

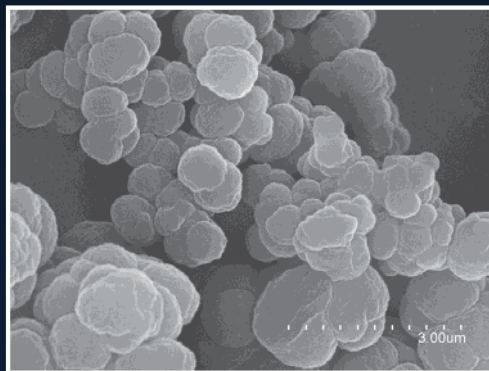
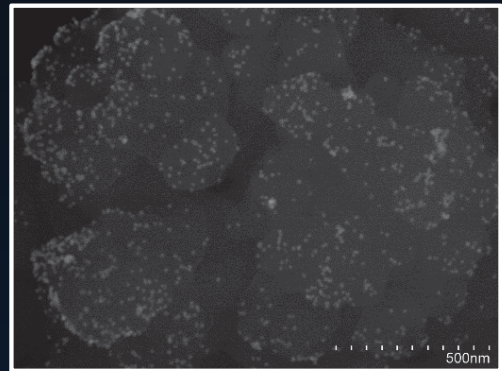
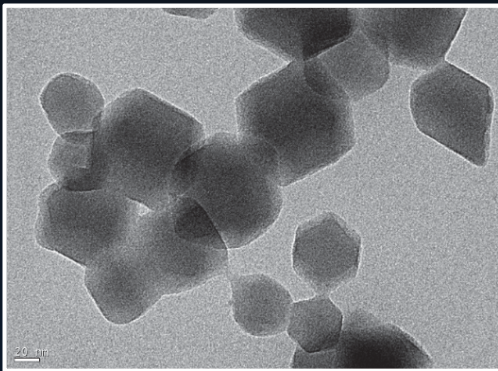


VNIVERSITAT  
DE VALÈNCIA

**Facultad de Química**

**Departamento de Química Analítica**

**DESARROLLO Y EVALUACIÓN DE  
MATERIALES POROSOS EN TÉCNICAS  
ANALÍTICAS DE EXTRACCIÓN Y  
SEPARACIÓN MINIATURIZADAS**



**Òscar Mompó Roselló  
Junio 2021**





VNIVERSITAT E VALÈNCIA

FACULTAD DE QUÍMICA

DEPARTAMENTO DE QUÍMICA ANALÍTICA

**DESARROLLO Y EVALUACIÓN DE MATERIALES POROSOS  
EN TÉCNICAS ANALÍTICAS DE EXTRACCIÓN Y  
SEPARACIÓN MINIATURIZADAS**

Memoria para alcanzar el grado de Doctor dentro del Programa de  
Doctorado en Química (R.D. 99/2011)

Autor:

**Òscar Mompó Roselló**

Directores:

**Dra. María Vergara Barberán**

**Dr. José Manuel Herrero Martínez**

**Dr. Ernesto F. Simó Alfonso**

València, junio de 2021



VNIVERSITAT (ò\*)  
E VALÈNCIA (ò\*)  
Facultat de Química

D. José Manuel Herrero Martínez y D. Ernesto F. Simó Alfonso, ambos catedráticos del Departamento de Química Analítica de la Universidad de Valencia y D<sup>a</sup>. María Vergara Barberán, doctora en Química.

Certifican

que la presente memoria, la cual lleva por título “*Desarrollo y evaluación de materiales porosos en técnicas analíticas de extracción y separación miniaturizadas*”, constituye la Tesis Doctoral de D. Òscar Mompó Roselló.

Asimismo, certifican haber dirigido y supervisado tanto los distintos aspectos del trabajo como su redacción.

Y para que así conste a los efectos oportunos y a petición del interesado, firmamos la presente en Burjasot, a 08 de junio de 2021.

MARIA|  
VERGARA|  
BARBERAN|  
Firmado digitalmente por MARIA|VERGARA| BARBERAN  
Fecha: 2021.07.16 13:20:13 +02'00'

Fdo.: María Vergara  
Barberán

JOSE  
MANUEL|  
HERRERO|  
MARTINEZ|  
Firmado digitalmente por JOSE MANUEL| HERRERO| MARTINEZ  
Fecha: 2021.07.16 13:25:17 +02'00'

Fdo.: José Manuel  
Herrero Martínez

ERNESTO  
FRANCISCO|  
SIMO|  
ALFONSO|  
Firmado digitalmente por ERNESTO FRANCISCO|SIMO| ALFONSO  
Fecha: 2021.07.16 13:10:33 +02'00'

Fdo.: Ernesto Francisco  
Simó Alfonso





VNIVERSITAT E VALÈNCIA

## *Prefacio*

Esta Tesis se acoge a la modalidad “compendio de publicaciones”, contemplada en el Reglamento de la Universidad de Valencia de 29/11/2011 (ACGUV 266/2011). De acuerdo con dicha normativa, la primera parte de la Tesis incluye un resumen global de la temática, resultados y conclusiones de los trabajos compendiados, justificando su temática y explicando la aportación original del doctorando. Seguidamente, se incluye una introducción general relacionada con la temática de la Tesis. A continuación, se incluyen los artículos ya publicados, los cuales corresponden en su totalidad a revistas indexadas. El doctorando ha contribuido sustancialmente en todas las etapas de desarrollo de todos los artículos, desde la elaboración de la idea, búsqueda bibliográfica, realización experimental, análisis e interpretación de los datos, redacción y preparación del manuscrito, y seguimiento y corrección final del mismo de acuerdo con las recomendaciones de los evaluadores. Todos los artículos han sido escritos por Òscar Mompó Roselló, con correcciones y revisión final por parte de los supervisores de esta Tesis.





Defèn el teu dret a  
pensar, perquè inclòs pensar  
erròniament és millor que no  
pensar.

Hypatia d'Alexandria



A la mea familia,

a ma uelo.



## AGRADECIMIENTOS

El camí ha sigut llarg, no ha sigut fàcil, però ha sigut disfrutat. Veient la fi tan propera, puc dir que ha merescut totalment la pena.

La realització d'aquesta tesi no haguera sigut possible sense la ajuda i el recolzament d'un gran nombre de persones.

En primer lugar, quisiera agradecer a mis directores, la Dra. María Vergara Barberán, el Dr. José Manuel Herrero Martínez y el Dr. Ernesto F. Simó Alfonso, su ayuda y dedicación en todo este tiempo. A ti doc, por todo el apoyo brindado, las largas tardes escribiendo cartas de respuesta a los *referees*, donde acabábamos hablando de todo menos de la carta a los *referees* y las abundantes noches de joda en las cenas de laboratorio y congresos varios. A María, la jefa suprema de todo el laboratorio 10, por tener la paciencia y la entereza necesaria para enseñarme, guiarme y ayudarme a convertirme en todo un doctor. Finalmente, a Erny, por lo muchísimo que me has ayudado, en lo profesional y sobretodo en lo personal, tú ya lo sabes, sin esas charlas no lo hubiese conseguido. Han sido muchos años juntos donde os he encontrado siempre disponibles y dispuestos a brindarme la mayor de las ayudas, gran parte de esta tesis es vuestra.

Agradecerle también a la Dra. María Jesús Lerma García su disponibilidad y predisposición, mención especial a la paciencia demostrada durante las interminables tardes corrigiendo mi TFG desde tierras milanesas.

Por otro lado, agradecer a mis compañeros del laboratorio 10. En estos años he aprendido mucho de vosotros, sobretodo villancicos (nunca había escuchado tantos villancicos y tan variados como en los diciembres vividos en el laboratorio 10). Enrique, el pequeño gran hombre del lab 10, siempre dispuesto a ayudar, muchas gracias por todo lo compartido durante estos años, dentro y también fuera del laboratorio. Héctor, el *fuertesito*, serio y reservado como nadie, pero una de las mejores personas y amigos que he encontrado en el camino, me llevo conmigo las largas charlas y consejos dados. Anca,

Ancuta, Ana C., otra de las personas que el laboratorio 10 ha cruzado en mi vida y que han acabado siendo importantes, sigue luchando por aquello que te haga feliz, es lo que realmente valdrá la pena al final. Isabel, en una casa de locos, siempre es necesario alguien que aporte algo de cordura, siempre me has dado los mejores consejos, sobretodo ayudándome a echar el freno en multitud de ocasiones, muchas gracias por ser, en ocasiones, la mami del lab 10. Carol, empezamos juntos en esto, desde el máster sabíamos que nos iba a tocar aguantarnos unos cuantos añitos más, y al final, ha merecido la pena, un orgullo haber compartido esta experiencia contigo. No me puedo olvidar de las viejas glorias del lab 10. Aarón, María Navarro y Miriam, me ayudasteis mucho en mis inicios y siempre os estaré agradecido. Me acuerdo también de los estudiantes que han pasado por el laboratorio, Iciar, Ernest, Jorge León, Mario, y un largo etcétera, gracias por compartir estos años.

Moltes gràcies a tots els meus amics, als Haters de la Torre, al Maxx Team, als químics guapos (de lo bueno lo mejor) i a tota la gent que ha passat per la *BurjaHouse*, gràcies per fer-me passar tots aquests anys més suportables.

I com no, agrair també a la meua família pel seu suport incondicional als bons i sobretot als no tan bons moments.

Por último, a Verónica. En estos últimos años has aguantado mis quejas, mis agobios, mis incertidumbres... Siempre con palabras de ánimo y apoyo. Pero por encima de todo, con una infinita PACIENCIA. Muchas gracias.

A tots els que, encara que no haja nomenat, han sigut partícips d'aquest projecte, GRÀCIES.

## **Resumen**





En esta sección, de acuerdo con la normativa sobre depósito, evaluación y defensa de la Tesis Doctoral de la Universidad de Valencia aprobada por Consejo de Gobierno el 29 de noviembre de 2011 y con última modificación el 31 de octubre de 2017, se presenta un resumen global de la temática, de los principales resultados y de las conclusiones del trabajo.

## **Objetivos**

La presente Tesis Doctoral contempla dos grandes líneas de actuación enmarcadas a su vez dentro de las líneas de investigación del grupo de investigación *Cromatografía Líquida, Electroforesis Capilar y Espectrometría de Masas* (CLECEM). La primera de ellas consiste en la síntesis, caracterización y modificación de materiales porosos para su uso como sorbentes en técnicas miniaturizadas de extracción en fase sólida (*Solid-Phase Extraction*, SPE) de analitos de interés biológico y medioambiental (fármacos, péptidos, proteínas, y contaminantes) utilizándose para ello diferentes formatos o soportes de extracción de uso común en el laboratorio químico tales como jeringas, columnas de centrífuga, etc. con diversos materiales híbridos desarrollados a este respecto (Objetivo *i*). La segunda línea de actuación consiste en la puesta a punto de metodologías sencillas y fiables en técnicas de separación miniaturizadas como la electrocromatografía capilar (*Capillary Electrochromatography*, CEC) empleándose para ello monolitos poliméricos como fases estacionarias capaces de ofrecer altas eficacias en la separación cromatográfica de solutos pequeños de diferentes polaridades y naturaleza química (Objetivo *ii*).

Así pues, para la consecución de los objetivos planteados en la presente memoria se ha considerado la experiencia previa del grupo de investigación en el diseño, síntesis y desarrollo de materiales poliméricos y su aplicación en el campo del tratamiento de muestra y de separación miniaturizadas.

De entre todas las etapas de un análisis químico, la etapa de tratamiento de muestras tanto de muestras biológicas como medioambientales constituye una

tarea complicada, debido al amplio espectro de interferentes que se pueden presentar en dichas matrices. Por lo que, el aislamiento, separación y preconcentración de los analitos de interés (fármacos, péptidos, proteínas y contaminantes) pueden verse comprometidas por las posibles interacciones de éstos con la matriz de la muestra dificultando así su extracción y posterior análisis. En este sentido, los métodos de extracción miniaturizados desarrollados en esta memoria (Objetivo *i*) suponen una interesante y prometedora alternativa al empleo de las metodologías tradicionales de extracción disponibles, las cuales suelen ser tediosas, poco selectivas y de dudosa sostenibilidad medioambiental. El resultado de este primer objetivo se traduce en el desarrollo de dispositivos miniaturizados para SPE eficaces con prestaciones mejoradas (selectividad, coste o reutilización, entre otros) y en consonancia con los principios de la Química Verde, que los hacen enormemente atractivos para ser empleados en laboratorios analíticos de rutina. Por otro lado, la metodología desarrollada en el Objetivo *ii*), relacionada con el empleo de una técnica de separación miniaturizada, presenta un gran interés debido a los buenos resultados que se han obtenido con el uso de monolitos poliméricos como fases estacionarias en nuestro grupo de investigación en la separación de moléculas pequeñas, tratándose de alcanzar mejores prestaciones (eficacia y tiempo de análisis) en el ámbito (electro)cromatográfico. Asimismo, el procedimiento desarrollado es sencillo, sostenible, y de bajo coste, lo cual podría permitir abordar el análisis de este tipo de solutos de una forma competitiva frente a técnicas cromatográficas más convencionales.

## **Estructura**

La presente memoria de Tesis Doctoral se divide en tres grandes bloques. El primer bloque consta de una breve introducción, donde se muestra en el **Capítulo 1**, una visión general del fundamento de la SPE y los posibles formatos miniaturizados de ésta, así como los tipos de sorbentes disponibles, centrándose en la descripción de aquellos que han sido empleados en esta

Tesis: los materiales porosos, incluyéndose por un lado, los materiales monolíticos de naturaleza orgánica sin modificar como modificados con nanopartículas de oro (*gold nanoparticles*, AuNPs), derivados de ácido borónico y líquidos iónicos (*ionic liquids*, ILs), y por el otro, las redes metalo-orgánicas (*metal-organic frameworks*, MOFs). Ambos tipos de materiales porosos han supuesto en los últimos años un avance significativo en el desarrollo de nuevas estrategias competitivas y prometedoras en el ámbito del tratamiento de muestra. A continuación, en el **Capítulo 2** se abordan las técnicas de electroseparación miniaturizadas, centrándose en la electrocromatografía capilar (*capillary electrochromatography*, CEC), describiendo brevemente su fundamento teórico y la instrumentación necesaria para llevarla a cabo. Además, se recogen las fases monolíticas comúnmente empleadas en CEC, así como las posibles estrategias que se pueden llevar a cabo para mejorar sus prestaciones, entre las que se encuentran modificaciones en la mezcla de polimerización y condiciones de reacción, el empleo del hiper-entrecruzamiento y la incorporación de nanomateriales. Estas estrategias han resultado esenciales de cara a poder desarrollar de manera relativamente sencilla la manipulación de las propiedades cromatográficas (eficacia, retención, selectividad) de las fases estacionarias y su adaptación a la separación de los analitos de interés.

Por su parte, el segundo bloque de la presente Tesis engloba los **Capítulos 3-6**, en los cuales se muestra la puesta a punto de diferentes sorbentes para su uso en SPE en diferentes formatos de extracción competitivos y sostenibles. Los materiales desarrollados se basan en materiales porosos de diferente naturaleza, como los monolitos poliméricos de metacrilato de glicidilo (*glycidyl methacrylate*, GMA), los cuales fueron posteriormente modificados químicamente con AuNPs e ILs. También, se describe el uso de otros materiales porosos como los MOFs para su posterior aplicación como sorbentes de extracción. A lo largo de estos capítulos se desarrollarán dispositivos extractivos en diversos soportes de uso común en el laboratorio

incluyéndose desde los cartuchos y jeringas convencionales de 1 mL, hasta minicolumnas de centrífuga. A su vez, los materiales desarrollados se han aplicado a diferentes familias de compuestos ( $\beta$ -bloqueantes, péptidos, glicoproteínas y benzomercaptanos) presentes en muestras de naturaleza biológica (orina, saliva y suero) y medioambiental (aguas y suelos).

El tercer bloque engloba el **Capítulo 7**, el cual se centra en el desarrollo de un método cromatográfico miniaturizado, en concreto de CEC, para la separación de moléculas pequeñas de diferente polaridad (alquilbencenos, sulfonamidas y compuestos organofosforados), empleando una fase estacionaria monolítica polimérica hiper-entrecruzada.

## **Resultados y conclusiones**

En este apartado, se describen los principales resultados obtenidos y las conclusiones derivadas de cada uno de los trabajos incluidos en la Tesis Doctoral. Los trabajos han sido divididos en dos grandes grupos (A y B), correspondientes a los bloques II y III de la presente memoria, donde se indica de forma desglosada por capítulos (cada capítulo corresponde a una publicación), la metodología adoptada en cada uno de ellos para alcanzar los objetivos planteados, así como los resultados y conclusiones más relevantes obtenidos de los mismos.

### **A. Evaluación del potencial de nuevos materiales porosos en técnicas de microextracción**

#### ***A.1. Diseño y aplicación de soportes poliméricos modificados con diversos nanomateriales o ligandos selectivos***

En estos trabajos (**Capítulos 3-5** de la memoria) se desarrollaron y evaluaron diferentes materiales monolíticos porosos como sorbentes de SPE para el aislamiento de diferentes analitos (fármacos, péptidos y

glicoproteínas). En concreto, los materiales seleccionados incluyen un monolito polimérico de GMA modificado con AuNPs (**Capítulo 3**), un monolito de GMA funcionalizado con un derivado del ácido borónico y posteriormente con AuNPs (**Capítulo 4**), y por último un monolito de GMA funcionalizado con un IL de tipo alquilpiridinio (**Capítulo 5**).

En el primer estudio que abre el bloque II (**Capítulo 3**) se llevó a cabo la síntesis de materiales poliméricos de GMA modificados con AuNPs y se evaluó su aplicación como sorbentes de SPE en formato jeringa para el aislamiento del polipéptido glutatión (GSH) en fluidos biológicos. Para ello, en primer lugar se prepararon sorbentes a partir de monolitos genéricos de GMA modificados con tres ligandos diferentes (amoníaco, cisteamina y cistamina) con el fin de dotar la superficie del sorbente de grupos amino (amoníaco) y grupos tiol (cisteamina y cistamina), para poder así modificar posteriormente la superficie de dicho sorbente con AuNPs. Para llevar a cabo la síntesis de los diferentes materiales poliméricos en el interior de jeringas, las paredes interiores de éstas fueron previamente vinilizadas para permitir el anclaje covalente de la fase monolítica, y así evitar su desprendimiento durante las operaciones de carga de muestra, lavado y elución. El tratamiento de la superficie interior de la jeringa se llevó a cabo en dos etapas. En primer lugar, se realiza una reacción de vinilización del polipropileno de la jeringa para facilitar el posterior anclaje del monolito, seguido de una polimerización *in-situ* de la fase monolítica en la jeringa mediante radiación UV. El resultado es un monolito híbrido unido covalentemente a la superficie interior de la jeringa, pero que presenta a su vez la suficiente estabilidad y permeabilidad para facilitar el proceso de extracción. Una vez realizada la modificación de la pared de la jeringa y generado el monolito de GMA, este polímero base conteniendo grupos epóxido en su superficie se funcionaliza con los ligandos anteriormente mencionados y posteriormente con AuNPs. Los materiales resultantes fueron caracterizados mediante técnicas tales como SEM (para evaluar la morfología) y microanálisis (para confirmar la presencia de Au). De

los tres materiales preparados, el material funcionalizado con cistamina fue el que proporcionó el mayor contenido de Au (entre 22 y 29%), y por ello se seleccionó este material para los estudios posteriores. Esto puede ser debido a que la cistamina produce mayor número de grupos reactivos (en este caso, tiol) sobre los cuales se puede depositar o inmovilizar mayor cantidad de AuNPs. Para demostrar la aplicabilidad del sorbente desarrollado, se seleccionó como analito diana, el GSH. Este compuesto es un tripéptido de vital importancia a nivel biológico que se produce dentro de los organismos y desempeña la función de antioxidante. Además, puede ser un marcador de algunas enfermedades como artritis reumatoide, distrofias musculares o Alzheimer. Por ello, su extracción de matrices complejas tales como fluidos biológicos y su posterior determinación resulta de enorme interés.

Con respecto al procedimiento SPE, se optimizó el pH de la muestra y la composición de la fase eluyente. Se obtuvieron las mejores condiciones de extracción ajustando la muestra a un pH final de 6, y usándose como eluyente una disolución de ditiotreitól (DTT) de una concentración de 500 mM. Si bien se ensayaron otros reactivos para producir la desorción del GSH del material híbrido diseñado, el DTT proporcionó rendimientos elevados así como no produjo interferencia, tras la reacción de derivatización oportuna con o-ftalaldehído, con el pico cromatográfico del analito. A continuación, se obtuvieron los parámetros de calidad del dispositivo, obteniéndose un satisfactorio volumen de ruptura (1,5 mL), una buena capacidad de carga (2,93 mg de GSH por g de sorbente polimérico modificado), y una adecuada reutilización del sorbente (hasta 15 ciclos de carga y desorción sin obtener pérdidas significativas en las recuperaciones del analito).

Tras llevar a cabo la optimización de las diferentes etapas del proceso de extracción, se analizaron muestras reales de saliva, lográndose valores de recuperación comprendidos entre 86 y 105%, y un LOD muy bajo ( $1,5 \text{ ng mL}^{-1}$ ). Estos resultados pusieron de manifiesto la buena efectividad del sorbente sintetizado tanto en el proceso de “clean-up” de la muestra como en la

preconcentración del GSH. El mecanismo de retención de este analito en el sorbente diseñado radica principalmente en la elevada afinidad que existe entre el grupo tiol presente en la molécula de GSH y las AuNPs que se encuentran localizadas en la superficie del monolito durante la etapa de extracción.

En comparación con otros métodos actuales que emplean nanomateriales para la preconcentración de GSH en diferentes muestras, la metodología aquí desarrollada resultó ser más simple y económica, gracias a la buena reutilización del material. Así pues, la metodología propuesta representa una alternativa alentadora para la extracción de compuestos relevantes que contengan grupos tiol en su estructura presentes en diferentes muestras biológicas.

En lo referente a los materiales monolíticos funcionalizados con grupos boronato (**Capítulo 4**), se sintetizaron dos materiales a partir de un monolito genérico de GMA en jeringas para su posterior uso como sorbentes en la extracción de glicopéptidos derivados de una proteína estándar, la proteína del rábano picante (*Horseradish peroxidase*, HRP), y las glicoproteínas presentes en suero humano. Para ello, se seleccionó el polimercaptopropilmetilsilosano (PMPMS) como politiol para reaccionar con los grupos epoxi presentes en la molécula de GMA, para posteriormente introducir el ácido vinil fenil borónico (*vinyl phenyl boronic acid*, VPBA) mediante una reacción de química click (reacción de acoplamiento tiol-alqueno). En concreto, en el primero de los materiales sintetizados, se partió del polímero de GMA, el cual se funcionalizó con PMPMS y VPBA de forma sucesiva. El polímero resultante de esta estrategia se designó como GMA-PMPMS-VPBA. Por su parte, el segundo material utilizó como polímero base un monolito de GMA modificado con cistamina (véase capítulo anterior), el cual fue funcionalizado con AuNPs. Posteriormente, este material híbrido se modificó con PMPMS y seguidamente con VPBA. El material híbrido obtenido siguiendo esta segunda estrategia se designó como GMA-SH@AuNP@PMPMS-VPBA. Se procedió

a llevar a cabo la caracterización de ambos materiales mediante SEM y microanálisis. Los resultados de esta caracterización morfológica condujo a la presencia de estructuras globulares en ambos materiales (características de los monolitos poliméricos), y además se obtuvo un contenido de silicio y boro de 2,48 y 2,78% en el primer material, y de 2,02% y de 3,04, en el segundo material. También, se determinó la cantidad de boro presente en el polímero total, no únicamente en la superficie, mediante espectrometría de masas con plasma acoplado inductivamente (ICP-MS), obteniéndose 0,10 y 0,45% en peso para el monolito GMA-PMPMS-VPBA y GMA-SH@AuNP@PMMPS-VPBA, respectivamente. Estos datos demuestran que los grupos boronato se anclaron de forma satisfactoria sobre la superficie del monolito. No obstante, la presencia de VPBA en el material resultante se confirmó/corrobó mediante las bandas de absorción en el infrarrojo características del derivado de ácido borónico. La alta cantidad de boro inmovilizado en el segundo material puede ser atribuido al mayor número de AuNPs disponible en este material, causado por el alto grado de recubrimiento que ofrece el ligando PMPMS, obteniéndose así un mayor número de sitios activos disponibles de NPs para una mayor inmovilización del VPBA.

En lo que respecta al protocolo SPE, los materiales preparados se emplearon como sorbentes SPE para el aislamiento de glicopéptidos tras la digestión de la proteína HRP. El material GMA-SH@AuNP@PMMPS-VPBA fue el que mostró una mayor eficacia extractiva de los glicopéptidos, lo cual puede ser atribuido a la mayor cantidad de grupos boronato presente en su estructura del polímero, tal y como se ha comentado anteriormente. Además, el material mostró una preconcentración selectiva de glicopéptidos (24 glicopéptidos de un total de 27), una elevada capacidad de adsorción (25 mg g<sup>-1</sup>), alta sensibilidad (0.5 fmol/μL) y selectividad, así como una buena reproducibilidad y reutilización (hasta 10 ciclos sin pérdidas apreciables en los valores de recuperación). También, se evaluó las prestaciones del material GMA-SH@AuNP@PMMPS-VPBA a la preconcentración de glicopéptidos



en una muestra de suero humana. El empleo de este material junto con el protocolo de extracción óptimo y con el análisis mediante nano-LC–MS/MS permitió obtener la identificación de un total de 85 péptidos N-glicosilados derivados de 42 proteínas N-glicosiladas sin necesidad de eliminar ninguna proteína abundante. La capacidad de preconcentrar e identificar péptidos del sorbente monolítico desarrollado en este trabajo fue ligeramente superior a otros monolitos de tipo hidrofílico descritos en bibliografía. Sin embargo, el rendimiento en la identificación de péptidos resultante fue menor que el obtenido utilizando monolitos híbridos con AuNPs inmovilizados y modificados con cisteína.

Los buenos resultados obtenidos en este trabajo hacen que la metodología propuesta represente una alternativa sencilla para el aislamiento y preconcentración de glicopéptidos en matrices biológicas complejas.

En este trabajo (**Capítulo 5**) se prepararon sorbentes monolíticos funcionalizados con IL de tipo imidazolio (cloruro de 1-alil-3-metilimidazolio, [AMIM] [Cl]) en columnas de microcentrífuga para su posterior aplicación en la extracción de  $\beta$ -bloqueantes en muestras de orina humana. Estos analitos generalmente se emplean en el tratamiento de algunas enfermedades cardíacas, y actúan relajando los músculos cardíacos y disminuyendo la frecuencia cardíaca. Por ello, se emplean de forma fraudulenta en algunos deportes siendo necesario llevar a cabo un control estricto de estas sustancias en muestras biológicas. Con el fin de desarrollar un sorbente capaz de extraer dichos analitos de muestras complejas, en primer lugar, se optimizó la relación monómeros/porógenos, proporcionando la ratio 60/40% (p/p) los mejores resultados en cuanto a estabilidad mecánica y resistencia durante la etapa de centrifugado. En segundo lugar, se llevó a cabo la incorporación del IL al monolito mediante su generación *in situ* sobre la superficie del monolito base (GMA). Esta estrategia dio lugar a sorbentes monolíticos frágiles los cuales se rompían durante la etapa de centrifugación. Por ello, se abordó una estrategia alternativa para llevar a cabo la introducción

del IL en el monolito que consistía en incorporar el IL a la mezcla de polimerización. El material resultante mostró una buena resistencia mecánica y unas propiedades de permeabilidad y porosidad apropiadas. Así pues, se seleccionó este segundo polímero como sorbente y se optimizó el protocolo SPE en términos de contenido de [AMIM] [Cl], el pH de carga de la muestra y la composición del eluyente con el fin de obtener el mayor rendimiento de extracción posible.

Así pues, la presencia de [AMIM] [Cl] en el sorbente polimérico resultante causó una mayor retención de los  $\beta$ -bloqueantes (en comparación con el polímero base de GMA) debido a interacciones electrostáticas, enlaces por puente de hidrógeno, interacciones  $\pi$ - $\pi$ , y fuerzas hidrofóbicas. Bajo las condiciones óptimas del procedimiento SPE, el sorbente desarrollado mostró altas recuperaciones ( $> 90\%$ ), LODs entre 1,4 y 40  $\mu\text{g L}^{-1}$ , una capacidad de carga de 2.5  $\mu\text{g}$  por mg sorbente y una reutilización de hasta 20 ciclos sin apreciar pérdidas de analitos significativas.

El método desarrollado se aplicó a la extracción del  $\beta$ -bloqueante propranolol en muestras de orina humana, observándose una limpieza efectiva (*clean up*) de la muestra, pudiéndose determinar de forma satisfactoria.

Por último, cabe destacar que, el método de tratamiento de muestra propuesto no sólo implica una reducción en la cantidad de reactivos necesaria, sino que, debido a la simplicidad asociada al manejo del material requerido, permite el procesamiento de un mayor número de muestras respecto a métodos de SPE tradicionales.

Los resultados de estos trabajos se encuentran publicados en:

Ó. Mompó-Roselló, M. Vergara-Barberán, E.F. Simó-Alfonso, J.M. Herrero-Martínez, In syringe hybrid monoliths modified with gold nanoparticles for selective extraction of glutathione in biological fluids prior to its determination by HPLC, *Talanta* 209 (2020) 120566.

Ó. Mompó-Roselló, M. Vergara-Barberán, M.J. Lerma-García, E.F. Simó-Alfonso, J.M. Herrero-Martínez, Boronate affinity sorbents based on thiol-functionalized polysiloxane-polymethacrylate composite materials in syringe format for selective extraction of glycopeptides, *Microchem. J.* 164 (2021) 106018.

Ó. Mompó-Roselló, A. Ribera-Castelló, E.F. Simó-Alfonso, M.J. Ruiz-Ángel, M.C. García-Álvarez-Coque, J.M. Herrero-Martínez, Extraction of  $\beta$ -blockers from urine with a polymeric monolith modified with 1-allyl-3-methylimidazolium chloride in spin column format, *Talanta* 214 (2020) 120860.

## ***A.2. Diseño y aplicación de sorbentes basados en redes metalo-orgánicas (MOF)***

En este trabajo (**Capítulo 6**) se sintetizaron y caracterizaron nanocristales de MOF con topología zeolítica, empleándose grupos imidazolato como ligandos orgánicos (*Zeolite imidazolate frameworks*, ZIFs). En concreto, el MOF sintetizado fue el ZIF-8, el cual se modificó con grupos amino empleándose como moduladores aminos orgánicos (concretamente, la *n*-butilamina, BA). El MOF resultante se evaluó como sorbente en SPE para la extracción de benzomercaptanos en muestras de agua y suelo.

En primer lugar, se estudió la influencia de la cantidad del modulador BA (en la mezcla de síntesis) sobre el tamaño de los cristales resultantes además de la capacidad de retención del MOF. La caracterización morfológica del material sintetizado por SEM mostró la estructura poliédrica característica de los nanocristales ZIF-8. Además, se determinó el tamaño de partícula mediante microscopía de transmisión electrónica (*Transmission electron microscopy*, TEM), situándose entre 47 y 89 nm. Asimismo, se apreció que un incremento del contenido de BA se tradujo en un aumento del tamaño de partícula. También, la presencia de grupos amino (proporcionados por la molécula BA) en los materiales obtenidos se confirmó mediante

microanálisis. Además, se determinó el área superficial de todos los materiales sintetizados mediante las isothermas de adsorción-desorción de nitrógeno, obteniéndose en todos los casos valores superiores a  $1000 \text{ m}^2 \text{ g}^{-1}$ . Todos los materiales sintetizados se testaron como sorbentes en SPE, y se obtuvieron los mejores resultados con ZIF-8 que contenía 10 mmol de BA como modulador.

Además, se investigaron varios parámetros experimentales del protocolo SPE que influyen en el rendimiento de extracción (pH de la muestra, composición y volumen del disolvente de elución o reutilización). Para llevar a cabo este estudio, se utilizaron 20 mg del material seleccionado y se colocaron en un cartucho convencional de 1 mL. Para poner de manifiesto la aplicabilidad del material fabricado como sorbente, se seleccionó una mezcla de benzomercaptanos como disolución test. Como resultado de este estudio, se estableció que el pH de la muestra no era un factor que implicara cambios significativos en la retención, mientras que la composición del eluyente sí afectaba a la retención de los solutos. En concreto, los mejores rendimientos de extracción (97-108%) se obtuvieron con un eluyente compuesto por 0,5 M NaOH en 50/50 % (v/v) MeOH/H<sub>2</sub>O, y un volumen de 250  $\mu\text{L}$ . Además, cabe destacar que el método propuesto permitió alcanzar factores de preconcentración de 100, obteniéndose LODs comprendidos entre 1,6 y 2  $\mu\text{g L}^{-1}$ . Por último, se aplicó la metodología desarrollada a la extracción de los benzomercaptanos en muestras de agua y suelos, alcanzándose unos rendimientos comprendidos entre 74 y 117%.

Este trabajo representa el primer estudio sobre la influencia del contenido de modulador en la morfología del sorbente, así como en el rendimiento de extracción de contaminantes orgánicos. La satisfactoria aplicación del material a la extracción de benzomercaptanos abre la puerta, sin duda, a su extensión a otro tipo de contaminantes como otras posibles aplicaciones de interés industrial.

Los resultados de estos trabajos se encuentran publicados en:

H. Martínez-Pérez-Cejuela, Ó. Mompó-Roselló, N. Crespí-Sánchez, C.P. Cabello, M. Catalá-Icardo, E.F. Simó-Alfonso, J.M. Herrero-Martínez, Determination of benzomercaptans in environmental complex samples by combining zeolitic imidazolate framework-8-based solid-phase extraction and high-performance liquid chromatography with UV detection, *J. Chromatogr. A* 1631 (2020) 461580.

## **B. Aplicación de materiales monolíticos en técnicas cromatográficas miniaturizadas**

En el trabajo descrito en el **Capítulo 7** se sintetizaron y caracterizaron una serie de columnas monolíticas basadas en polietilenglicol diacrilato (PEGDA) para la separación de moléculas pequeñas de diferentes polaridades mediante la técnica CEC. En este caso, el empleo de monómeros de PEGDA de diferentes longitudes de cadena del grupo alquilo permitió modificar la hidrofobicidad de la fase estacionaria resultante, así como también una manipulación en las eficacias de separación obtenidas. En primer lugar, se optimizó la composición de las mezclas de polimerización (concentración y longitud de cadena del PEGDA, concentración de porógenos y temperatura de polimerización). Se caracterizaron morfológicamente las fases monolíticas mediante SEM, y se evaluó la eficacia de separación cromatográfica de las columnas sintetizadas empleando una mezcla de alquilbencenos como soluto test, obteniéndose valores cercanos a 76.000 platos  $m^{-1}$  con una mezcla compuesta por el monómero de PEGDA 700.

Posteriormente, se demostró la viabilidad de esa misma fase estacionaria en la separación mediante CEC de pequeños solutos polares de naturaleza diferente como son los compuestos organofosforados, derivados del ácido benzoico y sulfonamidas, que se emplearon como soluto test en este trabajo. Cabe destacar la elevada eficacia cromatográfica que se obtuvo en la separación de sulfonamidas, en concreto 144.000 platos  $m^{-1}$ . Además, las columnas sintetizadas exhibieron excelentes reproducibilidades con valores de coeficiente de variación por debajo del 2,5 %, lo que confirma los beneficios

de utilizar el monómero de PEGDA en las mezclas de polimerización debido al alto grado de entrecruzamiento que genera.

Asimismo, cabe destacar que el empleo de PEGDA como único monómero en la mezcla de polimerización, sin la necesidad de recurrir a ningún otro agente entrelazante, facilita la preparación y la optimización de las diferentes variables que afectan a las propiedades morfológicas y cromatográficas del monolito resultante.

Los resultados de este trabajo se encuentran publicados en la siguiente referencia:

M. Vergara-Barberán, Ó. Mompó-Roselló, J.M. Herrero-Martínez, E.F. Simó-Alfonso, Poly (ethylene glycol) diacrylate based monolithic capillary columns for the analysis of polar small solutes by capillary electrochromatography, *J. Sep. Sci.* 41(12) (2018) 2632-2639.

# ÍNDICE

<b>Bloque I. Introducción .....</b>	<b>1</b>
<b>Capítulo 1. Sorbentes empleados en técnicas miniaturizadas de extracción en fase sólida .....</b>	<b>3</b>
1.1. La extracción en fase sólida.....	5
1.2. Materiales particulados.....	11
1.3. Materiales porosos.....	12
1.4. Referencias .....	29
<b>Capítulo 2. Aplicación de materiales monolíticos en técnicas de separación miniaturizadas.....</b>	<b>43</b>
2.1. Técnicas de (electro)separación miniaturizadas. Generalidades .....	45
2.2. Electro cromatografía capilar (CEC).....	47
2.3. Fases estacionarias monolíticas en técnicas de separación miniaturizadas .....	52
2.4. Referencias .....	63
<b>Bloque II. Evaluación del potencial de nuevos materiales porosos en técnicas de (micro)extracción.....</b>	<b>73</b>
<b>Capítulo 3. In syringe hybrid monoliths modified with gold nanoparticles for selective extraction of glutathione in biological fluids prior to its determination by HPLC .....</b>	<b>75</b>
3.1. Introduction .....	78
3.2. Experimental.....	81
3.3. Results and discussions .....	86
3.4. Conclusions .....	96
3.5. References .....	97

3.6. Supporting Material.....	102
<b>Capítulo 4. Boronate affinity sorbents based on thiol-functionalized polysiloxane-polymethacrylate composite materials in syringe format for selective extraction of glycopeptides.....</b>	<b>105</b>
4.1. Introduction .....	108
4.2. Experimental.....	112
4.3. Results and discussion.....	118
4.4. Conclusions .....	126
4.5. References .....	127
4.6. Supporting Material.....	134
<b>Capítulo 5. Extraction of <math>\beta</math>-blockers from urine with a polymeric monolith modified with 1-allyl-3-methylimidazolium chloride in spin column format .....</b>	<b>145</b>
5.1. Introduction .....	148
5.2. Experimental.....	150
5.3. Results and discussion.....	154
5.4. Conclusions .....	166
5.5. References .....	167
5.6. Supporting Material.....	173
<b>Capítulo 6. Determination of benzomercaptans in environmental complex samples by combining zeolitic imidazolate framework-8-based solid-phase extraction and high-performance liquid chromatography with UV detection .....</b>	<b>175</b>
6.1. Introduction .....	178
6.2. Experimental section .....	181



6.3. Results and discussion .....	185
6.4. Conclusions .....	199
6.5. References .....	200
6.6. Supporting Material .....	208
<b>Bloque III. Aplicación de materiales monolíticos en técnicas cromatográficas miniaturizadas .....</b>	<b>215</b>
<b>Capítulo 7. Poly(ethylene glycol) diacrylate based monolithic capillary columns for the analysis of polar small solutes by capillary electrochromatography.....</b>	<b>217</b>
7.1. Introduction .....	220
7.2. Materials and methods.....	222
7.3. Results and discussion.....	226
7.4. Conclusions .....	235
7.5. References .....	236
<b>Bloque IV. Resumen de resultados y conclusiones.....</b>	<b>241</b>
A. Evaluación del potencial de nuevos materiales porosos en técnicas de (micro)extracción.....	243
B. Aplicación de materiales monolíticos en técnicas cromatográficas miniaturizadas .....	247



# **Bloque I. Introducción**



**Capítulo 1. Sorbentes empleados en técnicas  
miniaturizadas de extracción en fase sólida**

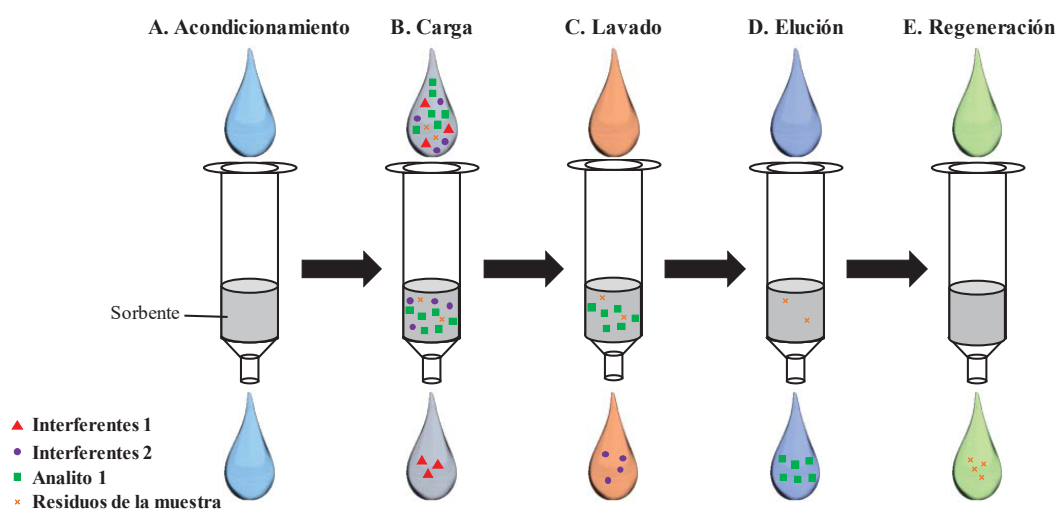


## 1.1. La extracción en fase sólida

### 1.1.1. Fundamento

La extracción en fase sólida (*Solid-Phase Extraction*, SPE) es una técnica empleada en Química Analítica, comúnmente utilizada en la preparación de muestras. Ésta se basa en el uso de un lecho cromatográfico para el aislamiento o extracción de diferentes analitos o grupos de interés en una matriz más o menos compleja (aguas de consumo, muestras biológicas, etc.). La terminología viene dada por el uso de un soporte sólido con afinidad por diversos analitos, a través del cual se hace pasar un líquido o gas que contiene a éstos. Los solutos son, por tanto, aislados de la muestra y eluidos posteriormente utilizando un disolvente o mezcla de ellos con una afinidad adecuada por el analito. El proceso de SPE se puede resumir en cinco etapas (véase **Figura 1.1**). Inicialmente tiene lugar el acondicionamiento del sorbente (**Figura 1.1A**), donde éste se activa mediante el uso de disolventes apropiados para cada tipo de lecho, por ejemplo, para sorbentes hidrofóbicos suele utilizarse metanol (MeOH) o acetonitrilo (ACN), mientras que para fases estacionarias hidrofílicas, se emplea hexano o cloruro de metileno. Posteriormente, tiene lugar la etapa de carga (**Figura 1.1B**), donde se introduce la muestra y ésta se hace pasar a través del sorbente, durante este proceso quedan retenidos los analitos de interés, siendo eliminados la mayoría de los interferentes. Con el fin de conseguir un proceso de eliminación de interferentes completo, se procede a una posterior etapa de lavado de la muestra (**Figura 1.1C**), en la cual se hace pasar un disolvente poco afín por los analitos a través del dispositivo de extracción, permitiendo así la eliminación de posibles interferentes que hubieran podido quedar retenidos junto al analito de interés. A continuación, en la etapa de elución (**Figura 1.1D**), se extrae el analito de interés pasando por el sorbente un disolvente afín a éste. Por regla general, se lleva a cabo una última etapa que consiste en la regeneración del lecho cromatográfico (**Figura 1.1E**), donde el sorbente se regenera completamente para poder ser reutilizado en posteriores análisis.

Cabe señalar que una correcta selección del disolvente de extracción puede permitir la posterior inyección directa del extracto en sistemas cromatográficos [1, 2]. Además, esta técnica puede permitir la preconcentración de los analitos, lo que facilita su posterior detección, disminuyendo considerablemente los límites de detección. También, se eliminan posibles efectos asociados a la naturaleza de la muestra (como el efecto matriz), que puedan afectar a la sensibilidad lo que conduce a una mejora en la detección cromatográfica o reducir fenómenos perjudiciales como la supresión iónica en la detección por espectrometría de masas (*Mass Spectrometry*, MS).



**Figura 1.1.** Representación esquemática de las etapas típicas en la SPE.

Por lo tanto, la SPE representa una alternativa real a la clásica extracción líquido-líquido (*Liquid-Liquid Extraction*, LLE) en el tratamiento de muestras, pues exhibe una serie de claras ventajas sobre ésta. Generalmente, el poder realizar un diseño de la selectividad del sorbente respecto a los analitos a estudiar, permite obtener mayores rendimientos de extracción, así como un incremento en la reproducibilidad y precisión. Además, permite procesar un número elevado de muestras simultáneamente. Finalmente, el empleo global de menores cantidades de disolventes, cuando se utilizan formatos de dimensiones reducidas, permite que las metodologías desarrolladas estén de acorde con los principios de la Química verde [3].



El uso de este tipo de metodología comenzó a ser intensamente estudiado al comienzo de la década de 1970, siendo la primera aplicación descrita por Sudben y col. [4], quienes usaron sorbentes basados en sílice para el aislamiento de histidinas presentes en vinos. Desde esa primera publicación, las metodologías han ido evolucionado con el estudio de sorbentes más selectivos y utilizando una amplia gama de soportes que se adaptan a las necesidades de cada análisis.

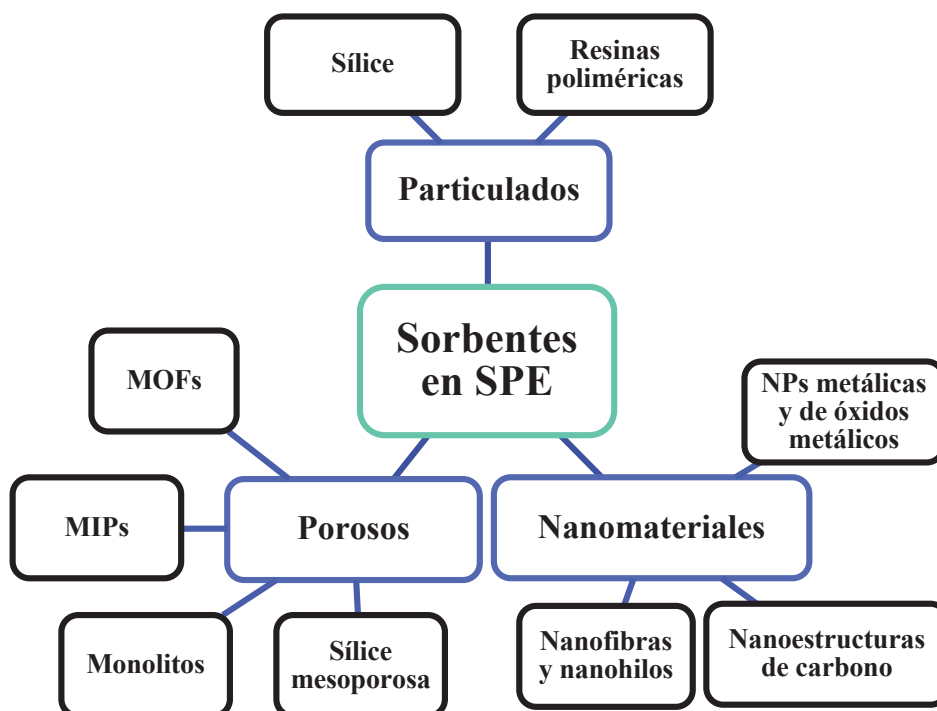
Atendiendo a los modos de aplicación de esta técnica de tratamiento de muestras, se puede llevar a cabo en línea (*on-line*), o fuera de línea (*off-line*). En el primer caso, dicha técnica se acopla directa y automáticamente a instrumento analítico (generalmente un sistema cromatográfico), mientras que en el segundo se requiere de la presencia de un analista para llevar a cabo todas las etapas de SPE, y posterior análisis. No obstante, éste último es el modo más utilizado debido a su sencillez y menor coste comparado con los métodos en línea. Existen ciertas limitaciones para realizar las extracciones *on-line* como pueden ser la compatibilidad de disolventes utilizados o las diferencias en cuanto a la tolerancia de caudal soportado por el sistema de análisis y el de extracción [5].

En los últimos años, el diseño y desarrollo de nuevos materiales dotados de una serie de prestaciones mejoradas para su uso como sorbentes en SPE ha despertado un gran interés en el campo del tratamiento de muestra, ya que se pueden obtener lechos con características modificables para maximizar así la afinidad por los analitos a estudiar [6]. Como consecuencia, se han mejorado considerablemente parámetros analíticos de la extracción, como la capacidad de carga, el volumen de ruptura, la selectividad/especificidad, o eficacia de preconcentración, lo que ha permitido detectar analitos a nivel de trazas en muestras complejas. Por otro lado, se han desarrollado materiales más estables tanto química como mecánicamente, de un menor coste en su síntesis y menor cantidad de residuos generada en su producción.

Las fases clásicas utilizadas como sorbente para SPE se componen en su mayoría por material de sílice particulado modificado superficialmente con cadenas alquílicas parecidas a las usadas para columnas de cromatografía líquida de alta resolución. Sin embargo, estas fases estacionarias convencionales presentan distintos inconvenientes, como su limitada estabilidad en un intervalo de pH reducido (pH 2-9) y la presencia de grupos reactivos accesibles en su estructura que pueden dar lugar a una menor retención y falta de selectividad.

Con la intención de superar estas desventajas, en los últimos años se han desarrollado materiales porosos con una serie de propiedades mejoradas, tales como mayor estabilidad, capacidad y dinámica de adsorción. Entre estos sorbentes, se encuentran los materiales mesoporosos basados en óxidos inorgánicos como óxidos de zirconio, hierro o titanio, los cuales presentan un área superficial muy elevada, estructuras muy ordenadas y tamaños de poro controlables durante el proceso de síntesis (2-50 nm) siendo candidatos perfectos para ser usados como sorbentes en SPE [7]. Más recientemente, se ha despertado el interés en el uso de materiales poliméricos como sorbentes dada su elevada porosidad, permeabilidad y la facilidad de poder llevar a cabo la modificación química de su superficie con el fin de aumentar la selectividad de los sorbentes por los analitos diana [8]. También, en los últimos años se ha descrito el uso de polímeros junto con materiales nanoestructurados como las NPs metálicas y de óxidos metálicos, nanoestructuras de carbono (nanotubos / nanocuernos / nanofibras), entre otros, aportando características como una gran área superficial, morfologías variables para modificar la interacción analito-sorbente y modificar su selectividad [9]. Por otro lado, las redes metalo-orgánicas también están siendo una revolución en el campo del SPE, pues se trata de materiales altamente porosos con cavidades nanométricas que proporcionan áreas superficiales extremadamente elevadas [10]. Aunque estos materiales presentan muchas propiedades ventajosas para su uso como sorbentes en SPE, el principal inconveniente es que poseen una limitada

selectividad cuando se aplican en muestras complejas. Para solventar esta limitación, se han desarrollado materiales altamente selectivos, o incluso específicos, basados en mecanismos de reconocimiento molecular como los polímeros de impronta molecular (*Molecularly Imprinted Polymers*, MIPs), inmunosorbentes y aptámeros. En la **Figura 1.2** se muestra los principales sorbentes utilizados en SPE, algunos de los cuales serán descritos posteriormente.



**Figura 1.2.** Clasificación de los sorbentes más utilizados en SPE en función de su naturaleza estructural.

### 1.1.2. Formatos de extracción en fase sólida

Actualmente los dispositivos de extracción en fase sólida presentan un amplio abanico de formatos disponibles: cartuchos, jeringas, discos de agitación, imanes, capilares, puntas de pipeta, placas multi-pocillo, etc., pudiéndose implementar metodologías semi-automáticas para el procesado de un gran número de muestras en poco tiempo. En este sentido, la aplicación de los 12 principios de la Química verde [3] en los laboratorios ha favorecido la

búsqueda de nuevos formatos que favorezcan el cumplimiento de estos requisitos. La miniaturización ha sido un elemento clave en la producción y el progreso de los nuevos formatos de SPE desde la preparación del primer dispositivo SPE en 1951, un cilindro de hierro con 1,5 kg de carbón activado granular [11]. En la **Tabla 1.1** se muestran los formatos más estudiados en los últimos años junto con las ventajas y desventajas de cada uno de ellos.

**Tabla 1.1.** Comparación de formatos usados en SPE.

Formato	Ventajas	Desventajas
Cartuchos/jeringas	Fácil preparación-combinación de sorbentes Bajo coste Bajo volumen de disolventes	Baja sección transversal Bajo caudal Alto volumen muerto Efecto de canalización Riesgo de obstrucción
Discos	Bajo volumen de disolventes Caudales elevados No presenta efectos de canalización Pequeño volumen muerto Elevada área superficial Bajo tiempo de extracción	Menor volumen de ruptura Elevado coste
Columnas de microcentrífuga	Facilidad de preparación Fácil automatización Bajo tiempo de extracción Tratamiento simultáneo de múltiples muestras	Necesidad de anclaje entre el sorbente y el soporte Menor volumen de ruptura
Puntas de pipeta	Preparación sencilla Pequeños volúmenes de muestra y disolventes Fácil automatización Bajo tiempo de extracción	Riesgo de obstrucción Alta generación de residuos plásticos

**Tabla 1.1.** (Continuación).

Formato	Ventajas	Desventajas
Placas multi-pocillo	Preparación sencilla Bajo volumen de disolventes Caudal elevado Bajo tiempo de extracción Flujos rápidos sin efectos de “canalización”	Baja homogeneidad en el procesamiento de muestras
SPE dispersiva	Bajos volúmenes de muestra y disolventes	Pérdida de sorbente

Una vez comentados los formatos habitualmente utilizados en SPE para llevar a cabo el tratamiento de muestra, se comentará en las secciones siguientes algunos de los materiales usados en SPE en función de su naturaleza estructural anteriormente indicados en la **Tabla 1.1**.

## 1.2. Materiales particulados

Se estima que la gran mayoría (>90%) de los sorbentes para SPE que se fabrican en el mundo utilizan con soporte un gel de sílice como material de partida [12], siendo el resultado un material con un área superficial comprendida entre 50 y 500 m<sup>2</sup>g<sup>-1</sup> y un tamaño de partícula entre 30 y 60 μm [6,12,13]. Este material contiene grupos silanoles libres en su superficie, los cuales actúan como centros reactivos responsables de sus propiedades. Así pues, estos materiales se pueden enlazar a distintos ligandos modificando su química superficial y su selectividad. De esta manera, se pueden obtener sorbentes que ofrezcan interacciones hidrofóbicas (C8, C18, fenilo...), hidrofílicas (diol, aminopropilo...) o de intercambio iónico (ácidos sulfónicos, aminas cuaternarias). Estos sorbentes presentan diversas ventajas como su fácil y económica preparación y elevada relación área superficial/volumen; sin embargo, presentan algunos inconvenientes como su restringido intervalo de estabilidad frente al pH (pH 2 - 9) y la presencia de grupos silanoles libres

en su estructura, los cuales pueden ejercer un efecto negativo en la retención de ciertos analitos [14].

Como alternativa a estos materiales, se encuentran materiales particulados de óxidos metálicos (alúmina o zirconia), y resinas sintéticas de tipo poliestireno-divinilbenceno (*polystyrene-divinylbenzene*, PS-DVB), entre otros [12]. El tipo de interacciones que puede ofrecer este último tipo de material es principalmente hidrofóbico (fuerzas de Van der Waals e interacciones  $\pi$ - $\pi$ ), si bien pueden ser sujetos a modificación con grupos polares con el fin de mejorar la retención de compuestos orgánicos hidrofílicos [15]. Sin embargo, la retención de compuestos altamente polares en matrices complejas sigue siendo una limitación de estos sorbentes.

En cualquier caso, la utilización de estos materiales particulados, bien sean de tipo sílice o resinas poliméricas, en los diferentes dispositivos de SPE es necesario el empleo de fritas para evitar la pérdida de sorbente. Estas fritas no son completamente inertes y pueden interactuar con los analitos, así como obturarse con partículas más pequeñas de sorbente, debido a la falta de homogeneidad de éste, impidiendo el uso continuado del dispositivo.

### 1.3. Materiales porosos

Los materiales porosos se pueden clasificar, atendiendo a criterios de la Unión Internacional de Química Pura y Aplicada (IUPAC), en función del tamaño de las cavidades que en ellos se encuentran. Los materiales con poros de tamaño inferior a 2 nm son los conocidos como estructuras microporosas, mientras que si el tamaño del poro se encuentra entre 2 - 50 nm se catalogan como mesoporosas, y los que contienen poros mayores a 50 nm se denominan materiales con estructuras macroporosas [16]. Estos materiales pueden presentar una elevada área superficial, con un mayor número de sitios activos donde se pueden adsorber/retener los analitos. Además, debido a su estructura altamente porosa se favorece la transferencia de masa, y velocidades de flujo o caudales de trabajo mayores. También, pueden ser modificados para mejorar

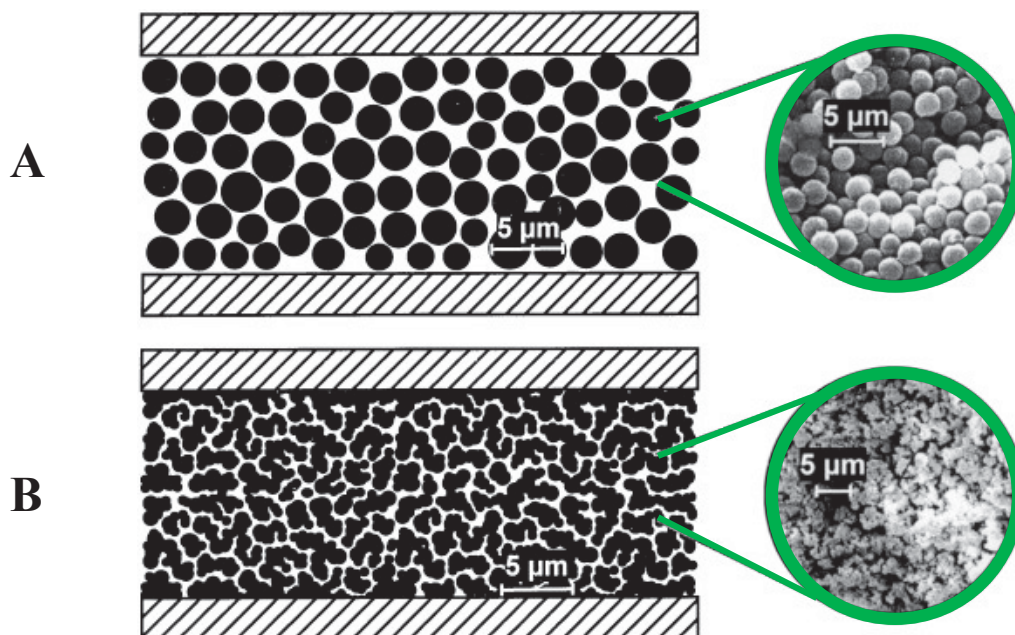
la selectividad/especificidad por las moléculas diana. Dentro de este grupo de materiales porosos se encuentran los materiales monolíticos y los MOFs, los cuales han sido utilizados en la presente Tesis. A continuación, se comentarán las características de estos materiales.

### 1.3.1. Materiales monolíticos

#### 1.3.1.A. Generalidades. Tipos de monolitos

Los materiales monolíticos son materiales formados por un único lecho o soporte. Etimológicamente, la palabra monolito procede del griego “*monólithos*” que se traduce como “una sola piedra”. La presencia de cavidades de distinto tamaño en estos materiales le confiere propiedades ventajosas para su utilización como fase estacionaria en el ámbito cromatográfico y en técnicas de preparación de muestra. Los materiales monolíticos se caracterizan por presentar una buena permeabilidad al paso del disolvente debido a la presencia de macroporos ( $> 50$  nm). Por otro lado, la existencia de mesoporos (2-50 nm) proporciona una alta área superficial, facilitándose un aumento de la eficacia en la separación cromatográfica o en el proceso extractivo de los analitos de interés. En la **Figura 1.3** se muestra de manera esquematizada las diferencias entre una columna particulada (**Figura 1.3A**) y un lecho monolítico (**Figura 1.3B**).

En comparación con los materiales particulados o empaquetados, los materiales monolíticos ofrecen una serie de ventajas. Además de la alta porosidad y permeabilidad anteriormente mencionadas, se pueden preparar *in-situ* en el molde que se quiera emplear (cartuchos de extracción, jeringas, puntas de pipeta, etc.), no requieren el uso de fritas, y resulta relativamente sencillo modificar su química superficial de manera sencilla. Todo ello, ha derivado en un aumento del empleo de estos materiales en preparación de muestra en los últimos años [18-21].



**Figura 1.3.** Características estructurales, incluyéndose microfotografías SEM, de un lecho particulado (A) y un lecho monolítico (B). Figura obtenida de [17].

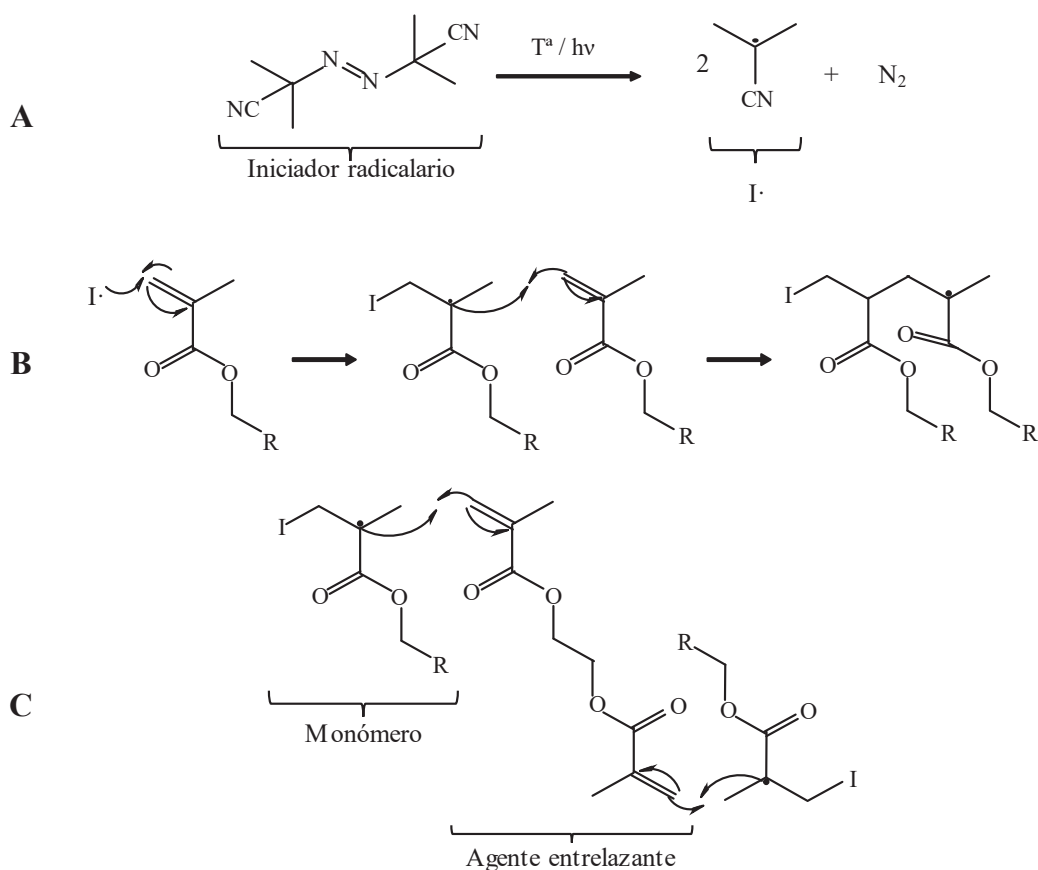
Dependiendo de su naturaleza, los materiales monolíticos se agrupan en tres grandes clases: inorgánicos (de base sílice), polímeros orgánicos (basados en estireno, acrilamida, metacrilato, entre otros) e híbridos de sílice-orgánicos.

La preparación de los monolitos de base sílice se suele llevar a cabo mediante el uso de procesos sol-gel [22]. Dichos monolitos presentan una mayor resistencia al uso de disolventes orgánicos y estabilidad mecánica que sus homólogos poliméricos; sin embargo, su síntesis no resulta tan sencilla y presentan problemas de estabilidad fuera del rango de pHs 2-7. Pese a estas limitaciones, se han descrito varios estudios utilizando este tipo de sorbentes para el aislamiento/preconcentración de compuestos en muestras ambientales y biológicas [23-25]. A modo de ejemplo, Nema y col. [23] construyeron un dispositivo usando este tipo de sorbente para la extracción de fármacos en muestras de orina usando como soporte una jeringa de 2 mL. En otros estudios se han utilizado dispositivos de extracción comerciales (p.ej. minicolumnas de centrifuga (*spin-columns*) MonoSpin<sup>TM</sup> y puntas de pipeta



MonoTip™) para la extracción de drogas y fármacos en matrices biológicas [18].

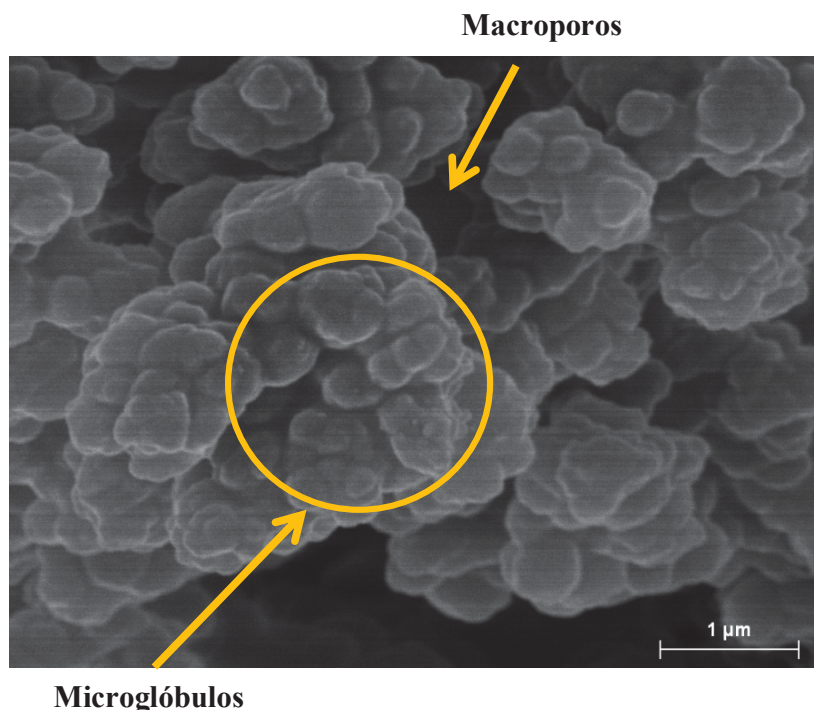
Atendiendo a los monolitos de polímero orgánicos, su preparación se realiza mediante polimerización radicalaria. Para ello, se prepara una mezcla de polimerización constituida por uno o varios monómeros, un agente entrelazante (*crosslinker*), una mezcla porogénica de disolventes y un iniciador radicalario, que se escogerá en función del tipo o modo de polimerización a realizar. La polimerización puede iniciarse térmicamente, mediante radiación UV o reacción química. En la **Figura 1.4**, se muestra de forma esquemática el mecanismo de polimerización de este tipo de materiales.



**Figura 1.4.** Mecanismo de polimerización. (A) Descomposición radicalaria del iniciador; (B) crecimiento de la cadena polimérica; (C) combinación del monómero y el agente entrelazante.

Primero, el iniciador radicalario se descompone para generar radicales libres y estos centros activos reaccionan con los monómeros que los rodean. Durante la etapa de propagación, la longitud de la cadena polimérica se incrementa hasta que no quedan más monómeros libres o hasta que el radical se desactiva al entrar en contacto con el disolvente porogénico. Al mismo tiempo, los monómeros activados reaccionan con el agente entrelazante dando lugar a una red formada por cadenas de monómero unidas entre ellas por agentes entrelazantes. Como resultado del proceso, se obtiene un sistema de dos fases, un lecho monolítico sólido y un líquido porogénico inerte que llena las cavidades que se han formado en la estructura monolítica durante la polimerización.

Los monómeros y agentes entrelazantes más utilizados son aquellos que contienen grupos reactivos fácilmente activables por polimerización radicalaria como pueden ser las acrilamidas, metacrilatos o estirenos [26]. Gracias al control que se puede realizar sobre la composición de la mezcla (elección de distintos disolventes porogénicos, monómeros y sus ratios) y las condiciones de polimerización (tipo de iniciador, temperatura, etc.), se pueden obtener monolitos con propiedades morfológicas “a la carta”, que presenten las propiedades más convenientes para el estudio posterior a realizar. Además, dada la variedad de monómeros disponibles, así como la posterior funcionalización de las superficies de los lechos obtenidos, ello permite adaptar las interacciones específicas necesarias para manipular o alcanzar una retención selectiva de los analitos de interés. La morfología resultante de este tipo de monolitos consiste en un sistema de microglóbulos parcialmente agregados, en forma de “racimos”, observándose también los huecos correspondientes a los macroporos del sorbente, tal y como se muestra en la **Figura 1.5**.



**Figura 1.5.** Micrografía SEM (10.000 x) de la estructura típica de un monolito de polímero orgánico. Adaptado de [27].

Respecto a los monolitos híbridos de sílice-orgánicos, éstos presentan ventajas de ambos grupos [28]. En concreto, dichos materiales ofrecen una mayor área superficial, una menor contracción en la presencia de disolventes orgánicos, y la resistencia mecánica propia de los monolitos de sílice, junto con la sencilla preparación de los monolitos orgánicos. Sin embargo, una parte importante de estos materiales sintetizados se basa en la química sol-gel seguida de procesos de post-funcionalización, siendo deseable alternativas más directas (*one-pot*) en los que se pueda disponer de una amplia gama de monómeros funcionales [29] Este tipo de fases se han usado en la extracción de pequeños solutos orgánicos [30-32] y trazas metálicas [33].

Una vez descrito los distintos tipos de monolitos, a continuación, se hará hincapié en los materiales usados en esta Tesis, en concreto, en los monolitos de ésteres de metacrilato y acrilato y sus posibles modificaciones para su aplicación al ámbito de tratamiento de muestra y separativo (véase **Capítulo 2**).

Estos monolitos se han utilizado como fases estacionarias en técnicas de separación miniaturizadas (véase **Capítulo 2**) así como en el tratamiento de muestra tanto en línea (*on-line*) [20] como fuera de línea (*off-line*) [18,19]. En esta última modalidad, los sorbentes monolíticos se han preparado en diversos formatos tales como en cartucho/jeringa de polipropileno [34], punta de micropipeta [35], o en un formato más miniaturizado como capilares de sílice fundida [36]. Este último procedimiento se conoce como microextracción usando lechos monolíticos (*Polymer Monolith Microextraction*, PMME) donde se utiliza un capilar relleno con el lecho polimérico, el cual se puede conectar a una jeringa, si bien se puede acoplar para su uso *on-line* con técnicas más sofisticadas [20,37]. A modo de ejemplo, Suo y col. [36] prepararon un capilar conteniendo un monolito de GMA y divinilbenceno (*Divinylbenzene*, DVB), el cual fue modificado con etilendiamina. Dicho sorbente se utilizó *on-line* con espectrometría de masas con plasma acoplado inductivamente (*Inductively coupled plasma mass spectrometry*, ICP-MS) para la determinación de trazas de metales en orina y cabello humano, alcanzándose LODs del orden de 20 ng L<sup>-1</sup>.

A pesar de las buenas prestaciones de estos materiales y la versatilidad que presentan, sus áreas superficiales son mucho menores que las de sus equivalentes de sílice debido a la menor cantidad de micro- y mesoporos presentes en su estructura, esto da lugar a menores capacidades de carga e interacciones más débiles con las moléculas de interés. Con el fin de contrarrestar esta limitación, en los últimos años se han descrito varias alternativas que han sido recogidas en diferentes revisiones [21,38,39]. Muchas de estas estrategias tales como la manipulación de las condiciones de polimerización, el hiper-entrecruzamiento (*hypercrosslinking*) y la incorporación de nanomateriales han sido aplicadas ampliamente en el ámbito de las técnicas de separación miniaturizadas, tal y como se comentará con más detalle en el **Capítulo 2**. No obstante, la alternativa de combinar con materiales nanoestructuradas ha sido utilizada con éxito en el área de

preparación de muestra [21]. Esta vía además de poder aliviar el problema de la baja área superficial de los sorbentes monolíticos abre la puerta a la modificación de su selectividad. En concreto, esta Tesis se centra en la incorporación de nanoestructuras de carbono y nanopartículas metálicas (fundamentalmente de oro) a lechos monolíticos. También, en ésta se aborda el uso de ciertos ligandos como los derivados del ácido borónico o el empleo de ILs como modificadores de la selectividad de los monolitos. A continuación, se comenta brevemente tanto el empleo de estas nanoestructuras y estos ligandos sobre los monolitos poliméricos y las prestaciones resultantes.

### *1.3.1.B. Estrategias de modificación de fases monolíticas poliméricas y su aplicación en preparación de muestra*

#### *i) Modificación de monolitos con nanomateriales*

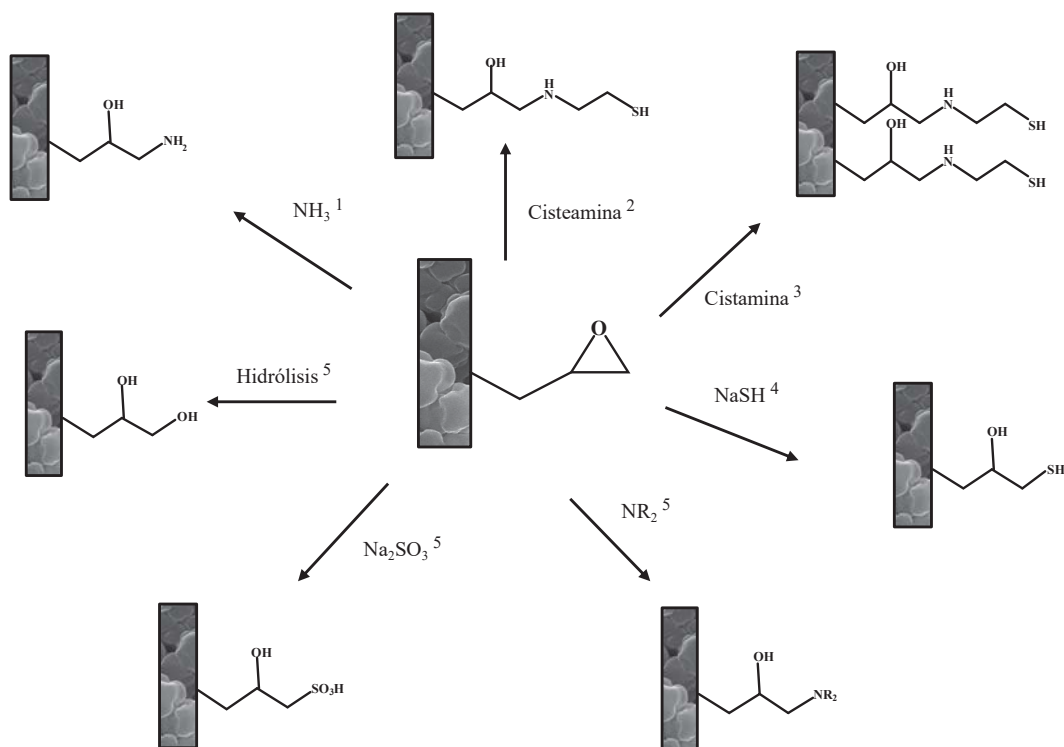
Para llevar a cabo la incorporación de las distintas nanomateriales o NPs, se pueden utilizar dos estrategias o aproximaciones. La primera se basa en la introducción de las NPs en la mezcla de polimerización, seguido de polimerización, obteniéndose un material con las NPs mayoritariamente embebidas. Por su parte, la segunda vía se basa en la post-funcionalización del polímero mediante diferentes reacciones, donde las NPs son ancladas a la superficie del monolito a través de interacciones electrostáticas o enlaces covalentes. Ambas estrategias poseen ventajas e inconvenientes. Así pues, la primera vía es mucho más rápida y sencilla que la segunda; sin embargo, la mayor parte de las NPs quedan en el interior del monolito, lo cual dificulta la interacción con los analitos [21,38,40]. Además, si la cantidad de NPs utilizada es alta, éstas se pueden agregar e incluso sedimentar, alterando la morfología porosa del monolito, lo cual puede ir en detrimento del proceso de extracción/separación [41].

Por su parte, la segunda vía requiere la post-modificación de la superficie del monolito con ligandos adecuados (por ejemplo, compuestos

conteniendo grupos tiol, amino, entre otros) para la posterior inmovilización de las NPs en base a la afinidad de éstas [21,39]. Sin embargo, la preparación de un recubrimiento uniforme de NPs sobre la superficie del monolito no es sencillo, ya que durante el proceso de interacción entre la dispersión de NPs y el monolito se puede producir fenómenos de agregación de éstas o la obstrucción de los poros del polímero.

Para llevar a cabo las reacciones de post-funcionalización de fases estacionarias monolíticas con diversos ligandos, se suele utilizar como monolitos de partida o base, aquellos que contiene GMA como monómero funcional. el cual posee un grupo epóxido reactivo, susceptible de ser modificado químicamente. En la **Figura 1.6** se observan de forma esquematizada distintas reacciones de modificación de monolitos de GMA con diversos ligandos. Los materiales modificados presentarán grupos o sitios afines por los nanomateriales, como por ejemplo, la presencia de grupos amino o tiol para la posterior inmovilización de NPs de Au o de Ag.

A continuación, se comentarán algunos de los materiales híbridos monolito-NM preparados a partir de nanoestructuras metálicas, y su aplicación en el área de tratamiento de muestra.



**Figura 1.6.** Representación esquemática de algunas reacciones de post-funcionalización de monolitos usando GMA como monómero funcional. Las condiciones de reacción de los diferentes ligandos se indican en las siguientes referencias: <sup>1</sup>[43], <sup>2</sup>[44], <sup>3</sup>[45], <sup>4</sup>[46], <sup>5</sup>[41].

En lo que respecta a la incorporación de NPs metálicas a monolitos se han descrito diversos artículos en el área de tratamiento de muestra [43,47,48]. A modo de ejemplo, Alwael y col. [47] desarrollaron en puntas de micropipeta, cuyas paredes fueron previamente modificadas con etilenglicol dimetacrilato (EDMA), la preparación de un monolito de vinil azolactona sobre el cual posteriormente se inmovilizaron AuNPs y lectinas (proteínas) para llevar a cabo una extracción selectiva de glicoproteínas. Recientemente, nuestro grupo de investigación ha desarrollado materiales poliméricos basados en GMA modificados con diversos ligandos (amoníaco, cisteamina, entre otros), y post-funcionalizados con NPs de Au o de Ag. Dichos materiales se han empleado como sorbentes en cartuchos de SPE para llevar a cabo la extracción de lectinas [48] y preconcentración de viscotoxinas procedentes del muérdago

[43]. Los materiales resultantes presentaron una adecuada selectividad y capacidades de carga de hasta 29,3 mg proteína g<sup>-1</sup> de sorbente [43].

En el **Capítulo 3** de esta Tesis, se describe la aplicación de monolitos poliméricos modificados con AuNPs en jeringas para la extracción de glutatión en muestras biológicas.

*ii) Modificación de monolitos con derivados del ácido borónico*

La incorporación de derivados del ácido borónico a materiales monolíticos ha sido estudiada en los últimos años, dada la elevada afinidad de estos ligandos para formar puentes diésteres con grupos *cis*-diol presentes en una variedad de azúcares y otros compuestos (p.ej. glicopéptidos y glicoproteínas), aprovechándose dicha interacción para llevar a cabo la retención de este tipo de biomoléculas [49-52]. Los materiales resultantes presentan la casi-especificidad de los boronatos por los grupos *cis*-diol junto con las ventajas de los materiales monolíticos descritas anteriormente, convirtiéndolos en candidatos ideales para el tratamiento de muestra. Además, dicha interacción boronato-*cis*-diol puede ser fácilmente manipulada mediante la variación del pH [49,53], controlándose de manera sencilla los procesos de adsorción/desorción. Sin embargo, la mayoría de los monolitos poliméricos descritos continúan presentando la limitación del área superficial, lo cual se traduce en una baja capacidad de carga. Para solventar esta limitación, algunos autores han llevado a cabo distintas estrategias para dotar el material de una mayor área superficial empleándose nanomateriales tales como el óxido de grafeno [49,54] o NPs metálicas [55] como paso intermedio previo a la incorporación de los derivados del ácido borónico (sitios activos). En particular, en este último estudio, se ha descrito el uso de AuNPs en combinación con derivados de ácido borónico (ácido 4-mercaptofenilborónico) para la extracción de la peroxidasa del rábano picante y peroxidasas de plasma humano en formato PMME. Sin embargo, la cantidad de boronato enlazado al soporte no se indica en dicho estudio, siendo un parámetro esencial a la hora de desarrollar sistemas de extracción eficaces



de glicopéptidos/glicoproteínas. Asimismo, es de señalar que hasta la fecha, la utilización de dispositivos miniaturizados de tratamiento de muestra se ha circunscrito al formato capilar, siendo deseable su extensión a formatos de mayor capacidad (puntas de micropipeta, cartuchos, etc).

En el **Capítulo 4** de esta Tesis, se describe el desarrollo de monolitos poliméricos modificados con AuNPs en jeringas, seguido de su funcionalización con politiol y un derivado vinil fenil borónico para la extracción de glicopéptidos en digestos de proteína estándar y la preconcentración de estas especies en muestras de suero.

### *iii) Modificación de monolitos con ILs*

En las últimas décadas, la introducción de los ILs en el área de Química Analítica ha jugado un papel relevante tanto en el ámbito de técnicas extractivas (extracción líquido-líquido, microextracción en fase líquida y microextracción en fase sólida (*Solid-Phase Microextraction*, SPME), entre otras) [56-66] como las de separación [63-66]. Los ILs son sales compuestas por un catión orgánico voluminoso y un anión de menor tamaño, que generalmente suelen estar fundidas por debajo de los 100°C. Entre los cationes más utilizados destacan los alquil-imidazolio, piridinio, amonio o fosfonio. Por otra parte, existe una gran variedad de aniones orgánicos, como acetato, trifluoroacetato y trifluorometilsulfato, e inorgánicos, como bromuro, cloruro, nitrato, perclorato, entre otros, asociados a estos cationes [57,58]. Así pues, los ILs muestran características interesantes como su baja volatilidad e inflamabilidad, su baja toxicidad, una alta estabilidad térmica y una miscibilidad con agua y disolventes orgánicos susceptible de manipulación [67]. Estas propiedades han permitido su uso como una “alternativa verde” a los disolventes orgánicos convencionales [68]. Además, las estructuras versátiles de los ILs con diferentes grupos funcionales han propiciado la posibilidad de generar diversas interacciones con los analitos de interés tales como hidrofóbicas/hidrofílicas, enlaces  $\pi$ - $\pi$ , puentes de hidrógeno,

intercambio iónico, etc [57,63]. Ello ha permitido la preparación de fases estacionarias en diferentes materiales (sílice y soportes poliméricos) destinados a técnicas de tratamiento de muestra y cromatográficas con objeto de mejorar la capacidad de extracción/eficacia de la separación, así como la manipulación de la selectividad. Sin embargo, la incorporación de ILs a monolitos poliméricos ha sido poco estudiada, tal y como recoge Chen y col. [69], y en particular, su aplicación al ámbito preparativo ha sido limitada [70-72]. Además, el formato preferentemente utilizado ha sido capilar o fibras para SPME, siendo deseable su extensión a otros formatos miniaturizados.

Al igual como se ha descrito anteriormente con la incorporación de nanomateriales a monolitos poliméricos, la introducción de ILs a éstos se puede llevar a cabo mediante dos enfoques: i) adición del IL a la mezcla de polimerización, o ii) post-funcionalización del monolito con el IL. La aproximación más común por su sencillez ha sido la primera, empleándose habitualmente un IL que contiene grupos vinilo o alilo en su estructura [73-75]. A modo de ejemplo, Feng y col. [72] desarrollaron un monolito polimérico copolimerizado con 1-(3-aminopropil)-3-(4-vinilbencil)imidazolio 4-estirenosulfonato para su uso como sorbente en SPME para la extracción de disruptores endocrinos en muestras de leche, obteniéndose recuperaciones satisfactorias (85,5-112%) y LODs comprendidos entre 1-2  $\mu\text{g L}^{-1}$ . Por su parte, el segundo enfoque basado en la post-funcionalización de la matriz monolítica con ILs [76-78] resulta más tedioso, si bien el material resultante presenta una mayor accesibilidad de los grupos funcionales del IL para su interacción con los analitos.

En el **Capítulo 5** de esta Tesis, se describe la preparación de materiales monolíticos modificados con ILs, donde se han explorado dos vías de incorporación de ILs: su generación in situ y la copolimerización. Los sorbentes resultantes se prepararon en columnas de minicentrífuga (*spin columns*) y se han aplicado a la extracción de  $\beta$ -bloqueantes en muestras de orina.

### *1.3.2. Redes metal-orgánicas (MOFs)*

Las redes metal-orgánicas, son una familia de estructuras porosas cristalinas, formadas por la unión de centros metálicos (habitualmente de transición) mediante enlaces de coordinación a una serie de ligandos orgánicos con alta densidad electrónica que pueden actuar como bases de Lewis [79]. El resultado son materiales con alta porosidad y elevada área superficial (pueden alcanzar hasta los 10.000 m<sup>2</sup>/g) con una satisfactoria estabilidad térmica y mecánica [80].

La estructura de los MOFs está enormemente influenciada por las propiedades de sus unidades básicas de construcción, esto es, por los centros metálicos que los forman y los ligandos orgánicos, cuya naturaleza puede ser muy variada. Debido a estas posibles variaciones en su composición, actualmente se han descrito más de 20.000 estructuras diferentes de MOFs [81,82]. Además de esta variabilidad, se puede controlar el tamaño de sus poros y cavidades, mediante la modificación de algunos factores tales como la relación metal/ligando, los disolventes, el pH o la introducción de algún aditivo durante su síntesis [83,84]. Asimismo, se pueden funcionalizar mediante un procedimiento post-síntesis [80], lo cual se traduce en una gran diversidad estructural y funcional.

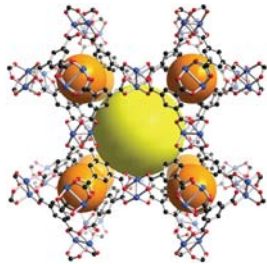
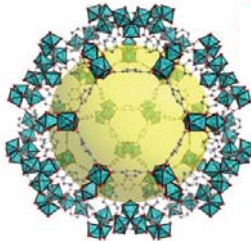

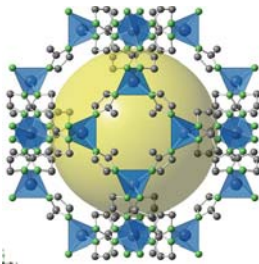
Debido a la gran variedad de centros metálicos combinados con los innumerables ligandos orgánicos posibles, no hay un método universal para la síntesis de todos ellos, si bien el método de síntesis más utilizado para MOFs es la reacción solvotermal o hidrotermal (si el disolvente utilizado es agua). En este método de síntesis, se mezclan dos disoluciones, una del ligando orgánico y otra de la sal del metal en un disolvente, o en una mezcla de ellos, y se coloca en un sistema cerrado, normalmente en un autoclave de teflón, y se sitúa en una estufa a temperaturas entre 80-260°C [85]. En esta modalidad de síntesis cabe tener en cuenta una serie de aspectos tales como: la naturaleza y concentración de la sal metálica y del ligando orgánico, la naturaleza del disolvente, el pH del medio, el uso de moduladores, la temperatura, la presión

y el tiempo de reacción, factores que pueden condicionar la morfología y cristalinidad del producto final. Sin embargo, la síntesis solvotermal presenta ciertos inconvenientes que cabe considerar, como son el alto tiempo de reacción (desde horas hasta semanas), el uso de altas cantidades de disolvente y la dificultad de llevar a cabo síntesis a gran escala. Estos inconvenientes han propiciado el desarrollo de síntesis alternativas, entre las cuales se encuentran la síntesis mediante aplicación de microondas [86,87], por ultrasonidos [88], la síntesis electroquímica [87] o mecanoquímica [87].

Gracias a las características anteriormente mencionadas, los MOFs son materiales muy versátiles con destacadas aplicaciones en áreas científicas muy diversas, tales como catálisis [89], adsorción de gases [90], almacenamiento y liberación de fármacos [91], entre otras.

También, gracias a sus propiedades, este tipo de materiales se han empleado en los últimos años en el ámbito de la Química Analítica como sorbentes para llevar a cabo la extracción y/o purificación de compuestos orgánicos e inorgánicos [81,92,93].

Existen varias clases de MOFs habitualmente empleados en las técnicas de tratamiento de muestra. Entre éstos se encuentran: los MOFs tipo MIL (desarrollados originalmente por *Matériaux de l'Institut Lavoisier*), los de la familia UiO (sintetizados por *University of Oslo*), las estructuras o redes zeolíticas de imidazol y MOFs isoreticulares (IRMOF). En la **Figura 1.7** se representan algunos ejemplos de los tipos de MOFs anteriormente mencionados, incluyéndose sus componentes y estructura.

MOF	Metal	Ligando	Estructura
HKUST-1	Cu (II)	Ácido benceno-1,3,5- tricarboxílico	
MIL-101	Cr (III)	Ácido benceno-1,4- dicarboxílico	
UiO-66	Zr (IV)	Ácido benceno-1,4- dicarboxílico	
ZIF-8	Zn (II)	2-metilimidazol	

**Figura 1.7.** Representación esquemática de algunos MOFs (incluyendo centro metálico y ligando) habitualmente utilizados como sorbentes en técnicas de extracción.

Si bien los MOFs de las diferentes familias pueden presentar diferencias en sus propiedades, la porosidad y el tamaño de poro presente en éstos puede facilitar o dificultar, sin duda, que los analitos difundan o no hacia el sorbente, contribuyendo a una mayor selectividad del mismo por los solutos. Así pues, el tamaño y forma de las moléculas de interés (*guest molecules*) junto con el

tamaño de poro del MOF representan aspectos esenciales a la hora de controlar o manipular la eficacia de extracción del material [94]. Además de estas variables, la selectividad de este tipo de materiales está fuertemente influenciada por la naturaleza de las interacciones entre analito-sorbente, entre las que se encuentran interacciones hidrofóbicas,  $\pi$ - $\pi$ , por puente de hidrógeno, electrostáticas, entre otras, las cuales se suelen producir mayoritariamente con los ligandos seleccionados en la preparación del MOF [95]. No obstante, el diseño y modificación del MOF a nivel molecular mediante funcionalización de su superficie a través de una selección cuidadosa de ligandos incluyendo grupos amino, tiol, hidroxilo, entre otros, puede permitir un control preciso para obtener materiales adsorbentes que proporcionen sitios de adsorción adicionales y así mejorar la selectividad del MOF [96]. Además, esta funcionalización puede mejorar la estabilidad química en agua, su dispersibilidad y la reutilización de este tipo de sorbentes [93,97].

Así pues, la introducción de funcionalidades tipo amino o tiol puede realizarse mediante un proceso de post-modificación del MOF, si bien es más directo la introducción de funcionalidades (en forma de ligandos) durante el proceso de síntesis del MOF [93]. Una vía alternativa a estas estrategias es la incorporación de moduladores (mediante adición de ácidos o bases) en el proceso de síntesis del MOF [98,99] que generen materiales con la funcionalidad deseada. Sin embargo, esta estrategia usando bases como moduladores (p.ej. aminas) para preparar MOFs con finalidades extractivas ha sido muy poco explorada en la literatura [100].

En el **Capítulo 6** de esta Tesis, se describe la preparación de un MOF (ZIF-8) modulado con butilamina durante su proceso de síntesis para llevar a cabo la extracción de contaminantes orgánicos (benzomercaptanos) en diversas muestras ambientales.

## 1.4. Referencias

- [1] M.C. Hennion, Solid-phase extraction: method development, sorbents, and coupling with liquid chromatography. *J. Chromatogr. A* 856(1–2)(1999) 3–54. doi: 10.1016/S0021-9673(99)00832-8
- [2] B. Buszewski, M. Szultka, Past, present, and future of solid phase extraction: a review, *Crit. Rev. Anal. Chem.* 42 (2012) 198–213. doi: 10.1080/07373937.2011.645413
- [3] 12 principles of green chemistry, disponible en: <https://www.acs.org/content/acs/en/greenchemistry/principles/12-principles-of-green-chemistry.html> (Fecha de acceso: 05/04/2020)
- [4] R.E. Subden, R.G. Brown, A.C. Noble, Determination of histamines in wines and musts by reversed-phase high-performance liquid chromatography, *J. Chromatogr. A* 166(1) (1978) 310–312. doi: 10.1016/s0021-9673(00)92280-5
- [5] Z. Lin, F. Yang, X. He, X. Zhao, Y. Zhang, Preparation and evaluation of a macroporous molecularly imprinted hybrid silica monolithic column for recognition of proteins by high performance liquid chromatography, *J. Chromatogr. A* 1216 (2009) 8612–8622. doi: 10.1016/j.chroma.2009.10.025
- [6] N.J.K. Simpson, *Solid-Phase Extraction. Principles, Techniques and Applications*, Marcel Dekker, Inc., New York, 2000.
- [7] Z. Wu, D. Zhao, Ordered mesoporous materials as adsorbents, *Chem. Comm.* 47 (2011) 3332–3338. doi: 10.1039/c0cc04909c
- [8] D. Chen, L. Wang, Y. Ma, W. Yang, Super-adsorbent material based on functional polymer particles with a multilevel porous structure, *NPG Asia Mat.* 8 (2016) e301. doi: 10.1038/am.2016.117
- [9] I. Ten-Doménech, H. Martínez-Pérez-Cejuela, E.F. Simó-Alfonso, S. Torres-Cartas, S. Messeguer-Lloret, J.M. Herrero-Martínez, *Talanta* 180 (2018) 162–167. doi: 10.1016/j.talanta.2017.12.042

- [10] T.C. Wang, W. Bury, D. A. Gómez-Gualdrón, N.A. Vermeulen, J.E. Mondolch, P. Deria, K. Zhang, P.Z. Moghadam, A.A. Sarjeant, R.Q. Snurr, J.F. Stoddart, J.T. Hupp, O.K. Farha, Ultrahigh surface area zirconium MOFs and insights into the applicability of the BET theory, *J. Am. Chem. Soc.* 137 (2015) 3585–3591. doi: 10.1021/ja512973b
- [11] H. Braus, F. M. Middleton, G. Walton, Organic chemical compounds in raw and filtered surface waters, *Anal. Chem.* 23(8) (1951) 1160–1164. doi: 10.1021/ac60056a031
- [12] Lane C. Sander, Silica-based solid phase extraction, en: M.J. Telepchak, T.F. August, G. Chaney (Eds.), *Forensic Clin. Appl. Solid Phase Extr.*, Humana Press Inc., Totowa, New Jersey, 2004: págs. 41–53.
- [13] T. Nema, The application of silica monolith for solid phase extraction, National University of Singapore, 2011.
- [14] J. Nawrocki, The silanol group and its role in liquid chromatography, *J. Chromatogr. A* 779 (1997) 29–71. doi: 10.1016/S0021-9673(97)00479-2
- [15] N. Fontanals, R.M. Marcé, F. Borrull, New materials in sorptive extraction techniques for polar compounds, *J. Chromatogr. A* 1152 (2007) 14–31. doi: 10.1016/j.chroma.2006.11.077
- [16] T.J. Mays, A new classification of pore sizes, *Stud. Surf. Sci. Catal.* 160 (2007) 57–62. doi: 10.1016/S0167-2991(07)80009-7
- [17] H. Oberacher, C.G. Huber, Capillary monoliths for the analysis of nucleic acids by high-performance liquid chromatography-electrospray ionization mass spectrometry, *Trends Anal. Chem.* 21 (2002) 166–174. doi: 10.1016/S0165-9936(02)00304-7
- [18] A. Namera, T. Saito, Advances in monolithic materials for sample preparation in drug and pharmaceutical analysis, *Trends Anal. Chem.* 45 (2013) 182–196. doi: 10.1016/j.trac.2012.10.017



- [19] T. Nema, E.C.Y. Chan, P.C. Ho, Applications of monolithic materials for sample preparation, *J. Pharm. Biomed. Anal.* 87 (2014) 130–141. doi: 10.1016/j.jpba.2013.05.036
- [20] J.C. Masini, F. Svec, Porous monoliths for on-line sample preparation: a review, *Anal. Chim. Acta* 964 (2017) 24–44. doi: 10.1016/j.aca.2017.02.002
- [21] B. Fresco-Cala, S. Cárdenas, Potential of nanoparticle-based hybrid monoliths as sorbents in microextraction techniques, *Anal. Chim. Acta.* 1031 (2018) 15–27. doi: 10.1016/j.aca.2018.05.069
- [22] K. Nakanishi, H. Minakuchi, N. Soga, N. Tanaka, Double pore silica gel monolith applied to liquid chromatography, *J. Sol-Gel Sci. Technol.* 8 (1997) 547–552. doi: 10.1023/a:1018331101606
- [23] T. Nema, E.C.Y. Chan, P.C. Ho, Application of silica-based monolith as solid phase extraction cartridge for extracting polar compounds from urine, *Talanta* 82(2) (2010) 488–494. doi: doi.org/10.1016/j.talanta.2010.04.063
- [24] X. Ma, M. Zhao, F. Zhao, H. Guo, J. Crittenden, Y. Zhu, Y. Chen, Application of silica-based monolith as solidphase extraction sorbent for extracting toxaphene congeners in soil, *J. Sol-Gel Sci. Technol.* 80(1) (2016). 87–95. doi: 10.1007/s10971-016-4054-8
- [25] A. Namera, T. Saito, S. Ota, S. Miyazaki, H. Oikawa, K. Murata, M. Nagao, Optimization and application of octadecyl-modified monolithic silica for solid-phase extraction of drugs in whole blood samples, *J. Chromatogr. A* 1517 (2017) 9–17. doi: 10.1016/j.chroma.2017.08.012
- [26] F. Svec, Porous polymer monoliths: amazingly wide variety of techniques enabling their preparation. *J. Chromatogr. A* 1217(6) (2010) 902–924. doi: 10.1016/j.chroma.2009.09.073
- [27] H. Martínez-Pérez-Cejuela, E.J. Carrasco-Correa, A. Shahat, E.F. Simó-Alfonso, J.M. Herrero-Martínez, Incorporation of metal-organic

framework amino-modified MIL-101 into glycidyl methacrylate monoliths for nano LC separation, *J. Sep. Sci.* 42 (2019) 834–842. doi: 10.1002/jssc.201801135

[28] Z. Zajickova, Advances in the development and applications of organic-silica hybrid monoliths, *J. Sep. Sci.* 40 (2017) 25–48. doi:10.1002/jssc.201600774

[29] J. Ou, Z. Liu, H. Wang, H. Lin, J. Dong, H. Zou, Recent development of hybrid organic-silica monolithic columns in CEC and capillary LC, *Electrophoresis* 36 (2014) 62–75. doi: 10.1002/elps.201400316

[30] T. Wang, Y. Chen, J. Ma, M. Chen, C. Nie, M. Hu, Y. li, Z. Jia, J. Fang, H. Gao, Ampholine-functionalized hybrid organic– inorganic silica material as sorbent for solid-phase extraction of acidic and basic compounds, *J. Chromatogr. A* 1308 (2013) 63–72. doi: 10.1016/j.chroma.2013.08.025

[31] X. Xiong, Z. Yang, Y. Huang, L. Jiang, Y. Chen, Y. Shen, B. Chen, Organic-inorganic hybrid fluoros monolithic capillary column for selective solid-phase microextraction of perfluorinated persistent organic pollutants, *J. Sep. Sci.* 36 (2013) 923–931. doi: 10.1002/jssc.201200913

[32] T. Wang, Y. Zhu, J. Ma, R. Xuan, H. Gao, Z. Liang, L. Zhang, Y. Zhang, Hydrophilic solid-phase extraction of melamine with ampholine-modified hybrid organic–inorganic silica material, *J. Sep. Sci.* 38(1) (2015) 87–92. doi: 10.1002/jssc.201400900

[33] L. Zhang, B. Chen, H. Peng, M. He, B. Hu, Aminopropyltriethoxysilane-silica hybrid monolithic capillary microextraction combined with inductively coupled plasma mass spectrometry for the determination of trace elements in biological samples, *J. Sep. Sci.* 34 (2011) 2247–2254. doi: 10.1002/jssc.201100173

[34] H. Wang, H. Zhang, Y. Lv, F. Svec, T. Tan, Polymer monoliths with chelating functionalities for solid phase extraction of metal ions from

water, J. Chromatogr. A 1343 (2014) 128–134. doi: 10.1016/j.chroma.2014.03.072

[35] C. Skoglund, F. Bassyouni, M. Abdel-Rehim, Monolithic packed 96-tips set for high-throughput sample preparation: determination of cyclophosphamide and busulfan in whole blood samples by monolithic packed 96-tips and LC-MS, Biomed. Chromatogr. 27(6) (2013) 714–719. doi: 10.1002/bmc.2849

[36] F. Suo, B. Chen, M. Hea, B. Hu, Monolithic capillary microextraction on-line combined with ICP-MS for determining Ni, Cu and Cd in biological samples, Anal. Methods 8 (2016) 4680–4688. doi: 10.1039/c6ay01008c

[37] F. Wei, Y.Q. Feng, Methods of sample preparation for determination of veterinary residues in food matrices by porous monolith microextraction-based techniques, Anal. Methods 3 (2011) 1246–1256. doi: 10.1039/c1ay05079f

[38] F. Svec, Y. Lv, Advances and recent trends in the field of monolithic columns for chromatography, Anal. Chem. 87 (2015) 250–273. doi: 10.1021/ac504059c

[39] J. Urban, Current trends in the development of porous polymer monoliths for the separation of small molecules, J. Sep. Sci. 39 (2015) 51–68. doi: 10.1002/jssc.201501011

[40] M. Navarro-Pascual-Ahuir, M.J. Lerma-García, G. Ramis-Ramos, E.F. Simó-Alfonso, J.M. Herrero-Martínez, Preparation and evaluation of lauryl methacrylate monoliths with embedded silver nanoparticles for capillary electrochromatography, Electrophoresis 34 (2013) 925–934. doi:10.1002/elps.201200408

[41] M.R. Buchmeiser, Polymeric monolithic materials: Syntheses, properties, functionalization and applications, Polymer 48 (2007) 2187–2198. doi: 10.1016/j.polymer.2007.02.045

- [42] M.R. Gama, F.R.P. Rocha, C.B.G. Bottoli, Monoliths: Synthetic routes, functionalization and innovative analytical applications, *Trends Anal. Chem.* 115 (2019) 39–51. doi: 10.1016/j.trac.2019.03.020
- [43] M. Vergara-Barberán, M.J. Lerma-García, E.F. Simó-Alfonso, J.M. Herrero-Martínez, Polymeric sorbents modified with gold and silver nanoparticles for solid-phase extraction of proteins followed by MALDI-TOF analysis, *Microchim. Acta* 184 (2017) 1683–1690. doi:10.1007/s00604-017-2168-5
- [44] Q. Cao, Y. Xu, F. Liu, F. Svec, J.M.J. Fréchet, Polymer monoliths with exchangeable chemistries: Use of gold nanoparticles as intermediate ligands for capillary columns with varying surface functionalities, *Anal. Chem.* 82 (2010) 7416–7421. doi: 10.1021/ac1015613
- [45] Y. Lv, F.M. Alejandro, J.M.J. Fréchet, F. Švec, Preparation of porous polymer monoliths featuring enhanced surface coverage with gold nanoparticles, *J. Chromatogr. A* 1261 (2012) 121–128. doi:10.1016/j.chroma.2012.04.007
- [46] B. Preinerstorfer, W. Bicker, W. Lindner, M. Lämmerhofer, Development of reactive thiol-modified monolithic capillaries and in-column surface functionalization by radical addition of a chromatographic ligand for capillary electrochromatography, *J Chromatogr A* 1044 (2004) 187–199. doi: 10.1016/j.chroma.2004.04.078
- [47] H. Alwael, D. Connolly, P. Clarke, R. Thompson, B. Twanley, B. O'Connor, B. Paul, Pipette-tip selective extraction of glycoproteins with lectin modified gold nano-particles on a polymer monolithic phase, *Analyst* 136 (2011) 2619–2629. doi: 10.1039/c1an15137a
- [48] M. Vergara-Barberán, M.J. Lerma-García, E.F. Simó-Alfonso, J.M. Herrero-Martínez, Solid-phase extraction based on ground methacrylate monolith modified with gold nanoparticles for isolation of proteins, *Anal. Chim. Acta* 917 (2016) 37–43. doi:10.1016/j.aca.2016.02.043

- [49] R. Wang, Z. Chen, Boronate affinity monolithic column incorporated with graphene oxide for the in-tube solid-phase microextraction of glycoproteins, *J. Sep. Sci.* 41(2018) 2767–2773. doi: 10.1002/jssc.201701417
- [50] Y. Liang, C. Wu, Q. Zhao, Q. Wu, B. Jiang, Y. Weng, Y. Zhang, Gold nanoparticles immobilized hydrophilic monoliths with variable functional modification for highly selective enrichment and on-line deglycosylation of glycopeptides, *Anal. Chim. Acta* 900 (2015) 83–89. doi: 10.1016/j.aca.2015.10.024
- [51] E. Alzahrani, Preparation of the polymeric-based microchip for protein extraction, *Int. J. Adv. Sci. Technical Res.* 1 (2015) 219–229.
- [52] Y.F. Shen, F.F. Yuan, X.Y. Liu, Y.P. Huang, Z.S. Liu, Synergistic effect of organic-inorganic hybrid monomer and polyhedral oligomeric silsesquioxanes in a boronate affinity monolithic capillary/chip for enrichment of glycoproteins, *Microchim. Acta* 186 (2019) 812. doi: 10.1007/s00604-019-3938-z
- [53] X.J. Zhou, C.E. Mo, M. Chen, Y.P. Huang, Z.S. Liu, Improving affinity of boronate capillary monolithic column for microextraction of glycoproteins with hydrophilic macromonomer, *J. Chromatogr. A* 1581 (2018) 8–15. doi: 10.1016/j.chroma.2018.11.005
- [54] C. Zhou, X. Chen, Z. Du, G. Li, X. Xiao, Z. Cai, A hybrid monolithic column based on boronate-functionalized graphene oxide nanosheets for online specific enrichment of glycoproteins, *J. Chromatogr. A* 1498 (2017) 90–98. doi: 10.1016/j.chroma.2017.01.049
- [55] C. Wu, Y. Liang, Q. Zhao, Y. Qu, S. Zhang, Q. Wu, Y. Zhang, Boronate affinity monolith with a gold nanoparticle-modified hydrophilic polymer as a matrix for the highly specific capture of glycoproteins, *Chem. Eur. J.* 20 (2014) 8737–8743. doi: 10.1002/chem.201402787

- [56] T.D. Ho, A.J. Canestraro, J.L. Anderson, Ionic liquids in solid-phase microextraction: a review, *Anal. Chim. Acta* 695 (2011) 18–43. doi: 10.1016/j.aca.2011.03.034
- [57] L. Vidal, M.L. Riekkola, A. Canals, Ionic liquid-modified materials for solid-phase extraction and separation: a review, *Anal. Chim. Acta* 715 (2012) 19–41. doi: 10.1016/j.aca.2011.11.050
- [58] N. Fontanals, F. Borrull, R.M. Marcé, Ionic liquids in solid-phase extraction, *Trends Anal. Chem.* 41 (2012) 15–26. doi: 10.1016/j.trac.2012.08.010
- [59] N. Miękus, I. Olędzka, N. Kossakowska, A. Plenis, P. Kowalski, A. Prahł, T. Bączek, Ionic liquids as signal amplifiers for the simultaneous extraction of several neurotransmitters determined by micellar electrokinetic chromatography, *Talanta* 186 (2018) 119–123. doi: 10.1016/j.talanta.2018.04.041
- [60] I. Rykowska, J. Ziemlińska, I. Nowak, Modern approaches in dispersive liquid-liquid microextraction (DLLME) based on ionic liquids: A review, *J. Mol. Liq.* 259 (2018) 319–339. doi: 10.1016/j.molliq.2018.03.043
- [61] M.J. Trujillo-Rodríguez, H. Nan, M. Varona, M.N. Emaus, I.D. Souza, J.L. Anderson, Advances of ionic liquids in analytical chemistry, *Anal. Chem.* 91 (2019) 505–531. doi: 10.1021/acs.analchem.8b04710
- [62] N. Kossakowska, I. Olędzka, A. Kowalik, N. Miękus, P. Kowalski, A. Plenis, E. Bień, A. Kaczorowska, M.A. Krawczyk, E. Adamkiewicz-Drożyńska, T. Bączek, Application of SPME supported by ionic liquids for the determination of biogenic amines by MEKC in clinical practice, *J. Pharm. Biomed. Anal.* 173 (2019) 24–30. doi: 10.1016/j.jpba.2019.05.021
- [63] C.F. Poole, S.K. Poole, Ionic liquid stationary phases for gas chromatography, *J. Sep. Sci.* 34 (2011) 888–900. doi: 10.1002/jssc.201000724

- [64] Y. Huang, S. Yao, H. Song, Application of ionic liquids in liquid chromatography and electrodriven separation, *J. Chromatogr. Sci.* 51 (2013) 739–752. doi: 10.1093/chromsci/bmt076
- [65] M.C. García-Alvarez-Coque, M.J. Ruiz-Angel, A. Berthod, S. Carda-Broch, On the use of ionic liquids as mobile phase additives in high-performance liquid chromatography. A review, *Anal. Chim. Acta* 883 (2015) 1–21. doi: 10.1016/j.aca.2015.03.042
- [66] A. Berthod, M.J. Ruiz-Angel, S. Carda-Broch, Recent advances on ionic liquid uses in separation techniques, *J. Chromatogr. A* 1559 (2018) 2–16. doi: 10.1016/j.chroma.2017.09.044
- [67] S.K. Singh, A.W. Savoy, Ionic liquids synthesis and applications: an overview, *J. Mol. Liq.* 297 (2020) 112038. doi: 10.1016/j.molliq.2019.112038
- [68] H. Passos, M.G. Freire, J.A.P. Coutinho, Ionic liquid solutions as extractive solvents for value-added compounds from biomass, *Green Chem.* 16 (2014) 4786–4815. doi: 10.1039/c4gc00236a
- [69] R. Chen, H. Zhou, M. Liu, H. Yan, X. Qiao, Ionic liquids-based monolithic columns: recent advancements and their applications for high-efficiency separation and enrichment, *Trends Anal. Chem.* 111 (2019) 1–12. doi: 10.1016/j.trac.2018.11.026
- [70] M. Tian, H. Yan, K.H. Row, Solid-phase extraction of caffeine and theophylline from green tea by a new ionic liquid-modified functional polymer sorbent, *Anal. Lett.* 43 (2009) 110–118. doi: 10.1080/00032710903276554
- [71] T.T. Wang, Y.H. Chen, J.F. Ma, M.J. Hu, Y. Li, J.H. Fang, H.Q. Gao, A novel ionic liquid-modified organic-polymer monolith as the sorbent for in-tube solid-phase microextraction of acidic food additives, *Anal. Bioanal. Chem.* 406 (2014) 4955–4963. doi: 10.1007/s00216-014-7923-4

- [72] J. Feng, M. Sun, Y. Bu, C. Luo, Development of a functionalized polymeric ionic liquid monolith for solid-phase microextraction of polar endocrine disrupting chemicals in aqueous samples coupled to high-performance liquid chromatography, *Anal. Bioanal. Chem.* 407 (2015) 7025–7035. doi: 10.1007/s00216-015-8888-7
- [73] T. Wang, Y. Chen, J. Ma, X. Zhang, L. Zhang, Y. Zhang, Ionic liquid-based zwitterionic organic polymer monolithic column for capillary hydrophilic interaction chromatography, *Analyst* 140 (2015) 5585–5592. doi: 10.1039/c5an00662g
- [74] J. Wang, L. Bai, Z. Wei, J. Qin, Y. Ma, H. Liu, Incorporation of ionic liquid into porous polymer monoliths to enhance the separation of small molecules in reversed-phase high-performance liquid chromatography, *J. Sep. Sci.* 38 (2015) 2101–2108. doi: 10.1002/jssc.201500061
- [75] P. Zhang, H. Yang, T. Chen, Y. Qin, F. Ye, Facile one-pot preparation of a novel imidazolium-based monolith by thiol-ene click chemistry for capillary liquid chromatography, *Electrophoresis* 38 (2017) 3013–3019. doi: 10.1002/elps.201600288
- [76] H. Han, Q. Wang, X. Liu, S. Jiang, Polymeric ionic liquid modified organic-silica hybrid monolithic column for capillary electrochromatography, *J. Chromatogr. A* 1246 (2012) 9–14. doi: 10.1016/j.chroma.2011.12.029
- [77] H. Huang, Z. Lin, Y. Lin, X. Sun, Y. Xie, L. Zhang, G. Chen, Preparation and evaluation of poly(4-vinylphenylboronic acid-co-pentaerythritol triacrylate) monolithic column for capillary liquid chromatography of small molecules and proteins, *J. Chromatogr. A* 1251 (2012) 82–90. doi: 10.1016/j.chroma.2012.06.032
- [78] C. Liu, Q. Deng, G. Fang, M. Dang, S. Wang, Capillary electrochromatography immunoassay for alpha-fetoprotein based on poly(guanidinium ionic liquid) monolithic material, *Anal. Biochem.* 530 (2017) 50–56. doi: 10.1016/j.ab.2017.04.014



- [79] Y. Yang, K. Shen, J.Z. Lin, Y. Zhou, Q.Y. Liu, C. Hang, H.N. Abdelhamid, Z.Q. Zhang, H. Chen, A Zn-MOF constructed from electron-rich  $\pi$ -conjugated ligands with an interpenetrated graphene-like net as an efficient nitroaromatic sensor, *RSC Adv.* 6 (2016) 45475–45481. doi: 10.1039/C6RA00524A
- [80] S.M. Cohen, Postsynthetic methods for the functionalization of metal-organic frameworks, *Chem. Rev.* 112 (2012) 970–1000. doi:10.1021/cr200179u
- [81] P. Rocío-Bautista, I. Pacheco-Fernández, J. Pasán, V. Pino, Are metal-organic frameworks able to provide a new generation of solid-phase microextraction coatings? – A review, *Anal. Chim. Acta* 939 (2016) 26–41. doi:10.1016/j.aca.2016.07.047
- [82] F. Maya, C. Palomino Cabello, R.M. Frizzarin, J.M. Estela, G. Turnes Palomino, V. Cerdà, Magnetic solid-phase extraction using metal-organic frameworks (MOFs) and their derived carbons, *Trends Anal. Chem.* 90 (2017) 142–152. doi:10.1016/j.trac.2017.03.004
- [83] H.Y. Cho, J. Kim, S.N. Kim, W.S. Ahn, High yield 1-L scale synthesis of ZIF-8 via a sonochemical route, *Microporous Mesoporous Mater.* 169 (2012) 180–184. doi: 10.1016/j.micromeso.2012.11.012
- [84] N. Stock, S. Biswas, Synthesis of metal-organic frameworks (MOFs): routes to various MOF topologies, morphologies, and composites. *Chem. Rev.* 112 (2012) 933–969. doi: 10.1021/cr200304e
- [85] G.I. Dzhardimalieva, R.K. Baimuratova, E.I. Knerelman, G.I. Davydova, S.E. Kudaibergenov, O.V. Kharissova, V. A. Zhinzhilo, I.E. Uflyand, Synthesis of copper(II) trimesinate coordination polymer and its use as a sorbent for organic dyes and a precursor for nanostructured material, *Polymers* 12 (2020) 1024. doi: 10.3390/polym12051024
- [86] I. Thomas-Hillman, A. Laybourn, C. Dodds, S.W. Kingman, Realising the environmental benefits of metal–organic frameworks: recent

advances in microwave synthesis, *J. Mater. Chem. A* 6 (2018). doi: 10.1039/c8ta02919a

[87] D. Sud, G. Kaur, A comprehensive review on synthetic approaches for metal-organic frameworks: From traditional solvothermal to greener protocols, *Polyhedron* 193 (2021) 114897. doi: 10.1016/j.poly.2020.114897

[88] C. Vaitsis, G. Sourkouni, C. Argirusis, Metal Organic Frameworks (MOFs) and ultrasound: A review, *Ultrason. Sonochem.* 52 (2019) 106–199. doi: 10.1016/j.ultsonch.2018.11.004

[89] Q. Wang, D. Astruc, State of the art and prospects in metal–organic framework (mof)-based and mof-derived nanocatalysis, *Chem. Rev.* 120 (2020) 1438–1511. doi: 10.1021/acs.chemrev.9b00223

[90] A. Uzun, S. Keskin, Site characteristics in metal organic frameworks for gas adsorption, *Prog. Surf. Sci.* 89 (2014) 56–79. doi: 10.1016/j.progsurf.2013.11.001

[91] J. Cao, X. Li, H. Tian, Metal-organic framework (MOF)-based drug delivery, *Curr. Med. Chem.* 27 (2020) 5949–5969. doi: 10.2174/0929867326666190618152518

[92] P. Rocío-Bautista, P. González-Hernández, V. Pino, J. Pasán, A.M. Afonso, Metal-organic frameworks as novel sorbents in dispersive-based microextraction approaches, *Trends Anal. Chem.* 90 (2017) 114–134. doi: 10.1016/j.trac.2017.03.002

[93] X. Li, W. Ma, H. Li, Y. Bai, H. Liu, Metal-organic frameworks as advanced sorbents in sample preparation for small organic analytes, *Coord. Chem. Rev.* 397 (2019) 1–13. doi: 10.1016/j.ccr.2019.06.014

[94] L. Feng, K.Y. Wang, X.L. Lv, T.H. Yan, H.C. Zhou, Hierarchically porous metal–organic frameworks: synthetic strategies and applications, *Natl. Sci. Rev.* 7 (2020) 1743–1758. doi: 10.1093/nsr/nwz170

- [95] V. Bon, N. Kavooosi, I. Senkovska, P. Müller, J. Schaber, D. Wallacher, D.M. Töbrens, U. Mueller, S. Kaskel, Tuning the flexibility in MOFs by SBU functionalization, *Dalton Trans.* 14 (2016) 4407–4415. doi: 10.1039/c5dt03504j
- [96] T. Duerinck, R. Bueno-Perez, F. Vermoortele, D.E. De Vos, S. Calero, G. V. Baron, J.F.M. Denayer, Understanding hydrocarbon adsorption in the uio-66 metal–organic framework: separation of (un)saturated linear, branched, cyclic adsorbates, including stereoisomers, *J. Phys. Chem. C.* 117 (2013) 12567–12578. doi: 10.1021/jp402294h
- [97] I.E. Uflyand, V.A. Zhinzhilo, V.O. Nikolaevskaya, B.I. Kharisov, C.M. Oliva-González, O.V. Kharissova, Recent strategies to improve MOF performance in solid phase extraction of organic dyes, *Microchem. J.* 168 (2021) 106387. doi: 10.1016/j.microc.2021.106387
- [98] B. Van de Voorde, I. Stassen, B. Bueken, F. Vermoortele, D. De Vos, R. Ameloot, J.C. Tan, T.D. Bennett, Improving the mechanical stability of zirconium-based metal–organic frameworks by incorporation of acidic modulators, *J. Mater. Chem. A* 3 (2015) 1737–1742. doi: 10.1039/c4ta06396a
- [99] J. Cravillon, R. Nayuk, S. Springer, A. Feldhoff, K. Huber, M. Wiebcke, Controlling zeolitic imidazolate framework nano- and microcrystal formation: insight into crystal growth by time-resolved in situ static light scattering, *Chem. Mater.* 23 (2011) 2130–2141. doi: 10.1021/cm103571y
- [100] F. Maya, C. Palomino-Cabello, S. Clavijo, J.M. Estela, V. Cerdà, G. Turnes-Palomino, Zeolitic imidazolate framework dispersions for the fast and highly efficient extraction of organic micropollutants, *RSC Adv.* 5 (2015) 28203–28210. doi: 10.1039/c5ra01079a.



## **Capítulo 2. Aplicación de materiales monolíticos en técnicas de separación miniaturizadas**



## 2.1. Técnicas de (electro)separación miniaturizadas. Generalidades

En las últimas décadas, las técnicas de separación a micro/nano escala como, por ejemplo, la cromatografía capilar (HPLC-capilar), la nanocromatografía de líquidos (HPLC-nano), la electroforesis capilar (*capillary electrophoresis*, CE) y la electrocromatografía capilar (*capillary electrochromatography*, CEC) se han convertido en herramientas esenciales en el área de la separación y análisis de un gran número de compuestos [1]. En este conjunto de técnicas se emplean columnas de separación de diámetros micrométricos que permiten miniaturizar el sistema de separación, disminuyendo el volumen de muestras, disolventes y otros reactivos usados durante el proceso analítico. Todo ello ha propiciado un acercamiento significativo a los principios de la Química Verde [2].

Así pues, la disminución del diámetro de la columna en HPLC ha facilitado el desarrollo y aplicación de micro-columnas de diferentes tipos (capilares/abiertas, parcialmente empaquetadas y empaquetadas) y con distintos tamaños (10-250  $\mu\text{m}$  de diámetro interno).

El uso de estas microcolumnas en estos sistemas miniaturizados ha conducido a una serie de ventajas sustanciales respecto a las columnas convencionales: i) incremento de la eficacia cromatográfica (de  $10^2$  a  $10^6$  veces) pudiéndose discriminar cientos de picos en un único cromatograma; ii) disminución drástica del consumo de la fase móvil y cantidad de muestra necesaria; iii) reducción de los residuos generados; iv) aumento de la sensibilidad con ciertos detectores; y v) mayor compatibilidad con detectores de altas prestaciones (p.ej. espectrometría de masas) en las hibridaciones instrumentales [3,4]. Sin embargo, el uso de estos sistemas miniaturizados también comporta una serie de limitaciones. Entre las más destacables se encuentran la adaptación del resto de componentes del cromatógrafo a la escala micro/nano, traduciéndose en una reducción del tamaño (p.ej. microinyectores, conectores con volúmenes muertos muy pequeños, microceldas de flujo, etc.).

Asimismo, la miniaturización de las celdas de flujo en HPLC ha conducido a la disminución de su volumen interno, con objeto de reducir la dispersión de los analitos, favoreciéndose así una mayor eficacia de los picos cromatográficos. Así pues, se ha pasado de las celdas convencionales de 20-50  $\mu\text{L}$  a microceldas de 2-5  $\mu\text{L}$  de volumen interno, y nanoceldas [5] del orden del nanolitro como las que usan los equipos más modernos de HPLC-nano.

Aprovechando las ventajas anteriormente citadas, estas técnicas cromatográficas miniaturizadas (particularmente, la HPLC-nano) se han utilizado ampliamente en distintos campos de muy diferente índole tales como alimentación [3], separación quiral [6] o análisis medioambiental [7], entre otras aplicaciones.

Una vía alternativa y complementaria a estas técnicas cromatográficas se halla en las técnicas de electroseparación capilar, basadas en la utilización de un campo eléctrico como fuerza motriz o impulsora para el avance de la fase móvil a través de un capilar hueco o relleno de sorbente. Estas técnicas habitualmente implican el movimiento diferencial de especies cargadas al aplicar un voltaje entre los extremos de la columna o capilar. Otro constituyente fundamental del funcionamiento de las técnicas enmarcadas dentro de la CE es el denominado flujo electroosmótico (*Electroosmotic flow*, EOF). Éste se trata del flujo neto de líquido en el capilar, y se debe a la carga superficial en el interior de la pared del capilar. En el caso de los capilares de sílice fundida la superficie de carga es generada por la ionización de los grupos silanol. En definitiva, el EOF es resultado del efecto del campo eléctrico aplicado en la doble capa de la disolución en la pared. Así pues, la separación de especies cargadas se producirá en función de su movilidad electroforética en un electrolito de fondo (*Background electrolyte*, BGE) a un pH determinado, y del EOF presente. En condiciones habituales, de polaridad directa (cátodo situado junto a la ventana de detección), los cationes son los que migrarán más rápidamente, seguidos de las especies neutras (transportadas todas a la velocidad del EOF), y por último, los aniones que migran más lentamente.



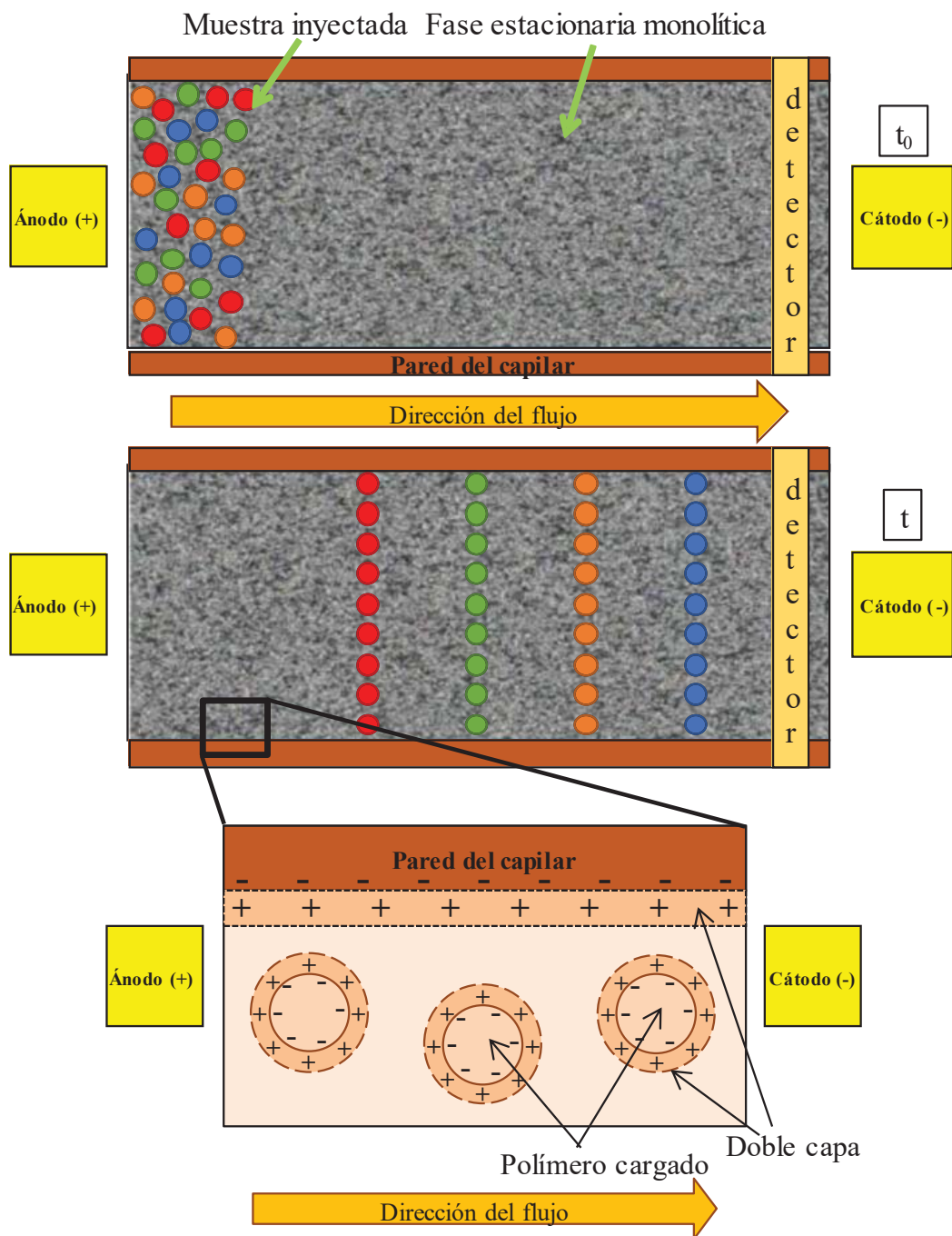
No obstante, existen modalidades o técnicas de la electroseparación capilar que permiten la separación de solutos neutros y cargados mediante un cambio en la composición del BGE (p.ej. mediante la introducción de un surfactante como la cromatografía capilar micelar electrocinética) o mediante la introducción de una fase estacionaria en capilares de sílice fundida (como la CEC). A continuación, se describirá brevemente esta técnica debido a su aplicación en la presente Tesis Doctoral.

Antes de pasar a describir brevemente esta técnica, es importante indicar que todas estas técnicas de electroseparación o electromigración capilar se caracterizan por su sostenibilidad medioambiental, al igual que los sistemas HPLC-capilar/nano, su bajo consumo de muestras (pocos nL), su alta eficacia, su sencillez y versatilidad en el desarrollo de metodologías y la posibilidad de realizar en éstas, la detección en el propio capilar.

## **2.2. Electrocromatografía capilar (CEC)**

### *2.2.1. Fundamento teórico*

La CEC es una técnica analítica de separación en fase líquida que combina la elevada eficacia de la CE con la alta selectividad y reproducibilidad proporcionadas por la HPLC. En CEC, la separación se lleva a cabo en columnas capilares rellenas total o parcialmente con una fase estacionaria, produciéndose una interacción entre los analitos y el sorbente semejante a la que sucede en los sistemas cromatográficos. Por otro lado, de forma análoga a como sucede en CE, se genera un flujo (EOF) a través de la columna al aplicar un voltaje a lo largo de la misma. No obstante, para que se genere EOF debe asegurarse la presencia de cargas sobre la superficie del relleno de la columna (ya sea particulada o monolítica). En la **Figura 2.1** se muestra de manera esquemática la separación de una serie de analitos en función de su afinidad por la fase estacionaria monolítica (cargada negativamente en su superficie) así como la generación de EOF resultante en la misma.



**Figura 2.1.** Esquema de la separación de analitos mediante CEC donde puede apreciarse la generación de EOF en la fase estacionaria.

Este EOF actúa como fuerza impulsora de la fase móvil y da lugar a un perfil plano en el movimiento del frente líquido presente en el interior del capilar, a diferencia del perfil parabólico que se obtiene en HPLC donde el avance de la fase móvil es producido por presión externa mediante bombas. Este perfil

prácticamente plano del flujo se traduce en mayores eficacias, esto es, en una disminución de la altura equivalente de plato teórico de la columna cromatográfica.

Como la CEC implica el uso de una fase estacionaria, los principios del ensanchamiento de banda son similares a los que tienen lugar en la HPLC convencional. En un proceso cromatográfico, el ensanchamiento o dispersión de los picos cromatográficos es habitualmente expresado mediante la ecuación de van Deemter [8]:

$$H=A+\frac{B}{u}+C u \quad (1)$$

donde  $H$  es la altura equivalente de plato teórico y hace referencia a la eficacia cromatográfica ( $N$ ) por unidad de longitud,  $u$  es la velocidad lineal de flujo de la fase móvil, y los términos  $A$ ,  $B$ , y  $C$  reflejan diversas contribuciones debidas a fenómenos que producen el ensanchamiento de banda. Dichas contribuciones, así como las expresiones matemáticas de los diferentes términos se indican en la **Tabla 2.1**.

**Tabla 2.1.** Contribución y expresión matemática de los términos de la ecuación de van Deemter.

Término	Contribución	Expresión
A	Multiplicidad de caminos	$A = 2\lambda d_p$
B	Difusión longitudinal	$B = 2\gamma D_m$
C	Resistencia a la transferencia de masa	$C = \frac{f_1(k)d_p^2}{D_m} + \frac{f_2(k)d_p^2}{D_s}$

dónde:  $\lambda$  es una constante de irregularidades,  $d_p$  es el diámetro de las partículas del relleno,  $\gamma$  es un factor de corrección provocado por la oposición del relleno a la difusión,  $D_m$  y  $D_s$  son los coeficientes de difusión de los analitos en las fases móvil y estacionaria, respectivamente, y  $f_1(k)$  y  $f_2(k)$  son funciones que dependen del factor de capacidad o retención de los analitos.

Como puede observarse, el empleo de partículas pequeñas conducirá a una mayor eficacia cromatográfica, dado que disminuirá  $H$ , la cual se relaciona con el ancho de pico cromatográfico de acuerdo con la siguiente ecuación:

$$H = \left(\frac{L}{5.54}\right) \left(\frac{w_{1/2}}{t_R}\right)^2 \quad (2)$$

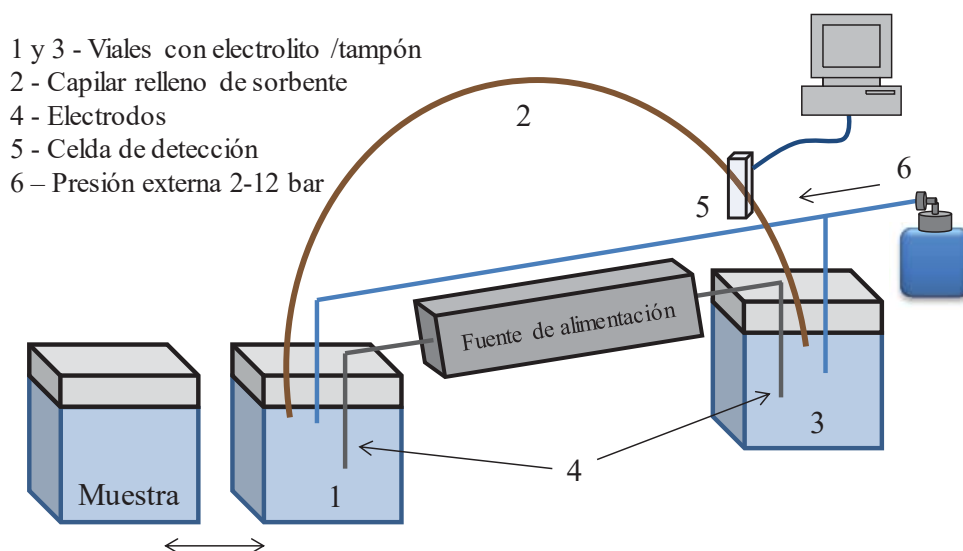
En CEC, el término  $A$  es sustancialmente debido al perfil plano causado por el EOF a diferencia de los sistemas convencionales y miniaturizados de HPLC. Además, este perfil de flujo también reduce la resistencia a la transferencia de masa (término  $C$ ), lo cual tiene implicaciones en el factor de retención. Estos perfiles planos en la curva de van Deemter han conducido a separaciones con altas eficacias en CEC, siendo superiores a las obtenidas en micro/nano-HPLC (alcanzándose mejores valores de  $H$  del orden de 2-2,5 veces) en diámetros de capilares de 50-100  $\mu\text{m}$  [9,10].

Así pues, el mecanismo de separación en CEC es doble [11]. Por un lado, existe un mecanismo cromatográfico, debido a que se produce un reparto de los solutos entre la fase móvil y la estacionaria. Los solutos que interactúan en mayor medida con la fase estacionaria presentan una mayor retención en la columna que aquéllos con mayor tendencia a permanecer en la fase móvil. Por otro lado, los solutos iónicos también se separan mediante un mecanismo electroforético, esto es, en base a las diferencias de movilidad electroforética, por lo que la naturaleza del relleno de la columna determina el EOF e influye sobre la selectividad de la separación [11].

### 2.2.2. Instrumentación en CEC

Un instrumento para CEC (véase esquema de la **Figura 2.2**) está constituido básicamente por una fuente de alto voltaje, un sistema de suministro de disolvente y/o muestras en los viales de entrada y de salida de la columna, una columna capilar con una fase estacionaria en la cual se genera el EOF y también tiene lugar la separación electrocromatográfica, un compartimento isotérmico

para la columna capilar, y un sistema de detección capaz de registrar los perfiles de concentración de los analitos en el eluyente.



**Figura 2.2.** Esquema de un instrumento de CEC.

La misma instrumentación utilizada en CE sirve para CEC [12], si bien, en este caso se debe de disponer de un sistema de presurización de los viales de entrada y salida. Esta presurización es necesaria para evitar la formación de burbujas, que podrían interrumpir la corriente. Las burbujas pueden originarse por diversas causas, ya sea por diferencias locales en la velocidad del EOF en el campo eléctrico, por pérdida del gas atrapado en los poros de la fase estacionaria, o por gas formado electroquímicamente, por calentamiento, o en el caso de columnas empaquetadas, por la presencia de las fritas que mantienen la integridad estructural del relleno [13,14]. La presurización se puede aplicar sobre el vial de entrada o en el de salida, aunque generalmente se aplica sobre ambos viales, ya que así se asegura un flujo reproducible. Para presurizar los viales se usa un gas inerte, normalmente  $N_2$ , a presiones próximas a 10 bares. Para obtener resultados reproducibles en CEC, es necesario el control de parámetros como la temperatura de la columna, el voltaje aplicado y la presión. En los equipos comerciales de CE, estos parámetros se controlan

automáticamente, lo que da lugar a mejoras significativas de la reproducibilidad y seguridad de las separaciones.

Por otro lado, la espectrofotométrica UV-Vis es la técnica de detección más utilizada en CEC [15], aprovechando que la detección se realiza en la misma columna (*on-column*), utilizando como celda de detección una pequeña sección de la misma, adyacente al relleno, y de la cual se ha retirado la capa protectora de polímero. Dado que la detección se realiza *on-column*, la sensibilidad está limitada por el paso óptico. En este sentido, se han desarrollado algunos diseños como capilares con celda burbuja (*bubble cell*) o celdas en forma de Z para aumentar el paso óptico, pero la resolución puede verse afectada [15]. Alternativamente, se han utilizado otras técnicas de detección más sensibles como son la fluorescencia inducida por láser [16], y la MS [17].

## **2.3. Fases estacionarias monolíticas en técnicas de separación miniaturizadas**

### *2.3.1. Tipos de columnas. Uso de monolitos orgánicos como fases estacionarias*

Habitualmente, las columnas para CEC se preparan normalmente a partir de capilares de sílice fundida con diámetros internos comprendidos entre 25 y 200  $\mu\text{m}$ . En base a las diferentes estructuras de los soportes cromatográficos utilizados, se pueden distinguir tres tipos de columnas: particuladas, abiertas y monolíticas.

Normalmente, las columnas empleadas en HPLC convencional han sido utilizadas para HPLC-capilar/nano y CEC. Estas fases estacionarias consistentes en lechos empaquetados de partículas de sílice porosa presentan excelentes propiedades para ser utilizadas como fase estacionaria, entre las que se encuentran su resistencia mecánica y su elevada área superficial [18]. Además, la derivatización de los grupos silanol permite llevar a cabo separaciones en CEC basadas en diferentes mecanismos (interacción hidrofílica o hidrofóbica, intercambio iónico, afinidad, etc) [19].

Sin embargo, la preparación de columnas empaquetadas robustas y estables no es un proceso sencillo, siendo frecuente la aparición de problemas derivados del propio proceso de fabricación de la columna, pudiendo crearse huecos en el relleno inducidos por repulsión electrostática entre las partículas [20]. También las mencionadas fritas son a menudo responsables de la formación de burbujas que pueden producir caídas en la corriente. Por otro lado, estas fritas son difíciles de fabricar de manera reproducible, y al estar elaboradas con material sinterizado pueden crear zonas de heterogeneidad en el interior de los capilares empaquetados.

Además de los problemas inherentes a la elaboración de las columnas, pueden surgir otros debido a la interacción de los analitos con el lecho empaquetado y en particular con las fritas. Éste es el caso de moléculas con cargas múltiples como las proteínas, que pueden, en ocasiones, adsorberse permanentemente sobre la frita y quedar atrapadas en el interior de la columna.

Una alternativa al empleo de fritas y sencillez de preparación se encuentra en las columnas abiertas (*open-tubular columns*), donde la fase estacionaria se fija a modo de recubrimiento sobre la pared interna del capilar; modificando la naturaleza del recubrimiento se puede incidir sobre la selectividad de la separación [21]. Sin embargo, presentan ciertas limitaciones tales como una menor relación de fases y una capacidad de carga bastante limitada [22]. No obstante, pueden obtenerse eficacias de separación bastante elevadas respecto a las columnas particuladas convencionales al haberse eliminado la contribución de la difusión de remolino o torbellino (término A de la ecuación de van Deemter) [21, 23].

Una posibilidad a las columnas particuladas y a las limitaciones de las columnas abiertas es el empleo de fases estacionarias monolíticas debido a sus interesantes ventajas implícitas comentadas en el anterior capítulo. Así pues, dada su estructura continua, no es necesario el empleo de fritas de retención, ya que el lecho monolítico se ancla directamente a la pared del soporte (en este caso, capilar). Además, pueden prepararse *in situ*, por lo que la fabricación de

lechos cromatográficos tanto en columnas capilares como en microchips es relativamente sencilla en comparación con las técnicas de empaquetado de partículas. En condiciones óptimas, las columnas monolíticas constituyen fases estacionarias altamente permeables y uniformes, con una relación de fases y una capacidad de carga relativamente elevadas, lo que les confiere buenas propiedades de retención y selectividad.

Entre los diferentes tipos de fases monolíticas, el interés de la presente Tesis se centra en el desarrollo de fases estacionarias monolíticas poliméricas de ésteres de metacrilato y acrilato. Si bien la extensión de estas fases al ámbito de preparación de muestra en la última década, su aplicación como columnas cromatográficas fue introducida por Svec y Fréchet en los primeros años de la década de los 90 [24,25].

Tal y como se ha comentado la preparación de los polímeros monolíticos sigue un proceso simple y directo (véase **Capítulo 1**). La mezcla de polimerización es una combinación de monómeros entre los que se encuentra un agente entrelazante o *crosslinker*, una mezcla porogénica de disolventes y un iniciador radicalario. Si es necesario se puede exaltar la hidrofobicidad añadiendo grupos funcionales alquílicos [26]. El EOF, necesario para CEC, se asegura mediante la incorporación de grupos funcionales ionizables, tales como monómeros derivados del ácido sulfónico, o si se desea invertir el EOF pueden añadirse monómeros que contengan sales de amonio cuaternario [26]. El capilar se rellena con la mezcla de polimerización y se sellan los extremos. La mezcla se polimeriza en la mayoría de los casos por calentamiento en un baño u horno, por la acción de iniciadores químicos o mediante radiación UV. Esta última posibilidad también permite formar monolitos en una zona específica mediante el empleo de capilares transparentes, haciendo pasar la radiación a través de una máscara en un proceso pseudo-litográfico. Una vez que la polimerización se completa, se retiran los sellos y se conecta el capilar a una bomba, para pasar un disolvente a través de la columna y eliminar porógenos y otros compuestos solubles que pudieran quedar en el monolito.



Para evitar que la fase móvil desplace el lecho monolítico a lo largo de la columna, es necesario un adecuado anclaje del polímero a la pared interna del capilar, recurriéndose a menudo a la silanización de dicha pared, lo que suele llevarse a cabo con metacrilato de 3-(trimetoxisilil)propilo (*silano binding*) para anclar covalentemente el monolito.

Además de su aplicación en el ámbito de la preparación de muestra, tal y como se ha indicado en el anterior capítulo, las fases monolíticas poliméricas se han utilizado de forma satisfactoria en la separación rápida en técnicas cromatográficas de macromoléculas tales como proteínas/péptidos, ácidos nucleicos y polímeros sintéticos [27-30]. Sin embargo, la baja área superficial de los monolitos orgánicos (del orden de unos pocos  $m^2/g$ ) y su estructura fundamentalmente macroporosa de éstos (con escasa o inexistente presencia de mesoporos) ha dificultado separaciones competitivas de solutos pequeños a diferencia de lo que ocurre con los monolitos de sílice. En este sentido, en la última década, se han descrito diversas estrategias para mejorar las prestaciones cromatográficas de estas columnas monolíticas poliméricas [31,32]. En el siguiente apartado, se describirán algunas de las estrategias realizadas para manipular sus propiedades con objeto de mejorar sus prestaciones como fases estacionarias en técnicas de (electro)separación miniaturizadas.

### 2.3.2. Manipulación de las prestaciones de columnas monolíticas poliméricas

Las estrategias utilizadas para manipular o controlar las prestaciones cromatográficas de las fases monolíticas se pueden agrupar en torno a diferentes ítems: a) modificaciones en la mezcla de polimerización y condiciones de reacción, b) hiper-entrecruzamiento (*hypercrosslinking*) y c) incorporación de nanomateriales. A continuación, se describirán estas aproximaciones, y en particular, la última de ellas ya mencionada en el capítulo anterior (véase **apartado 1.3.1B**) se mencionará brevemente haciendo hincapié en su aplicación a columnas de formato capilar para técnicas HPLC-capilar/nano y CEC.

*A) Modificaciones en la mezcla de polimerización y condiciones de reacción*

Tal y como se ha comentado en el anterior capítulo, las propiedades de los lechos monolíticos de metacrilato y acrilato pueden optimizarse ajustando la composición de la mezcla de polimerización (monómeros, crosslinker, disolvente porogénico y/o iniciador), así como el tipo de iniciación empleada [33]. La modificación de cada uno de estos factores altera el proceso de polimerización y produce un efecto diferente sobre las características del monolito final, traduciéndose en un cambio en sus propiedades morfológicas y cromatográficas. A continuación, se comentará brevemente algunas de las variables principales sobre las que se puede ejercer un control, así como los recientes estudios realizados sobre éstas.

- *Influencia del monómero funcional*

Actualmente, existe una amplia variedad de monómeros que permite ajustar la naturaleza de la superficie del monolito a las características de la separación que se desea realizar. Así, en el caso de los monolitos basados en ésteres de metacrilato pueden destacarse el metacrilato de butilo (BMA) [34,35], el metacrilato de hexilo (HMA) [34], el metacrilato de laurilo (LMA) y octadecilo (ODA) [34,36,37], permitiendo así manipular la hidrofobicidad de la fase estacionaria. También es de señalar el GMA, que como ya se ha dicho permite derivatizar fácilmente el lecho monolítico, y proporcionar columnas con funcionalidades diversas [34, 38]. En el caso de los monolitos de ésteres de acrilato pueden citarse entre otros, el acrilato de butilo [39,40], el acrilato de acrilato de laurilo y octadecilo [39,41], entre otros.

Por su parte, en CEC, aparte de este monómero funcional que determina la hidrofobicidad y las características químicas de la superficie del lecho resulta necesario la inclusión de un pequeño porcentaje de un monómero con carga, positiva o negativa, para generar el EOF que garantice el transporte de los diferentes analitos a través de la columna.

En los últimos años, se han descrito la incorporación de ILs como comonómeros a la mezcla de polimerización tanto en HPLC-capilar/nano [42] como CEC [43]. Así, por ejemplo, se ha observado un aumento en la selectividad de las separaciones de solutos con anillos aromáticos en base a la interacción  $\pi$ - $\pi$  que ofrecen estos reactivos; sin embargo, las eficacias de las separaciones obtenidas con monolitos modificados con ILs se sitúan por debajo de los 25.000 platos teóricos/m [42].

Una alternativa reciente e interesante al empleo de los monómeros funcionales tradicionales es el uso de silsesquioxanos oligoméricos poliédricos (*Polyhedral oligomeric silsesquioxane*, POSS). Estas nanoestructuras híbridas de naturaleza inorgánica/orgánica de elevada simetría contienen un núcleo inorgánico (-Si-O-Si-) térmicamente estable que suele estar cubierto externamente por sustituyentes orgánicos [44]. Éstos pueden presentar una estructura desordenada, en forma de jaula o en forma de jaula parcial y son fáciles de modificar químicamente [45]. La morfología globular de los monolitos híbridos metacrilato-POSS es semejante a los monolitos de sílice y han proporcionado eficacias de hasta 190.000 platos teóricos/m en separaciones de moléculas pequeñas [46].

- *Influencia del crosslinker*

En el caso de columnas monolíticas de metacrilato se suelen utilizar dimetacrilatos de alcoholes saturados divalentes, siendo el etilenglicol dimetacrilato (*Ethylene glycol dimethacrylate*, EDMA) el más popular. Por su parte, para las columnas basadas en ésteres de acrilato, el crosslinker más utilizado es el diacrilato de 1,3-butanodiol (*1,3-butanediol diacrylate*, BDDA).

Un cambio en el porcentaje de agente entrelazante utilizado en la mezcla de monómeros afecta tanto a la composición química del lecho monolítico como a sus propiedades porosas y cromatográficas, de modo que en general un incremento del contenido de *crosslinker* produce una disminución del tamaño medio de poro debido a la temprana formación de microglóbulos con un alto

grado de entrecruzamiento [33]. Además, el porcentaje de agente entrelazante afecta a la rigidez y homogeneidad del monolito. Así pues, la polimerización de mezclas con un alto contenido de crosslinker puede resultar útil para obtener lechos monolíticos de elevada área superficial, de hasta más de 100 m<sup>2</sup>/g; no obstante, estos monolitos pueden presentar una permeabilidad limitada, restringiéndose su uso en HPLC-capilar/nano y CEC.

Además del contenido del crosslinker en la mezcla de polimerización, se ha demostrado que su tamaño, su polaridad y los grupos funcionales presentes en éste pueden afectar al tamaño de poros, la permeabilidad y la eficacia cromatográfica [33,47]. En este sentido, se han utilizado crosslinkers conteniendo diversos grupos de acrilato que ha proporcionado eficacias de hasta 165.000 platos teóricos/m en la separación de alquilbencenos por HPLC capilar [48]. Otra alternativa sencilla a preparar columnas con alta eficacia en la separación de moléculas pequeñas es la propuesta por el grupo de Lee y colaboradores [49,50], donde se hace uso de crosslinkers (dimetacrilato de 1,3-butanodiol, dimetacrilato de ciclohexanodiol, diacrilato de 1,4-fenileno, polietilenglicol diacrilato (PEGDA), entre otros) como monómero para preparar fases estacionarias altamente entrelazadas en HPLC capilar, alcanzándose eficacias que van desde los 100.000 a los 186.000 platos/m [51]. Esta estrategia propuesta simplifica el proceso de optimización de la mezcla de polimerización, mejora la estabilidad mecánica de los lechos y la reproducibilidad entre columnas.

- *Influencia de la composición del disolvente porogénico*

La elección del disolvente porogénico y su proporción en la mezcla de polimerización también representa un factor esencial en la optimización de las propiedades porosas de los monolitos de metacrilato y acrilato.

El mecanismo de la formación de poros mediante la utilización de agentes porogénicos puede explicarse teniendo en cuenta la solubilidad del polímero en los distintos porógenos. La polimerización tiene lugar en un medio de reacción

inicialmente homogéneo hasta que se separan las cadenas de polímero que aumentan de tamaño y se entrecruzan. Los cambios en la naturaleza o en la composición del disolvente porogénico influyen sobre la solvatación de las cadenas de polímero en las primeras etapas de la polimerización, de manera que en general se obtienen poros de mayor tamaño si se utilizan disolventes con pobre capacidad solvatante hacia el polímero. Por el contrario, si el porógeno es un buen disolvente del polímero, la separación de fases se enlentece y los poros son menores [52,53].

Por otro lado, la disminución de la relación monómeros/porógenos proporciona un método directo de incrementar el tamaño de poro y por tanto reducir la resistencia al flujo de las columnas, si bien con ello disminuye la homogeneidad y rigidez del polímero formado [52].

Habitualmente, disolventes como alcoholes (metanol, 1-propanol, 1,4-butanediol, ciclohexanol, decanol, dodecanol) y ciertos hidrocarburos (hexano y tolueno) han sido ampliamente utilizados en la preparación de monolitos, en los últimos años disolventes como ILs, surfactantes u otros han sido utilizados en la manipulación de las propiedades morfológicas y cromatográficas. A modo de ejemplo, la introducción de ILs como disolventes porogénicos ha conducido a la formación de estructuras más uniformes, con mayor área superficial (150-250 m<sup>2</sup>/g) [54,55] si bien las eficacias obtenidas han sido discretas (25.000 platos/m).

- *Influencia de las condiciones de reacción*

La polimerización de lechos monolíticos de metacrilato y acrilato es una reacción radicalaria iniciada generalmente por una temperatura elevada, un proceso de irradiación o la presencia de agentes químicos.

En la iniciación térmica, la temperatura del proceso de polimerización debe controlarse cuidadosamente debido a su fuerte influencia sobre la velocidad de crecimiento de los núcleos. A temperaturas elevadas, a las que tanto la descomposición del iniciador como la velocidad de propagación son muy

rápidas, aumenta el número de núcleos con la consiguiente reducción del tamaño final de poro. Polimerizaciones rápidas dan lugar a estructuras porosas menos uniformes, por lo que desde esta perspectiva sería preferible utilizar temperaturas de polimerización más bajas. Sin embargo, el uso de bajas temperaturas puede inhibir el efecto del iniciador o afectar a la cinética del proceso en su conjunto, enlenteciéndolo demasiado [56].

Otro de los aspectos a controlar es el tiempo de reacción. Habitualmente, la polimerización por iniciación térmica suele requerir 20-24 h, si bien se puede reducir este tiempo (“*early termination of polymerization reaction*”) con el fin de lograr monolitos con mejores prestaciones cromatográficas. A tiempos cortos de polimerización (90-180 min), se obtiene un polímero con suficiente estructura mesoporosa que ofrece mayor área superficial (418 m<sup>2</sup>/g frente a 120 m<sup>2</sup>/g a 24 h) y adecuadas eficacias (hasta 116.000 platos/m) de solutos neutros en HPLC-capilar [57,58]. Sin embargo, la conversión de los monómeros no es del todo completa, lo cual puede comprometer la reproducibilidad en la preparación de los lechos.

Por su parte, la polimerización iniciada por radiación UV se efectúa normalmente a temperatura ambiente, y tal como se ha indicado en el capítulo anterior, el proceso de polimerización puede completarse en tiempos muy cortos, del orden de pocos minutos. En términos generales, a igualdad de composición de mezcla de polimerización, las columnas obtenidas mediante este modo son más permeables que las obtenidas por vía térmica [59].

### *B) Hiper-entrecruzamiento*

Esta estrategia se ha descrito para columnas monolíticas basadas en estireno-divinilbenzeno, las cuales se someten a una funcionalización con un reactivo bifuncional apropiado que actúa como puente para obtener un polímero con una estructura rica en meso o microporos, traduciéndose en un aumento del área superficial. Este incremento en área superficial ha mejorado las prestaciones de estos monolitos para separar moléculas pequeñas, alcanzándose eficacias

comprendidas entre 70.000 y 85.000 platos/m [60,61]. Sin embargo, esta aproximación no ha sido extendida al uso de otros lechos monolíticos como los basados en metacrilato y acrilato.

### *C) Incorporación de nanomateriales variados*

Una de las estrategias que ha recibido enorme atención en la última década ha sido la incorporación de nanomateriales en los lechos monolíticos para mejorar sus prestaciones cromatográficas como fases estacionarias en HPLC capilar/nano y CEC. En este sentido, se han utilizado nanopartículas de muy diversa naturaleza tales como nanoestructuras de carbono (nanotubos de C, fullerenos, etc) [62-64], nanopartículas metálicas (de oro y plata) [65-67], de sílice [68,69], magnéticas [70], de látex [68] y MOFs [71,72]. Tal y como se ha comentado en el capítulo anterior, estos nanomateriales se han incorporado mediante simple adición de éstos a la mezcla de polimerización o mediante una reacción de modificación de la superficie del lecho polimérico, empleándose habitualmente como polímeros de partida, monolitos de GMA. Aunque la primera vía es sencilla y directa, ésta posee la limitación de que altas concentraciones de nanopartículas presentes en la mezcla de polimerización conducen a fenómenos de agregación y sedimentación. Por su parte, la vía de post-funcionalización con el nanomaterial seleccionado puede requerir de varias etapas, lo cual puede hacer lento y tedioso la obtención del monolito híbrido o modificado con NPs.

En general, la incorporación de nanomateriales en los lechos monolíticos en técnicas de separación miniaturizadas [53,73] ha producido cambios en la retención y eficacia en comparación con los monolitos base o control. En algunos de los nanomateriales incorporados, se han obtenido eficacias que pueden ir desde 110.000 a 180.000 platos/m (como en el caso de NPs de sílice y magnéticas) en la separación de solutos pequeños, y en otros, solamente unas decenas de miles de platos/m. Por otro lado, esta estrategia ha proporcionado una manipulación ventajosa de la retención y de la selectividad de la separación

en base a las interacciones hidrofóbicas, por puente de hidrógeno o de otra índole entre el lecho monolítico modificado con el nanomaterial y los solutos de interés, lo cual la convierte en una herramienta interesante para abordar la selectividad en un problema cromatográfico determinado.

Dado que esta última vía ha sido explorada en detalle en los últimos años por nuestro grupo de investigación, en el **Bloque III** de la presente Tesis (**Capítulo 8**), se ha considerado abordar el desarrollo de fases monolíticas altamente entrelazadas a partir de un solo monómero/crosslinker con las ventajas anteriormente indicadas, y su aplicación a la separación mediante CEC de solutos pequeños de diferente polaridad.



## 2.4. Referencias

- [1] M. Szumski, B. Buszewski, State of the art in miniaturized separation techniques, *Crit. Rev. Anal. Chem.* 32 (2010) 1–46. doi: 10.1080/10408340290765434
- [2] M. de la Guardia, S. Garrigues, *Handbook of green analytical chemistry*. John Wiley & Sons, Ltd; 2012
- [3] C. Fanali, L. Dugo, P. Dugo, L. Mondello, Capillary-liquid chromatography (CLC) and nano-LC in food analysis, *Trends Anal. Chem.* 52 (2013) 226–238. doi: 10.1016/j.trac.2013.05.021
- [4] S.R. Wilson, T. Vehus, H.S. Berg, E. Lundanes, Nano-LC in proteomics: recent advances and approaches, *Bioanalysis* 7(14) (2015) 1799–1815. doi: 10.4155/bio.15.92
- [5] S. Fanali, An overview to nano-scale analytical techniques: Nano-liquid chromatography and capillary electrochromatography, *Electrophoresis* 38 (2017) 1822–1829. doi: 10.1002/elps.201600573.
- [6] S. Fanali, Nano-liquid chromatography applied to enantiomers separation, *J. Chromatogr. A* 1486 (2017) 20–34. doi: 10.1016/j.chroma.2016.10.028
- [7] Z. Aturki, A. Rocco, S. Rocchi, S. Fanali, Current applications of miniaturized chromatographic and electrophoretic techniques in drug analysis, *J. Pharm. Biomed. Anal.* 101 (2014) 194–220. doi: 10.1016/j.jpba.2014.03.041
- [8] J. Cazes, R.P.W. Scott, *Chromatography Theory*. Marcel Dekker, Nueva York, 2002.
- [9] S. Fanali, G. D’Orazio, T. Farkas, B. Chankvetadze, Comparative performance of capillary columns made with totally porous and core–shell particles coated with a polysaccharide-based chiral selector in nano-liquid chromatography and capillary electrochromatography, *J. Chromatogr. A* 1269 (2012) 136–142. doi: 10.1016/j.chroma.2012.06.021

- [10] S. Fanali, B. Chankvetadze, History, advancement, bottlenecks, and future of chiral capillary electrochromatography, *J. Chromatogr. A* 1637 (2021) 461832. doi: 10.1016/j.chroma.2020.461832
- [11] K. Bartle, P. Myers, Theory of capillary electrochromatography, *J. Chromatogr. A* 916 (2001) 3–23. doi: 10.1016/S0021-9673(01)00709-9
- [12] F. Steiner, B. Scherer, Instrumentation for capillary electrochromatography, *J. Chromatogr. A* (2000) 55–83. doi: 10.1016/S0021-9673(00)00551-3
- [13] R.A. Carney, M.M. Robson, K.D. Bartle, P. Myers, Investigation into the formation of bubbles in capillary electrochromatography, *J. High Resolut. Chromatogr.* 22 (1999) 29–32. Doi: 10.1002/(sici)1521-4168(19990101)22:1<29::aid-jhrc29>3.0.co;2-u
- [14] A.S. Rathore, Theory of electroosmotic flow, retention and separation efficiency in capillary electrochromatography, *Electrophoresis* 23 (2002) 3827–3846. doi: 10.1002/elps.200290004
- [15] C. Yan, Y. Wang, Y. Xue, Capillary electrochromatography. *Encyclopedia of analytical chemistry*. West Sussex, England: John Wiley & Sons, Ltd; 2016
- [16] C. Liu, Q. Deng, G. Fang, M. Dang, S. Wang, Capillary electrochromatography immunoassay for alpha-fetoprotein based on poly(guanidinium ionic liquid) monolithic material, *Anal. Biochem.* 530 (2017) 50–56. doi: 10.1016/j.ab.2017.04.014
- [17] E. Barceló-Barrachina, E. Moyano, M.T. Galceran, State-of-the-art of the hyphenation of capillary electrochromatography with mass spectrometry, *Electrophoresis* 25 (2004) 1927–1948. doi: 10.1002/elps.200305908
- [18] J.J. Kirkland, F.A. Truszkowski, R.D. Ricker, Atypical silica-based column packings for high-performance liquid chromatography, *J. Chromatogr. A* 965 (2002) 25–34. doi: 10.1016/s0021-9673(01)01339-5get

- [19] J. Nawrocki, The silanol group and its role in liquid chromatography, *J. Chromatogr. A* 779 (1997) 29–71. doi: 10.1016/s0021-9673(97)00479-2
- [20] P. D. Angus, C. W. Demarest, T. Catalano, J. F. Stobaugh, Aspects of column fabrication for packed capillary electrochromatography, *J. Chromatogr. A* 887 (2000) 347–365. doi: 10.1016/s0021-9673(00)00529-x
- [21] F.M. Tarongoy Jr., P.R. Haddad, R.I. Boysen, M.T.W. Hearn, J.P. Quirino, *Electrophoresis* 37 (2015) 66–85. doi: 10.1002/elps.201500339
- [22] C.P. Kapnissi-Christodoulou, X. Zhu, I.M. Warner, Analytical separations in open-tubular capillary electrochromatography, *Electrophoresis* 24 (2003) 22–23. doi: 10.1002/elps.200305640
- [23] Z. Mao, Z. Chen, *Advances in capillary electro-chromatography*, *J. Pharm. Anal.* 9(4) (2019) 227–237. doi: 10.1016/j.jpha.2019.05.002
- [24] F. Svec, J.M.J. Frechet, Continuous rods of macroporous polymer as high-performance liquid chromatography separation media, *Anal. Chem* 64(7) (1992) 820–822. doi: 10.1021/ac00031a022
- [25] F. Svec, J.M.J. Frechet, Modified poly(glycidyl methacrylate-co-ethylene dimethacrylate) continuous rod columns for preparative-scale ion-exchange chromatography of proteins, *J. Chromatogr. A* 702 (1995) 89–95. doi: 10.1016/0021-9673(94)01021-6
- [26] F. Svec, Recent developments in the field of monolithic stationary phases for capillary electrochromatography, *J. Sep. Sci* 28(8) (2005) 729–745. doi: 10.1002/jssc.200400086
- [27] X. Chen, H.D. Tolley, M.L. Lee, Monolithic capillary columns synthesized from a single phosphate-containing dimethacrylate monomer for cation-exchange chromatography of peptides and proteins, *J. Chromatogr. A* 1218 (2011) 4322–4331. doi: 10.1016/j.chroma.2011.04.074
- [28] R.D. Arrua, M. Talebi, T.J. Causon, E.F. Hilder, Review of recent advances in the preparation of organic polymer monoliths for liquid

chromatography of large molecules, *Anal. Chim. Acta* 783 (2012) 1–12. doi: 10.1016/j.aca.2012.05.052

[29] H. Lei, L. Bai, X. Zhang, G. Yang, Preparation of a tetrazolyl monolithic column via the Combination of ATRP and click chemistry for the separation of proteins, *J. Chromatogr. Sci.* 52 (2014) 1211–1216. doi: 10.1093/chromsci/bmt179

[30] D. Bicho, Â. Sousa, F. Sousa, J. Queiroz, C. Tomaz, Effect of chromatographic conditions and plasmid DNA size on the dynamic binding capacity of a monolithic support, *J. Sep. Sci* 37 (2014) 2284–2292. doi: 10.1002/jssc.201400127

[31] F. Svec, Y. Lv, Advances and Recent Trends in the Field of Monolithic Columns for Chromatography, *Anal. Chem.* 87 (2015) 250–273. doi: 10.1021/ac504059c

[32] J. Urban, Current trends in the development of porous polymer monoliths for the separation of small molecules, *J. Sep. Sci* 39 (2015) 51–68. doi: 10.1002/jssc.201501011

[33] I. Nischang, Porous polymer monoliths: Morphology, porous properties, polymer nanoscale gel structure and their impact on chromatographic performance, *J. Chromatogr. A* 1287 (2013) 39–58. doi: 10.1016/j.chroma.2012.11.016

[34] M. Merhar, A. Podgornik, M. Barut, M. Žigon, A. Štrancar, Methacrylate monoliths prepared from various hydrophobic and hydrophilic monomers – Structural and chromatographic characteristics, *J. Sep. Sci* 26 (2003) 322–330. doi: 10.1002/jssc.200390038

[35] S. Eeltink, J.M. Herrero-Martinez, G.P. Rozing, P.J. Schoenmakers, W.T. Kok, Tailoring the morphology of methacrylate ester-based monoliths for optimum efficiency in liquid chromatography, *Anal. Chem.* 77 (2005) 7342–7347. doi: 10.1021/ac051093b

- [36] V. Bernabé-Zafón, A. Cantó-Mirapeix, E.F. Simó-Alfonso, G. Ramis-Ramos, J.M. Herrero-Martínez, Comparison of thermal- and photopolymerization of lauryl methacrylate monolithic columns for CEC, *Electrophoresis* 30 (2009) 1929–1936. doi: 10.1002/elps.20080055
- [37] Z. Jiang, N.W. Smith, P.D. Ferguson, M.R. Taylor, Preparation and characterization of long alkyl chain methacrylate-based monolithic column for capillary chromatography, *J. Biochem. Biophys. Methods* 70 (2007) 39–45. doi: 10.1016/j.jbbm.2006.08.009
- [38] R. Rathnasekara, S. Khadka, M. Jonnada, Z. El Rassi, Polar and nonpolar organic polymer-based monolithic columns for capillary electrochromatography and high-performance liquid chromatography, *Electrophoresis* 38 (2017) 60–79. doi: 10.1002/elps.201600356
- [39] M.P. Barrioulet, N. Delaunay-Bertoncini, C. Demesmay, J.L. Rocca, Development of acrylate-based monolithic stationary phases for electrochromatographic separations, *Electrophoresis* 26 (2005) 4104–4115. doi: 10.1002/elps.200500251
- [40] A. Cantó-Mirapeix, J.M. Herrero-Martínez, C. Mongay-Fernández, E.F. Simó-Alfonso, Preparation and evaluation of butyl acrylate-based monolithic columns for CEC using ammonium peroxodisulfate as a chemical initiator, *Electrophoresis* 29 (2008) 3858–3865. doi: 10.1002/elps.200700918
- [41] C. Puangpila, T. Nhujak, Z. El Rassi, Investigation of neutral monolithic capillary columns with varying n-alkyl chain lengths in capillary electrochromatography, *Electrophoresis* 33 (2012) 1431–1442. doi: 10.1002/elps.201200018
- [42] J. Wang, L. Bai, Z. Wei, J. Qin, Y. Ma, H. Liu, Incorporation of ionic liquid into porous polymer monoliths to enhance the separation of small molecules in reversed-phase high-performance liquid chromatography, *J. Sep. Sci* 38 (2015) 2101–2108. doi: 10.1002/jssc.201500061

- [43] Z. Mao, Z. Chen, Monolithic column modified with bifunctional ionic liquid and styrene stationary phases for capillary electrochromatography, *J. Chromatogr. A* 1480 (2017) 99–105. doi: 10.1016/j.chroma.2016.12.030
- [44] S.H. Phillips, T.S. Haddad, S.J. Tomczak, Developments in nanoscience: polyhedral oligomeric silsesquioxane (POSS)-polymers, *Curr. Opin. Solid State Mater. Sci.* 8 (2004) 21–29. Doi: 10.1016/j.cossms.2004.03.002
- [45] H. Lin, J. Ou, Z. Zhang, J. Dong, H. Zou, Ring-opening polymerization reaction of polyhedral oligomeric silsesquioxanes (POSSs) for preparation of well-controlled 3D skeletal hybrid monoliths, *Chem. Comm.* 49 (2013) 231–233. doi: 10.1039/c2cc36881a
- [46] H. Zhang, J. Ou, Z. Liu, H. Wang, Y. Wei, H. Zou, Preparation of hybrid monolithic columns via “one-pot” photoinitiated thiol–acrylate polymerization for retention-independent performance in capillary liquid chromatography, *Anal. Chem.* 87 (2015) 8789–8797. doi: 10.1021/acs.analchem.5b01707
- [47] P. Jandera, M. Staňková, V. Škeříková, J. Urban, Cross-linker effects on the separation efficiency on (poly)methacrylate capillary monolithic columns. Part I. Reversed-phase liquid chromatography, *J. Chromatogr. A* 1274 (2013) 97–106. doi: 10.1016/j.chroma.2012.12.003
- [48] H. Zhang, J. Ou, Y. Wei, H. Wang, Z. Liu, L. Chen, H. Zou, A novel polymeric monolith prepared with multi-acrylate crosslinker for retention-independent efficient separation of small molecules in capillary liquid chromatography, *Anal. Chim. Acta* 883 (2015) 90–98. doi: 10.1016/j.aca.2015.04.001
- [49] K. Liu, H.D. Tolley, J.S. Lawson, M.L. Lee, Highly crosslinked polymeric monoliths with various C6 functional groups for reversed-phase capillary liquid chromatography of small molecules, *J. Chromatogr. A* 1321 (2013) 80–87. doi: 10.1016/j.chroma.2013.10.071

[50] K. Liu, P. Aggarwal, H.D. Tolley, J.S. Lawson, M.L. Lee, Fabrication of highly cross-linked reversed-phase monolithic columns via living radical polymerization, *J. Chromatogr. A* 1367 (2014) 1367–1390. doi: 10.1016/j.chroma.2014.09.046

[51] P. Aggarwal, H.D. Tolley, J.S. Lawson, M.L. Lee, High efficiency polyethylene glycol diacrylate monoliths for reversed-phase capillary liquid chromatography of small molecules, *J. Chromatogr. A* 1364 (2014) 96–106. doi: 10.1016/j.chroma.2014.08.056

[52] F.R. Mansour, S. Waheed, B. Paull, F. Maya, Porogens and porogen selection in the preparation of porous polymer monoliths, *J. Sep. Sci* 43 (2019) 56–69. doi: 10.1002/jssc.201900876

[53] X. Ding, J. Yang, Y. Dong, Advancements in the preparation of high-performance liquid chromatographic organic polymer monoliths for the separation of small-molecule drugs, *J. Pharm. Anal* 8 (2018) 75–85. doi: 10.1016/j.jpha.2018.02.001

[54] J. Qin, C. Yang, Y. An, E. Liu, L. Bai, H. Liu, Preparation of an ionic liquid-functionalized polymer monolith and its application in the separation of Chinese herb with HPLC, *J. Liq. Chromatogr. Relat. Technol.* 39 (2016) 568–573. doi: 10.1080/10826076.2016.1204552

[55] L. Bai, J. Wang, H. Zhang, S. Liu, J. Qin, H. Liu, Ionic liquid as porogen in the preparation of a polymer-based monolith for the separation of protein by high performance liquid chromatography, *Anal. Methods* 7 (2015) 607–613. doi: 10.1039/c4ay02200a

[56] F. Svec, Porous polymer monoliths: Amazingly wide variety of techniques enabling their preparation, *J. Chromatogr. A* 1217 (2010) 902–924. doi: 10.1016/j.chroma.2009.09.073

[57] R. Koeck, M. Fischnaller, R. Bakry, R. Tessadri, G.K. Bonn, Preparation and evaluation of monolithic poly(N-vinylcarbazole-co-1,4-divinylbenzene) capillary columns for the separation of small molecules,

Anal. Bioanal. Chem. 406 (2014) 5897–5907. doi: 10.1007/s00216-014-8007-1

[58] R. Koeck, R. Bakry, R. Tessadri, G.K. Bonn, Monolithic poly(N-vinylcarbazole-co-1,4-divinylbenzene) capillary columns for the separation of biomolecules, *Analyst* 138 (2013) 5089–5098. doi: 10.1039/c3an00377a

[59] V. Bernabé-Zafón, M. Beneito-Cambra, E.F. Simó-Alfonso, G. Ramis-Ramos, J.M. Herrero-Martínez, Photo-polymerized lauryl methacrylate monolithic columns for CEC using lauroyl peroxide as initiator, *Electrophoresis* 30 (2009) 3748–3756. doi: 10.1002/elps.200900038

[60] F. Maya, F. Svec, A new approach to the preparation of large surface area poly(styrene-co-divinylbenzene) monoliths via knitting of loose chains using external crosslinkers and application of these monolithic columns for separation of small molecules, *Polymer* 55 (2014) 340–346. doi: 10.1016/j.polymer.2013.08.018

[61] S. Janků, V. Škeříková, J. Urban, Nucleophilic substitution in preparation and surface modification of hypercrosslinked stationary phases, *J. Chromatogr. A* 1388 (2015) 151–157. doi: 10.1016/j.chroma.2015.02.038

[62] S.D. Chambers, F. Svec, J.M.J. Fréchet, Incorporation of carbon nanotubes in porous polymer monolithic capillary columns to enhance the chromatographic separation of small molecules, *J. Chromatogr. A* 1218 (2011) 2546–2552. doi: 10.1016/j.chroma.2011.02.055

[63] M. Navarro-Pascual-Ahuir, R. Lucena, S. Cárdenas, G. Ramis-Ramos, M. Valcárcel, J.M. Herrero-Martínez, UV-polymerized butyl methacrylate monoliths with embedded carboxylic single-walled carbon nanotubes for CEC applications, *Anal Bioanal Chem* 406 (2014) 6329–6336. Doi: 10.1007/s00216-014-8050-y

[64] S.D. Chambers, T.W. Holcombe, F. Svec, J.M.J. Fréchet, Porous polymer monoliths functionalized through copolymerization of a C60 fullerene-containing methacrylate monomer for highly efficient separations



of small molecules, *Anal. Chem.* 83 (2011) 9478–9484. doi: 10.1021/ac202183g

[65] Q. Cao, Y. Xu, F. Liu, F. Svec, J.M.J. Fréchet, Polymer monoliths with exchangeable chemistries: use of gold nanoparticles as intermediate ligands for capillary columns with varying surface functionalities, *Anal. Chem.* 82 (2010) 7416–7421. doi: 10.1021/ac1015613

[66] Y. Lv, F. Maya-Alejandro, J.M.J. Fréchet F. Svec, Preparation of porous polymer monoliths featuring enhanced surface coverage with gold nanoparticles, *J. Chromatogr. A* 1261 (2012) 121–128. doi: 10.1016/j.chroma.2012.04.007

[67] M. Navarro-Pascual-Ahuir, M.J. Lerma-García, G. Ramis-Ramos, E.F. Simó-Alfonso, J.M. Herrero-Martínez, Preparation and evaluation of lauryl methacrylate monoliths with embedded silver nanoparticles for capillary electrochromatography, *Electrophoresis* 34 (2013) 925–934. doi: 10.1002/elps.201200408

[68] W. Lei, L.Y. Zhang, L. Wan, B.F. Shi, Y.Q. Wang, W.B. Zhang, Hybrid monolithic columns with nanoparticles incorporated for capillary electrochromatography, *J. Chromatogr. A* 1239 (2012) 64–71. doi: 10.1016/j.chroma.2012.03.065

[69] A. Weller, E.J. Carrasco-Correa, C. Belenguer-Sapiña, A. Mauri-Aucejo, P. Amorós, J.M. Herrero-Martínez, Organo-silica hybrid capillary monolithic column with mesoporous silica particles for separation of small aromatic molecules, *Microchim. Acta* 184 (2017) 3799–3808. doi: 10.1007/s00604-017-2404-z

[70] E.J. Carrasco-Correa, G. Ramis-Ramos, J.M. Herrero-Martínez, Hybrid methacrylate monolithic columns containing magnetic nanoparticles for capillary electrochromatography, *J. Chromatogr. A* 1385 (2015) 77–84. doi: 10.1016/j.chroma.2015.01.044

[71] S. Yang, F. Ye, Q. Lv, C. Zhang, S. Shen, S. Zhao, Incorporation of metal-organic framework HKUST-1 into porous polymer monolithic

capillary columns to enhance the chromatographic separation of small molecules, *J. Chromatogr. A* 1360 (2014) 143-149. doi: 10.1016/j.chroma.2014.07.067

[72] E.J. Carrasco-Correa, A. Martínez-Vilata, J.M. Herrero-Martínez, J.B. Parra, F. Maya, V. Cerdà, C. Palomino-Cabello, G. Turnes-Palomino, F. Svec, Incorporation of zeolitic imidazolate framework (ZIF-8)-derived nanoporous carbons in methacrylate polymeric monoliths for capillary electrochromatography, *Talanta* 164 (2017) 348-354. doi: 10.1016/j.talanta.2016.11.027

[73] F. Maya, C. Palomino-Cabello, A. Figuerola, G. Turnes-Palomino, V. Cerdà, Immobilization of metal–organic frameworks on supports for sample preparation and chromatographic separation, *Chromatographia* 82 (2019) 361–375. doi: 10.1007/s10337-018-3616-z

**Bloque II. Evaluación del potencial de  
nuevos materiales porosos en técnicas  
de (micro)extracción**



**Capítulo 3. In syringe hybrid monoliths modified with gold nanoparticles for selective extraction of glutathione in biological fluids prior to its determination by HPLC**





## In syringe hybrid monoliths modified with gold nanoparticles for selective extraction of glutathione in biological fluids prior to its determination by HPLC

Oscar Mompó-Roselló, María Vergara-Barberán, Ernesto F. Simó-Alfonso, José Manuel Herrero-Martínez  

Department of Analytical Chemistry, Faculty of Chemistry, University of Valencia, Dr Moliner 50, 46100, Burjassot, Valencia, Spain

In this work, a simple device for extraction glutathione (GSH) in biological fluids using a hybrid monolithic material within a polypropylene syringe is developed. For this purpose, glycidyl methacrylate-based monolith was firstly prepared within this housing material, and the polymer was modified with different ligands (ammonia, cysteamine and cystamine). The resulting materials (containing amine or thiol groups, respectively) were then functionalized with gold nanoparticles (AuNPs). The hybrid material that gave the largest AuNPs coverage was selected as solid-phase (SPE) sorbent and several variables affecting the extraction recovery of this compound were investigated. Under optimal conditions, GSH was quantitatively retained at pH 6.0, and then it was desorbed with aqueous dithiothreitol solution and determined, after derivatization with o-phthaldialdehyde, via reversed-phase LC with fluorometric detection. The limit of detection was *ca.* 1.5 ng mL<sup>-1</sup>, and the reproducibility between extraction units was below 8% (expressed as relative standard deviation), which demonstrates the robustness of the method. The developed material was also applied for the extraction of GSH in saliva and urine samples yielding recoveries ranging from 86 to 105%.

**Keywords:** hybrid monolith; gold nanoparticles; solid-phase extraction; glutathione; biological fluids

### **3.1. Introduction**

Glutathione ( $\gamma$ -L-glutamyl-L-cysteinyl-glycine, GSH) is the most relevant low-molecular weight antioxidant synthesized in the prokaryotic and eukaryotic cells [1]. This tripeptide has involved in several roles in biological systems. Thus, one well-characterized role of GSH concerns its involvement as a reaction partner in the detoxification of xenobiotics. Besides, GSH is essential for the regulation of cell proliferation [2], and keeps the thiol redox potential in the cells by preserving thiol groups of proteins in the reduced form [1]. The GSH system is also very significant for the cellular defense against oxidative stress and diseases derived from this undesirable phenomenon [1]. Indeed, its depletion in certain biological fluids could be implicated in aging and the pathogenesis of many diseases, such as rheumatoid arthritis, muscular dystrophy and Alzheimer's disease, among others [3]. Thus, the accurate analysis of this compound in biological fluids is a relevant issue for the diagnosis of these serious diseases.

However, the determination of GSH in these matrices represents a challenge due to the ease GSH oxidation jointly with the enzymatic proteolysis of GSH by  $\gamma$ -glutamyl transpeptidase [4, 5]. Thus, precautions that minimize its oxidation and proteolysis during sample collection and treatment including refrigeration and protein precipitation by acidification have been adopted. In addition, the absence of a strong chromophore or fluorophore group in GSH requires a suitable derivatization protocol followed by HPLC analysis [6]. In this sense, several pre-column derivatization methodologies using several reagents such as 5,5'-dithiobis(2-nitrobenzoic acid) [7], o-phthaldialdehyde (OPA) [8] monobromobimane [9] and 4-chloro-3,5-dinitrobenzotrifluoride [10], among others, have been adopted in many fields to improve selectivity and detection properties.

On the other hand, due to the low-concentration of this analyte in biosamples (such as tissue, blood, serum, and urine), a pre-concentration step using solid-phase extraction (SPE) or other extraction techniques is



indispensable to achieve a sensitive determination. In any case, the strong polarity and instability of GSH represent a challenge, since it is difficult to extract polar GSH from aqueous samples by use of conventional methods. However, the eluent solution (mixed directly with the derivatizing reagent) used to achieve a proper extraction yield and high enrichment factor can strongly influence on the efficiency of derivatization reaction, and even produce a non-uniform tagging [11].

In the last decade, nanostructured materials have led to a wide variety of challenging possibilities in sample preparation. Their particular features such as large available surface area and multiform morphologies, which can be used to increase analyte-sorbent interactions, speed up mass transfer and modify selectivity, turning them into excellent sorbents for SPE. In particular, gold nanoparticles (AuNPs) have received attention as sorbents due to their strong affinity towards compounds containing thiol moieties. Thus, citrate-stabilized AuNPs have been applied as trapping support of GSH in white wines [12], whereas these NPs capped with non-ionic surfactants have been used to determine aminothiols in human urine and protein-bound aminothiols in human plasma [13-16]. Recently, Wei *et al.* [17] have reported the use of polystyrene nanofibers coated with CuNPs as SPE-based material applied to the extraction of GSH in urine samples. Most of these works [13-15] are based on dispersive SPE; however, this extraction mode can produce analyte loss or desorption from the surface of NPs during washing or centrifugation steps. In this sense, the extraction and enrichment of GSH in complex mixtures could be improved by incorporating AuNPs onto a carrier or support to act as new kind of SPE sorbent.

In recent years, the incorporation of NPs to monoliths have emerged as smart strategy to enhance selectivity and to improve the extraction efficiencies of polymer-based monoliths as well as NP-based materials. Thus, studies of polymeric monoliths modified with AuNPs for peptide and protein enrichment purposes have been reported [18-19]. For example, Vergara-

Barberán *et al.* [20] have demonstrated the potential of a gold modified polymeric material within a 1 mL SPE cartridge for the selective extraction of lectins and viscotoxins (sulphur-rich proteins) in mistletoe extracts. The sorbents showed large recovery efficiencies ( $> 82\%$ ), loading capacities (up to  $29.3 \text{ mg g}^{-1}$  sorbent) and satisfactory reusabilities (at least 20 times). In spite of these good features, the scale-up or extension of hybrid monolithic materials to efficient and miniaturized-based systems devoted to sample treatment remains scarce.

In this study, a hybrid material based on a polymer monolith modified with AuNPs was used as SPE sorbent within a polypropylene syringe for the selective and efficient extraction of GSH in biological fluid samples. For this purpose, glycidyl methacrylate (GMA)-based monolith was firstly prepared within polypropylene syringes, which were previously modified by photografting with ethylene glycol dimethacrylate to assure a covalent attachment of monolith. Then, the polymer was treated with different ligands (ammonia, cysteamine and cystamine). The resulting materials (containing amine or thiol groups, respectively) were subsequently functionalized with AuNPs. The hybrid material that provided the largest AuNPs coverage was then selected as SPE sorbent and it was investigated in terms of extraction efficiency through parameters such as the sample pH, elution solvent, etc. Under the optimized conditions, the hybrid monolithic microdevices were successfully applied to the extraction of glutathione in saliva and urine samples followed its analysis by HPLC coupled with fluorescence detection, thus demonstrating the fruitful combination of these materials with (micro)analytical systems for sample treatment purposes.

## **3.2. Experimental**

### *3.2.1. Reagents and standards*

Glycidyl methacrylate (GMA), ethylene glycol dimethacrylate (EDMA), benzophenone (BP), cyclohexanol, 1-dodecanol, 2,2-dimethoxy-2-phenylacetophenone (DMPA), cystamine dihydrochloride, cysteamine, tris(2-carboxyethyl)phosphine hydrochloride (TCEP), L-glutathione reduced (GSH), o-phthaldialdehyde (OPA), DL-dithiothreitol (DTT) were obtained from Sigma-Aldrich (Milwaukee, WI, USA). Acetonitrile (ACN), methanol (MeOH), trifluoroacetic acid (TFA), trichloroacetic acid (TCA), boric acid, sodium chloride, ethylenediaminetetraacetic acid (EDTA), hydrochloric acid, nitric acid, calcium chloride, sodium hydroxide ammonia solution (25%) were purchased from Scharlab (Barcelona, Spain). Gold nanoparticles (AuNPs) suspension stabilized with sodium citrate (particle size, 20 nm,  $6.54 \cdot 10^{11}$  particles  $\text{mL}^{-1}$ ) were from Alfa Aesar (Lancashire, United Kingdom). Monosodium and disodium phosphate, magnesium sulphate heptahydrate and orthophosphoric acid were from Merck (Darmstadt, Germany). Deionized water was prepared in Crystal B30 EDI Adrona deionizer (Riga, Latvia) was used in all procedures. Stock solution of GSH was daily prepared by dissolving appropriate amounts of this aminothiols in deionized water in brown flask, and working standard solutions were obtained by dilution of the stock solution. Phosphate buffer solutions (PBS) of 25  $\text{mmol L}^{-1}$  at several pH values were prepared by mixing appropriate amounts of  $\text{Na}_2\text{HPO}_4$ ,  $\text{NaH}_2\text{PO}_4$  and  $\text{H}_3\text{PO}_4$  according to the required pH. Polypropylene syringes of 1 mL (used as support for the SPE sorbent) were purchased from Henke Sass Wolf (Keltenstraße4, Tuttlingen, Germany).

### *3.2.2. Instrumentation*

Photografting of polypropylene wall surface and photopolymerization of monoliths were carried out using a UV radiation chamber CL-1000 (UVP, Upland, Canada). A syringe pump (model 101, KD Scientific, Holliston, MA,

USA) was used to perform functionalization of monolithic beds. The morphology of the materials was characterized using a scanning electron microscope (S-4800, Hitachi, Ibaraki, Japan) equipped with a backscattered electron detector and a X-ray microanalysis system (EDAX Genesis 400). The determination of gold content in the hybrid monoliths was also done by using an inductive coupling plasma equipment connected to mass spectrometer (ICP-MS) (model 7900, Agilent Technologies, Waldbronn, Germany). A micro star 17R from VWR chemicals (Radnor, USA) centrifuge was used for the sample treatment protocol.

Chromatographic experiments were conducted on Jasco Analytica (Madrid, Spain), composed of a PU-2089 quaternary gradient pump, an AS-2055 autosampler with a 20  $\mu\text{L}$  injection loop and FP-2020 Plus fluorescence detector (Jasco Analytica). The system was controlled using the LC-NETII/AFC interface also supplied by Jasco. Acquisition and data treatment was performed using the ChromNAV software (version 1.17.01, Jasco).

### *3.2.3. Surface modification of polypropylene syringes*

Prior to preparation of monolithic phase into the syringe, the inner surface of this support was modified by photografting with BP and EDMA [18] in order to achieve a covalent attachment of monolithic beds. Briefly, the inner surface of 1 mL polypropylene syringe was sequentially washed with MeOH and acetone, and dried under a nitrogen stream. Then, the syringe was filled with 100  $\mu\text{L}$  of a deoxygenated 5% (w/v) methanolic BP solution and sequentially irradiated with UV light ( $1 \text{ J}\cdot\text{cm}^{-2}$ ) for 10 min followed by a MeOH rinse and drying step with nitrogen. Next, the syringe was filled with 100  $\mu\text{L}$  of a 15% (v/v) methanolic EDMA solution and irradiated again with UV light for 10 min. Finally, the modified syringe was washed thoroughly with acetone and dried under a nitrogen stream before use.

#### *3.2.4. Preparation of generic monolith within the syringe*

A poly (GMA-*co*-EDMA) monolith was prepared in the vinylized syringe (50  $\mu\text{L}$  of the polymerization mixture, 20 mg of monolith after polymerization) by UV-initiated radical polymerization. The composition of the polymerization mixture was as follows: 40 wt% monomers (32 wt% GMA and 8 wt% EDMA) and 60 wt% porogens (56 wt% cyclohexanol and 4 wt% 1-dodecanol), in the presence of 0.1 wt% DMPA (out of the total weight of the monomers). Next, the mixture was homogenized by sonication for 10 min, and then purged with nitrogen for 10 more min. Once the mixture was filled into the syringe, it was placed under UV light for 2 h. After that, the monolith was rinsed with MeOH during 30 min at 5  $\mu\text{L min}^{-1}$  to remove the porogenic solvents and possible unreacted monomers. Then, the monoliths were dried in the oven at 60°C overnight.

#### *3.2.5. Modification of GMA-based monolith with amino- or thiol-groups and posterior functionalization with AuNPs*

After the polymerization, the porous material was treated with 3 different nucleophilic reagents (ammonia, cysteamine and cystamine) according to the following procedures. In the first protocol [19], the GMA-based monolith was modified by passing through aqueous 4.5 mol L<sup>-1</sup> ammonia at 60 °C (water bath) at 5  $\mu\text{L min}^{-1}$  using a syringe pump for 2 h. Upon completion of the reaction, the material was washed with deionized water to remove the excess of ammonia until the eluent was neutral pH. This reaction generates amino groups on the surface of the monolith.

In the second procedure, the monolith was modified using cysteamine in order to provide thiol moieties [21]. For this purpose, 2.5 mol L<sup>-1</sup> cysteamine aqueous solution was pumped through the parent monolith at a flow rate of 5  $\mu\text{L min}^{-1}$  for 2 hours at room temperature. The syringe was then rinsed with water to remove excess reagents until neutral pH.

The last used protocol [22], a 1.0 mol L<sup>-1</sup> cystamine dihydrochloride solution (prepared in 2.0 mol L<sup>-1</sup> aqueous sodium hydroxide), which it was first pumped through the monolith at 60 °C at a flow rate of 5 μL min<sup>-1</sup> for 2 h and then washed until neutral pH. Then, a TCEP solution (0.25 mol L<sup>-1</sup> in an equal concentration NaOH solution) was also pumped through the monolith at room temperature at a flow rate of 5 μL min<sup>-1</sup> for 2 h to achieve cleavage of disulphide bonds. The column was then washed with water until neutral pH.

The resulting materials were treated by passing through the syringe a commercial AuNPs dispersion at 0.3 mL min<sup>-1</sup> until saturation of the monolithic materials with NPs, by monitoring the UV-vis spectra of the supernatants as we previously described [20]. The presence of the AuNPs was also easily recognizable by the colour-change of the material, which it passed from clear white to intense pink.

The prepared hybrid materials were characterized by SEM. Moreover, their Au content was evaluated by using energy dispersive analysis of X-rays (EDAX) and ICP-MS. For these latter measurements, all materials were previously calcined at 550°C for 1 h, and the resulting pellets were dissolved in *aqua regia*, properly diluted with water and analyzed by ICP-MS.

### *3.2.6. Sample extraction and pretreatment*

Human biological fluids (saliva and urine) were obtained from a healthy adult volunteer. For the saliva, a prior gargling with distilled water for 5 minutes was done to remove all the possible pollutes. After that, the donor kept tongue in touch with palate and made the saliva naturally flow down into 2 mL tubes. Then, the saliva and urine samples were stored at -20 °C until analysis. The pretreatment method of both samples was adapted from Zhang *et al.* [10] with certain modifications. After thawing, 1000 μL of sample (saliva or urine) was mixed with 100 μL of a solution of TCEP (50 mmol L<sup>-1</sup> in borate buffer at pH 7.4) in a vial and incubated at 25 °C for 10 min. Then, 900 μL of a solution containing 1 % (m/v) TCA and 1 mmol L<sup>-1</sup> EDTA was

added and the resulting solution was centrifuged for 10 min at 10000 g. The obtained supernatant was properly neutralized and collected for the subsequent pretreatment or analysis.

### *3.2.7. microSPE protocol*

A (micro)SPE procedure was applied to the selected hybrid material for the extraction of GSH in aqueous solutions and biological fluid samples. Thus, a preactivating step of sorbent was done with ACN (500  $\mu\text{L}$ ) and equilibrated with 25 mM PBS at pH 6.0 (500  $\mu\text{L}$ ). Next, 200  $\mu\text{L}$  of standard solutions (prepared in in the same buffer) or biological samples (treated as above) were loaded onto the syringe. Then, the material was washed with PBS solution (200  $\mu\text{L}$ ), and the retained analyte was eluted with DTT 0.5 mol L<sup>-1</sup> (200  $\mu\text{L}$ ). The regeneration of sorbent was done with water at 80°C during 2 h [19]. The same procedure was applied to prepare a blank sorbent (GMA-based monolith).

### *3.2.8. GSH derivatization and LC analysis*

The OPA functionalization protocol was adapted from Wei *et al.* [17]. Thus, 100  $\mu\text{L}$  of the collected fraction (in the different SPE steps) and the same volume of the derivatization reagent (100 mM OPA in 0.7 M borate buffer at pH 9, 20 % MeOH solution) were mixed and let to react for 1.0 minute at room temperature. The resulting solution was filtered through a 0.45  $\mu\text{m}$  filter membrane (Millipore Corporation, Belfast, MA, USA) and injected into the chromatographic system.

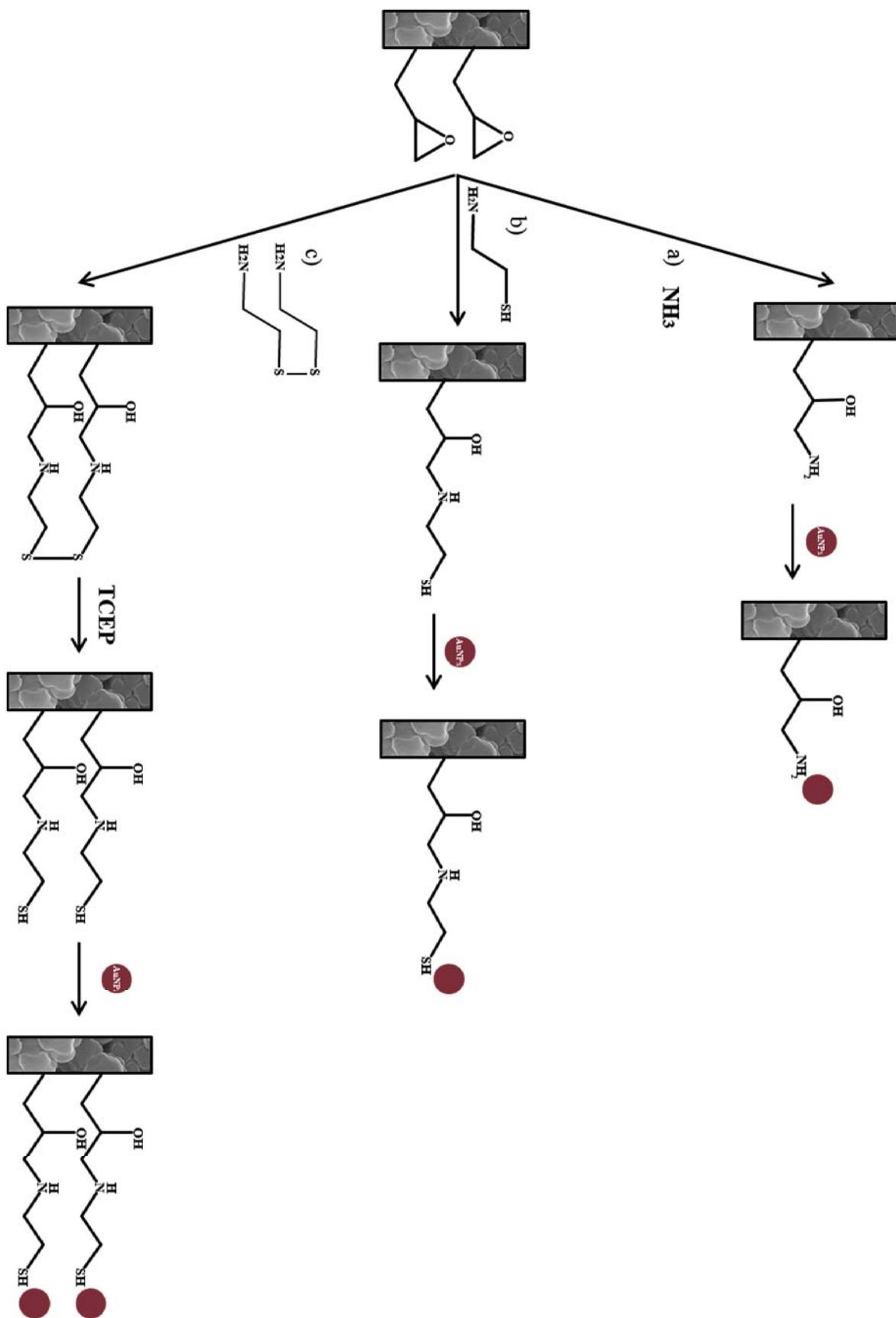
The separation of fluorescent isoindole derivative (GSH-OPA) was done on a Kinetex C18 column (150 x 4.6 mm, 2.6  $\mu\text{m}$ , 100 Å, Phenomenex, Torrance, USA). The HPLC system was operated under isocratic mode using a mobile phase consisted of 23/77 (v/v) MeOH/H<sub>2</sub>O mixture containing 20 mM PBS at pH 6.0. The flow rate was 0.75 ml min<sup>-1</sup> and the column temperature was 25°C. The GSH was measured at excitation and emission wavelengths set at 340 nm and 462 nm, respectively.

### **3.3. Results and discussions**

#### *3.3.1. Choice of hybrid monoliths functionalized with AuNPs*

As we mentioned in the Introduction, polymeric materials modified with AuNPs has been previously used in our research group as sorbents in SPE cartridges for isolation of proteins. In particular, GMA-based monoliths were synthesized to be subsequently chemically modified by using two different ligands (ammonia and cysteamine). AuNPs were then assembled to the amino or thiol groups present in the resulting polymers. In spite of the good features of these sorbents, a reduction in the preparation protocol (by avoiding grinding and sieving processes) is highly desirable. In this sense, a simple approach based on in situ UV-initiated polymerization of GMA-monolith within activated polypropylene syringes (according ref. [23, 24]) was adopted. Then, this monolith was modified with the two prior ligands as well as another ligand (cystamine) was included. This ligand has been previously used by Svec and coworkers [22] to provide monoliths with enhanced surface coverage with AuNPs. **Figure 3.1** shows the scheme of modification reactions of GMA-based material with mentioned ligands and posterior immobilization of AuNPs. Thus, the AuNPs functionalized materials (with different ligands) were analyzed by ICP-MS (as described in Section 2.5) to determine the total Au content, giving 0.029, 0.27 and 0.79 wt% for the ammonia-, cysteamine-, and cystamine-modified monoliths, respectively. Also, EDAX was used to evaluate the amount of Au in the surface of hybrid monoliths. For this purpose, different areas (1 and 10  $\mu\text{m}^2$ ) in several regions of hybrid materials were measured (see Supplementary Information, **Figures 3.S1-S2**, respectively). For example, the content in Au ranged from 22.3 to 29.2 wt% for the cystamine-modified monolith. Thus, these values were similar to that observed by Connolly et al. [25], but lower than those reported by Svec's group [22].

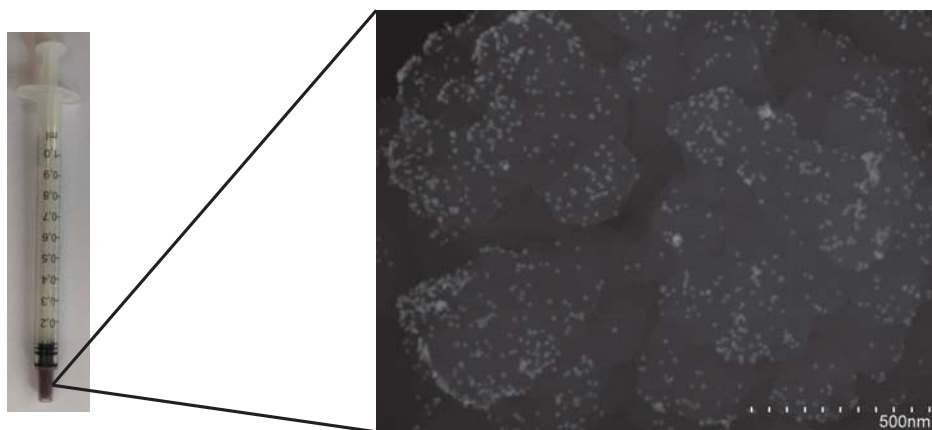




**Figure 3.1.** Scheme of functionalization of GMA-based material in syringe with: (a) ammonia, (b) cysteamine and (c) cysteamine, and subsequently immobilization with AuNPs.

These dissimilarities in terms of Au content could be explained taking into account several factors. On the one side, the format used here (syringe) in the synthesis of bulk monoliths is rather different from that (fused-silica capillaries) described in ref. [22], which might affect the accessible number of reactive sites in the parent monolith [26]. On the other hand, other important issue to be considered is the technique used for the Au evaluation in the resulting hybrid monoliths. Thus, EDX analysis (used in this study and refs. [22, 25]) provides only a semi-quantitative estimation (“local analysis”) of Au content in the surface of the material, while ICP allows the determination of bulk Au content in the materials.

On the basis of the results obtained above, polymer monoliths modified with cysteamine and functionalized with AuNPs was chosen as sorbent for extraction of GSH. Moreover, SEM micrographs of this hybrid material were obtained (**Figure 3.2**), showing the presence of a large number of AuNPs covering the monolith surface.



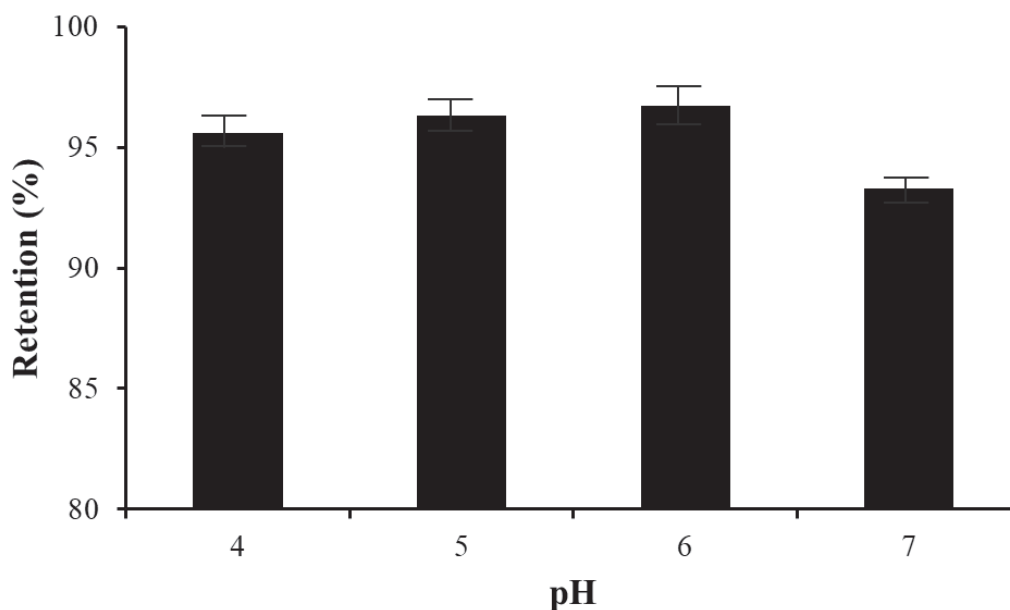
**Figure 3.2.** Photograph of AuNP-modified monolithic syringe using cysteamine-modified monolith and its corresponding SEM micrograph (at 80 000 $\times$  magnification).

### *3.3.2. Optimization of microSPE conditions*

Using the selected hybrid monolith, the parameters that may influence on the extraction efficiency of GSH such as the sample pH and elution conditions

were studied. Sample pH is an important factor that affects ionization state of target analyte and also the effective surface charge of the sorbent, which can influence on the extraction performance of GSH. For this reason, the effect of sample pH (in the range of 4 - 7) on the loading SPE step was studied. Thus, solutions (200  $\mu\text{L}$ ) containing 30  $\mu\text{mol L}^{-1}$  of GSH ( $\text{pK}_{\text{as}}$  of 2.50 and 3.40 for glutamate and glycine carboxylic acids, respectively, and 9.49 for the glutamate amino group) were selected to perform the retention studies. As shown in **Figure 3.3**, large retentions ( $> 95\%$ ) in the loading step were obtained along 4.0–6.0. This result is in agreement with the findings reported in literature, where the maximum adsorption of amino thiols onto the metal surface is usually observed at zwitterion form of these molecules [27, 28]. Under these conditions, the electrostatic interactions between the amino thiol molecule and the sorbent are favoured. When the pH was modified out of zwitterionic form range, a less favorable retention was obtained. At basic pH, the GSH molecules become less zwitterionic leading to repulsion interactions between these molecules and the citrate-coated Au surfaces and/or between adjacent adsorbed GSH molecules onto Au surface. On the other hand, at lower pH, the carboxylic groups of GSH become protonated and favorable hydrogen bonding between GSH molecules are promoted in detrimental of its adsorption onto AuNPs surface [27, 28]. At sight of these results, a pH of 6.0 was selected as compromise to achieve the highest extraction recovery. Then, the washing step was done at this pH, where no significant losses ( $< 0.2\%$ ) were obtained.

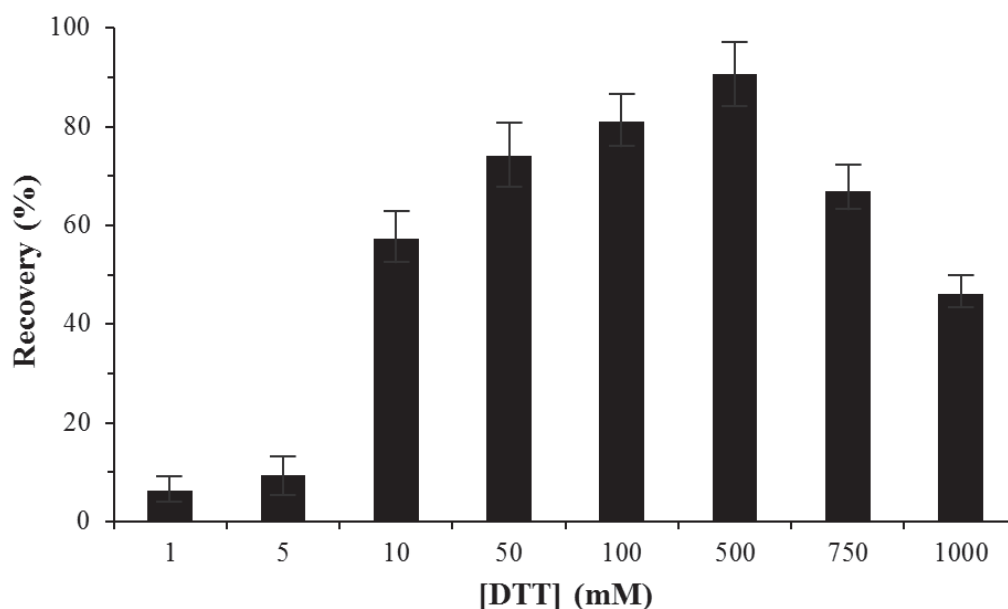
Once the retention of GSH was studied, its elution from the AuNP surface was investigated. Due to strong affinity of these NPs for thiol-containing ligands, the desorption of this molecule from the nanostructured sorbent is not an easy task. For this purpose, several thiol-compound solutions have been described in literature to achieve an efficient desorption [13, 14, 15, 17] via ligand-exchange reaction.



**Figure 3.3.** Influence of pH on retention of GSH using AuNP-modified monolithic syringe. Error bar = SD (n = 3).

In order to ensure a successful completion of the ligand exchange in short time, an excess of the incoming thiol is commonly used (approximately 90-200 molar equivalents with respect to the NP for most thiols) [29]. Smaller amounts of thiol result in incomplete exchange, giving worse recovery efficiencies. Thus, thioglycolic acid was firstly considered as ligand to remove the adsorbed GSH onto the gold surface. However, this reagent gave low extraction yields (up to 100 mM was tested) and interfered with derivatization reaction with OPA. Then, 1,4-dithiothreitol (DTT) was examined as thiol reagent for the desorption of the extracted compound. **Figure 3.4** shows the effect of the DTT concentration (1-1000 mM) on the extraction recovery of GSH at a concentration of 30  $\mu\text{M}$  (*ca.* 9  $\mu\text{g mL}^{-1}$ ). As can be observed, the extraction recovery increased with increasing DTT concentration up to 500 mM. Concentrations above this value led to a decrease in the recovery efficiency of GSH, which can be explained by interferences of the excess of this reagent with OPA derivatization of GSH. Hence, the concentration of DTT might be kept at an appropriate level to obtain satisfactory extraction efficiencies. Thus, a solution containing 500 mM DTT was chosen as

desorption solvent for all subsequent experiments. Once the working SPE conditions were optimized, several analytical parameters such as breakthrough volume, loading capacity and reusability of sorbent were evaluated. Thus, the breakthrough volume of the (micro)SPE device was tested by percolating variable volumes (0.2–1.5 mL) of GSH standard solution (**Figure 3.S3**). Experimental results showed recoveries above 90% up to 1.25 mL, whereas a considerable decrease in the recoveries of this analyte was observed at larger volumes. The loading capacity was also measured by passing through the syringe SPE device by keeping constant the working conditions of SPE procedure, giving a maximum value of 2.93 mg of GSH per g of hybrid monolithic material. Below this value, excellent performance of sorbent with recoveries higher than 75% was observed. The reusability of this sorbent (200  $\mu$ L of 30  $\mu$ M GSH) was also evaluated (**Figure 3.S4**). For this purpose, the proposed SPE sorbent was repeatedly used by employing the regeneration protocol described in Section 5.2.7. An excellent performance with recoveries higher than 90% for GSH was observed after 15 re-cycles.



**Figure 3.4.** Effect of DTT concentration on recovery of GSH using AuNP-modified monolithic syringe. Error bar = SD (n = 3).

Besides, the proposed (micro)extraction procedure needed a small total volume of liquid solution (< 1 mL, including all SPE steps), which was lower than that required for conventional SPE cartridges (around 5-20 mL), being a significant advance in terms of green aspects of sample preparation. Furthermore, the required volume of sample was 200  $\mu\text{L}$ , being a great benefit to monitor GSH in biological fluids as we demonstrated below.

### *3.3.3. Validation of the method and application to real samples*

The proposed SPE protocol combined with LC coupled to fluorescence detection was validated in terms of linearity, sensitivity and precision. A good linearity ( $R > 0.9998$ ) was obtained in the range of  $4.6 \cdot 10^{-3}$ -1500  $\mu\text{g mL}^{-1}$  ( $1.5 \cdot 10^{-2}$ -5700  $\mu\text{M}$ ) for GSH. The limit of detection (LOD) and limit of quantitation (LOQ) were also estimated based on signal-to-noise ratios of 3 and 10, respectively. Thus, the LOD and LOQ values were 5 and 15 nM (1.53 and 4.59  $\text{ng mL}^{-1}$ ), respectively. The reproducibility of preparation of in syringe hybrid monoliths as sorbent was tested. Thus, the precision for the intra- and inter-(micro)extraction devices was evaluated. By using the same device, the extraction recoveries of GSH for intra- and inter-day ( $n = 3$ ) were below than 2.8% and 5.3%, respectively. The device-to-device precision was less than 7.8% RSDs with 83.7-90.4% recoveries ( $n = 3$ ). Therefore, the above results suggest the good repeatability and reproducibility of hybrid polymer monoliths. Another analytical parameter evaluated was the enrichment factor, which was calculated by comparison of the slopes of the calibration graphs before and after extraction process, giving a value of 5.8 for the proposed methodology.

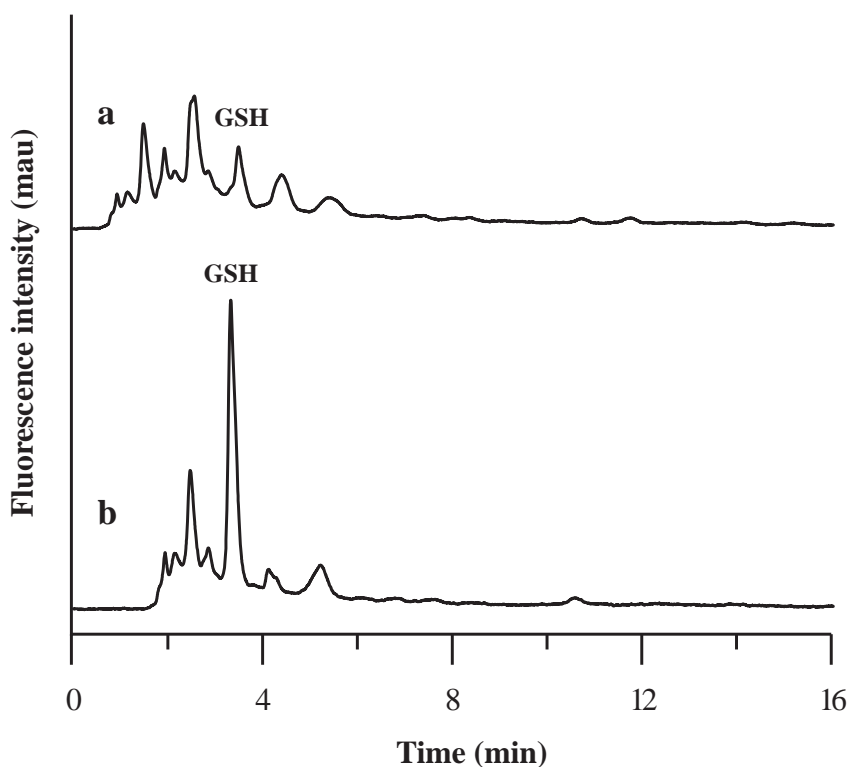
Then, the SPE sorbent described here was compared with reports related to the use of other nanomaterials for GSH extraction in biological fluids (**Table 3.1**).

**Table 3.1.** Comparison with other reported nanomaterial-based methods for GSH extraction.

<b>Material</b>	<b>Extraction technique</b>	<b>Detection method</b>	<b>Recoveries (%)</b>	<b>LOD</b>	<b>Ref</b>
Tween 20-capped AuNPs	dsPE	UV detection	97.1-99.4	3.1	[14]
CuNPs-assembled nanofibers	PFSPE	Fluorescence	94.6-98.6	1.1	[16]
MnO <sub>2</sub> nanosheet-gated mesoporous silica NPs	No extraction	Electrochemical glucose meter	97.5-102.5	10.4	[28]
AuNPs	dsPE	Graphene-based MALDI-TOF	-	625	[29]
Carbon dots-Cu <sup>2+</sup>	dsPE	Fluorescence	93.8-103.6	26.4	[30]
AuNPs modified-monolith	microSPE	Fluorescence	86-105	1.5	

dsPE: dispersive SPE, PFSPE: packed-fiber SPE

Regarding extraction recovery values obtained in this study, these were similar to those found in reported studies. Concerning the LODs, our LOD value was similar [15, 17] or lower [30-32] than studies described in **Table 3.1**. Besides, our SPE support method offers an increased surface area-to-volume ratio, without losses of material and analyte compared to dispersive SPE [15, 31, 32], where analyte loss or desorption from the surface of NPs occurred during washing or centrifugation steps. Moreover, other strength of our sorbent is its satisfactory reusability (see data above). In this regard, in the related studies of NP-based materials (see **Table 3.1**), this important parameter was not evaluated or this information was missing.



**Figure 3.5.** Chromatograms of urine without (a) and with pretreatment (b) using AuNP-modified monolithic syringe. Chromatographic conditions as in section 5.2.8.



This fact confirms the suitability of the hybrid material to be used as sorbent in SPE for clean-up purposes. **Table 3.2** shows the recovery values obtained in all matrices investigated. The mean recoveries for GSH at two spiked levels were in the range of 86-105 %. Moreover, standard addition calibration curves were obtained by adding to the samples at least four solutions with increasing concentrations, taking into account the linearity range given above. For saliva samples, the slope of calibration curve did not differ significantly from that obtained with the external calibration method, in contrast with that found for real urine samples. From these results, it can be derived that standard addition method was required for the determination of this analyte in real urine samples. On the basis of these considerations, the concentrations of GSH in saliva and urine samples were estimated, being  $7.88 \pm 0.04$  and  $17.0 \pm 0.6 \mu\text{mol L}^{-1}$ , respectively.

**Table 3.2.** Recovery study of GSH in spiked samples analyzed following AuNPs-modified monolithic syringe device.

Sample	Spiked level ( $\mu\text{M}$ )	
	3	30
Saliva	$89.2 \pm 5.2$	$86.1 \pm 6.4$
Artificial urine	$105.2 \pm 3.1$	$96.8 \pm 4.2$
Urine	$94.3 \pm 10.1$	$92.9 \pm 8.4$

### **3.4. Conclusions**

This study presents the preparation of AuNPs-modified monoliths in a syringe by UV-initiated polymerization to be used as SPE sorbents for the selective and sensitive determination of GSH in biological fluids. For this purpose, generic monoliths modified with several ligands (ammonia, cysteamine and cystamine) and then functionalized with AuNPs were prepared, giving the materials containing cystamine functionalities the largest coverage of AuNPs onto the monolith surface. The presence of the AuNPs in the monolith results in a better sensitivity since GSH can be easily retained on the basis of the strong interaction between thiol group and AuNP surface during the retention step. After optimization of extraction protocol, high recovery values and very low LOD value ( $1.5 \text{ ng mL}^{-1}$ ) were achieved. The performance of the AuNPs-modified monolithic syringe unit was demonstrated by its application to biological samples, where an effective clean-up of sample and preconcentration of GSH was done. Compared with other current nanomaterial-based methods for sample preparation of GSH, our SPE protocol is simpler and more cost-effective and it shows a good reusability of material. Thus, the proposed methodology represents an encouraging alternative for the extraction of relevant thiol-containing compounds from biological samples.

### **3.5. References**

- [1] H.J. Forman, H. Zhang, A. Rinna, Glutathione: Overview of its protective roles, measurement, and biosynthesis, *Mol. Aspects Med.* 30 (2009) 1–12. doi: 10.1016/j.mam.2008.08.006
- [2] M. Poot, H. Teubert, P. S. Rabinovitch, T. J. Kavanagh, De novo synthesis of glutathione is required for both entry into and progression through the cell cycle, *J. Cell. Physiol.* 163 (1995) 555–560. doi: 10.1002/jcp.1041630316
- [3] M.P. Gamcsik, M.S. Kasibhatla, S.D. Teeter, O.M. Colvin, Glutathione levels in human tumors, *Biomarkers* 17 (2012) 671–691. doi: 10.3109/1354750x.2012.715672
- [4] J.L. Luo, F. Hammarqvist, I.A. Cotgreave, C. Lind, K. Andersson, J. Wernerman, Determination of intracellular glutathione in human skeletal muscle by reversed-phase high-performance liquid chromatography, *J. Chromatogr. B* 670 (1995) 29–36. doi: 10.1016/0378-4347(95)00137-8
- [5] D.J. Anderson, B. Guo, Y. Xu, L.M. Ng, L.J. Kricka, K.J. Skogerboe, D.S. Hage, L. Schoeff, J. Wang, L.J. Sokoll, D.W. Chan, K.M. Ward, K.A. Davis, Clinical chemistry, *Anal. Chem.* 69 (1997) 165R–229R. doi: 10.1021/a1970008p
- [6] T. Santa, Recent advances in analysis of glutathione in biological samples by high-performance liquid chromatography: a brief overview, *Drug. Discov. Ther.* 5 (2013) 172–177. doi: 10.5582/ddt.2013.v7.5.172
- [7] A.E. Katrusiak, P.G. Paterson, H. Kamencic, A. Shoker, A.W. Lyon, Pre-column derivatization high-performance liquid chromatographic method for determination of cysteine, cysteinyl-glycine, homocysteine and glutathione in plasma and cell extracts, *J. Chromatogr. B* 758 (2001) 207–212. doi: 10.1016/s0378-4347(01)00182-7
- [8] Y. Mukai, T. Togawa, T. Suzuki, K. Ohata, S. Tanabe, Determination of homocysteine thiolactone and homocysteine in cell cultures using high-

performance liquid chromatography with fluorescence detection, *J. Chromatogr. B* 767 (2002) 263–268. doi: 10.1016/s0378-4347(01)00554-0

[9] X.A. Conlan, N. Stupka, G.P. McDermott, P.S. Francis, N.W. Barnett, Determination of intracellular glutathione and cysteine using HPLC with a monolithic column after derivatization with monobromobimane, *Biomed. Chromatogr.* 24 (2010) 455–457. doi: 10.1002/bmc.1327

[10] W. Zhang, P. Li, Q. Geng, Y. Duan, M. Guo, Y. Cao, Simultaneous determination of glutathione, cysteine, homocysteine, and cysteinylglycine in biological fluids by ion pairing high-performance liquid chromatography coupled with precolumn derivatization, *J. Agric. Food Chem.* 62 (2014) 5845–5852. doi: 10.1021/jf5014007

[11] C.K. Zacharis, P.D. Tzanavaras, D. Theano, T.D. Karakostaa, D. G. Themelis, Zwitterionic hydrophilic interaction chromatography coupled with post-column derivatization for the analysis of glutathione in wine samples, *Anal. Chim. Acta* 795 (2013) 75–81. doi: 10.1016/j.aca.2013.07.015

[12] A. Sarakbi, J.M. Kauffmann, A new chemical criteria for white wine: The glutathione equivalent capacity, *Food Chem.* 153 (2014) 321–326. doi: 10.1016/j.foodchem.2013.12.090

[13] C.C. Shen, W.L. Tseng, M.M. Hsieh, Selective enrichment of aminothiols using polysorbate 20-capped gold nanoparticles followed by capillary electrophoresis with laser-induced fluorescence, *J. Chromatogr. A* 1216 (2009) 288–293. doi: 10.1016/j.chroma.2008.11.044

[14] M.D. Li, T.L. Cheng, W.L. Tseng, Nonionic surfactant-capped gold nanoparticles for selective enrichment of aminothiols prior to CE with UV absorption detection, *Electrophoresis* 30 (2009) 388–395. doi: 10.1002/elps.200800364

[15] C.W. Chang, W.L. Tseng, Gold nanoparticle extraction followed by capillary electrophoresis to determine the total, free, and protein-bound

aminothiols in plasma, *Anal. Chem.* 82 (2010) 2696–2702. doi: 10.1021/ac902342c

[16] A.Z. Zhang, F.G. Ye, J.Y. Lu, Z. Wei, Y. Peng, S.L. Zhao, Preparation and characterization of polymer solid-phase microextraction monolith modified with gold nanoparticles, *Chin. J. Anal. Chem.* 39 (2011) 1247–1250. doi: 10.1016/s1872-2040(10)60464-1

[17] L. Wei, Y. Song, P. Liu, K. Xuejun, Polystyrene nanofibers capped with copper nanoparticles for selective extraction of glutathione prior to its determination by HPLC, *Microchim. Acta* 185 (2018) 321–329. doi: 10.1007/s00604-018-2845-z

[18] H. Alwael, D. Connolly, P. Clarke, C. Thompson, B. Twamley, B. O'Connor, B. Paull, Pipette-tip selective extraction of glycoproteins with lectin modified gold nano-particles on a polymer monolithic phase, *Analyst* 136 (2011) 2619–2629. doi: 10.1039/c1an15137a

[19] M. Vergara-Barberán, M.J. Lerma-García, E.F. Simó-Alfonso, J.M. Herrero-Martínez, Solid-phase extraction based on ground methacrylate monolith modified with gold nanoparticles for isolation of proteins, *Anal. Chim. Acta* 917 (2016) 37–43. doi: 10.1016/j.aca.2016.02.043

[20] M. Vergara-Barberán, M.J. Lerma-García, E.F. Simó-Alfonso, J.M. Herrero-Martínez, Polymeric sorbents modified with gold and silver nanoparticles for solid-phase extraction of proteins followed by MALDI-TOF analysis, *Microchim. Acta* 184 (2017) 1683–1690. doi: 10.1007/s00604-017-2168-5

[21] Y. Xu, Q. Cao, F. Svec, J.M. Fréchet, Porous polymer monolithic column with surface-bound gold nanoparticles for the capture and separation of cysteine-containing peptides, *Anal. Chem.* 82 (2010) 3352–3358. doi: 10.1021/ac1002646

[22] Y. Lv, F. Maya, J.M. Fréchet, F. Svec, Preparation of porous polymer monoliths featuring enhanced surface coverage with gold nanoparticles, *J. Chromatogr. A* 1261 (2012) 121–128. doi: 10.1016/j.chroma.2012.04.007

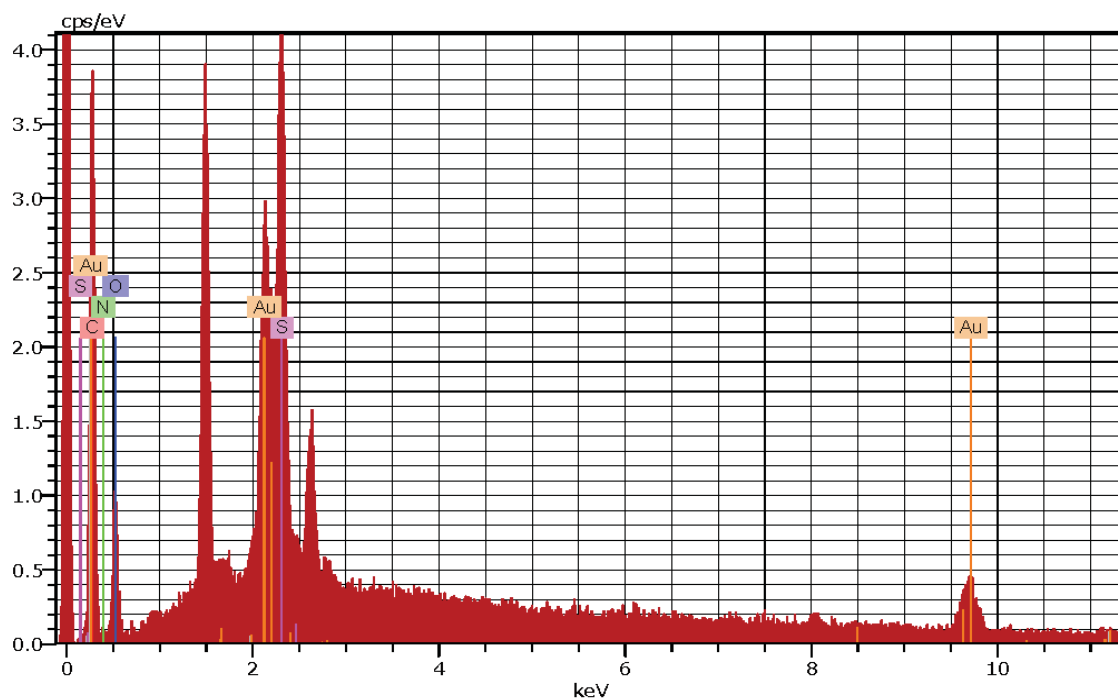
- [23] B. Fresco-Cala, O. Mompó-Roselló, E.F. Simó-Alfonso, S. Cárdenas, J.M. Herrero-Martínez, Carbon nanotube-modified monolithic polymethacrylate pipette tips for (micro)solid-phase extraction of antidepressants from urine samples, *Microchim. Acta* 185 (2018) 127. doi: 10.1007/s00604-017-2659-4
- [24] H. Alwael, D. Connolly, P. Clarke, R. Thompson, B. Twamley, B. O'Connor, B. Paull, Pipette-tip selective extraction of glycoproteins with lectin modified gold nano-particles on a polymer monolithic phase, *Analyst* 136 (2011) 2619–2628. doi: 10.1039/c1an15137a
- [25] D. Connolly, B. Twamley, B. Paull, High-capacity gold nanoparticle functionalised polymer monoliths, *Chem. Commun.* 46 (2010) 2109–2111. doi: 10.1039/b924152c
- [26] E.J. Carrasco-Correa, G. Ramis-Ramos, J.M. Herrero-Martínez, Evaluation of 2,3-epoxypropyl groups and functionalization yield in glycidyl methacrylate monoliths using gas chromatography, *J. Chromatogr. A* 1379 (2015) 100–105. doi: 10.1016/j.chroma.2014.12.050
- [27] S. Lim, D. Mott, W. Ip, P.N. Njoki, Y. Pan, S. Zhou, C.J. Zhong, Interparticle interactions in glutathione mediated assembly of gold nanoparticles, *Langmuir* 24 (2008) 8857–8863. doi: 10.1021/la800970p
- [28] M.R. Hormozi-Nezhada, E. Seyedhosseini, H. Robotjazi, Spectrophotometric determination of glutathione and cysteine based on aggregation of colloidal gold nanoparticles, *Sci. Iran* 19 (2012) 958–963. doi: 10.1016/j.scient.2012.04.018
- [29] H.G. Woehrle, L.O. Brown, J.E. Hutchison, Thiol-functionalized 1.5-nm gold nanoparticles through ligand exchange reactions: scope and mechanism of ligand exchange, *J. Am. Chem. Soc.* 127 (2005) 2172–2183. doi: 10.1021/ja0457718
- [30] Q. Tan, R. Zhang, R. Kong, W. Kong, W. Zhao, F. Qu, Detection of glutathione based on MnO<sub>2</sub> nanosheet-gated mesoporous silica nanoparticles and target induced release of glucose measured with a

portable glucose meter, *Microchim. Acta* 185 (2018) 44. doi: 10.1007/s00604-017-2603-7

[31] D. Wan, M. Gao, Y. Wang, P. Zhang, X. Zhang, A rapid and simple separation and direct detection of glutathione by gold nanoparticles and graphene-based MALDI-TOF-MS, *J. Sep. Sci.* 36 (2013) 629–635. doi: 10.1002/jssc.201200766

[32] Y. Guo, L. Yang, W. Li, X. Wang, Y. Shang, B. Li, Carbon dots doped with nitrogen and sulfur and loaded with copper(II) as a “turn-on” fluorescent probe for cysteine, glutathione and homocysteine, *Microchim. Acta* 183 (2016) 1409–1416. doi: 10.1007/s00604-016-1779-6

### 3.6. Supporting Material

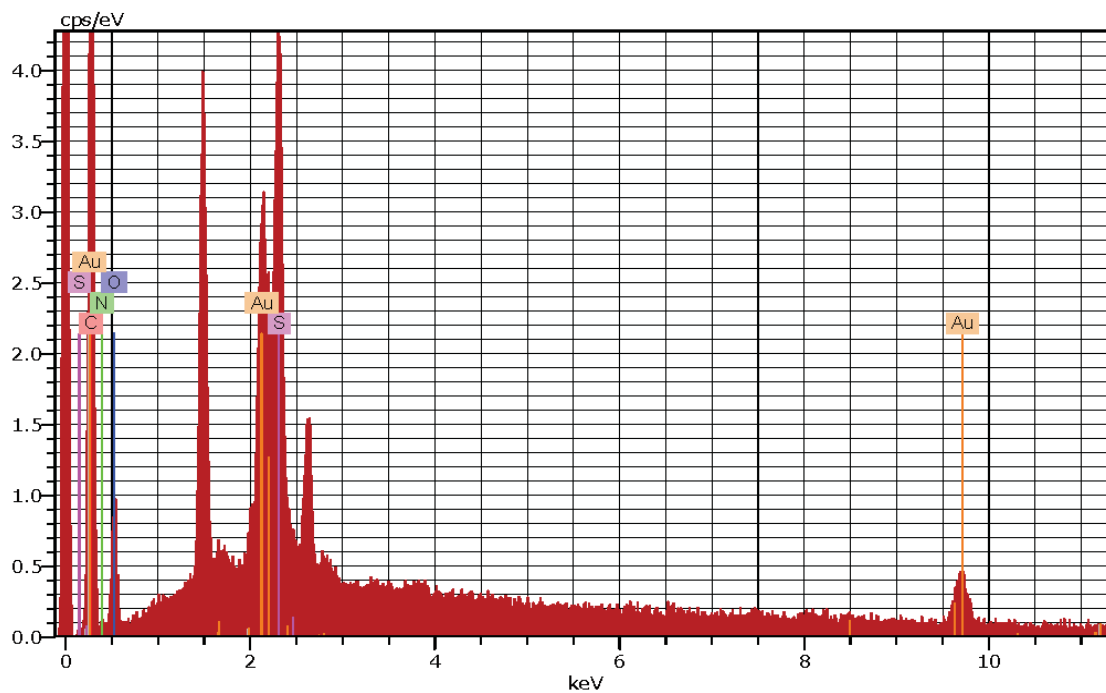


Spectrum: 1

Element	Series	unn. C [wt.%]	norm. C [wt.%]	Atom. C [at.%]	Error [wt.%]
Carbon	K-series	29.05	48.05	75.77	4.4
Nitrogen	K-series	1.16	1.92	2.60	0.6
Oxygen	K-series	6.63	10.97	12.99	1.3
Sulfur	K-series	5.97	9.88	5.83	0.3
Gold	L-series	17.64	29.18	2.81	0.7
Total:		60.46	100.00	100.00	

**Figure 3.S1.** Electron dispersive X-ray spectrometry data collected in a  $1 \mu\text{m}^2$  area of AuNP-modified monolith using cystamine-modified polymer as parent support.

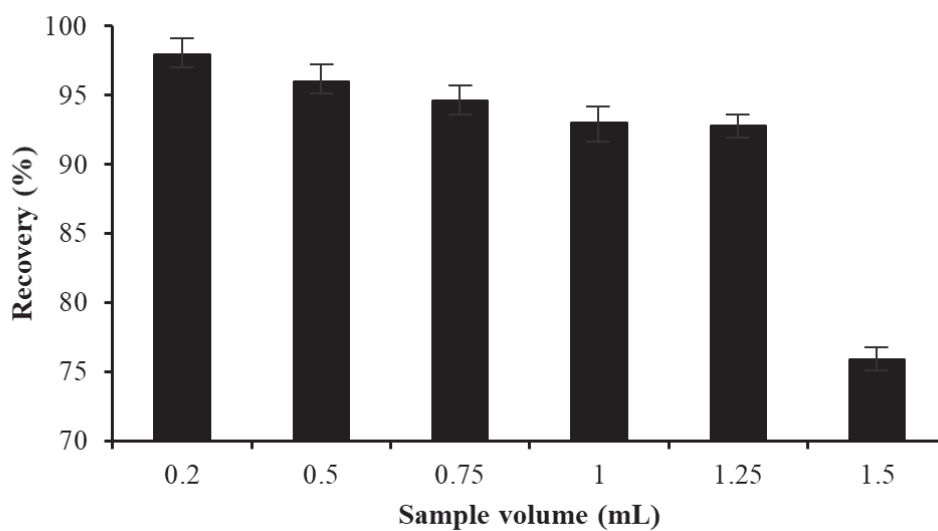




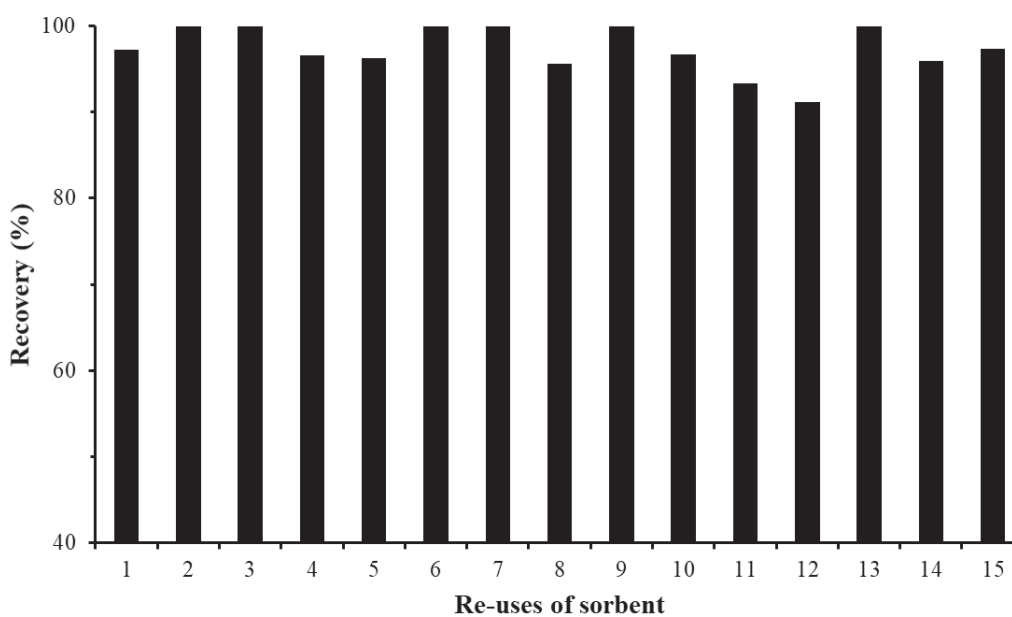
Spectrum: 1

Element	Series	unn. C [wt.%]	norm. C [wt.%]	Atom. C [at.%]	Error [wt.%]
Carbon	K-series	32.67	57.13	80.59	4.6
Nitrogen	K-series	1.27	2.22	2.69	0.6
Oxygen	K-series	5.50	9.62	10.19	1.1
Sulfur	K-series	5.00	8.74	4.62	0.2
Gold	L-series	12.74	22.29	1.92	0.5
Total:		57.19	100.00	100.00	

**Figure 3.S2.** Electron dispersive X-ray spectrometry data collected in a 10  $\mu\text{m}^2$  area of AuNP-modified monolith using cystamine-modified polymer as parent support.



**Figure 3.S3.** Effect of sample volume on the recoveries of GSH using the AuNP-modified monolithic syringe.



**Figure 3.S4.** Recovery values of GSH in (micro)SPE devices as a function of increasing number of reuses.

**Capítulo 4. Boronate affinity sorbents based on thiol-functionalized polysiloxane-polymethacrylate composite materials in syringe format for selective extraction of glycopeptides**





## Boronate affinity sorbents based on thiol-functionalized polysiloxane-polymethacrylate composite materials in syringe format for selective extraction of glycopeptides

Óscar Mompó-Roselló, María Vergara-Barberán, María Jesús Lerma-García, Ernesto F. Simó-Alfonso, José Manuel Herrero-Martínez  

In this work, two novel boronate affinity monolithic materials able to extract glycopeptides within a polypropylene syringe are described and compared. The first material was synthesized from glycidyl methacrylate (GMA)-based monoliths modified with poly-3-mercaptopropyl-methylsiloxane (PMPMS) followed by attachment of 4-vinylphenylboronic acid (VPBA) via thiol-ene click reaction. The second material was prepared by using gold nanoparticle (AuNP)-modified monoliths as substrate followed by subsequent attachment of PMPMS and VPBA. The resulting materials were used as sorbents for solid-phase extraction (SPE) to selectively preconcentrate glycopeptides from horseradish peroxidase (HRP) digests. The material that gave the superior performance was that prepared with AuNPs due to the presence of abundant boronic acid groups, being its practical applicability also examined. The hybrid material exhibited a satisfactory efficiency of glycopeptide enrichment (identifying 24 glycopeptides from a total of 27) in mixture of tryptic digests of HRP and bovine serum albumin (BSA) (1:100, w/w) were tested (or as testing sample). The sorbent shows low sensitivity (0.5 fmol/ $\mu\text{L}$ ), good adsorption capacity (25 mg  $\text{g}^{-1}$ ) and suitable reusability (over 10 times). Moreover, the hybrid monolith was successfully applied to the selective enrichment of glycopeptides from human serum digests, without any pretreatment, in which 85 glycopeptides were identified by nano-LC-MS/MS, suggesting a great potential for application in glycoproteome field.

**Keywords:** Monoliths; gold nanoparticles; poly-3-mercaptopropyl methylsiloxane; thiol-ene click reaction; composite material; glycopeptides enrichment

## **4.1. Introduction**

Glycoproteins play an essential role in diverse biological and clinical events, such as inter and intracellular transport, signal transduction, immune response, and molecular recognition [1-4]. In addition, they have been associated with many diseases, being used as biomarkers and therapeutic targets in clinical diagnostics [5]. However, the low abundance of glycoproteins in biological samples, jointly with the complexity of these matrices, make that the direct identification of these compounds remains challenging [3,4,6]. Consequently, a sample treatment is required before proceeding with their determination. Several methods have been described for glycoproteins enrichment such as lectin affinity chromatography [7,8], hydrophilic interaction chromatography [9], hydrazide chemistry [10], or boronate affinity chromatography [3-6]. In particular, boronate-based supports present particular affinity properties towards solutes (e.g. glycoproteins) containing cis-diol groups, where the interaction based on a specific covalent binding can be easily tailored by adjusting the pH of medium [3,5]. Additionally, these boronic-based supports can avoid irreversible glycan variations during extraction process [11]. Indeed, various boronate affinity materials have been synthesized, such as boronic acid-functionalized magnetic nanoparticles (NPs) [12], mesoporous silica particles [13], molecularly imprinted polymers (MIPs) [14,15] and monolithic supports [2-4,6].

The well-known features of monolithic materials, particularly polymer monoliths (viz. simple and cost-effective fabrication, high stability over a wide pH range, low back-pressure and fast separation of macromolecules) [16] combined with boronic ligands represent an attractive support for sample pretreatment methodologies as evidenced by several reviews [11,17]. Thus, these materials have been prepared using hydrophilic boronic acid ligands as functional monomers such as 3-acrylamidophenylboronic acid [18], 4-vinylphenylboronic acid (VPBA) [19], 2,4-difluoro-3-formyl-phenylboronic

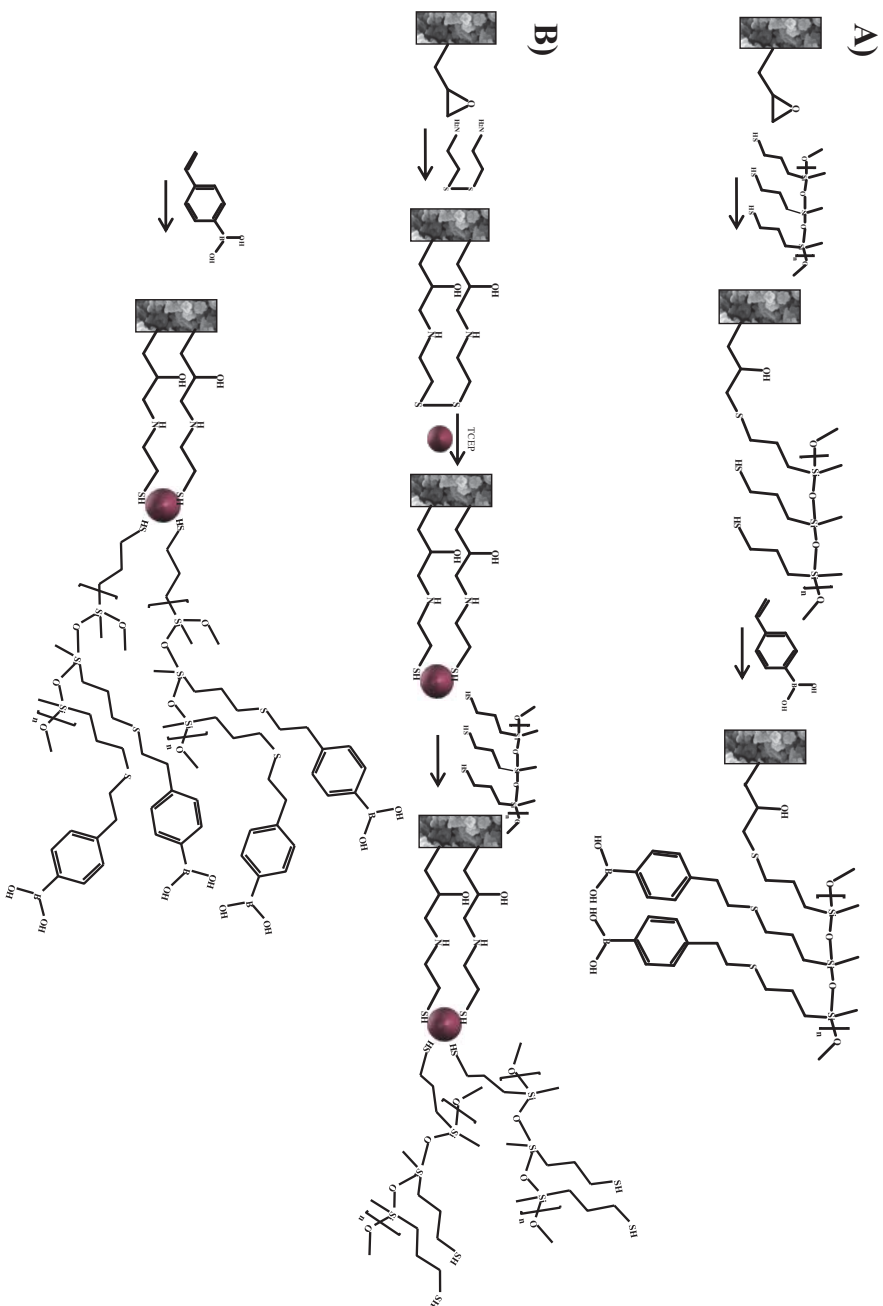
acid [20] and 3-(acrylamido)phenylboronic acid [5], among others. Nevertheless, due to the small surface area of the resulting polymer monoliths, glycoprotein binding capacity needs to be enhanced. Also, organic/inorganic hybrid boronate affinity monoliths [4,21,22] have been adopted to extract these target analytes. Although a slight improvement in surface area is produced in these hybrid monoliths, the nonspecific adsorption of non-glycoproteins on such monoliths was delicate, which decreased the selectivity. Therefore, the development of boronate affinity monolithic sorbents with large surface areas and high selectivity is strongly required to efficiently accomplish the selective capture of glycopeptides.

In the last years, the incorporation of nanomaterials into the monoliths has been considered a valuable strategy to increase the effective surface area of polymer monoliths as well as to tailor their selectivity [23,24]. Several nanomaterials such as gold nanoparticles (AuNPs) [1,3,25] and graphene oxide (GO) [3,26] have been used to prepare boronate affinity-based materials for (micro)extraction purposes. Most of these works have been applied in-capillary format; however, their scale-up to other usual (micro)extraction formats (with enhanced loading capacity) have been scarcely investigated [25]. In this respect, AuNPs have attracted much interest among scientists of monolith field [25,27-29], since AuNP-modified monoliths could be considered perfect candidates as host matrices for selective glycopeptides enrichment [1,30]. For example, Wu et al. [1] reported the modification of a GMA-based monolith with AuNPs (using cysteamine) to attach 4-mercaptophenylboronic acid (MPBA) and 2-mercaptoethylamine. The resulting hybrid monolithic capillaries were applied to enrich horseradish peroxidase (HRP) and glycoproteins from human plasma. The same authors [30] used the same AuNP-modified monolithic platform to attach cysteine and PNGase F for glycopeptide enrichment and on-line deglycosilation, respectively. Despite these contributions, it is still necessary to improve the immobilized amount of boronic acid groups of supports, which would

consequently enhance its binding capacity. Additionally, this information is commonly missing in most works reported on this topic. Therefore, it is essential to develop novel materials with high coverage density of boronate ligands.

In this work, with the aim of obtaining hybrid boronate affinity materials with a large surface area and enhanced surface coverage of boronate functionalities, poly-3-mercaptopropyl-methylsiloxane (PMPMS) was attached to the surface of the epoxide groups of a poly(GMA-co-EDMA) monoliths. Although this polymer has been used to generate large thiol-covered monolith surfaces, which has been posteriorly functionalized (by thiol-ene click reaction) with chiral selectors in miniaturized separation techniques [31,32], its use to develop boronate affinity sorbents has not been yet explored. Besides, the development of these novel hybrid monolithic sorbents in miniaturized devices (such as syringe) has been proposed for the first time. In order to prepare the boronate affinity sorbents, two distinct approaches were adopted: i) functionalization of the poly(GMA-co-EDMA) monolith with the PMPMS polymer followed by thiol-ene click attachment of VPBA, and ii) synthesis of an AuNP-modified poly(GMA-co-EDMA) monolith to be used as host material for binding PMPMS polymer followed by attachment of VPBA ligand by click thiol-ene chemistry (**Figure 4.1**). The resulting materials obtained by these approaches were morphologically characterized. Also, their potential as solid-phase extraction (SPE) sorbents to selectively preconcentrate glycopeptides from horseradish peroxidase (HRP) digests as model protein was evaluated. Then, the best material was investigated in terms of adsorption capacity, sensitivity, selectivity, reusability and reproducibility. Furthermore, the practical applicability of selected material was evaluated by enriching glycopeptides from a biological sample such as human serum.





**Figure 4.1.** Scheme of synthesis of (A) GMA-PMPMS-VPBA and (B) GMA-SH@AuNP@PMPMS-VPBA monolithic materials

## **4.2. Experimental**

### *4.2.1. Chemicals and reagents*

Glycidyl methacrylate (GMA), ethylene glycol dimethacrylate (EDMA), cyclohexanol, 1-dodecanol, 2,2-dimethoxy-2-phenylacetophenone (DMPA), cystamine dihydrochloride, poly-3-mercaptopropyl methylsiloxane (PMPMS), 4-vinylphenylboronic acid (VPBA), tris(2-carboxyethyl)phosphine hydrochloride (TCEP), benzophenone (BP),  $\alpha$ -cyano-4-hydroxycinnamic acid (HCCA), trifluoroacetic acid (TFA), dithiothreitol (DTT), ammonium bicarbonate, trypsin, iodoacetamide, sodium hydroxide (NaOH), formic acid (FA), horseradish peroxidase (HRP) and bovine serum albumin (BSA) were obtained from Sigma-Aldrich (Milwaukee, WI, USA). PNGase F Glycan cleavage kit was acquired from Thermo Fisher Scientific (Bremen, Germany). Azobisisobutyronitrile (AIBN) was purchased from Fluka (Buchs, Switzerland). Gold nanoparticles (AuNPs) suspension stabilized with sodium citrate (particle size, 20 nm,  $6.54 \cdot 10^{11}$  particles mL<sup>-1</sup>) and Coomassie Blue were from Alfa Aesar (Lancashire, UK). Acetonitrile (ACN), ethanol (EtOH), acetone and methanol (MeOH) were purchased from Scharlab (Barcelona, Spain). Deionized water was prepared in Crystal B30 EDI Adrona deionizer (Riga, Latvia) was used in all procedures.

Polypropylene syringes of 1 mL (used as support for monolithic phases) were purchased from Henke Sass Wolf (Keltenstrasse4, Tuttlingen, Germany).

### *4.2.2. Instrumentation*

Photografting of polypropylene wall surface and photopolymerization of monoliths were carried out using a UV radiation chamber CL-1000 (UVP, Upland, Canada). A syringe pump (model 101, KD Scientific, Holliston, MA, USA) was used to perform functionalization (or modification) of monolithic beds. The morphology of resulting materials was characterized by a scattering electron microscope (S-4800, Hitachi, Ibaraki, Japan) equipped with a

backscattered electron detector and a X-ray microanalysis system (EDAX Genesis 400). High-resolution transmission electron microscopy (TEM) analysis of sorbents was performed in a JEOL microscope (JEM 2100F, Freising, Germany) operated at 200 kV. The determination of gold and boron content in the materials was also done by using an inductive coupling plasma equipment connected to mass spectrometer (ICP-MS) (model 7900, Agilent Technologies, Waldbronn, Germany). For these latter measurements, all materials were previously calcined at 550°C for 1 h, and the resulting pellets were dissolved in aqua regia, properly diluted with water and analyzed by ICP-MS.

An EA 1110 CHNS elemental analyzer (CE Instruments, Milan, Italy) was used for elemental analysis of synthesized materials. Fourier-transform infrared (FTIR) spectroscopy was also conducted in characterization studies. For this purpose, a FTIR spectrometer model Tensor 27 from Bruker (Bremen, Germany) was used. Measurements were recorded using a DLaTGS detector and a Dura Sample IR II attenuated total reflection (ATR) accessory from Smiths Detection Inc. (Warrington, UK) equipped with a nine-reflection diamond/ZnSe DuraDisk plate was used. Spectra were collected in the region compressed between 4000 and 550  $\text{cm}^{-1}$  at a resolution of 4  $\text{cm}^{-1}$  with 15 scans. Background spectrum was acquired under the same measurement conditions.

An 8453 diode-array UV-vis spectrophotometer (Agilent Technologies, Waldbronn, Germany) was used to obtain HRP content by Bradford assay.

A 5800 MALDI-TOF/TOF-MS (AB SCIEX, Foster City, CA, USA) was used to establish peptide masses.

Peptides were also analyzed by using an Eksigent 425 nano-LC system (Dublin, CA) which was connected to a TripleTOF 6600plus mass spectrometer (AB Sciex).

#### *4.2.3. Synthesis of GMA-based monolith within the syringe*

The inner surface of the syringe was firstly modified by photografting with BP and EDMA [33] in order to enable a covalent attachment of monolithic bed to the wall. The parent monolith consisted of a poly (GMA-co-EDMA) material, which was prepared in the vinylized syringe (50  $\mu\text{L}$  of the polymerization mixture, 20 mg of monolith after polymerization) by UV-initiated radical polymerization. The composition of polymerization mixture was taken from a previous work [33]: 40 wt% monomers (32 wt% GMA and 8 wt% EDMA) and 60 wt% porogens (56 wt% cyclohexanol and 4 wt% 1-dodecanol), in the presence of 0.1 wt% DMPA (out of the total weight of the monomers). This mixture was next sonicated for 10 min and purged with nitrogen for 10 more min and then filled into the pretreated syringe. Polymerization was carried out with UV light for 2 h at 1 J  $\text{cm}^{-2}$ . To remove possible unreacted monomers and rests of porogenic solvents, the monolith was then washed with MeOH and the obtained material was dried in the oven at 60°C overnight.

#### *4.2.4. Synthesis of the different boronate affinity monolithic materials*

Using the parent monolith previously synthesized, two different materials to be tested as SPE sorbents were prepared as illustrated in **Figure 4.1**. The first monolithic material (route A) was obtained by passing through the parent monolith a 10% (v/v) PMPMS solution in ACN at 5  $\mu\text{L min}^{-1}$  using a syringe pump at 60°C for 2 h. Then, a VPBA solution (40 mg  $\text{mL}^{-1}$  of VPBA in ACN and also containing 1% AIBN) was used to fill the syringe and its end was sealed with rubber stoppers and kept in an oven at 60°C for 24 h. The resulting material (GMA-PMPMS-VPBA) was washed with ACN and dried in an oven at 60°C overnight.

To prepare the second material (route B), the GMA-based monolith was chemically modified with cystamine (to provide thiol moieties) and further attached with AuNPs following a procedure previously described [33,34].

Briefly, a 1.0 mol L<sup>-1</sup> cystamine dihydrochloride solution (prepared in 2.0 mol L<sup>-1</sup> aqueous NaOH) was flushed through the bare monolith at 60°C at a flow rate of 5 μL min<sup>-1</sup> for 2 h and then washed until neutral pH. Subsequently, to achieve the reduction of disulfide bonds, a TCEP solution (0.25 mol L<sup>-1</sup> in an equal concentration NaOH solution) was pumped through the monolith at room temperature at the same flow rate for 2 h. After washing with water until neutral pH, the resulting thiol-modified monolith was treated with a commercial AuNPs dispersion at 0.3 mL min<sup>-1</sup> as previously described [35]. The resulting hybrid monoliths were identified as GMA-SH@AuNP. After that, a solution of 10% PMPMS (v/v) in acetone passed through the hybrid monolith at room temperature for 2 h, and then washed with acetone. Afterwards, a solution of VPBA (with the same composition as indicated above) was used to fill the PMPMS-modified material and subjected to the same click thiol-ene reaction conditions as above. Finally, the resulting material (namely GMA-SH@AuNP@PMPMS-VPBA) was washed with ACN and dried in an oven at 60°C overnight.

#### *4.2.5. HRP and human serum digestion*

The standard glycoprotein was dissolved in 1 mL of 50 mM NH<sub>4</sub>HCO<sub>3</sub> (pH 7.8) and denatured at 100°C for 15 min and then allowed to cool at room temperature. Next, the resulting solution was reduced with 1.5 mg mL<sup>-1</sup> DTT (in 50 mM NH<sub>4</sub>HCO<sub>3</sub> 7.8) at 56 °C for 1 h and alkylated with 10 mg mL<sup>-1</sup> iodoacetamide (in the same buffer solution) at room temperature for 45 min. To obtain the glycopeptides, the solution was digested with 0.02 μg μL<sup>-1</sup> trypsin (in 25 mM NH<sub>4</sub>HCO<sub>3</sub> pH 7.8) at 37 °C overnight. The digestion was stopped with FA up to a final concentration of 10%.

10 μL of human serum were diluted with 400 μL of 50 mM NH<sub>4</sub>HCO<sub>3</sub> (pH 7.8) and centrifuged at 12000 rpm (ca. 15000 g) for 5 min. Supernatant was collected and heated at 100 °C for 10 min. Next, the sample was incubated with 100 μL de 30 mg mL<sup>-1</sup> DTT (in 50 mM NH<sub>4</sub>HCO<sub>3</sub> 7.8) at

60°C for 20 min. The cooled solution was alkylated by 10 mg mL<sup>-1</sup> iodoacetamide (in the same buffer solution) for 30 min at room temperature in the dark. Finally, trypsin (40 µg) was added and digestion was left at 37°C overnight.

#### *4.2.6. MicroSPE protocol*

The syringe with the different boronate affinity monolithic sorbents were firstly activated with 500 µL ACN and equilibrated with 500 µL of loading buffer (50 mM NH<sub>4</sub>HCO<sub>3</sub> pH 7.8). Then, 500 µL HRP digest (prepared in the loading buffer) was passed through the syringe at 0.1 mL min<sup>-1</sup> flow rate. The washing step was carried out with the same loading solution and the retained glycopeptides were eluted with 100 µL of ACN/H<sub>2</sub>O (50:50, v/v) containing 0.5% TFA prior to the subsequent MS analysis.

#### *4.2.7. MALDI-TOF analysis*

The resulting eluates (1 µL) were spotted onto a MALDI plate, and after the droplets were air-dried at room temperature. 1 µL of matrix (10 mg mL<sup>-1</sup> HCCA in ACN/H<sub>2</sub>O (1:1, v/v) containing 0.1% TFA) was added and allowed to air-dry at room temperature for MALDI-TOF/TOF MS analysis. Peptide mass maps were acquired in the positive ion mode (1500 shots every position) in a m/z range of 800-6000. The MS and MS/MS information was sent to be identified by the MASCOT software (v 2.3.02; Matrix Science) via the Protein Pilot (ABSciex).

#### *4.2.8. Glycopeptides enrichment from human serum*

To enrich glycopeptides from the tryptic digest of human serum, the adopted microSPE protocol was the same that described in Section 2.6. Once the retained glycopeptides were eluted, this solution was evaporated to dryness, and the residue was dissolved in 50 µL of ammonium bicarbonate. Then, the resulting solution was deglycosylated using the PNGase F Glycan

Cleavage Kit following the supplier instructions. Finally, the deglycosylated peptides were subjected to nano-LC-MS/MS.

#### *4.2.9. Nano-LC-MS/MS analysis*

Briefly, 2  $\mu\text{L}$  of deglycosylated peptides was loaded onto a trap column (NanoLC Column, 3  $\mu\text{m}$ , C18-CL, 350  $\mu\text{m} \times 0.5$  mm, Eksigent) and desalted using TFA 0.1% as mobile phase at a flow of 5  $\mu\text{L min}^{-1}$  during 5 min. The peptides were then loaded onto an analytical column (3C18-CL-120, 3  $\mu\text{m}$ , 120  $\text{\AA}$ , 75  $\mu\text{m} \times 15$  cm, Eksigent) equilibrated in 5% ACN and 0.1% FA. The elution was done using a linear gradient of 7–40% B in A for 20 min at a flow rate of 300  $\text{nL min}^{-1}$ , where A is deionized water with 0.1% FA and B is ACN with 0.1% FA. Analysis of peptides by MS was carried out in a data-dependent mode. Survey MS1 scans were acquired from 350 to 1400  $m/z$  for 250 ms. The quadrupole resolution was set to ‘LOW’ for MS2 experiments, which were acquired from 100 to 1500  $m/z$  for 25 ms in ‘high sensitivity’ mode. Main conditions in the MS analysis were ions from 2<sup>+</sup> to 4<sup>+</sup> with a minimum intensity of 250 cps. Up to 100 ions were selected for fragmentation after each survey scan. Dynamic exclusion was set to 15 s.

The analysis of the obtained spectra was done using ProteinPilot v5.0 search engine. Protein-Pilot default parameters were used to generate a peak list directly from the nano-LC-MS/MS instrument. The Paragon algorithm [36] of ProteinPilot was used to search the SwissProt database (200601, 562246 proteins) and Uniprot Trematoda database (200604, 362615). Search criteria included fixed and variable modifications as carbamidomethylation (C) and oxidation (M), respectively. Only peptides with N-!P-S/T were identified as N-linked glycopeptides.

#### *4.2.10. Quality control and quality assurance (QC/QA)*

The application of QA/QC procedures has been carried out in order to provide accurate and reproducible results.

Adsorption capacity of boronate affinity monoliths for glycopeptides was adapted according to the protocols described in literature [37,38]. Briefly, 500  $\mu\text{L}$  of HRP digest at  $1 \text{ mg mL}^{-1}$  were passed through microSPE devices containing different sorbent amounts (from 10 to 40 mg). After enrichment, the eluted fraction was analyzed by MALDI-TOF-MS. The adsorption capacity was calculated by the amount of HRP tryptic digest (500  $\mu\text{g}$ ) to the amount of sorbent.

An estimation of the limit of detection (LOD) was obtained by analyzing digested HRP at low-concentrations (close to the LOD level, as determined from the approach based on  $S/N = 3$ ).

To evaluate the selectivity of boronate affinity sorbents for glycopeptides, a mixture of HRP and BSA tryptic digests (at a mass ratio of 1:100, w/w) was enriched by the affinity-based monolith and analyzed by MALDI-TOF-MS.

The reusability of the sorbent in syringe devices was evaluated by repeatedly analyzing digested HRP at a concentration of  $0.1 \text{ mg mL}^{-1}$ .

### **4.3. Results and discussion**

#### *4.3.1. Preparation and characterization of boronate affinity monolithic materials*

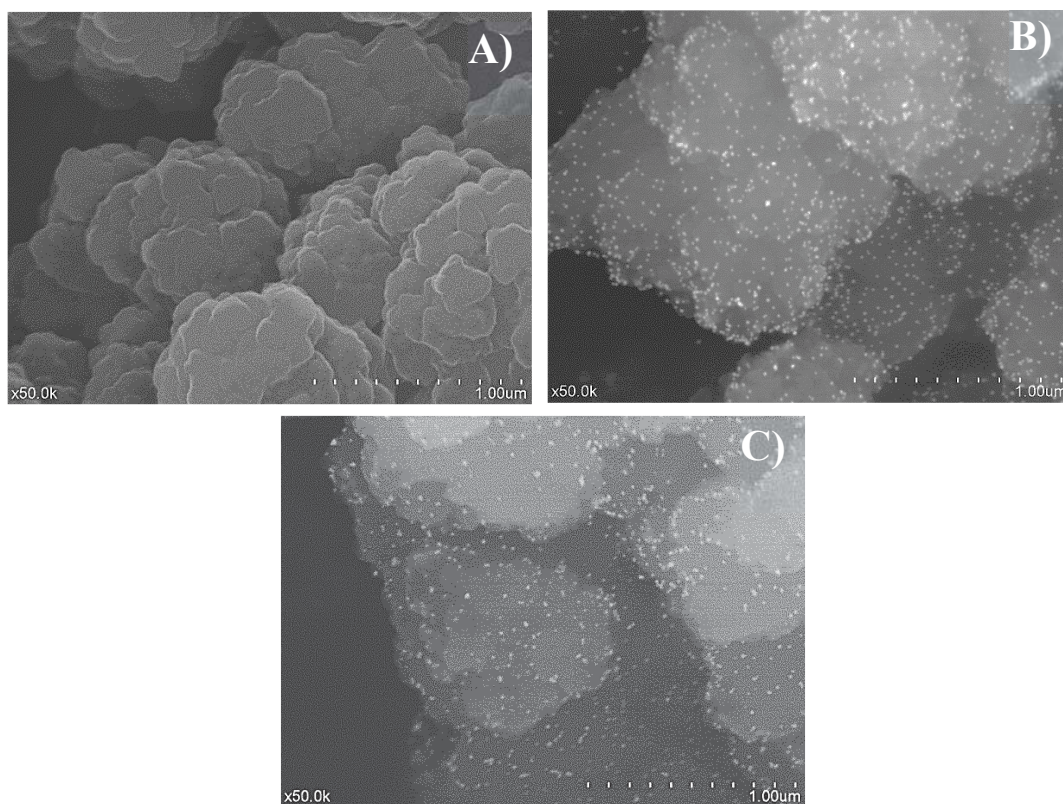
**Figure 4.1** shows the preparation routes of the different boronate affinity monoliths synthesized in this work. Firstly, poly (GMA-co-EDMA) monolith described in previous works of our research group [33,35,39] was selected as starting host material for the preparation of polymeric phases due to the presence of reactive epoxy groups in its structure, which facilitates the modification with different functional groups [1]. Then, two distinct strategies were pursued to increase the density of reactive boronate groups on the surface of the modified monoliths. For this purpose, in the route A, PMPMS was selected as polythiol reagent to modify epoxy groups by nucleophilic substitution following the reaction conditions described elsewhere [31]. The



attached PMPMS significantly enhanced the hydrophilicity of parent polymer due to its abundant thiol groups. Then, the available unreacted thiol groups present on the PMMPS-modified monolith surface reacted with VPBA ligands via thiol-ene click chemistry to produce the material named as GMA-PMPMS-VPBA. Alternatively, in the second strategy (route B), AuNPs were immobilized onto the GMA-based monolith surface (previously treated with cystamine [27,28,33]), which provides a smart way not only to increase the surface area for enhancing the active sites, but also to perform a facile surface modification [27,28,33,35,39]. Then, the hybrid monolith was used as support for immobilizing PMPMS and further bonding of VPBA to prepare GMA-SH@AuNP@PMMPS-VPBA composites.

The resulting materials were firstly characterized by SEM to get information of their morphology. The morphology of the GMA-PMPMS-VPBA (see **Figure 4.2A**) resembled the typical microglobular structure of polymethacrylate monoliths, with large-through pores, which is beneficial for flow-through purposes. EDAX analysis of this material gave silicon and boron contents of 2.48 and 2.78 wt%, respectively (see **Table 4.S1**), thus demonstrating the incorporation of the PMPMS and VMNPs to the polymeric matrix. Next, SEM/BSE image of the cystamine-modified monolith obtained after AuNP immobilization (**Figure 4.2B**) showed a remarkable AuNPs coverage. This surface coverage was also estimated by EDAX, giving the presence of ca. 22 wt% Au (see **Table 4.S1**), which provided enough sites for further functionalization. Due to the high affinity between gold and the thiol groups of PMPMS, this reagent was used to functionalize AuNP-modified monolith and subsequently to attach VPBA. SEM micrographs of this material (GMA-SH@AuNP@PMMPS-VPBA) were also taken (**Figure 4.2C**). As observed, AuNPs were also evidenced on monolith surface, although most of them were covered by the layer of bonded polythiol, and posterior attachment of VPBA ligand. Although there were no clear morphological differences between both materials (**Figure 4.2B** and **4.2C**),

EDAX analysis of this latter material (see **Table 4.S1**) showed the presence of silicon (2.02 wt%) and boron (3.04 wt%) demonstrating the successful attachment of PMPMS and VPBA onto AuNPs. Additionally, TEM measurements of these latter materials was carried out (**Figure 4.S1**). From these measurements, AuNPs showed diameters of ca. 17 and 19 nm, respectively. The increase in AuNP diameter in GMA-SH@AuNP@PMPMS-VPBA corroborated the presence of the bonded ligands (PMPMS and VPBA) onto the AuNP surface.



**Figure 4.2.** SEM micrographs of (A) GMA-PMPMS-VPBA, (B) AuNP-modified monolith and (C) GMA-SH@AuNP@PMPMS-VPBA monolithic materials. Images taken at 80 000 × magnification.

As mentioned in the Introduction, the immobilized amount of boronate groups played an important role in the extraction performance of glycopeptides. Thus, the determination of bulk boron content in both materials was also done by ICP-MS (as described in Section 2.2), giving 0.10

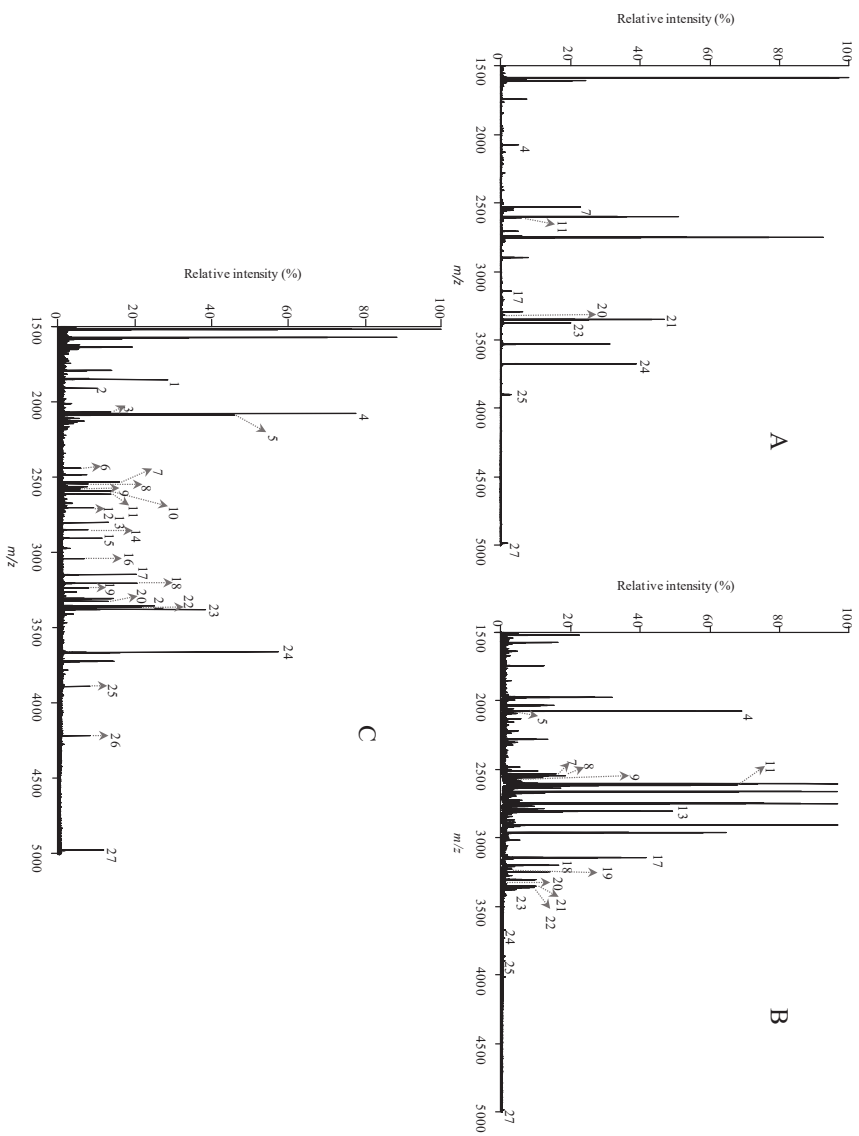
and 0.45 wt% for the GMA-PMPMS-VPBA monolith and the GMA-SH@AuNP@PMMPS-VPBA, respectively. The high immobilization amount observed for the composite might be attributed to the large number of AuNPs available, which provided enhanced reactive thiol coverage (via PMPMS) sites for the attachment of VPBA.

The successful preparation of both monoliths was also confirmed by FT-IR (see **Figure 4.S2**). The GMA-based monolith (parent monolith) presented an adsorption band due to the C-H stretching of epoxy groups at around 3000  $\text{cm}^{-1}$  (**Figure 4.S2A**). This band decreased in both boronic affinity-based materials (**Figure 4.S2B and C**), which proved the epoxide ring-opening reactions with the different ligands (see **Figure 4.1**). Moreover, the band at 1361  $\text{cm}^{-1}$ , which correspond to the B-O stretching vibration bond in the phenylboronic acid moieties was observed in the two synthesized materials [5,6], which demonstrated the successful immobilization of VPBA onto the resulting hybrid monoliths. A broad absorption band at 3450 (or 3500)  $\text{cm}^{-1}$ , which was attributed to O-H stretching arising from the diol moieties present in VPBA, was also observed in these materials, which confirmed VPBA binding to the polymer surface.

#### *4.3.2. Glycopeptide enrichment performance of synthesized monolithic materials*

In order to evaluate the enrichment performance of boronate affinity sorbents, a standard glycoprotein (HRP) tryptic digest was used as a model sample. According to previous or studies [40,41],  $\text{NH}_4\text{HCO}_3$  (50 mM, pH 7.8) and ACN/ $\text{H}_2\text{O}$ /TFA (50/50, v/v) containing 0.5% TFA were used as loading and elution buffers, respectively.

The MALDI-TOF mass spectra of the HRP tryptic digest without enrichment and with enrichment using the synthesized materials are presented in **Figure 4.3**. Without enrichment, 10 peaks attributed to glycopeptides or their fragments were identified (see **Figure 4.3A**).



**Figure 4.3.** MALDI-TOF mass spectra of HRP tryptic digests: (A) without enrichment and after enrichment using (B) GMA PMPMS-VPBA and (C) GMA-SH@AuNP@PMPMS-VPBA materials. Glycopeptide peak identification as in Table 6.S2

However, after enrichment, as shown in **Figure 4.3B** and **C**, 17 and 27 glycopeptides were identified with enhanced MS intensities using the GMA-PMPMS-VPBA and GMA-SH@AuNP@PMPMS-VPBA materials, respectively. The detailed information of identified glycopeptides is shown in **Table 4.S2**. The superior performance found in this last material was attributed to high immobilized amount of boronic acid groups in this composite, and consequently, large capability for capturing target molecules with cis-diol moieties (in this case, glycopeptides) according to the recognition mechanism depicted in **Figure 4.S3**. On the basis of these results, this composite was preferentially chosen as sorbent for extraction of glycopeptides, and several analytical parameters of this material were evaluated as follows.

### *5.3.3. Adsorption capacity, detection sensitivity, enrichment selectivity, reproducibility and reusability of hybrid material*

The adsorption capacity of the GMA-SH@AuNP@PMPMS-VPBA composite was evaluated by enriching the glycopeptides from a fixed amount of HRP digest using different amounts of sorbent. As shown in **Figure 4.S4**, the signal intensities of 6 high-abundant glycopeptides firstly increased reaching a maximum value when 20 mg of sorbent were used. With higher sorbent amounts, signal intensities have not been significantly improved. Therefore, the adsorption capacity of the proposed sorbent is calculated to be 25 mg g<sup>-1</sup>. This adsorption capacity value is comparable or even higher than those obtained by other hydrophilic materials [38,42].

The detection sensitivity of the aforementioned hybrid monolith was investigated by using different concentrations of HRP tryptic digest. When the concentration was reduced to 0.5 fmol μL<sup>-1</sup>, 3 glycopeptide peaks with S/N ratios over 6 can still be detected (see **Figure 4.S5**). Therefore, the limit of detection (LOD) of the composite was 0.5 fmol μL<sup>-1</sup>. This result suggests that the prepared material has a good sensitivity towards glycopeptides. This value

was comparable to others previously reported using HILIC-based monoliths (without boronic functionalities) [42-45] and magnetic materials [46,47], thus indicating that the prepared hybrid monolith had great sensitivity toward glycopeptides.

To evaluate the enrichment selectivity of the hybrid monolith for glycopeptides, a mixture of tryptic digests of HRP and BSA at a mass ratio of 1:100 (w/w) was used as the testing sample. As shown in **Figure 4.S6A** for the direct analysis of this mixture, only two glycopeptide peaks could be observed. However, after enrichment with the proposed material, 24 glycopeptide peaks (from the 27 peaks detected when only HRP digest was enriched) were identified (see **Figure 4.S6B**). These results proved that the GMA-SH@AuNP@PMPMS-VPBA had high selectivity for glycopeptide enrichment.

To investigate the material reusability performance, the sorbent (within device) was repeatedly used to enrich HRP. Similar mass spectra were obtained after using the same material for 10 consecutive uses, which demonstrated its good stability. Furthermore, the device-to-device reproducibility for glycopeptide enrichment was also evaluated. The number of identified glycopeptides from HRP digests enriched by three in syringe devices was the same with similar signal intensities, thus indicating the good preparation and enrichment reproducibility of GMA-SH@AuNP@PMPMS-VPBA monolithic material.

#### *4.3.4. N-Glycopeptides enrichment from tryptic digest of human serum*

To demonstrate the enrichment performance of the proposed material, a real complex biological sample such as human serum (without any pretreatment) was used. For this purpose, as previously stated, the human serum sample (10  $\mu$ L) was digested with trypsin and passed through the microSPE device. After washing and elution steps, the resulting eluate was deglycosylated with PNGase F and further analyzed by nano-LC-MS/MS. As

a result, a total of 85 N-glycosylated peptides derived from 42 N-glycosylated proteins were identified without removing any high-abundant protein (see **Table 4.S3** for detailed information). The enrichment and identification performance of this boronate affinity hybrid monolith was higher than the identification results reported in some papers using hydrophilic monoliths [42,44,45]. However, the resulting identification performance was lower than that obtained using hybrid monoliths with immobilized AuNPs and modified with cysteine [2], although in this work, a previous removal of high-abundant proteins was carried out in combination with a long pretreatment (70 min).

#### **4.4. Conclusions**

This study presents the preparation of novel boronate affinity monolithic materials in a syringe format for the capture and preconcentration of glycopeptides. For this purpose, two materials were synthesized using polythiol-functionalized monoliths as host substrates to produce sorbents with high boronic functionalities for glycopeptides enrichment. Thus, the first material was prepared from a generic monolith (GMA) modified with PMPMS and VPBA, whereas the second one used an AuNP-modified monolith as parent support. This last material showed higher efficiency to trap glycopeptides, which can be attributable to the increased binding sites of the resulting material. The hybrid material showed good performances in selective enrichment of glycopeptides, such as satisfactory adsorption capacity, high sensitivity, selectivity and good reusability. Also, the proposed methodology is of facile operation and it was feasibly applied to enrich glycopeptides from complex biological samples such as human serum, without any pretreatment. Thus, the work described here not only offered the description and application of novel boronate affinity materials, but also opened its application to large-scale glycoproteome analysis.



## 4.5. References

- [1] C. Wu, Y. Liang, Q. Zhao, Y. Qu, S. Zhang, Q. Wu, Y. Zhang, Boronate affinity monolith with a gold nanoparticle-modified hydrophilic polymer as a matrix for the highly specific capture of glycoproteins, *Chem. Eur. J.* 20 (2014) 8737-8743. doi: 10.1002/chem.201402787
- [2] Y. Liang, C. Wu, Q. Zhao, Q. Wu, B. Jiang, Y. Weng, Y. Zhang, Gold nanoparticles immobilized hydrophilic monoliths with variable functional modification for highly selective enrichment and on-line deglycosylation of glycopeptides, *Anal. Chim. Acta* 900 (2015) 83-89. doi: 10.1016/j.aca.2015.10.024
- [3] R. Wang, Z. Chen, Boronate affinity monolithic column incorporated with graphene oxide for the in-tube solid-phase microextraction of glycoproteins, *J. Sep. Sci.* 41 (2018) 2767-2773. doi: 10.1002/jssc.201701417
- [4] Y.F. Shen, F.F. Yuan, X.Y. Liu, Y.P. Huang, Z.S. Liu, Synergistic effect of organic-inorganic hybrid monomer and polyhedral oligomeric silsesquioxanes in a boronate affinity monolithic capillary/chip for enrichment of glycoproteins, *Microchim. Acta* 186 (2019) 812. doi: 10.1007/s00604-019-3938-z
- [5] X.J. Zhou, C.E. Mo, M. Chen, Y.P. Huang, Z.S. Liu, Improving affinity of boronate capillary monolithic column for microextraction of glycoproteins with hydrophilic macromonomer, *J. Chromatogr. A* 1581 (2018) 8-15. doi: 10.1016/j.chroma.2018.11.005
- [6] E. Alzahrani, Organic boronate affinity sorbent for capture of cis-diol containing compounds, *Asian J.Chem.* 31 (2019) 2073-2082. doi: 10.14233/ajchem.2019.22108
- [7] Y. Liu, D. Fu, L. Yu, Y. Xiao, X. Peng, X. Liang, Oxidized dextran facilitated synthesis of a silica-based concanavalin a material for lectin

- affinity enrichment of glycoproteins/glycopeptides, *J. Chromatogr. A* 1455 (2016) 147-155. doi: 10.1016/j.chroma.2016.05.093
- [8] S. Nauom, B.R. da Silva Neto, M.S. Ribeiro, W.R. Pedersoli, C.J. Ulhoa, R.N. Silva, V.N. Monteiro, Biochemical and molecular study of *Trichoderma harzianum* enriched secretome protein profiles using lectin affinity chromatography, *Biotechnol. Appl. Bioc.* 187 (2019) 1-13. doi: 10.1007/s12010-018-2795-2
- [9] M.H. Selman, M. Hemayatkar, A.M. Deelder, M. Wuhler, Cotton HILIC SPE microtips for microscale purification and enrichment of glycans and glycopeptides, *Anal. Chem.* 83 (2011) 2492-2499. doi: 10.1021/ac1027116
- [10] Y. Zhang, M. Kuang, L. Zhang, P. Yang, H. Lu, An accessible protocol for solid-phase extraction of N-linked glycopeptides through reductive amination by amine-functionalized magnetic nanoparticles, *Anal. Chem.* 85 (2013) 5535-5541. doi: 10.1021/ac400733y
- [11] H. Li, Z. Liu. Recent advances in monolithic column-based boronate-affinity chromatography, *TrAC Trends Anal. Chem.* 37 (2012) 148-161. doi: 10.1016/j.trac.2012.03.01
- [12] Z. Shi, L. Pu, Y. Guo, Z. Fu, W. Zhao, Y. Zhu, J. Wu, F. Wang, Boronic acid-modified magnetic Fe<sub>3</sub>O<sub>4</sub>@mTiO<sub>2</sub> microspheres for highly sensitive and selective enrichment of N-glycopeptides in amniotic fluid, *Sci. Rep.* 7 (2017) 4603. doi: 10.1038/s41598-017-04517-8
- [13] L. Liu, Y. Zhang, L. Zhang, G. Yan, J. Yao, P. Yang, H. Lu, Highly specific revelation of rat serum glycopeptidome by boronic acid-functionalized mesoporous silica, *Anal. Chim. Acta* 753 (2012) 64-72. doi: 10.1016/j.aca.2012.10.002
- [14] Z. Lin, J. Wang, X. Tan, L. Sun, R. Yu, H. Yang, G. Chen, Preparation of boronate-functionalized molecularly imprinted monolithic column with polydopamine coating for glycoprotein recognition and

enrichment, *J. Chromatogr. A* 1319 (2013) 141-147. doi: 10.1016/j.chroma.2013.10.059

[15] Z. Lin, L. Sun, W. Liu, Z. Xia, H. Yang, G. Chen, Synthesis of boronic acid-functionalized molecularly imprinted silica nanoparticles for glycoprotein recognition and enrichment, *J. Mater. Chem. B* 2 (2014) 637-643. doi: 10.1039/c3tb21520b

[16] E. Alzahrani, Preparation of the polymeric-based microchip for protein extraction, *Int. J. Adv. Sci. Technol.* 1 (2015) 219-229. doi: 10.1021/ac802359e

[17] D. Li, Y. Chen, Z. Liu, Boronate affinity materials for separation and molecular recognition: structure, properties and applications, *Chem. Soc. Rev.* 44 (2015) 8097-8123. doi: 10.1039/c5cs00013k

[18] M. Chen, Y. Lu, Q. Ma, L. Guo, Y.Q. Feng, Boronate affinity monolith for highly selective enrichment of glycopeptides and glycoproteins, *Analyst* 134(2009) 2158-2164. doi: 10.1039/b909581k

[19] Z. Lin, H. Huang, S. Li, J. Wang, X. Tan, L. Zhang, G. Chen, Preparation of phenylboronic acid-silica hybrid monolithic column with one-pot approach for capillary liquid chromatography of biomolecules, *J. Chromatogr. A* 1271 (2013) 115-123. doi: 10.1016/j.chroma.2012.11.038

[20] Q. Li, C. Lü, Z. Liu, Preparation and characterization of fluorophenylboronic acid-functionalized monolithic columns for high affinity capture of cis-diol containing compounds, *J. Chromatogr. A* 1305 (2013) 123-130. doi: 10.1016/j.chroma.2013.07.007

[21] Z. Lin, J. Pang, H. Yang, Z. Cai, L. Zhang, G. Chen, One-pot synthesis of an organic-inorganic hybrid affinity monolithic column for specific capture of glycoproteins, *Chem. Commun.* 47 (2011) 9675-9677. doi: 10.1039/c1cc13082j

[22] F. Yang, J. Mao, X.W. He, L.X. Chen, Y.K. Zhang, Synthesis of boronate-silica hybrid affinity monolith via a one-pot process for specific

capture of glycoproteins at neutral conditions, *Anal. Bioanal. Chem.* 405 (2013) 6639-6648. doi: 10.1007/s00216-013-7026-7

[23] F. Svec, Y. Lv, Advances and recent trends in the field of monolithic columns for chromatography, *Anal. Chem.* 87 (2015) 250-273. doi: 10.1021/ac504059c

[24] B. Fresco-Cala, S. Cardenas, Potential of nanoparticle-based hybrid monoliths as sorbents in microextraction techniques, *Anal. Chim. Acta* 1031 (2018) 15-27. doi: 10.1016/j.aca.2018.05.069

[25] H. Alwael, D. Connolly, P. Clarke, R. Thompson, B. Twamley, B. O'Connor, B. Paull, Pipette-tip selective extraction of glycoproteins with lectin modified gold nano-particles on a polymer monolithic phase, *Analyst* 136 (2011) 2619-2628. doi: 10.1039/c1an15137a

[26] C. Zhou, X. Chen, Z. Du, G. Li, X. Xiao, Z. Cai, A hybrid monolithic column based on boronate-functionalized graphene oxide nanosheets for online specific enrichment of glycoproteins, *J. Chromatogr. A* 1498 (2017) 90-98. doi: 10.1016/j.chroma.2017.01.049

[27] Q. Cao, Y. Xu, F. Liu, F. Svec, J.M. Fréchet, Polymer monoliths with exchangeable chemistries: use of gold nanoparticles as intermediate ligands for capillary columns with varying surface functionalities, *Anal. Chem.* 82 (2010) 7416-7421. doi: 10.1021/ac1015613

[28] Y. Xu, Q. Cao, F. Svec, J.M. Fréchet, Porous polymer monolithic column with surface-bound gold nanoparticles for the capture and separation of cysteine-containing peptides, *Anal. Chem.* 82 (2010) 3352-3358. doi: 10.1021/ac1002646

[29] L. Terborg, J.C. Masini, M. Lin, K. Lipponen, M.L. Riekolla, F. Svec, Porous polymer monolithic columns with gold nanoparticles as an intermediate ligand for the separation of proteins in reverse phase-ion exchange mixed mode, *J. Adv. Res.* 6 (2015) 441. doi: 10.1016/j.jare.2014.10.004

- [30] Y. Liang, C. Wu, Q. Zhao, Q. Wu, B. Jiang, Y. Weng, Y. Zhang, Gold nanoparticles immobilized hydrophilic monoliths with variable functional modification for highly selective enrichment and on-line deglycosylation of glycopeptides, *Anal. Chim. Acta* 900 (2015) 83-89
- [31] E.J. Carrasco-Correa, G. Ramis-Ramos, J.M. Herrero-Martínez, M. Lämmerhofer, Polymethacrylate monoliths with immobilized poly-3-mercaptopropyl methylsiloxane film for high-coverage surface functionalization by thiol-ene click reaction, *J. Chromatogr. A* 1367 (2014) 123-130. doi: 10.1016/j.chroma.2014.09.066
- [32] M. Wolter, M. Lämmerhofer, In-situ functionalized monolithic polysiloxane-polymethacrylate composite materials from polythiol-ene double click reaction in capillary column format for enantioselective nano-high-performance liquid chromatography, *J. Chromatogr. A* 1497 (2017) 172-179. doi: 10.1016/j.chroma.2017.03.070
- [33] O. Mompó-Roselló, M. Vergara-Barberán, E.F. Simó-Alfonso, J.M. Herrero-Martínez, In syringe hybrid monoliths modified with gold nanoparticles for selective extraction of glutathione in biological fluids prior to its determination by HPLC, *Talanta* 209 (2020) 120566. doi: 10.1016/j.talanta.2019.120566
- [34] Y. Lv, F.M. Alejandro, J.M. Fréchet, F. Svec, Preparation of porous polymer monoliths featuring enhanced surface coverage with gold nanoparticles, *J. Chromatogr. A* 1261 (2012) 121-128. doi: 10.1016/j.chroma.2012.04.007
- [35] M. Vergara-Barberán, M.J. Lerma-García, E.F. Simó-Alfonso, J.M. Herrero-Martínez, Polymeric sorbents modified with gold and silver nanoparticles for solid-phase extraction of proteins followed by MALDI-TOF analysis, *Microchim. Acta* 184 (2017) 1683-1690. doi: 10.1007/s00604-017-2168-5
- [36] I.V. Shilov, S.L. Seymour, A.A. Patel, A. Loboda, W.H. Tang, S.P. Keating, C.L. Hunter, L.M. Nuwaysir, D.A. Schaeffer, *The Paragon*

algorithm, a next generation search engine that uses sequence temperature values and feature probabilities to identify peptides from tandem mass spectra, *Mol. Cell. Proteomics* 6 (2007) 1638-1655. Doi: 10.1074/mcp.t600050-mcp200

[37] X.M. He, X.C. Liang, X. Chen, B.F. Yuan, P. Zhou, L.N. Zhang, Y.Q. Feng, High strength and hydrophilic chitosan microspheres for the selective enrichment of N-glycopeptides, *Anal. Chem.* 89 (2017) 9712-9721. doi: 10.1021/acs.analchem.7b01283

[38] L. Zhang, S. Ma, Y. Chen, Y. Wang, J. Ou, H. Uyama, M. Ye, Facile fabrication of biomimetic chitosan membrane with honeycomb-like structure for enrichment of glycosylated peptides, *Anal. Chem.* 91 (2019) 2985-2993. doi: 10.1021/acs.analchem.8b05215

[39] M. Vergara-Barberán, M.J. Lerma-García, E.F. Simó-Alfonso, J.M. Herrero-Martínez, Solid-phase extraction based on ground methacrylate monolith modified with gold nanoparticles for isolation of proteins, *Anal. Chim. Acta* 917 (2016) 37-43. doi: 10.1016/j.aca.2016.02.043

[40] X. Zou, D. Liu, L. Zhong, B. Yang, Y. Lou, Y. Yin, Synthesis and characterization of a novel boronic acid-functionalized chitosan polymeric nanosphere for highly specific enrichment of glycopeptides, *Carbohydr. Polym.* 90 (2012) 799-804. doi: 10.1016/j.carbpol.2012.05.090

[41] L. Zhang, Y. Xu, H. Yao, L. Xie, J. Yao, H. Lu, P. Yang, Boronic acid functionalized core-satellite composite nanoparticles for advanced enrichment of glycopeptides and glycoproteins, *Chem. Eur. J.* 15 (2009) 10158-10166. doi: 10.1002/chem.200901347

[42] W. Zhang, L. Jiang, D. Wang, Q. Jia, Preparation of copper tetra (N-carboxylacrylic) aminephthalocyanine functionalized zwitterionic-polymer monolith for highly specific capture of glycopeptides, *Anal. Bioanal. Chem.* 410 (2018) 6653-6661. Doi:10.1007/s00216-018-1278-1

[43] H. Jiang, H. Yuan, Y. Qu, Y. Liang, B. Jiang, Q. Wu, N. Deng, Z. Liang, L. Zhang, Y. Zhang, Preparation of hydrophilic monolithic

capillary column by in situ photo-polymerization of N-vinyl-2-pyrrolidinone and acrylamide for highly selective and sensitive enrichment of N-linked glycopeptides, *Talanta* 146 (2016) 225-230. doi: 10.1016/j.talanta.2015.08.037

[44] W. Zhang, N. Song, H. Zheng, W. Feng, Q. Jia, Cobalt phthalocyanine tetracarboxylic acid functionalized polymer monolith for selective enrichment of glycopeptides and glycans, *Proteomics* 18 (2018), 1700399. Doi: 10.1002/pmic.201700399

[45] W. Zhang, L. Jiang, L. Fu, Q. Jia, Selective enrichment of glycopeptides based on copper tetra (N-carboxylacrylic) aminophthalocyanine and iminodiacetic acid functionalized polymer monolith, *J. Sep. Sci.* 42 (2019) 1037-1044. doi: 10.1002/jssc.201801030

[46] H. Wang, F. Jiao, F. Gao, J. Huang, Y. Zhao, Y. Shen, Y. Zhang, X. Qian, Facile synthesis of magnetic covalent organic frameworks for the hydrophilic enrichment of N-glycopeptides, *J. Mat. Chem. B* 5 (2017) 4052-4059. doi: 10.1039/c7tb00700k

[47] M. Wang, X. Zhang, C. Deng, Facile synthesis of magnetic poly (styrene-co-4-vinylbenzene-boronic acid) microspheres for selective enrichment of glycopeptides, *Proteomics* 15 (2015), 2158-2165. doi: 10.1002/pmic.201300523

## 4.6. Supporting Material

Monolithic material	C (wt%)	N (wt%)	O (wt%)	Si (wt%)	S (wt%)	B (wt%)	Au (wt%)
GMA-PMPPMS-VPBA	72.78	-	18.01	2.48	3.95	2.78	-
AuNP-modified monolith	58.27	2.32	9.60	-	7.73	-	22.08
GMA-SH@AuNP@PMPPS-VPBA	70.56	3.13	8.87	2.02	6.09	3.04	6.30

**Table 4.S1.** Elemental compositions and relative contents of synthesized materials obtained from EDAX analysis.



**Table 4.S2.** Detailed information of the observed glycopeptides obtained from HRP tryptic digests.

Nº	Observed $m/z$	Amino acid sequence	Glycan composition
1	1842.9	NVGLN#R	XylMan3FucGlcNAc2
2	1895.7	LHFHDCFVNGCDASILLDN#TTSFR	XylMan3FucGlcNAc2
3	2068.9	PN#VSNIVR	XylMan3FucGlcNAc2
4	2073.0	DSFRNVGLN#R	Man3GlcNAc2
5	2276.2	SILLDN#TTSFR	XylMan2FucGlcNAc2
6	2438.0	SILLDN#TTSFR	XylMan3FucGlcNAc2
7	2533.3	SFANSTQTFNFAVEAMDR	FucGlcNAc
8	2543.2	SFANSTQTFNFAVEAMDR	FucGlcNAc
9	2575.2	QLTPTFYDN SCPN#VSNIVR	GlcNAc2
10	2591.3	PTLN#TTYLQTLR	XylMan3FucGlcNAc2
11	2612.1	MGN#ITPLTGTQGQIR	Xyl1Man3GlcNAc2
12	2703.3	SFAN#STQTFNFAVEAMDR	XylMan2GlcNAc2
13	2805.4	MGN#ITPLTGTQGQIRLNCR	Man2GlcNAc2
14	2851.2	GLCPLNGN#LSALVDFDLR	XylMan3FucGlcNAc2
15	2908.0	GLIQSDQELFSSPN#ATDTIPLVR	GlcNAc2
16	3041.0	SFAN#STQTFNFAVEAMDR	XylMan2GlcNAc2
17	3147.2	GLIQSDQELFSSPN#ATDTIPLVR	XylMan3GlcNAc2
18	3206.4	SFAN#STQTFNFAVEAMDR	XylMan3GlcNAc2
19	3233.0	GLIQSDQELFSSPN#ATDTIPLVR	Man2GlcNAc2
20	3321.6	QLTPTFYDN SCPN#VSNIVR	XylMan3FucGlcNAc2
21	3353.0	SFAN#STQTFNFAVEAMDR	XylMan3FucGlcNAc2
22	3369.9	SFAN#STQTFNFAVEAM*DR	XylMan3FucGlcNAc2
23	3384.7	DSFRNVGLN#R	XylHex6Fuc2HexNAc4
24	3671.9	GLIQSDQELFSSPN#ATDTIPLVR	XylMan3FucGlcNAc2
25	3895.0	LHFHDCFVNGCDASILLDN#TTSFR	XylMan3FucGlcNAc2
26	4223.2	QLTPTFYDN SC(AAVESACPR)PN#VSNIVR	XylMan3FucGlcNAc2
27	4984.1	LYN#FSNTGLPDPTLN#TTYLQTLR	XylMan3FucGlcNAc2 / XylMan3FucGlcNAc2

**Table 4.S3.** Detail information of the glycopeptides enriched from tryptic digests of human serum using GMA-SH@AuNP@PMPMS-VPBA material.

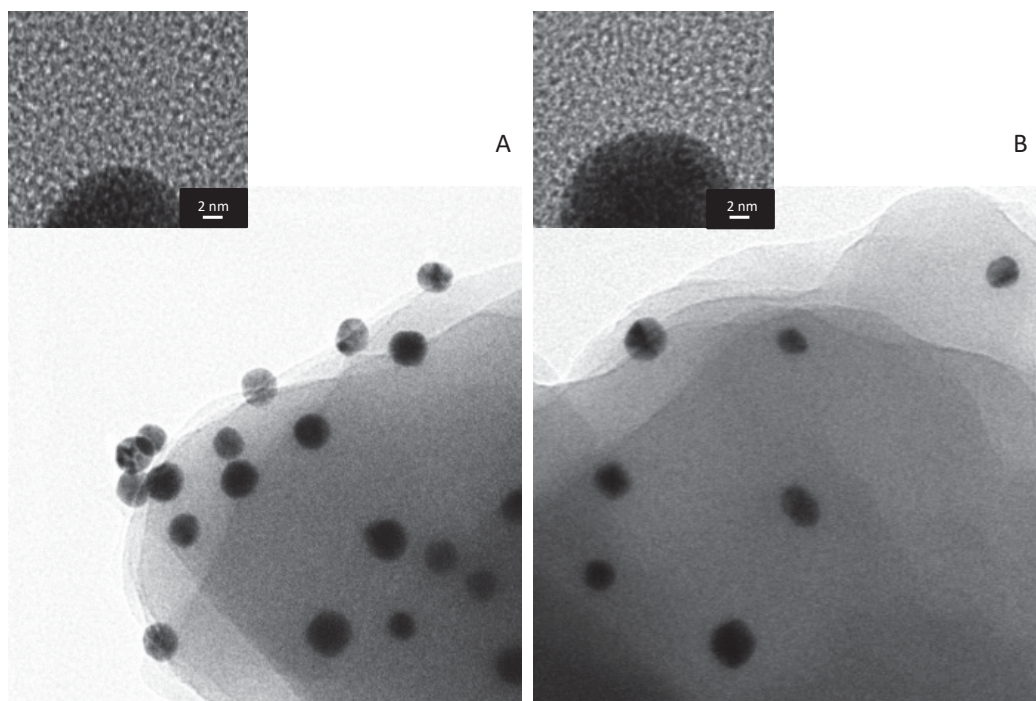
<b>N°</b>	<b>Accessions</b>	<b>Peptide sequence</b>
1	Q7Z6E9	ASLKEPYNSGIN*RSR
2	P00450	DVDKEFYLFPTVFDEN*ESLLEDNIR
3	P00450	QKDVDKEFYLFPTVFDEN*ESLLEDNIR
4	P00734	SEGSSVN*LSPPLEQCVPCR
5	P00734	GHVN*ITR
6	P00734	SEGSSVN*LSPPLEQCVPCRGGQQYQGR
7	P00734	SRYPHKPEIN*STTHPGADLQENFCRNPDSSTTGPWCYTTDPTVR
8	P00738	MVSHHN*LTTGATLINEQWLLTTAK
9	P00738	NLFLN*HSENATAKDIAPTLTLYVGK
10	P00738	NLFLN*HSENATAKDIAPTLTLYVGKK
11	P00738	QLVEIEKVVLPN*YSQVDIGLIK
12	P00738	VVLHPN*YSQVDIGLIK
13	P00739	MVSHHN*LTTGATLINEQWLLTTAK
14	P01008	SLTFN*ETYQDISELVYGAK
15	P01009	ADTHDEILEGLNFN*LTEIPEAQIHEGFQELLR
16	P01009	NTKSPLFMGKVVN*PTQK
17	P01009	SPLFMGKVVN*PTQK
18	P01009	VVN*PTQK
19	P01009	YLGN*ATAIFFLPDEGK
20	P01009	YLGN*ATAIFFLPDEGKLQHLENELTHDIITK
21	P01011	HPNSPLDEEN*LTQENQDR
22	P01011	NSPLDEEN*LTQENQDR
23	P01011	PNSPLDEEN*LTQENQDR
24	P01011	SPLDEEN*LTQENQDR
25	P01023	VSN*QTLSSLFFTVLQDVPVR
26	P01024	HYLMWGLSSDFWGEKPN*LSYIIGK
27	P01024	KHYLMWGLSSDFWGEKPN*LSYIIGK
28	P01031	YN*FSFR
29	P01042	YNSQN*QSNNQFVLYR
30	P01042	KYNSQN*QSNNQFVLYR
31	P01591	EN*ISDPTSPLR
32	P01591	IIVPLNNREN*ISDPTSPLR
33	P01859	EEQFN*STFRVVSVLTVVHQDWLNGK

N°	Accessions	Peptide sequence
34	P01859	TKPREEQFN*STFR
35	P01860	IAVEWESSGQPENNYN*TPPMLDSDGSFFLYSK
36	P01871	TVDKSTGKPTLYN*VSLVMSDTAGTCY
37	P01871	YKN*NSDISSTR
38	P01876	LAGKPTHVN*VSVVMAEVDGTC
39	P01876	LAGKPTHVN*VSVVMAEVDGTCY
40	P01876	LSLHRPALEDLLLGSEAN*LTCTLTGLR
41	P01876	LSLHRPALEDLLLGSEAN*LTCTLTGLRDASGVFTFTWTPSSGK
42	P01876	SLHRPALEDLLLGSEAN*LTCTLTGLR
43	P01876	TIDRLAGKPTHVN*VSVVMAEVDGTC
44	P01876	TIDRLAGKPTHVN*VSVVMAEVDGTCY
45	P01877	LSLHRPALEDLLLGSEAN*LTCTLTGLR
46	P01877	SAVQGPPELDLCGCYSVSSVLPGCAQPWNHGETFTCTAAHPELKT PLTAN*ITK
47	P01877	SLHRPALEDLLLGSEAN*LTCTLTGLR
48	P01877	TPLTAN*ITK
49	P01877	LSLHRPALEDLLLGSEAN*LTCTLTGLR
50	P02671	GSAGHWTSESSVSGSTGQWHSESGSFRPDSPGSGNARPNPDWGT FEEVSGN*VSPGTR
51	P02671	GGSTSYGTGSETESPRN*PSSAGSWNSGSSGPGSTGNR
52	P02671	GSAGHWTSESSVSGSTGQWHSESGSFRPDSPGSGNARPNPDWGT FEEVSGN*VSPGTRR
53	P02671	N*PSSAGSWNSGSSGPGSTGNR
54	P02671	SAGHWTSESSVSGSTGQWHSESGSFRPDSPGSGNARPNPDWGT EEVSGN*VSPGTRR
55	P02749	VYKPSAGN*NSLYR
56	P02749	VYKPSAGN*NSLYRDTAVFECLPQHAMFGNDTITCTTHGNWTKLP ECR
57	P02750	DGFDISGNPWICDQN*LSDLYR
58	P02751	DTLTSRPAQGVVTTLEN*VSPPR
59	P02765	AALAAFNAQNN*GSNFQLEEISR
60	P02766	ALGISPFHEHAEVVFTAN*DSGPR
61	P02774	LCDN*LSTK
62	P02787	CGLVPVLAENYN*KSDNCEDTPEAGYFAIAVVKK
63	P02787	ILRQQHFLFGSN*VTDCSGNFCLFR
64	P02787	QQQHFLFGSN*VTDCSGNFCLFR
65	P02790	ALPQPQN*VTSLLGCTH
66	P04114	VNQNLVYESGSLN*FSK
67	P04114	N*LTDFAEQYSIQDWAK

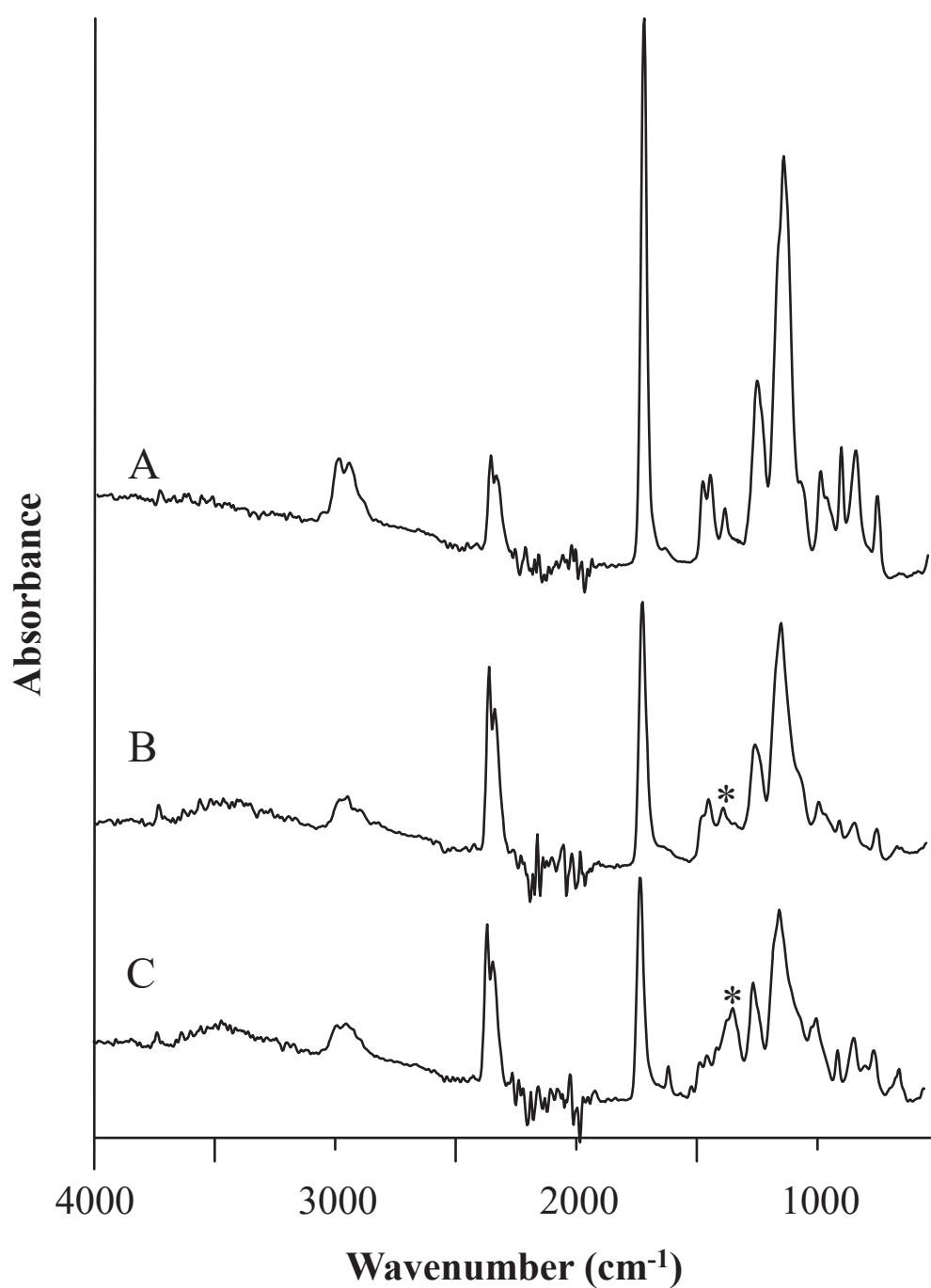
---

<b>N°</b>	<b>Accessions</b>	<b>Peptide sequence</b>
68	P08571	ATVN*PSAPR
69	P08603	SPDVIN*GSPISQK
69	P08603	SPDVIN*GSPISQK
70	P08603	CVEISCKSPDVIN*GSPISQK
71	P08603	WQSIPLCVEKIPCSQPPQIEHGTIN*SSR
72	P08697	NPN*PSAPR
73	P0DOX2	LSLHRPALEDLLLGSEAN*LTCTLTGLR
74	P0DOX3	EVN*TSGFAPARPPPQPGSTTFWAWSVLR
75	P0DOX5	TKPREEQYN*STYR
76	P0DOX8	AN*PTVTLFPPSSEELQANK
77	P10909	EILSVDCSTNN*PSQAK
78	P10909	CREILSVDCSTNN*PSQAK
79	P10909	EIRHN*STGCLR
80	P19823	VVN*NSPQPQNVVFDVQIPK
81	P27169	SLDFNTLVDN*ISVDPETGDLWVGCHPNGMK
82	P36980	LQNNENN*ISCVER
83	Q03591	LQNNENN*ISCVER
84	Q12805	RNPADPQRIPSN*PSHR
85	Q8WZ64	LITEN*LSK

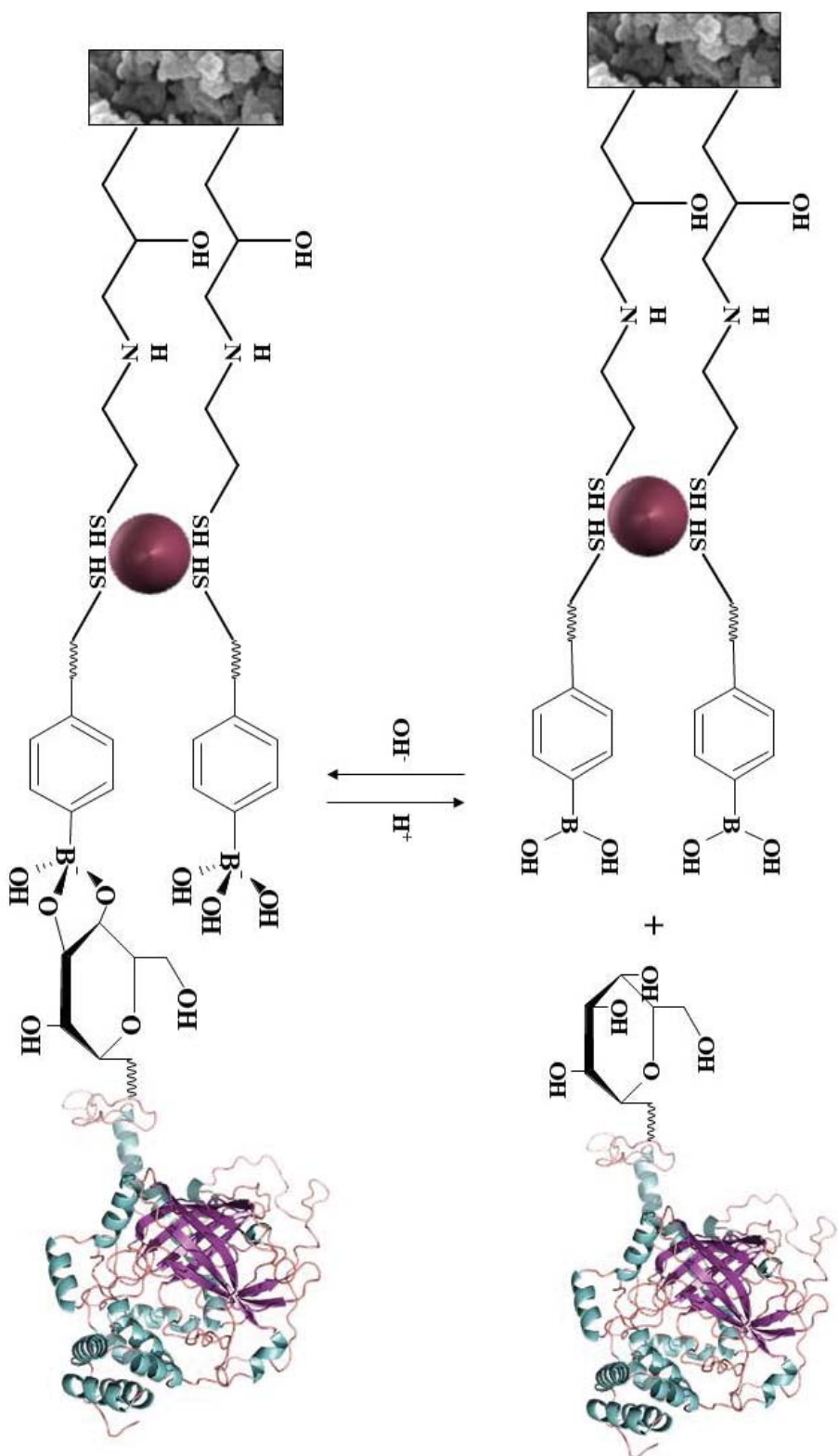
---



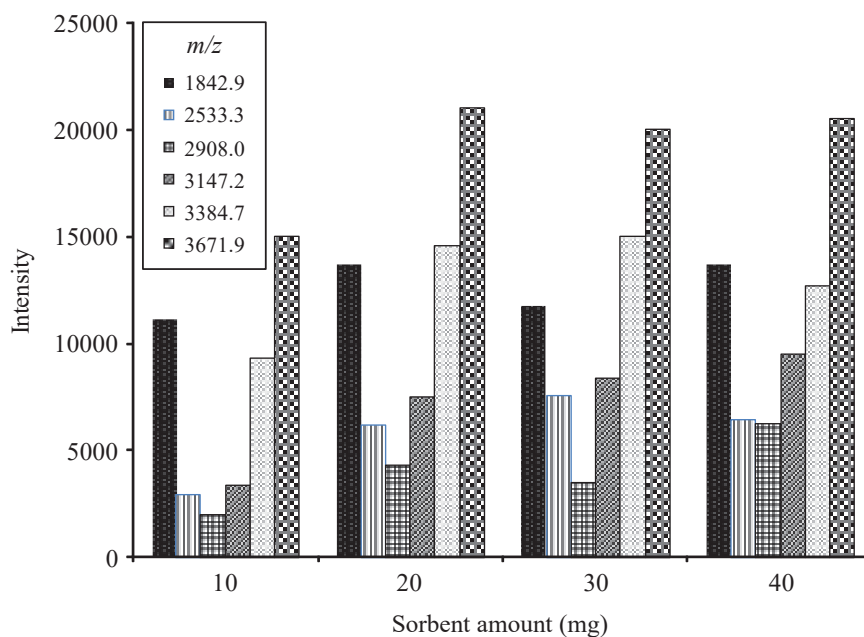
**Figure 4.S1.** TEM images of (A) AuNP-modified monolith and (B) GMA-SH@AuNP@PMMPS-VPBA material.



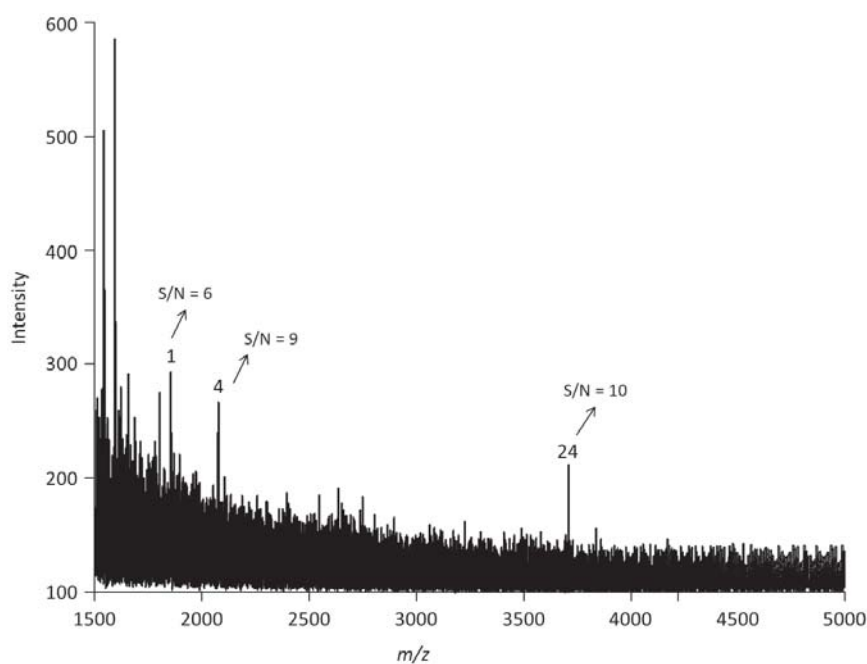
**Figure 4.S2.** FTIR spectra of (A) GMA, (B) GMA-PMPMS-VPBA and (C) GMA-SH-@AuNP@PMPMS-VPBA monolithic materials. The band observed at 1361 cm<sup>-1</sup> was labeled with an asterisk.



**Figure 4.S3.** Recognition mechanism of hybrid affinity monolith (GMA-SH-@AuNP@PMPMS-VPBA) toward glycopeptides.

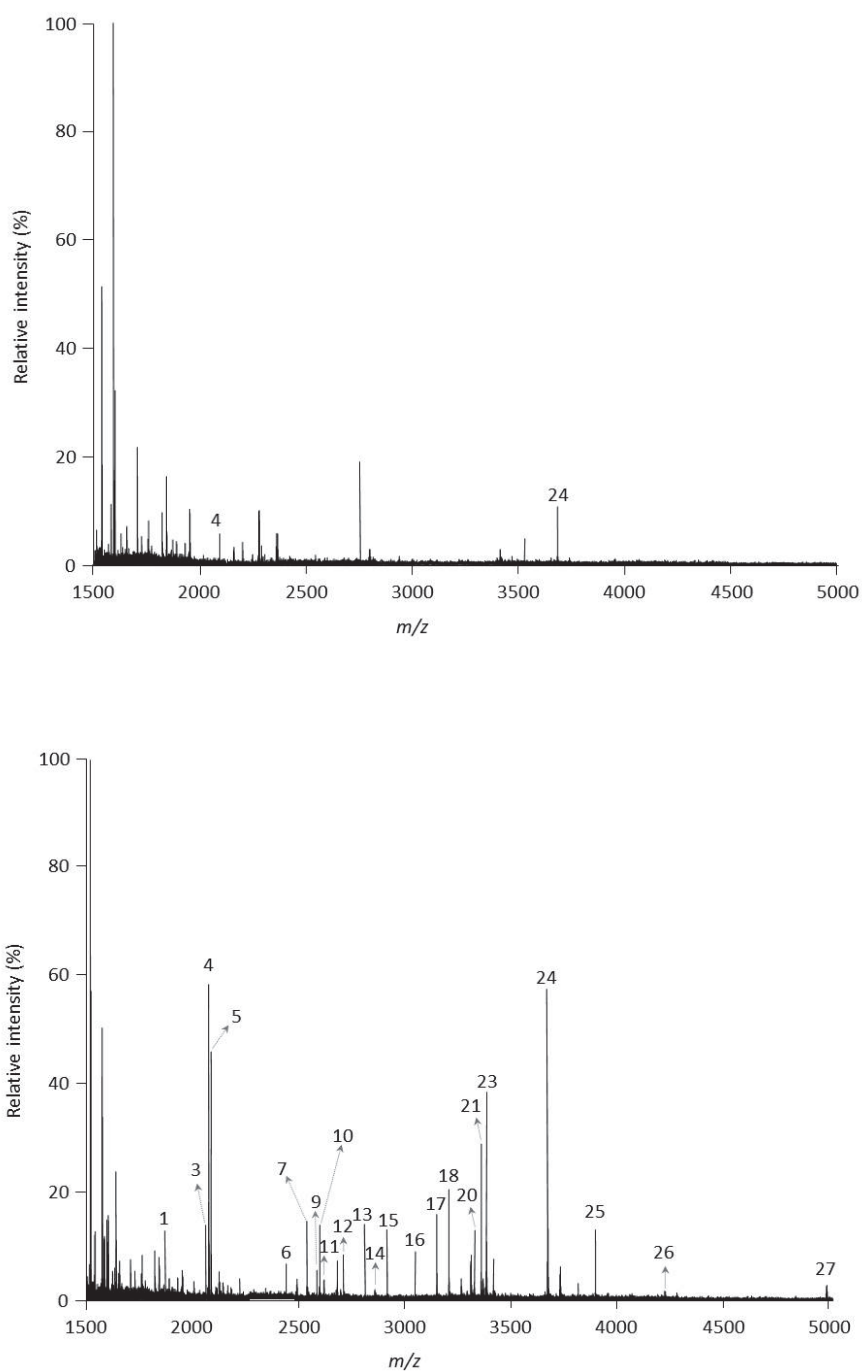


**Figure 4.S4.** MS intensities of 6 selected glycopeptides from tryptic digest of HRP after enrichment with different amounts of GMA-SH@AuNP@PMPMS-VPBA material.



**Figure 4.S5.** MALDI-TOF mass spectrum of HRP digest at 0.5 fmol/ $\mu$ L using GMA-SH@AuNP@PMPMS-VPBA material. Glycopeptide peak identification as in Table S2.





**Figure 4.S6.** MALDI-TOF mass spectra of the mixture containing HRP and BSA tryptic digests at a mass ratio 1:100. (A) direct analysis and (B) after enrichment with the hybrid monolith. Glycopeptide peak identification as in Table S2.



**Capítulo 5. Extraction of  $\beta$ -blockers from urine with a  
polymeric monolith modified with 1-allyl-3-  
methylimidazolium chloride in spin column format**





## Extraction of $\beta$ -blockers from urine with a polymeric monolith modified with 1-allyl-3-methylimidazolium chloride in spin column format ☆

Oscar Mompó-Roselló, Ana Ribera-Castelló, Ernesto F. Simó-Alfonso, María José Ruiz-Angel, María Celia García-Alvarez-Coque, José Manuel Herrero-Martínez  

Department of Analytical Chemistry, Faculty of Chemistry, University of Valencia, Dr. Moliner 50, 46100, Burjassot, Valencia, Spain

A glycidyl methacrylate-based monolith was modified with imidazolium-based ionic liquid (IL) to be used as stationary phase for solid-phase extraction (SPE). The host monolithic support was prepared by *in-situ* UV polymerization in spin column format. Two approaches were developed to incorporate the IL into the polymeric monolithic matrix: generation of IL onto the surface monolith, and copolymerization by addition of the IL to the polymerization mixture, which gave the best results. The resulting sorbent materials were morphologically characterized and used for the isolation of five  $\beta$ -blockers from human urine samples. All SPE steps were accomplished by centrifugation, which reduces significantly costs and time in sample treatment. Under optimal conditions,  $\beta$ -blockers were quantitatively retained in the modified monolith at pH 12, and desorbed with a water-methanol mixture, to be subsequently determined via HPLC with UV detection. The limits of detection ranged between 1.4 and 40  $\mu\text{g L}^{-1}$ , and the reproducibility among extraction units (expressed as relative standard deviation) was below 8.2%. The novel phase was successfully applied to the extraction of propranolol in urine samples with recoveries above 90%.

**Keywords:** Hybrid monoliths; Ionic liquids; Spin columns; Solid-phase extraction;  $\beta$ -Blockers; Biological fluids

## 5.1. Introduction

Heart diseases are a worldwide matter of concern, as confirmed by the World Health Organization (WHO) in its 2012 report [1], which indicates that approximately 33.3% of the population suffers from cardiac problems (data from 194 countries).  $\beta$ -Blockers are commonly used in the treatment of heart diseases like *angina pectoris*, arrhythmia and hypertension. These drugs act by relaxing muscles and reducing the heart rate. Owing to these effects,  $\beta$ -blockers have been also used to improve performance in sports that require accurate steadiness, equilibrium and deftness, being forbidden for some sports by the International Olympic Committee (IOC) and the World Anti-Doping Agency (WADA) [2].

The control of this type of doping substances is commonly carried out by analyzing their presence in urine samples using sophisticated techniques, such as gas chromatography (GC) or liquid chromatography (HPLC) coupled to mass spectrometry (MS) detection [3–6]. Although these methodologies provide low limits of detection, efficient isolation and sample cleanup prior to analysis are still required. Different sample preparation techniques such as solid-phase extraction (SPE) [5] and solid-phase microextraction (SPME) [6] have been commonly reported for the trace level determination of  $\beta$ -blockers in complex matrices. However, SPE procedures show certain disadvantages, such as low selectivity and poor reusability, while the fibers used in SPME are fragile and relatively expensive. Thus, there is considerable interest in developing novel selective and efficient sorbents for extracting and pre-concentrating these drugs in biological fluids using miniaturized formats.

In this context, organic polymer monoliths have recently revealed as attractive sorbents in sample treatment [7–10], due to their inherent advantages, which include relatively easy preparation, large porosity, tailorable surface chemistry and excellent pH stability. However, the use of these sorbents in micro-extraction formats for the extraction of  $\beta$ -blockers from urine samples has not been yet described.

In the last decade, the introduction of ionic liquids (ILs) in different materials (silica- and polymeric supports), as novel stationary phases, has been addressed in order to improve the selectivity and separation efficiency in separation techniques [11-13]. However, the combined merits of polymer monoliths and ILs have been scarcely exploited [14]. ILs are salts composed of a bulky organic cation and a smaller anion, which are usually melted below 100 °C. ILs show interesting features, such as low volatility and flammability, negligible vapor pressure, low toxicity, high thermal stability, and tunable miscibility with water and organic solvents [15]. These properties have enhanced their use as serious green alternative to conventional organic solvents [16]. ILs have been widely used in several fields of analytical chemistry, including separation techniques [11,17] and sample preparation [11,18-21].

The introduction of ILs into polymer monoliths can be carried out by adopting two approaches. The most common route for preparation of ILs-based monoliths implies the addition of ILs containing vinyl or allyl moieties into the polymerization mixture [22–24]. The second approach is based on the post-functionalization of the monolithic matrix with ILs [25,26], which is more complex and time-consuming. In any case, these approaches have been scarcely reported in the field of sample preparation using polymeric monolithic supports [27,28].

In this work, 1-allyl-3-methylimidazolium chloride ([AMIM][Cl]) was introduced in hybrid monolithic sorbents within a miniaturized device (spin column) to be used for extraction of  $\beta$ -blockers. For this purpose, different pathways were tested to introduce the IL into the monolith: (i) *in situ* generation of the IL, and (ii) copolymerization. The resulting composites were characterized, and their potential as (micro)SPE sorbents was comparatively evaluated. The best hybrid monolith was studied in terms of extraction performance of  $\beta$ -blockers through variables including sample pH and elution solvent, among others. The resulting spin column devices were employed for

the extraction and pre-concentration of  $\beta$ -blockers in urine samples prior HPLC-UV analysis.

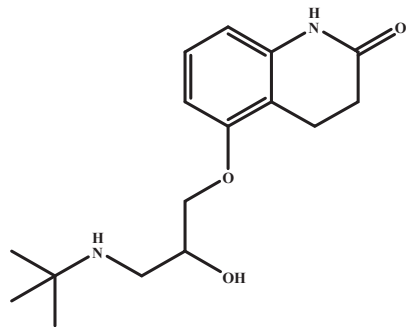
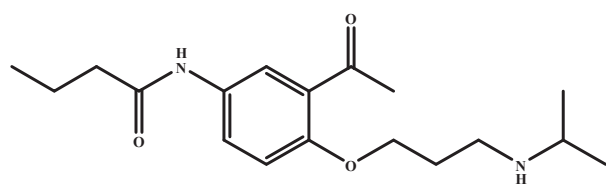
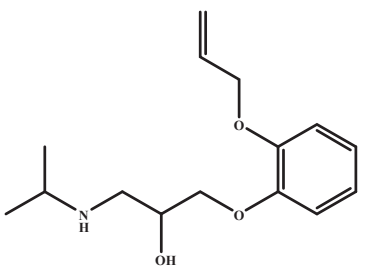
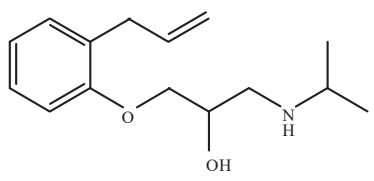
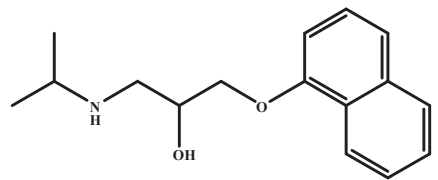
## **5.2. Experimental**

### *5.2.1. Reagents and materials*

Five  $\beta$ -blockers were selected for this study (**Table 5.1**): acebutolol, carteolol, oxprenolol, alprenolol and propranolol, all purchased from Sigma-Aldrich (Milwaukee, WI, USA). Benzophenone (BP), glycidyl methacrylate (GMA), ethylene glycol dimethacrylate (EDMA), 2,2-dimethoxy-2-phenylacetophenone (DMPA), 1-dodecanol, cyclohexanol, 1-methylimidazol (MIM) and 1-hexyl-3-methylimidazolium chloride ( $[\text{C}_6\text{MIM}][\text{Cl}]$ ) (see structure in **Table 5S.1**) were also purchased from Sigma-Aldrich. 1-Allyl-3-methylimidazolium chloride ( $[\text{AMIM}][\text{Cl}]$ ) (see structure in **Table 5.S1**) was acquired from Alfa Aesar (Lancashire, UK). Sodium hydrogen phosphate and sodium dihydrogen phosphate were obtained from Panreac Quimica (Barcelona, Spain). Acetonitrile (ACN), methanol (MeOH) and acetone were from VWR International Eurolab (Barcelona). Deionized water was obtained in Crystal B30 EDI Adrona deionizer (Riga, Latvia). All other reagents were of analytical grade, unless otherwise stated. Individual standard solutions of  $\beta$ -blockers ( $1000 \mu\text{g mL}^{-1}$ ) were prepared in MeOH:water (50:50, v/v) and stored at 4 °C. Working standard solutions were daily prepared by appropriate dilution with water. Spin columns with 700  $\mu\text{L}$  maximal volume were also supplied by Sigma-Aldrich.



**Table 5.1.** Structures and properties of the studied  $\beta$ -blocker

Compound	Structure	$pK_a^a$	$\text{Log}P_{o/w}^b$
Carteolol		ND	1.42
Acebutolol		9.12	1.83
Oxprenolol		9.13	2.30
Alprenolol		ND	3.10
Propranolol		9.67	3.48

<sup>a</sup> Calculated with ACD/pK database 4.06 from Advanced Chemistry Development Corporation. ND: No determined.

<sup>b</sup> C. J. Drayton, Comprehensive Medicine Chemistry, eds; Vol. 6, Pergamon Press, Oxford, 1990.

### 5.2.2. Instrumentation

Photo-polymerization studies in the spin column devices were carried out using a UV crosslinker (model CL-1000 Ultraviolet Crosslinker) from UPV Inc. (Upland, Canada, USA), containing five UV lamps ( $5 \times 8$  W, 254 nm). Elemental analysis of the synthesized materials was done with an EA 1110 CHNS elemental analyzer (CE Instruments, Milan, Italy). Scanning electronic microscopy (SEM) images of materials were carried out with a scanning electron microscope (S-4800, Hitachi, Ibaraki, Japan). A micro star 17R from VWR centrifuge was employed for the SPE protocol.

The chromatographic instrument consisted of a modular HPLC system from Agilent Technologies (Waldbronn, Germany), equipped with quaternary pump (Series 1200), autosampler (Series 1260 Infinity II), thermostated column compartment (Series 1290 Infinity II), and diode array detector (Series 1100). The flow rate was  $1 \text{ mL min}^{-1}$  and the column temperature,  $25 \text{ }^\circ\text{C}$ . The  $\beta$ -blockers were monitored at 254 nm. An HP Chemstation (Agilent, C.01.07) was used for data acquisition. The chromatographic column was a Zorbax Eclipse XDB-C18 ( $150 \times 4.6$  mm,  $5 \text{ }\mu\text{m}$  particle size, Agilent Technologies). The mobile phase contained 15% (v/v) ACN and 10 mM  $[\text{C}_6\text{MIM}][\text{Cl}]$ , and was buffered at pH 3 with 10 mM sodium dihydrogen phosphate and HCl. These separation conditions were adapted from Ref. [29].

### 5.2.3. Preparation of monolithic sorbent in spin column devices

Prior to polymerization, and with the purpose of achieving a covalent binding of monolithic beds to wall support, the inner surface of polypropylene centrifugal devices was treated with BP and EDMA, according to a protocol based on previous reports [30, 31]. The polymerization mixture was adapted from a previous work [31], and consisted of 60 wt% monomers (48 wt% GMA and 12 wt% EDMA), 40 wt% porogens (37 wt% cyclohexanol and 3 wt% 1-dodecanol), and 0.4 wt% DMPA (out of the total weight of the monomers) as free-radical initiator. The polymerization mixture was

introduced into an ultrasonic bath for 10 min and purged under N<sub>2</sub> stream for other 10 min. Then, 70 µL of the polymerization mixture was placed into the modified-wall spin column and photopolymerization was proceeded (2 h at 1 J cm<sup>-2</sup>). The resulting sorbent was designed as bare or parent monolith spin column. After the polymerization, the monolith was rinsed with MeOH several times to remove completely the porogens, oligomers and unreacted monomers, followed by centrifugation at 500 g during 15 min.

#### *5.2.4. Incorporation of ILs to GMA-based monoliths*

The incorporation of ILs was performed through two different approaches. The first route consisted in the functionalization of the GMA parent monolith with 1-methylimidazole (MIM) to generate the IL onto the monolith surface (see reaction in **Figure 5.S1**). The conditions were adapted from Ref. [27]. A MIM solution (25% (w/w) in ACN) was passed through the bare polymer (described above) at 75° C during 8 h. The resulting material was washed with MeOH. The second strategy consisted in the introduction of [AMIM][Cl] at two percentages (16 and 24 wt%) in the polymerization mixture. The resulting hybrid monoliths were prepared as described in Section 7.2.3, including the washing steps.

#### *5.2.5. (Micro)extraction procedure*

An SPE protocol using the prepared monolithic materials was applied to the extraction of β-blockers in aqueous solutions and urine samples. For this purpose, the spin column was pre-conditioned with ACN (500 µL) and 25 mM phosphate buffer at pH 12 (500 µL), at 500 g for 5 min. Next, 500 µL of buffered standard or sample solutions were loaded onto the (micro)SPE devices at 220 g for 10 min. The sorbent was washed with phosphate buffer (500 µL) by centrifugation at 500 g for 10 min. Finally, the retained drugs were eluted with 80:20 MeOH-water (v/v) (500 µL) at 220 g for 10 min for subsequent HPLC analysis. The devices were regenerated with this

methanolic solution (three times) at 500 g. All SPE steps were carried out at 20 °C. Other assayed conditions will be commented below.

### **5.3. Results and discussion**

#### *5.3.1. Preparation and characterization of the IL-modified monoliths*

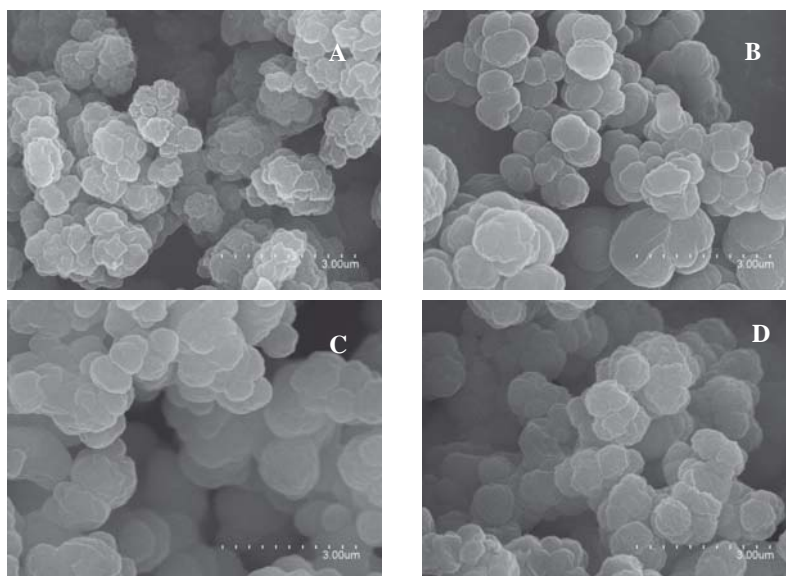
An important property of an SPE sorbent used in spin column format is the possibility of offering appropriate flow resistance, with enough loading capacity to retain the target analytes in a short processing time. To fulfill these requests, a GMA-based monolith as host polymer was adapted from Ref. [31], making modifications centered on the monomers/porogens ratio to assure a mechanically stable polymer with good flow-through properties. **Figure 5.1** shows the SEM micrographs corresponding to polymer monoliths prepared at several ratios (% w/w): 60/40 (**Figure 5.1A**), 50/50 (**Figure 5.1B**) and 40/60 (**Figure 5.1C**). As observed, an increase in the globule size and voids was yielded with increasing porogenic solvent content. Besides, the monoliths prepared with 50/50 and 40/60 (% w/w) ratios (**Figures 5.1B** and **5.1C**, respectively) were too porous, which led to their break in the centrifugation step. In contrast, the 60/40 ratio (% w/w) (**Figure 5.1A**) resulted in a strongly permeable porous monolith, with satisfactory mechanical resistance. This ratio was selected for further experiments.

Once the host polymer was selected, the bare monolith was modified with an IL using two approaches: (i) *in situ* generation of the IL onto the surface of the monolith by post-functionalization of the parent material, and (ii) incorporation of the IL as a monomer into the polymerization mixture (copolymerization). To carry out the first route, the GMA-based monolith was modified by adapting the conditions of Tian *et al.* [27], as described in Section 2.4, by passing a MIM solution through the spin column. After percolation of this solution, the resulting IL-monolith phase showed a too porous structure that broke down during the centrifugation step. In order to

enhance the mechanical resistance of the material, percolation through the polymer network of solutions with low contents of MIM (up to 1 wt%) was also tested. However, the resulting hybrid materials showed also fragile structures. Taking into account that the original structure of parent monolith was sufficiently rigid, the reason of the appearance of fragility could be the high temperature (75 °C) applied during a long time (8 hours) needed to obtain the desired modification. In view of these results, we decided to explore a different strategy based on the incorporation of the IL into the polymerization mixture.

Hybrid materials were prepared by incorporating two different amounts (16 and 24 wt%) of [AMIM][Cl] to the polymerization mixture, following the procedure described in Section 7.2.4. The introduction of the IL into the mixture was done at the expense of reducing the GMA content in the mixture, but always keeping constant the percentage of monomers at 60% (w/w). The resulting sorbents showed a proper rigid structure that avoided their breakage during the flow-through of the solutions, thus encouraging their reusability.

**Figure 5.1D** shows the SEM micrograph of the composite obtained in the presence of 24 wt% [AMIM][Cl]. Similar morphological structure was observed for the hybrid monolith prepared with 16 wt% IL. As observed, the incorporation of [AMIM][Cl] into the monolith produced larger globules than those found in the bare monolith (**Figure 5.1A**). Additionally, in order to confirm the presence of [AMIM][Cl] in the polymer matrix, the nitrogen content was evaluated by elemental analysis, obtaining  $0.125 \pm 0.007\%$  and  $0.190 \pm 0.014\%$  of N in the materials prepared with 16 and 24 wt% [AMIM][Cl], respectively. From these values, the percentage of IL incorporated into the monolith (0.71 and 1.07% AMIM-Cl, respectively) can be derived. Apart from showing good permeability, these materials allowed sufficient retention for the target  $\beta$ -blockers (as described in **Section 5.3.2**).



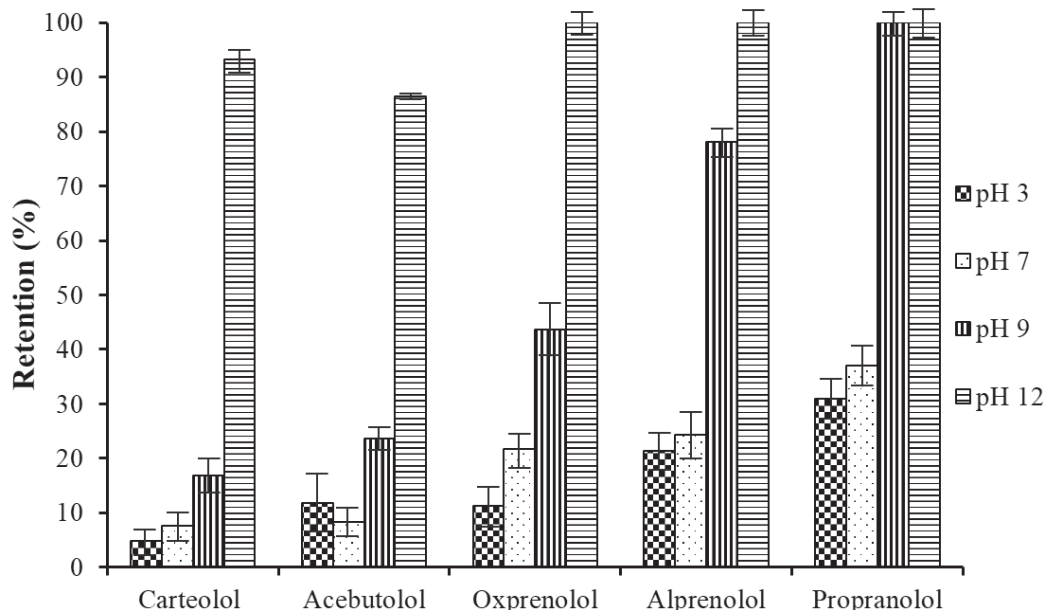
**Figure 5.1.** SEM micrographs of GMA-based monoliths prepared at different monomer/porogen ratios (wt/wt): (A) 60/40, (B) 50/50 and (C) 40/60. (D) is a SEM image corresponding to hybrid monolithic material prepared with [AMIM][Cl] at 24 wt% in the polymerization mixture. Magnification at 15000  $\times$ .

### *5.3.2. Evaluation of the IL-modified polymers as (micro)SPE sorbents*

Prior to performing the SPE optimization, a preliminary study was carried out with the two composites developed in the previous section, obtained by copolymerization of [AMIM][Cl]. In this study, a spin column containing a GMA-based monolith (bare polymer) was used as control sorbent for comparison purposes. To evaluate the extraction efficiency of all these sorbents, a solution containing 20  $\mu\text{g mL}^{-1}$  propranolol was used as test mixture. The centrifugation and conditioning conditions are described in **Section 5.2.5**. The percent retention of analytes onto the sorbent was evaluated as follows. The amount of a solute that is retained in the sorbent compared to the amount that was loaded onto the (micro)SPE device and that found in the percolated solution. Thus, the retention of propranolol was *ca.* 40% and 90% for the hybrid monoliths prepared with 16 and 24 wt% [AMIM][Cl], respectively. Meanwhile, the retention with bare GMA-based

material was below 10%. Based on these results, the composite synthesized (copolymerized) with 24 wt% [AMIM][Cl] was chosen for further studies.

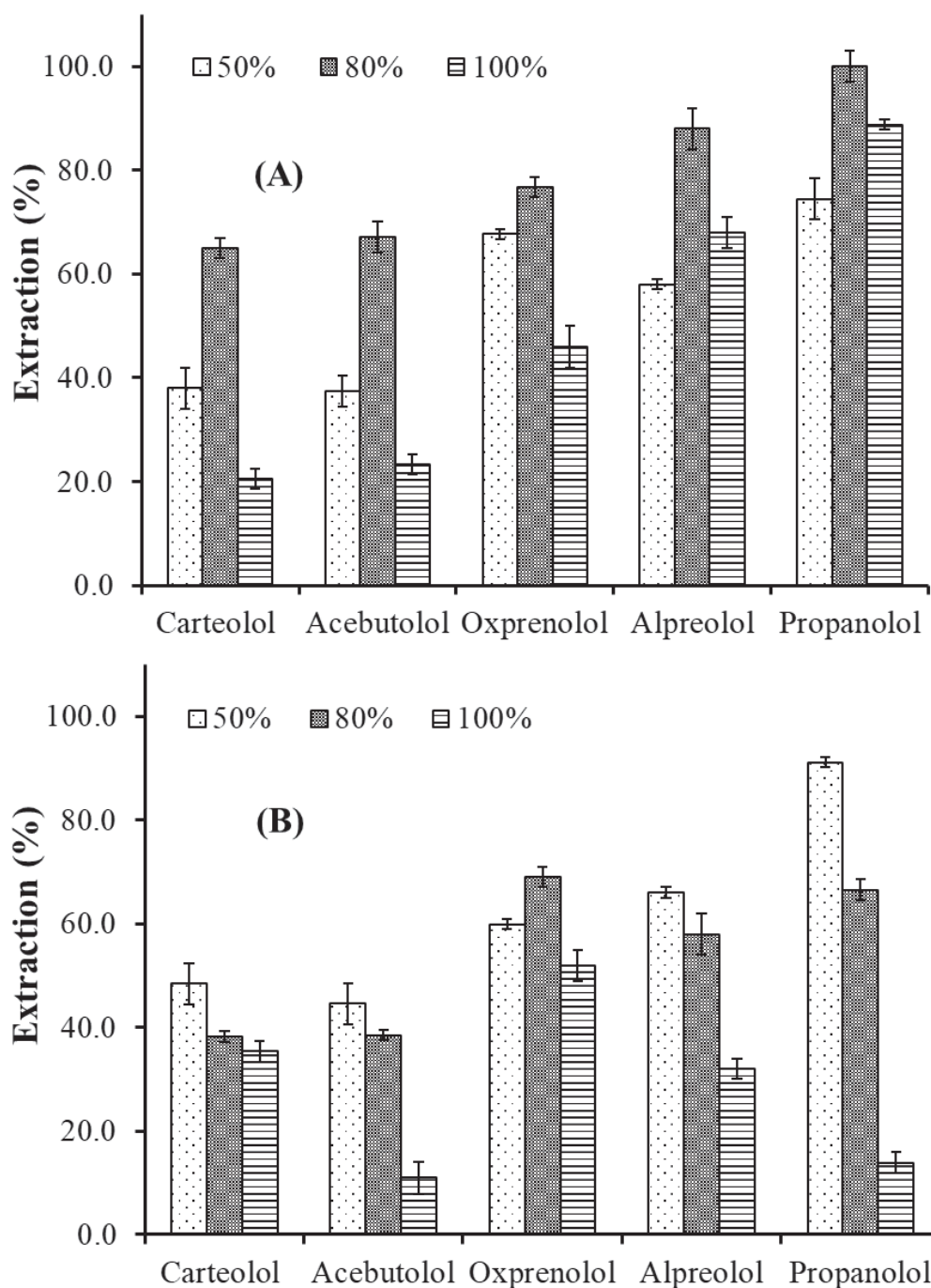
The parameters that may affect the extraction efficiency of  $\beta$ -blockers were next studied, using the hybrid monolith prepared with 24 wt% [AMIM][Cl]. Sample pH is a key variable that modifies the ionization degree of the target analytes and the effective surface charge of the sorbent. This may affect the extraction performance of the investigated analytes. The effect of sample pH on the loading SPE step was investigated in the range from 3 to 12. Solutions containing  $20 \mu\text{g mL}^{-1}$  of each  $\beta$ -blocker (500  $\mu\text{L}$ ) were passed-through the spin columns at several pH values, following the steps described in Section 7.2.5. The obtained retention for each drug is shown in **Figure 5.2** (see also **Table 5.1** for  $\log P_{o/w}$  data, where the compounds are ordered according to their hydrophobicity). As observed, the retention of  $\beta$ -blockers was stronger at increasing pH, with the highest retention at pH 12. These results can be explained taking into account the ionization state of the  $\beta$ -blockers and their interaction with the hybrid IL-monolith phase. At acidic or neutral pH, the amino moieties of  $\beta$ -blockers are protonated (see **Table 5.1** for  $\text{p}K_a$  data), and the repulsion between these groups and the imidazole ring (positively charged) of the IL is translated into lower retention of the analytes. At pH 12, the molecular form of the  $\beta$ -blockers is dominant, and the electrostatic repulsion with the IL-monolith phase is minimized, thus favoring their retention on the sorbent. The results are consistent with those found by other authors for basic compounds (aromatic amines) separated with IL-modified silica materials [32]. In any case, the obtained results suggest that the electrostatic interaction plays a key role in the extraction, although other interactions such as hydrophobic,  $\pi$ - $\pi$  stacking and hydrogen bonding also may participate in the retention mechanism of the  $\beta$ -blockers. Based on the obtained results, pH 12 was selected for sample loading and extended for the washing step, where small losses (<1%) of these compounds were found at this pH.



**Figure 5.2.** Influence of pH on retention of  $\beta$ -blockers using a hybrid monolith prepared with 24 wt% [AMIM][Cl]. Error bar = SD ( $n = 3$ ).

The elution of  $\beta$ -blockers from the hybrid monolith surface was next considered. For this purpose, several aqueous-organic mixtures were assayed in order to achieve the highest eluting efficiencies (**Figure 5.3**, parts A-B). As can be seen, 80/20 (v/v) MeOH-water mixture (**Figure 5.3A**) exhibited the best recoveries. This can be explained by the protic behavior of MeOH compared with ACN, which can favor the easy desorption of the analytes from the sorbent.





**Figure 5.3.** Influence of the composition of the elution solvent on the recovery of the tested  $\beta$ -blockers: (A) MeOH-water and (B) ACN-water mixtures. Error bar = SD ( $n = 3$ ).

The established SPE protocol was applied to the bare GMA-based sorbent, obtaining recoveries close to 30% for all  $\beta$ -blockers, which are quite lower

with respect to those found for the IL-modified material. These results underlined the significant role of the IL in the extraction efficiency of these compounds.

Once the optimal extraction conditions were found, several quality parameters of the sorbent, such as the loading capacity and reusability were evaluated. The loading capacity of the IL-modified monolith was established by passing through the spin column different concentrations of propranolol (from 2 to 100  $\mu\text{g mL}^{-1}$ ) in a fixed volume (500  $\mu\text{L}$ ). A maximal value of 2.5  $\mu\text{g}$  per mg sorbent (with recoveries close to 100%) was obtained. The reusability of the hybrid monolith was carried out using the recommended SPE procedure (see Section 7.2.5). It was checked that the developed sorbent could be reused at least 20 times without losing significant properties in its features (with recoveries above 90%).

Finally, to assay the pre-concentration factor, different volumes of elution solvent (50-500  $\mu\text{L}$ ) were tested to assure the minimal (but enough) volume necessary to elute the retained analytes with the highest sensitivity. This study indicated that the minimal elution volume that provided a quantitative recovery of the analytes (> 80%) was 100  $\mu\text{L}$ .

### *5.3.3. Figures of merit and application to real samples*

The optimized (micro)SPE procedure, in combination with HPLC-UV detection, was validated in terms of linearity, sensitivity and precision. High correlation coefficients ( $r > 0.998$ ) were achieved within the range  $4.6\text{--}1 \times 10^5$   $\mu\text{g L}^{-1}$  for the target compounds. The limits of detection (LOD) and quantitation (LOQ) were calculated as the concentration of analyte that provided a detector response with a signal-to-noise ratio of 3 and 10, respectively (see **Table 5.2**). The LODs were in the range  $1.4\text{--}40$   $\mu\text{g L}^{-1}$ , whereas the LOQs were comprised between 4.6 and 132  $\mu\text{g L}^{-1}$ . The precision of the method (intra- and inter-device) was evaluated for standard solutions of  $\beta$ -blockers containing 2  $\mu\text{g mL}^{-1}$ , where RSD values below 8.2% were

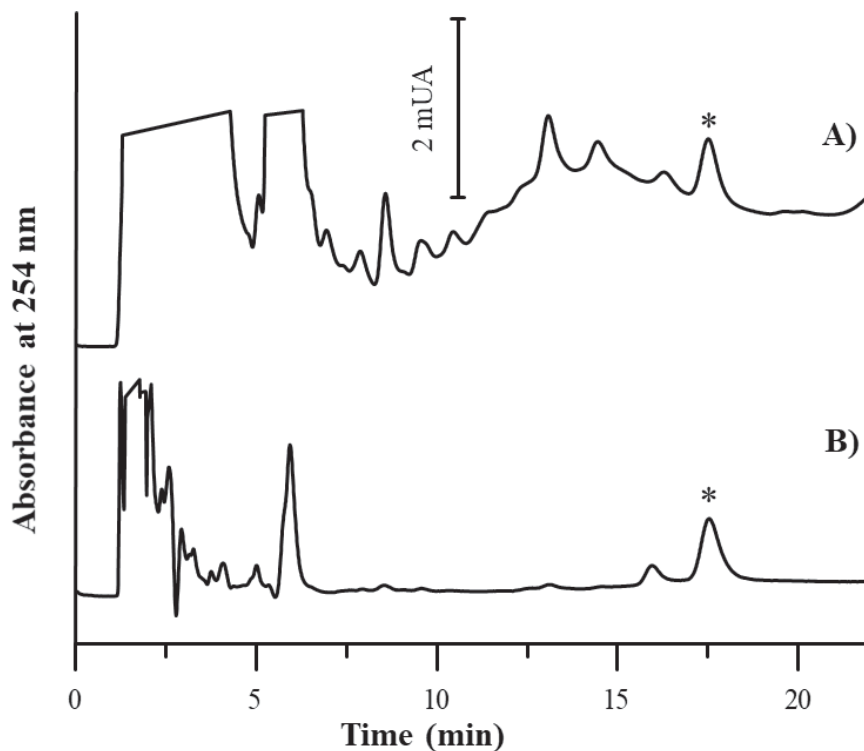
found. This demonstrated the reproducibility in the preparation of IL-modified monolithic units.

**Table 5.2.** Analytical figures of merit of the [AMIM][Cl] modified monolithic (micro)extraction device for the determination of the target  $\beta$ -blockers.

Analyte	LOD ( $\mu\text{g}\cdot\text{L}^{-1}$ )	LOQ ( $\mu\text{g}\cdot\text{L}^{-1}$ )	Precision	
			Intra-spin column	Inter-spin columns
			RSD (% , n = 3)	RSD (% , n = 3)
Carteolol	2.0	6.6	5.4	8.2
Acebutolol	1.4	4.6	4.2	7.7
Oxprenolol	40.0	132.0	5.1	8.0
Alprenolol	40.0	132.0	3.3	6.9
Propranolol	20.0	66.0	6.5	7.8

LOD: limit of detection, LOQ: limit of quantification, RSD: relative standard deviation

The proposed procedure was applied to the extraction of propranolol in human urine. For this purpose, blank urine samples were fortified with the target analyte at two concentration levels (1 and 5  $\mu\text{g mL}^{-1}$ ), and analyzed using the extraction protocol. The recoveries of propranolol were satisfactory, ranging between 90.3 and 110.6%. **Figure 5.4** shows the chromatograms for blank urine samples spiked with the analyte, before and after SPE treatment. From these results, it is clear that an effective clean-up of the sample showing no matrix interference of endogenous urine compounds was achieved, thus allowing a proper quantitative determination of the drug.



**Figure 5.4.** Chromatograms of spiked urine with propranolol (peak labelled with asterisk), extracted using the IL-modified monolithic spin column, without pretreatment (A) and with pretreatment (B). Chromatographic conditions as in **Section 5.2.2**. The final concentration of propranolol in the spiked samples was  $20 \mu\text{g mL}^{-1}$ .

The developed (micro)SPE sorbent was compared with other recent sample preparation approaches used for the extraction of  $\beta$ -blockers in biological samples (**Table 5.3**). In terms of linearity, the method reported in this work provided a wider application range than other sample preparation methods (see for instance, Refs. [6, 33–38]), and similar to that reported in Ref. [39]. Concerning the recovery values found, these were similar to those obtained in some reported studies [6, 34–36, 39], although the values in this work were better than those given in Refs. [33, 35, 37, 38]. The LODs were similar to those reported using UV detection [33, 34, 38], and higher than those obtained when MS was employed as detector system [6, 35, 39].

**Table 5.3.** Comparison of the proposed method with other recently reported methods for the determination of  $\beta$ -blockers in biological samples.

Material used	Analytes	Sample	Method	Figures of merit (LODs, $\mu\text{g}\cdot\text{L}^{-1}$ ; Linearity $\mu\text{g}\cdot\text{L}^{-1}$ , ER, %)
C18 cartridge	alprenolol, acebutolol, carazolol	Human plasma	SPE / HPLC- UV	
Oasis HLB cartridges	rinone, sotolol, metoprolol, propranolol	uman urine	SPE / UPLC- UV	8.9-66.2; 40-20000; 70.4-98.6
Oasis HLB and Plexa cartridges	norol, pindolol, acebutolol, metoprolol, labetalol, propranolol	uman urine	SPE / HPLC- DAD	-; -; 70-80
Commercial MIP (SupelMIP <sup>®</sup> )	metoprolol, labetalol, propranolol	uman urine	SPE / HPLC- DAD	0.6-2.0; 10-1000; 94-105
MIP-modified membrane	Propranolol	and plasma	MISPE / HPLC- MS/MS	-; 10-1500; 85.2-114
MIP	Atenolol	uman urine	MISPE / Fluorescence	32; 100-2000; 74.5-75.3

Table 5.3. Continuation

Material used	Analytes	Sample	Method	Figures of merit (LODs, $\mu\text{g}\cdot\text{L}^{-1}$ ; Linearity $\mu\text{g}\cdot\text{L}^{-1}$ , ER, %)	Ref.
HLB and C18 sorbents	Acebutolol, atenolol, fenoterol, nadolol, pindolol, procaterol, sotalol, timolol	Human urine and plasma	Thin-film SPME / HPLC-MS/MS	0.018-1.15; -; 83.4-122.3	[6]
Dichlorometane (organic extractant phase)	Metoprolol, propranolol	Human plasma	Tandem DLLME / HPLC-UV	0.8-1.0; 2.5-2500; 34-45	[38]
IL-modified magnetic core-shell nanoparticles	Propranolol, metoprolol, atenolol, alprenolol	Human plasma	EP-DSPE / HPLC-MS/MS	0.03-0.44; 0.5-10000; 75-91	[39]
Poly(GMA-co-[AMIM][Cl]-co-EDMA) monolith	Carteolol, acebutolol, oxprenolol, alprenolol, propranolol	Human urine	(micro)SPE / HPLC-UV	1.4-40; 4.6-100000; 90.3-110.6	This work

DLLE: dispersive liquid-liquid microextraction; DSPME: dispersive solid-phase microextraction, EP-DSPE: effervescent powder-dispersive SPE, MISPE: molecularly-imprinted SPE

In any case, our methodology is sensitive enough to quantify the maximal allowable urinary concentration (minimal required performance level, MRPL) of  $\beta$ -blockers, which has been set at  $0.1 \mu\text{g mL}^{-1}$  by WADA [40]. Furthermore, our (micro)SPE sorbent offers easy preparation and satisfactory reusability, it is environment-friendly, and allows the handling of many samples simultaneously (with a sample throughput of  $> 40 \text{ samples h}^{-1}$ ), which undoubtedly speeds the sample treatment. Additionally, the cheap synthesis of the material, in combination with the absence of sophisticated instrumentation, makes this methodology an attractive alternative for routine sample analysis.

## 5.4. Conclusions

The study carried out in this work shows the preparation of novel hybrid IL-monoliths in spin columns, for the isolation of  $\beta$ -blockers in human urine. For this purpose, two routes were followed: (i) *in situ* generation of IL onto the surface of GMA-based monolith, and (ii) the incorporation of IL into the polymerization mixture. The first approach was unsuccessful due to the observed sorbent fragility after IL incorporation. The second approach gave appropriate mechanical resistance and good flow-through properties for the synthesized materials. In particular, the composites containing 24 wt% [AMIM][Cl] provided the largest retention of the target compounds (a set of  $\beta$ -blockers).

The SPE protocol was optimized in terms of pH of the loading solution and the composition of the elution solvent that yielded the best performance. The presence of [AMIM][Cl] in the resulting composite provided an enhanced retention of the  $\beta$ -blockers (compared with the bare polymer), due to several interactions (such as electrostatic, hydrogen bonding,  $\pi$ - $\pi$  and hydrophobic forces). Under the optimized SPE conditions, the novel IL-modified phase showed an effective sample clean-up with high recoveries (above 90%) in the extraction of propranolol in human urine. Compared with other published methods for sample preparation of  $\beta$ -blockers, the SPE devices showed reduced environmental impact, low cost and easy synthesis of the sorbent material, which can be suitably reused (> 20 times after a simple regeneration step). Additionally, the format of the polymeric monolith in spin column format is highly competitive for multiple sample processing, and can be extended to routine bioanalytical applications.



## 5.5. References

- [1] World Health Statistics 2012 report. World Health Organization, Geneva, 2012.
- [2] [https://www.wada-ama.org/sites/default/files/wada\\_2019\\_english\\_prohibited\\_list.pdf](https://www.wada-ama.org/sites/default/files/wada_2019_english_prohibited_list.pdf) (accessed November 2019).
- [3] M.J. Paik, J. Lee, K.R. Kim, Simultaneous screening analysis of multiple  $\beta$ -blockers in urine by gas chromatography-mass spectrometry in selected ion monitoring mode, *Anal. Chim. Acta* 601 (2007) 230–233. doi: 10.1016/j.aca.2007.08.036
- [4] S. Magiera, C. Uhlschmied, M. Rainer, Ch. W. Huck, I. Baranowska, G.K. Bonn. GC-MS method for the simultaneous determination of  $\beta$ -blockers, flavonoids, isoflavones and their metabolites in human urine, *J. Pharm. Biomed. Anal.* 56 (2011) 93–102. doi: 10.1016/j.jpba.2011.04.024
- [5] K. Saleem, I. Ali, U. Kulsum, H.Y. Aboul-Enein, Recent developments in HPLC: analysis of  $\beta$ -blockers in biological samples, *J. Chromatogr. Sci.* 51 (2013) 807–818. doi: 10.1093/chromsci/bmt030
- [6] K. Goryński, A. Kiedrowicz, B. Bokjo, Development of SPME-LC-MS method for screening of eight beta-blockers and bronchodilators in plasma and urine samples, *J. Pharm. Biomed. Anal.* 127 (2016) 147–155. doi: 10.1016/j.jpba.2016.03.001
- [7] T. Nema, E.C.Y. Chan, P.C. Ho, Applications of monolithic materials for sample preparation, *J. Pharm. Biomed. Anal.* 87 (2014) 130–141. doi: 10.1016/j.jpba.2013.05.036
- [8] J.C. Masini, F. Svec, Porous monoliths for on-line sample preparation: a review, *Anal. Chim. Acta* 964 (2017) 24–44. doi: 10.1016/j.aca.2017.02.002

- [9] B. Fresco-Cala, S. Cárdenas, Potential of nanoparticle-based hybrid monoliths as sorbents in microextraction techniques, *Anal. Chim. Acta* 1031 (2018) 15–27. doi: 10.1016/j.aca.2018.05.069
- [10] M. Vergara-Barberán, E.J. Carrasco-Correa, M.J. Lerma-García, E.F. Simó-Alfonso, J.M. Herrero-Martínez, Current trends in affinity-based monoliths in microextraction approaches: a review, *Anal. Chim. Acta* 1084 (2019) 1–20. doi: 10.1016/j.aca.2019.07.020
- [11] L. Vidal, M.L. Riekkola, A. Canals, Ionic liquid-modified materials for solid-phase extraction and separation: a review, *Anal. Chim. Acta* 715 (2012) 19–41. doi: 10.1016/j.aca.2011.11.050
- [12] M. Zhang, A.K. Mallik, M. Takafuji, H. Ihara, H. Qu, Versatile ligands for high-performance liquid chromatography: an overview of ionic liquid-functionalized stationary phases, *Anal. Chim. Acta* 887 (2015) 1–16. doi: 10.1016/j.aca.2015.04.022
- [13] X. Shi, L. Qiao, G. Xu, Recent development of ionic liquid stationary phases for liquid chromatography, *J. Chromatogr. A* 1420 (2015) 1–15. doi: 10.1016/j.chroma.2015.09.090
- [14] R. Chen, H. Zhou, M. Liu, H. Yan, X. Qiao, Ionic liquids-based monolithic columns: recent advancements and their applications for high-efficiency separation and enrichment, *Trends Anal. Chem.* 111 (2019) 1–12. doi: 10.1016/j.trac.2018.11.026
- [15] S.K. Singh, A.W. Savoy, Ionic liquids synthesis and applications: an overview, *J. Mol. Liq.* 297 (2020) 112038. doi: 10.1016/j.molliq.2019.112038
- [16] H. Passos, M.G. Freire, J.A.P. Coutinho, Ionic liquid solutions as extractive solvents for value-added compounds from biomass, *Green Chem.* 16 (2014) 4786–4815. doi: 10.1039/C4GC00236A

- [17] A. Berthod, M.J. Ruiz-Angel, S. Carda-Broch, Recent advances on ionic liquid uses in separation techniques, *J. Chromatogr. A* 1559 (2018) 2–16. doi: 10.1016/j.chroma.2017.09.044
- [18] M.J. Trujillo-Rodríguez, H. Nan, M. Varona, M.N. Emaus, I.D. Souza, J.L. Anderson, Advances of ionic liquids in analytical chemistry, *Anal. Chem.* 91 (2019) 505–531. doi: 10.1021/acs.analchem.8b04710
- [19] N. Fontanals, F. Borrull, R.M. Marcé, Ionic liquids in solid-phase extraction, *Trends Anal. Chem.* 41 (2012) 15–26. doi: 10.1016/j.trac.2012.08.010
- [20] N. Miękus, I. Olędzka, N. Kossakowska, A. Plenis, P. Kowalski, A. Prahł, T. Bączek, Ionic liquids as signal amplifiers for the simultaneous extraction of several neurotransmitters determined by micellar electrokinetic chromatography, *Talanta* 186 (2018) 119–123. doi: 10.1016/j.talanta.2018.04.041
- [21] N. Kossakowska, I. Olędzka, A. Kowalik, N. Miękus, P. Kowalski, A. Plenis, E. Bień, A. Kaczorowska, M.A. Krawczyk, E. Adamkiewicz-Drożyńska, T. Bączek, Application of SPME supported by ionic liquids for the determination of biogenic amines by MEKC in clinical practice, *J. Pharm. Biomed. Anal.* 173 (2019) 24–30. doi: 10.1016/j.jpba.2019.05.021
- [22] P. Zhang, H. Yang, T. Chen, Y. Qin, F. Ye, Facile one-pot preparation of a novel imidazolium-based monolith by thiol-ene click chemistry for capillary liquid chromatography, *Electrophoresis* 38 (2017) 3013–3019. doi: 10.1002/elps.201600288
- [23] T. Wang, Y. Chen, J. Ma, X. Zhang, L. Zhang, Y. Zhang, Ionic liquid-based zwitterionic organic polymer monolithic column for capillary hydrophilic interaction chromatography, *Analyst* 140 (2015) 5585–5592. doi: 10.1039/C5AN00662G
- [24] J. Wang, L. Bai, Z. Wei, J. Qin, Y. Ma, H. Liu, Incorporation of ionic liquid into porous polymer monoliths to enhance the separation of small

molecules in reversed-phase high-performance liquid chromatography, *J. Sep. Sci.* 38 (2015) 2101–2108. doi: 10.1002/jssc.201500061

[25] C. Liu, Q. Deng, G. Fang, M. Dang, S. Wang, Capillary electrochromatography immunoassay for alpha-fetoprotein based on poly(guanidinium ionic liquid) monolithic material, *Anal. Biochem.* 530 (2017) 50–56. doi: 10.1016/j.ab.2017.04.014

[26] H. Han, Q. Wang, X. Liu, S. Jiang, Polymeric ionic liquid modified organic-silica hybrid monolithic column for capillary electrochromatography, *J. Chromatogr. A* 1246 (2012) 9–14. doi: 10.1016/j.chroma.2011.12.029

[27] M. Tian, H. Yan, K.H. Row, Solid-phase extraction of caffeine and theophylline from green tea by a new ionic liquid-modified functional polymer sorbent, *Anal. Lett.* 43 (2009) 110–118. doi: 10.1080/00032710903276554

[28] T.T. Wang, Y.H. Chen, J.F. Ma, M.J. Hu, Y. Li, J.H. Fang, H.Q. Gao, A novel ionic liquid-modified organic-polymer monolith as the sorbent for in-tube solid-phase microextraction of acidic food additives, *Anal. Bioanal. Chem.* 406 (2014) 4955–4963. doi: 10.1007/s00216-014-7923-4

[29] M.T. Ubeda-Torres, C. Ortiz-Bolsico, M.C. García-Alvarez-Coque, M.J. Ruiz-Angel, Gaining insight in the behaviour of imidazolium-based ionic liquids as additives in reversed-phase liquid chromatography for the analysis of basic compounds, *J. Chromatogr. A* 1380 (2015) 96–103. doi: 10.1016/j.chroma.2014.12.064

[30] B. Fresco-Cala, S. Cárdenas, J.M. Herrero Martínez, Preparation of methacrylate monoliths with oxidized single-walled carbon nanohorns for the extraction of nonsteroidal anti-inflammatory drugs from urine samples, *Microchim. Acta* 184 (2017) 1863–1871. doi: 10.1007/s00604-017-2203-6

- [31] M. Giesbers, E.J. Carrasco-Correa, E.F. Simó-Alfonso, J.M. Herrero-Martínez, Hybrid monoliths with metal-organic frameworks in spin columns for extraction of non-steroidal drugs prior to their quantitation by reversed-phase HPLC, *Microchim. Acta* 186 (2019) 759. doi: 10.1007/s00604-019-3923-6
- [32] L. Vidal, J. Parshintsev, K. Hartonen, A. Canals, M.L. Riekkola, Ionic liquid-functionalized silica for selective solid-phase extraction of organic acids, amines and aldehydes, *J. Chromatogr. A* 1266 (2012) 2–10. doi: 10.1016/j.chroma.2011.08.075
- [33] I. Ali, U. Kulsum, K. Saleem, N. Nagae, V.D. Gaitonde, Novel SPE-HPLC method for analyses of  $\beta$ -blockers in human plasma using new generation phenyl-ethyl column, *Am. J. Adv. Drug Deliv.* 3 (2015) 32–51.
- [34] I. Baranowska, S. Magiera, J. Baranowski, UHPLC method for the simultaneous determination of  $\beta$ -blockers, isoflavones, and flavonoids in human urine, *J. Chromatogr. Sci.* 49 (2011) 764–773. doi: 10.1093/chrsci/49.10.764
- [35] W. Boonjob, H. Sklenářová, F.J. Lara, A.M. García-Campaña, P. Solich, Retention and selectivity of basic drugs on solid-phase extraction sorbents: application to direct determination of  $\beta$ -blockers in urine, *Anal. Bioanal. Chem.* 406 (2014) 4207–4215. doi: 10.1007/s00216-014-7753-4
- [36] T. Renkecz, G. Ceolin. V. Horváth, Selective solid phase extraction of propranolol on multiwell membrane filter plates modified with molecularly imprinted polymer, *Analyst* 136 (2011) 2185–2172. doi: 10.1039/C0AN00906G
- [37] Y. Gorbani, H. Yilmaz, H. Basan, Spectrofluorimetric determination of atenolol from human urine using high-affinity molecularly imprinted solid-phase extraction sorbent, *Luminiscence* 32 (2017) 1391–1397. doi: 10.1002/bio.3335
- [38] M. Hemmati, A. Asghari, M. Bazregar, M. Rajabi, Rapid determination of some beta-blockers in complicated matrices by tandem

dispersive liquid-liquid microextraction followed by high performance liquid chromatography, *Anal. Bioanal. Chem.* 408 (2016) 8163–8176. doi: 10.1007/s00216-016-9922-0

[39] S. Jamshidi, M.K. Rofouei, G. Thorsen, Using magnetic core-shell nanoparticles coated with an ionic liquid dispersion assisted by effervescence powder for the micro-solid-phase extraction of four beta blockers from human plasma by ultra-high performance liquid chromatography with mass spectrometry detection, *J. Sep. Sci.* 42 698–705. doi: 10.1002/jssc.201800834

[40] [https://www.wada-ama.org/sites/default/files/resources/files/td2019mrpl\\_eng.pdf](https://www.wada-ama.org/sites/default/files/resources/files/td2019mrpl_eng.pdf) (accessed december 2019).

## 5.6. Supporting Material

Table 5.S1. Structures of ILs used in this study.

Name	Use	Structure
1-Hexyl-3-methyl imidazolium ([HMIM][Cl])	Mobile phase additive	
1-Allyl-3-methyl imidazolium ([AMIM][Cl])	Monomer	

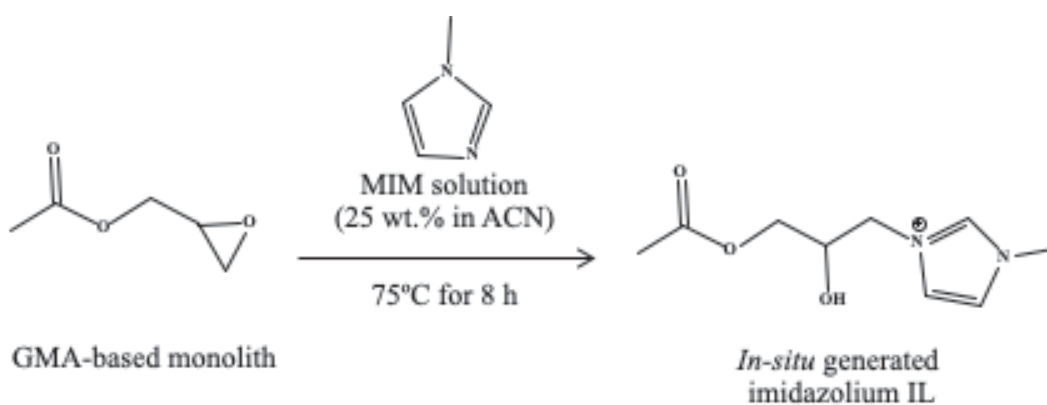


Figure 5.S1. Post-modification reaction scheme of GMA-based monolith.





**Capítulo 6. Determination of benzomercaptans in environmental complex samples by combining zeolitic imidazolate framework-8-based solid-phase extraction and high-performance liquid chromatography with UV detection**





## Determination of benzomercaptans in environmental complex samples by combining zeolitic imidazolate framework-8-based solid-phase extraction and high-performance liquid chromatography with UV detection

Héctor Martínez-Pérez-Cejuela <sup>a, \*</sup>, Óscar Mompó-Roselló <sup>a, \*</sup>, Neus Crespi-Sánchez <sup>b</sup>, Carlos Palomino Cabello <sup>b</sup>, Mónica Catalá-Icardo <sup>c</sup>, Ernesto F. Simó-Alfonso <sup>a</sup>, José Manuel Herrero-Martínez <sup>a</sup>  

In this work, the synthesis of zeolitic imidazolate framework-8 (ZIF-8) crystals and their subsequent application as effective sorbents for extraction and preconcentration of several benzomercaptans from environmental complex samples is described. These materials were prepared by solvothermal approach varying the concentration of n-butylamine modulator to modify the surface of the metal-organic framework. The resulting materials were characterized by scanning and transmission electron microscopy, powder X-ray diffraction and Fourier transform infrared spectroscopy. The ZIF-8 material that gave the best features was selected as extractive phase and the influence of various parameters (sample pH and elution solvent composition, among others) on the extraction efficiency of target compounds were investigated. Under the optimal conditions of the method, the tested analytes (2-mercaptobenzothiazole, 2-mercaptobenzoxazole and 2-mercapto-6-nitrobenzothiazole) were retained and eluted quantitatively with alkaline 50:50 (v:v) methanol-water mixture. Using the proposed method, low limits of detection, in the range of 16-21 ng L<sup>-1</sup> for aqueous samples and 0.4-0.5 µg kg<sup>-1</sup> for soil samples, were achieved whereas the precision (expressed as relative standard deviation) was lower than 7%. The resulting solid-phase extraction protocol, using the zeolitic material as sorbent, was combined with liquid chromatography and ultraviolet-vis detector and successfully applied to determine traces of these organic pollutants in environmental samples.

**Keywords:** Metal-organic frameworks; environmental pollutants; soil and aqueous samples; solid-phase extraction; sorbent; sample preparation

## **6.1. Introduction**

Metal-organic frameworks (MOFs) have aroused a great interest over the last decades. These coordination polymers are a class of highly porous materials composed of metal ions or clusters linked by organic ligands. Their crystalline structures, including their pore sizes and surfaces, can be controlled by a careful selection of their precursors. MOFs are characterized by a large specific surface area and intrinsic porosity, as well as profuse active sites [1]. Many applications have been proposed for this type of materials, and surely, their number will grow in the coming years. Some of those applications include gas/electrical storage and catalysis [2], removal of contaminants in air or water by adsorption and separation [3-4], sensors [5] and sorbents for sample preparation [6]. In particular, zeolitic imidazolate frameworks (ZIFs) are a subfamily of MOFs consisting of Zn or Co metal ions tetrahedrally coordinated by anionic imidazolate ligands [7, 8]. ZIF-8 [Zn(2-methylimidazolate)<sub>2</sub>] has been widely used due to its easy synthesis, high thermal and chemical stabilities [9, 10], great pore volume and surface area [9]. ZIF-8 shows a very large adsorption capacity, which is attributed to its high porosity and the different ways in which it can interact with adsorbates, such as  $\pi$ -stacking, hydrogen bonding and ionic interactions [11, 12]. Such good features have become this material in one of the most attractive MOFs for the extraction and preconcentration of analytes. Related to this, solid-phase microextraction (SPME) [6] has been commonly reported as a suitable sample preparation technique in the extraction of amines [13], polycyclic aromatic hydrocarbons [14], BTEX [15] and fluoroquinolones [16] from environmental water samples. Despite its advantages, SPME has certain disadvantages such as the limited fiber lifetime, its fragility and its relatively high cost. In this sense, other alternatives based on conventional solid-phase extraction (SPE) format (syringe/cartridges) [17], magnetic SPE [18] or the use of membrane as support medium [19-21] have been developed. However, the preparation of homogenous ZIF-8 membranes is a difficult task presenting

some drawbacks such as possible sedimentation phenomena of MOF crystals during the preparation stage, the formation of bubbles during stirring (poor reproducibility) and limited reusability (blockage of pores of membrane). Besides, in most of these works, the selectivity of sorbent has been attributed to the hydrophobic and  $\pi$ -interactions of solutes with the 2-methylimidazole ligands instead of taking advantages of their tunable pore size and feasible chemical functionalization [22].

The pollution of the environment by organic compounds is always of great concern due to the toxicity risks for aquatic organisms and human posed by their occurrence and increasing concentration in water bodies. Among organic pollutants, benzomercaptans, such as 2-mercaptobenzothiazole (MBT) and 2-mercaptobenzoxazole (MBO), deserve special attention due to their broad use in many industrial processes. These compounds are commonly used as vulcanization accelerators in the rubber industry, as biocorrosion inhibitors, as coating agents of metallic surfaces, and as biocides in medical applications [23-24]. As consequence, such compounds have been found in different environmental compartments such as surface waters, wastewater effluents, sewage treatment plants, soils, roadsides, etc. These poorly biodegradable pollutants may cause allergic reactions, induce tumours, and be toxic to aquatic organisms [25-26]. According to the NSF International Standard/American National Standard (NSF/ANSI 60-2016), the drinking water criteria (Annex C) for MBT is maximum contamination levels or maximum allowable concentration, respectively of total allowable concentration is  $20 \mu\text{g L}^{-1}$ , single product allowable concentration is  $2 \mu\text{g L}^{-1}$  [27]. In order to reach these low concentrations, determination techniques mainly based on LC combined with mass spectrometry detectors have been reported [28-31]. In any case, sample preparation techniques are required in order to reduce matrix interferences and to improve sensitivity to benzomercaptans in environmental complex samples, being SPE the most common technique used for extraction and preconcentration of these kind of

analytes [23, 24, 28, 30, 31]. However, SPE shows some disadvantages, such as limited selectivity and poor reusability.

In order to overcome the above-mentioned drawbacks, there is a recent interest concerned to functionalized MOFs, which are obtained by incorporation of ligands including additional functional groups ( $-\text{OH}$ ,  $-\text{NH}_2$ , ...). Particularly, amine-functionalized MOFs have mainly attracted attention since they improved MOF water stability and provided the possibility of forming hydrogen bonds and even electron transfer capability towards analytes [32]. Recently, these materials have applied for capturing of several polar guests from different matrices. Thus,  $\text{NH}_2\text{-MIL-101(Fe)}$  and  $\text{NH}_2\text{-MIL-53(Al)}$  have been used for the removal of imidacloprid in water [33] and to selectively recognize tetracyclines from milk [34], respectively. Also, amino-functionalized UiO-66 combined with magnetic  $\text{Fe}_3\text{O}_4$  microspheres has been used for the selective extraction of bisphenols in river water samples [35]. In these works, the introduction of amino moieties is accomplished by one-pot solvothermal synthesis MOFs, which has the advantage of avoiding the complicated steps required in post-modification approach. Alternatively, amino moieties can be incorporated through the addition of organic amines as modulators in the synthesis mixture of MOF [22]. However, this approach has not been explored in literature with sample treatment purposes.

In this work, amine-modulated ZIF-8 (nano)crystals ( $\text{NH}_2\text{-ZIF-8}$ ) was used as sorbent for the extraction of these target compounds (MBO, MBT and its nitro derivative) in environmental samples. The incorporation of n-butylamine molecules to the framework structure resulted appropriate to tailor the surface properties improving the selectivity of the extraction of these polar compounds. Although this type of material has been previously used in hydrophobic compounds in dispersive mode with sophisticated technique (GC-MS) [36], its application to hydrophilic compounds in cartridge format with accessible instrumentation (LC-UV) has not been explored. Taking into account the key role of butylamine (BA) as modulator, in this work, its

content on crystal structure and posterior interaction with analytes was studied. The resulting MOF that provided the best features was selected as SPE sorbent and parameters affecting the extraction process such sample pH and eluent solvent composition (among others) were investigated. Finally, the applicability of the method for the analysis of these compounds by HPLC-UV was evaluated in environmental samples obtained from different sources.

## 6.2. Experimental section

### 6.2.1. Reagents and materials

Zinc nitrate hexahydrate, 2-methylimidazole (Hmim), n-butylamine (BA), ethylamine and hexylamine were purchased from Sigma-Aldrich (Milwaukee, WI, USA). Sodium hydroxide was obtained from Panreac Química SA (Barcelona, Spain). Acetonitrile (ACN), methanol (MeOH), acetic acid (HAcO) and hydrochloric acid were from VWR International Eurolab (Barcelona, Spain). The benzomercaptans selected in this work were: 2-mercaptobenzoxazole (MBO), 2-mercaptobenzothiazole (MBT) and 6-nitrobenzo[d]thiazole-2-thiol (NMBT), all purchased from Sigma-Aldrich. The structures of these compounds are given in **Table 6.S1**. Deionized water was prepared in Crystal B30 EDI Adrona deionizer (Riga, Latvia). All other reagents were of analytical grade unless otherwise stated. 1 mL empty propylene disposable SPE cartridge and frits (1/16', 20 µm) were from Análisis Vínicos (Tomelloso, Spain). Individual standard solutions of benzomercaptans (1000 mg L<sup>-1</sup>) were prepared in MeOH and stored at 4 °C until its use. Working standard solutions were done daily by appropriate dilution from these stock solutions.

### 6.2.2. Instrumentation

Scanning electron microscopy (SEM) images were obtained with a Hitachi S-4800 electron microscope (Ibaraki, Japan) equipped with a retrodispersive electron detector and an energy dispersive spectrometer (EDAX Genesis

4000). A transmission electron microscope (TEM) coupled to a digital camera AMT RX80 model JEM-1010 JEOL (Akishima, Japan) was used to obtain the transmission electron micrographs. Adsorption-desorption isotherms of nitrogen were registered in a S5 Micromeritics ASAP2020 instrument (Norcross, USA) at 77 K. The Brauner-Emmet-Teller (BET) model was used to calculate the specific surface area using the low-pressure range. Powder X-ray Diffraction (p-XRD) patterns were obtained in a D8 Advance A25 diffractometer (Bruker). Attenuated total reflection Fourier-transform infrared (FT-IR) spectra of powdered materials were registered with a DuraSamplIR II accessory from Smiths Detection Inc. (Warrington, UK) equipped with a nine reflection diamond/ZnSe DuraDisk plate, installed on a Bruker FT-IR spectrometer (Bremen, Germany) model Tensor 27. The zeta potential measurements were performed with Zetasizer Nano ZS equipment (Malvern Instruments, Malvern, UK). NH<sub>2</sub>-ZIF-8-BA 1 was dispersed in distilled water at a concentration of 1 g L<sup>-1</sup> and sonicated during 1 min. Measurements were carried out per triplicate at 25 °C. The final zeta potential value was estimated from the particle mobility using the Smoluchowski model.

Chromatographic separation of standards and samples was performed on a 1260 Infinity II HPLC from Agilent Technologies (Waldbronn, Germany) with a UV-Vis diode-array detector. The separation conditions of benzomercaptans were adapted from Parham *et al.* [30]. The chromatographic column was a Kromasil C18 (250 × 4.0 mm, 5 μm particle size, Análisis Vínicos). Separation was done under gradient elution mode (at flow rate of 1.0 mL min<sup>-1</sup>) using as solvents: (A) water and (B) ACN containing both 0.1% (v/v) of HAcO. The gradient elution and the detection wavelength programs are given in supplementary information (see **Table 6.S2**).

### 6.2.3. *Synthesis of ZIF-8 crystals*

ZIF-8 materials were synthesized following protocols reported in the literature by Cravillon *et al.* [22, 37]. To obtain ZIF-8 (nano)crystals (without



modulator), two methanolic solutions were needed. Solution (A) composed of  $\text{Zn}(\text{NO}_3)_2 \cdot 6\text{H}_2\text{O}$  (9.87 mmol) in MeOH (200 mL) and solution (B) of 2-methylimidazole (79.04 mmol) in MeOH (200 mL). The later solution was added to the former under stirring. After keeping at room temperature for 24 h, a white dispersion of ZIF-8 was formed, and separated by centrifugation at 6000 rpm for 10 min. Then, the resulting solid was washed with MeOH three times and dried at 40°C overnight. On the other hand, ZIF-8 nanocrystals using BA ( $\text{NH}_2$ -ZIF-8-BA) as modulator agent were prepared as given elsewhere [22]. A ligand solution (B) (9.874 mmol of Hmim in 50 mL MeOH) including the modulator agent (9.874 mmol of n-BA) was poured slowly into a solution (A) containing the metallic cation (2.469 mmol of  $\text{Zn}(\text{NO}_3)_2 \cdot 6\text{H}_2\text{O}$  in 50 mL of MeOH) under stirring and left at room temperature for 24 h. The resulting white solid (namely,  $\text{NH}_2$ -ZIF-8-BA 1) was recovered and washed with the same protocol that is described above for ZIF-8 (nano)crystals. Also, different molar contents of BA as modulator (5 and 20 mmol,  $\text{NH}_2$ -ZIF-8-BA 2 and 3, respectively) were tested by keeping constant the molar ratio of other starting reagents. Additionally, other alkyl amines (ethyl- and hexylamine) were investigated as modulator agent (at 10 mmol) following the abovementioned protocol for  $\text{NH}_2$ -ZIF-8-BA materials.

#### *6.2.4. Sample collection and treatment*

The sampling of water was performed from different locations in Valencia. Approximately, 500 mL were collected in dark containers and refrigerated at 4 °C until their use.

Several soil samples from different sources were collected, air-dried at room temperature, crushed and then sieved through a 1 mm sieve. These samples were stored on polypropylene bags in darkness at 25°C. The pH, humidity and electrical conductivity of soil samples were measured following ISO rules [38]. pH and electrical conductivity were measured in a 1:5 (soil:deionized water) extract shaken for 5 min and measured after 2 h. For the

determination of humidity, 1 g of each sample was heated at 70°C overnight until constant weight. These soil parameters are listed in **Table 6.S3**. The extraction of benzomercaptans from soil samples was adapted from Zhang *et al* [39], as follows. Briefly, 0.1 g approx. of each sample was weighed and spiked at 500  $\mu\text{g kg}^{-1}$  with the investigated pollutants. After vortex-assisted and ultrasonic homogenization, the samples were allowed to stand with the analytes for 2 h. Then, 5 mL of MeOH were added, shaken during 20 min and centrifuged at 6000 rpm for 3 min. The supernatant was collected and the extraction procedure was repeated twice. All methanolic fractions were combined and evaporated at low pressure up to small volume (ca. 100  $\mu\text{L}$ ) and reconstituted up to 5 mL with water before application of SPE protocol described below.

#### *6.2.5. Extraction procedure*

A SPE protocol using the developed materials as sorbents was applied to the extraction of aromatic benzomercaptans in environmental samples. For the preparation of SPE devices, 20 mg of the metal-organic framework was packed between two frits into 1 mL empty polypropylene cartridges. Prior to loading, the sewage waters were sonicated and centrifuged, and the extraction was carried out following the protocol described above. The material was firstly conditioned with MeOH (500  $\mu\text{L}$ ) and water (500  $\mu\text{L}$ ), and after that, a known volume of standard solution or sample (5 mL and 25 mL for soil and water samples, respectively) was passed through the cartridge. The sorbent was finally washed with water (500  $\mu\text{L}$ ). The retained analytes were later eluted with 250  $\mu\text{L}$  of 50% (v/v) MeOH containing 0.5 mol L<sup>-1</sup> NaOH. The extraction units were regenerated with water (10 mL) in order to eliminate the NaOH excess. Prior to HPLC injection, the elution fraction was properly neutralized with hydrochloric acid.

## 6.3. Results and discussion

### 6.3.1. Preliminary considerations

As it was mentioned in the Introduction, the selection of the adequate MOF as SPE sorbent is a key aspect since it strongly influences on the selective retention and the way of interaction with the target analytes. In this sense, ZIF-8 material, due to its pore size and the kind of interactions it can establish with the analytes, has advantageous features making it a good SPE phase candidate. As shown in Figure 6.S1, the molecular sizes of MBO and MBT are smaller than the pore size of ZIF-8 (3.4 Å) [40, 41]; whereas for NMBT, a partial embedding process may happen into ZIF-8 structure.

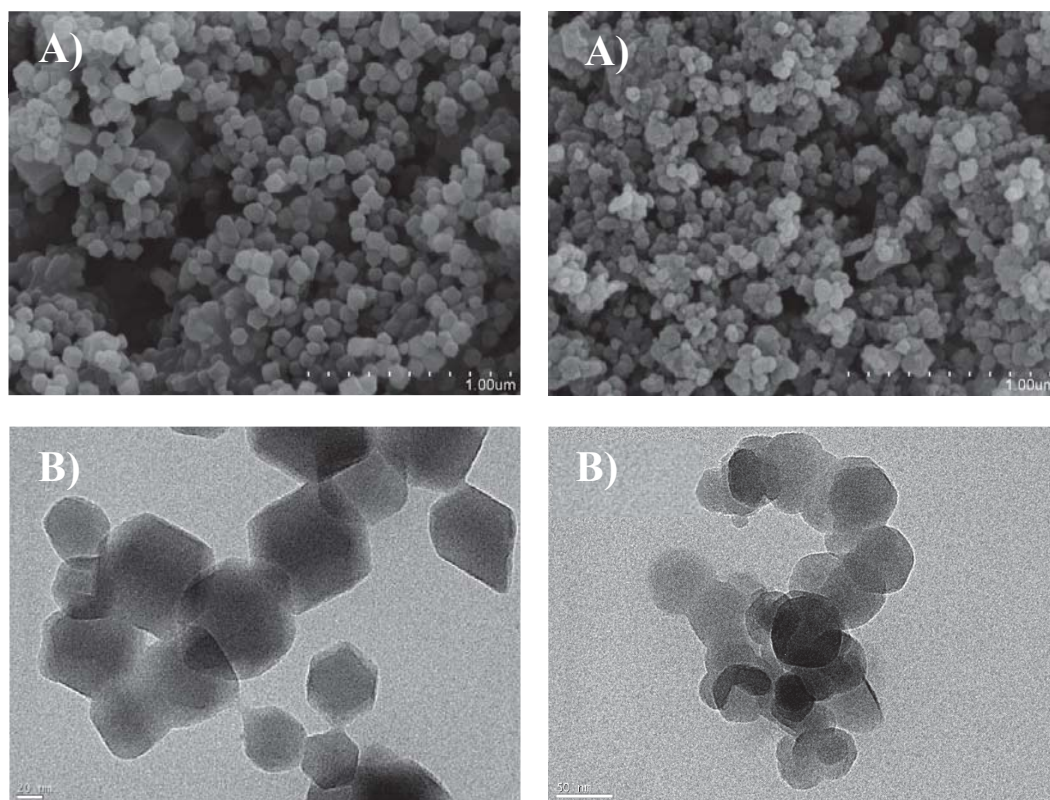
Regarding the interaction forces involved, there are different possible interaction modes between this MOF and benzomercaptans: i) hydrophobic effects and  $\pi$ -interaction between the imidazole rings of ZIF-8 and the aromatic moieties of these analytes (see structures in **Figure 6.S1**); ii) hydrogen bonding between NH groups in ZIF-8, and certain hydrogen-bond accepting groups (*e.g.* ether, organo sulfurs, nitro, among others) present in the analytes (**Figure 6.S1**) thus enhancing the hydrophilic binding and improving the selectivity; and iii) electrostatic interaction between ZIF-8 and benzomercaptan molecules. In this sense, the surface charge of ZIF-8 nanocrystals and the ionization degree of benzomercaptans (see **Table 6.S1**) should be considered (as we discussed below). Additionally, other potential contributions due to the amine moiety such as cation- $\pi$  interaction between aromatic ring and amino protonated ZIF-8 structure can occur [42], which have been previously reported with other amino functionalized MOFs and compounds with structural similarities [43]. In this regard, the synergetic contribution of BA modulator of the NH<sub>2</sub>-ZIF-8-BA in these last interactions can be explained by its presence onto the surface of ZIF-8 crystals as previously demonstrated [36].

Indeed, the use of modulators during MOF synthesis has proven to be a promising strategy through which the internal MOF structure (crystal size and morphology), and outer surface functionalities, can be controlled by using monodentate ligands [44]. The modulators then compete with conventional multidentate ligands for coordination to the metal cations [45, 46]. In order to study the influence of BA upon the crystal growth of ZIF-8 and other features, several materials were synthesized varying its molar ratio. Taking into account all these considerations, the ability of these synthesized materials as SPE phases is here evaluated (see **Table 6.1**).

### *6.3.2. Characterization of material*

The morphology and crystal size of the prepared materials (ZIF-8 and NH<sub>2</sub>-ZIF-8 with different modulators) were investigated by SEM and TEM analysis, respectively. **Figure 6.1A** and **B** shows the SEM micrograph of the ZIF-8 (without modulator) and NH<sub>2</sub>-ZIF-8-BA 1 (corresponding to *ca.* 10 mmol of BA) materials, respectively. In both images, a polyhedral shape of the nanocrystals was evidenced, which is in agreement with the typical form of ZIF-8 nanocrystals [40, 41]. Also, SEM images of MOFs prepared at other BA contents were taken (**Figure 6.S2**). As it can be seen, the morphology did not change substantially with modulator content. The TEM images of the resulting materials for this set of experiments are summarized in **Figure 6.S2**, and the mean sizes of the crystals are given in **Table 6.1**. As it can be seen, an increase of the concentration of BA modulator led to the increased mean size of the resulting crystals. The tendency observed for BA-modulated MOFs is consistent with that reported in previous studies focused on the addition of monocarboxylic acid modulators [44, 47]. These results can be explained taking into account that modulating ligands can tailor crystal nucleation and growth via both coordination and deprotonation equilibria [22]. Thus, the addition of a basic ligand (L) as BA (pK<sub>a</sub> value in aqueous media is 10.7) can deprotonate the [Zn(Hmim)<sub>m</sub>L<sub>n</sub>] species, and thus producing an acceleration of rate of ligand exchange reactions, resulting in a higher nucleation rate and

therefore in a smaller final crystal size. When a low amount of BA is added a, a large number of nuclei were formed and rapidly grow at the same time affording smaller crystals. However, higher concentration of BA provides a slow nucleation (fewer nuclei) of the MOF giving as result larger crystals. This is due to this additive starts to have a relevant role as a competitive ligand in the complex formation. On the other hand, in absence of modulating ligand (BA), there is not a deprotonation reaction, which led to small concentration of  $[\text{Zn}(\text{Hmim})_m\text{L}_n]$  species decreasing the nucleation rate, and consequently in a large final crystal size.



**Figure 6.1.** SEM (A) and TEM (B) micrographs of ZIF-8 (left part) and  $\text{NH}_2$ -ZIF-8-BA 1 (right part) materials.

Additionally, energy dispersive X-ray spectroscopy (EDX) of the synthesized materials were performed. As shown in **Table 6.1**, nitrogen content increased with increasing BA content, which confirmed not only the presence of BA onto the surface of ZIF-8 crystals but also the possibility of tailoring the loading of surface amine moieties.

**Table 6.1.** Influence on different BA content modulator of textural parameters of synthesized MOFs and their extraction performances.

MOF	Modulator	Particle size (nm)	Surface area (m <sup>2</sup> g <sup>-1</sup> )	N amount (atomic, %)	R <sup>a</sup> (%)
ZIF-8	None	89 ± 6	1456	45.3	60-63
NH <sub>2</sub> -ZIF-8-BA 1	BA, 10 mmol	61 ± 2	1365	52.6	94-102
NH <sub>2</sub> -ZIF-8-BA 2	BA, 5 mmol	47 ± 5	856	47.7	64-77
NH <sub>2</sub> -ZIF-8-BA 3	BA, 20 mmol	72 ± 7	1213	56.3	99-102

<sup>a</sup>Extraction conditions: sample concentration, 500 µg L<sup>-1</sup>; volume, 5 mL; eluting solvent, 0.5 mL of 50:50 MeOH:H<sub>2</sub>O (v/v) with 0.5 M NaOH.

To determine the surface area, nitrogen adsorption/desorption isotherms of the synthesized materials were performed. They exhibited typical Type I isotherms (a representative example is depicted in **Figure 6.S3**), which are indicative of their microporous nature. The specific surface area, calculated using the BET equation, are shown in the **Table 6.1**. As it can be observed, high surface areas (> 1000 m<sup>2</sup>/g) were obtained from BA contents of 10 mmol or higher.

Furthermore, X-ray powder diffraction patterns, depicted in **Figure 6.S4**, were in good agreement with the simulated one, thus indicating that the current materials were successfully prepared. Also, FT-IR spectra of ZIF-8 materials were taken (**Figure 6.S5**). All the spectra display the typical bands of the ZIF-8 MOF [36, 40], corroborating their successful preparation. In addition, a small band close to 2900 cm<sup>-1</sup> appeared in the NH<sub>2</sub>-ZIF-8-BA, which can be assigned to the aliphatic stretching C–H of BA.

Next, the synthesized MOFs were evaluated as SPE sorbents in order to study the influence of modulation and choose the phase that provided the highest extraction efficiency. As shown in **Table 6.1**, the NH<sub>2</sub>-ZIF-8-BA 1 showed high recoveries jointly with exposed surfaces having enough amino moieties for the selective capture of analytes. Additionally, this material was

superior to that synthesized without modulator, which clearly demonstrated the important contribution of the amount of attached BA onto ZIF-8 crystals in the extraction efficiency of these pollutants. It is evident from the previous discussion and experimental results that amine group of BA modulator plays a key role in the crystal growth of MOF as well as in his subsequent retention properties. For this purpose, other organic amines (ethyl and hexyl) with similar basicity ( $pK_a$  values ranged between 10.6-10.9) were studied as modulators using the same conditions of  $NH_2$ -ZIF-8-BA 1. The characterization of the resulting materials gave mean sizes of the crystals similar to those obtained with BA modulated material and surface area values ranged between 1150 and 1324  $m^2 g^{-1}$ . Both materials were tested as SPE sorbents, giving recoveries up to 90%. These results suggested that the alkyl chain has not a relevant effect, whereas the introduction of amine in the final framework is an important issue to improve the retention performance. At sight of these results,  $NH_2$ -ZIF-8-BA 1 was selected for further studies.

### 6.3.3. Optimization of SPE protocol

In order to obtain the maximal extraction performance, various parameters such as sample pH value, elution solvent composition and volume were investigated. During optimization of SPE conditions, an aqueous solution containing 250  $\mu g L^{-1}$  of each benzomercaptan was employed as a test mixture.

Sample pH is an important variable that influences the extraction performance since it affects the ZIF-8 charge surface as well as the analyte charge state. According to previous reports, ZIF-8 material is charged positively in the pH range of 2-10 due to its imidazole moieties [48, 49]. In any case, zeta potential measurements of the selected material were performed at loading/elution conditions (**Figure 6.S6**). Thus, the positive value of this parameter at loading step (pH close to 7.0) implied a positive surface charge of MOF nanoparticles, whereas that it reversed from positive to negative

when eluting solution was tested ( $\text{pH} > 12$ ). These results were consistent with the above-mentioned studies. On the other hand, the heterocyclic benzomercaptans may exist as thione and/or thiol forms, and the thiol form can be further ionized in aqueous solutions (see  $\text{pK}_a$  values in **Table 6.S1**). In this study, the effect of the sample pH value was evaluated from 5 to 9 (data not shown), by considering aspects such as the structural integrity of this framework ( $\text{pH} > 4$ ) [50] as well as the usual pH range found in surface water systems (6.5 to 8.5). Recoveries in the tested pH range were almost constant for each benzomercaptan. These results can be explained as follows. On the one side, the existence of electrostatic interactions can be present taking into account the surface charge of MOF and the ionization state of benzomercaptans. Particularly, when the solution pH was below 6.0, these compounds are predominantly as neutral (molecular) species, while the surface of ZIF-8 remained positive, which made the electrostatic attraction between them become weak. When solution pH increased from 6.0 to 8.5, the anionic form of benzomercaptans begin to have greater significance due to progressive deprotonation of these molecules (see  $\text{pK}_a$  values), and the electrostatic attraction between these solutes and ZIF-8 became a main factor in the interaction mechanism. Nevertheless, the recovery values of target compounds on ZIF-8 along the tested pH range remained nearly constant. This fact suggested that the factor controlling the retention of probe compounds was not just electrostatic interaction, and there should be other modes of action that influence on the adsorption process (such as  $\pi$ -stacking and hydrogen bonding interactions). Therefore, no pH adjustment was required in sample solutions.

The selection of an appropriate eluting solvent is of major concern for the optimization of the SPE process. To obtain the highest eluting efficiencies, several eluting solvents were investigated (see **Figure 6.2**, left part). Desorption solvents as pure MeOH gave very low recovery values of analytes ( $< 8\%$ ). As can be observed, when MeOH-water mixtures (50/50, v/v) were



used, higher recoveries were obtained (up to 29%), which subsequently increased up to around 79% when using mixtures of MeOH-water basified with 0.1 M NaOH. This increment can be explained taking into account the surface charge of MOF and the ionization state of benzomercaptans. As it was mentioned before, the point of zero charge for ZIF-8 is approximately at pH 9.8 [48, 49]. Consequently, at pH above this value, an electrostatic repulsion between the negatively charged ZIF-8 surfaces and the benzomercaptan anions is produced, which favors the desorption of these analytes from the sorbent. Consequently, the content of NaOH (from 0.1 to 0.5 M) in MeOH-water mixtures was optimized. It was found that a content of 0.5 M NaOH gave recoveries ranging between 97 and 108%. So, as in agreement with previous studies [50], the MOF structure was stable at this pH, a 0.5 M NaOH concentration was selected for further studies.

The volume of eluent can affect not only the elution efficiency, but also the concentration of the analytes in the eluent. Therefore, the effect of the solvent volume (100-1000  $\mu\text{L}$ ) was also investigated (**Figure 6.S7**). As can be seen, recoveries of analytes higher than 87.3% (< 6.1% relative standard deviation, RSDs) were obtained for 250  $\mu\text{L}$ , and this value was selected for further experiments.

Another essential parameter in a SPE protocol, especially to monitor trace pollutants in environmental analysis, is the breakthrough volume. Thus, the effect of sample volume was evaluated using the  $\text{NH}_2$ -ZIF-8 as sorbent. Several volumes (in the range 1-100 mL) were loaded by keeping constant the total amount of each pollutant (500 ng) (see **Figure 6.2**, right part). As can be seen, the extraction recoveries of all the benzomercaptans were higher than 80% up to 50 mL, however, higher volumes caused a diminution in the extraction efficiency. Consequently, considering the minimum elution volume found (250  $\mu\text{L}$ ) and the maximum sample loading volume (25 mL) with average recoveries values *ca.* 100%, a preconcentration factor of 100 was estimated.

Finally, the reusability of sorbent was also evaluated, and the obtained results indicated that the MOF could be reused at least 10 times without significant decrease of efficiency extraction (between 87-104% with RSD below to 8%).

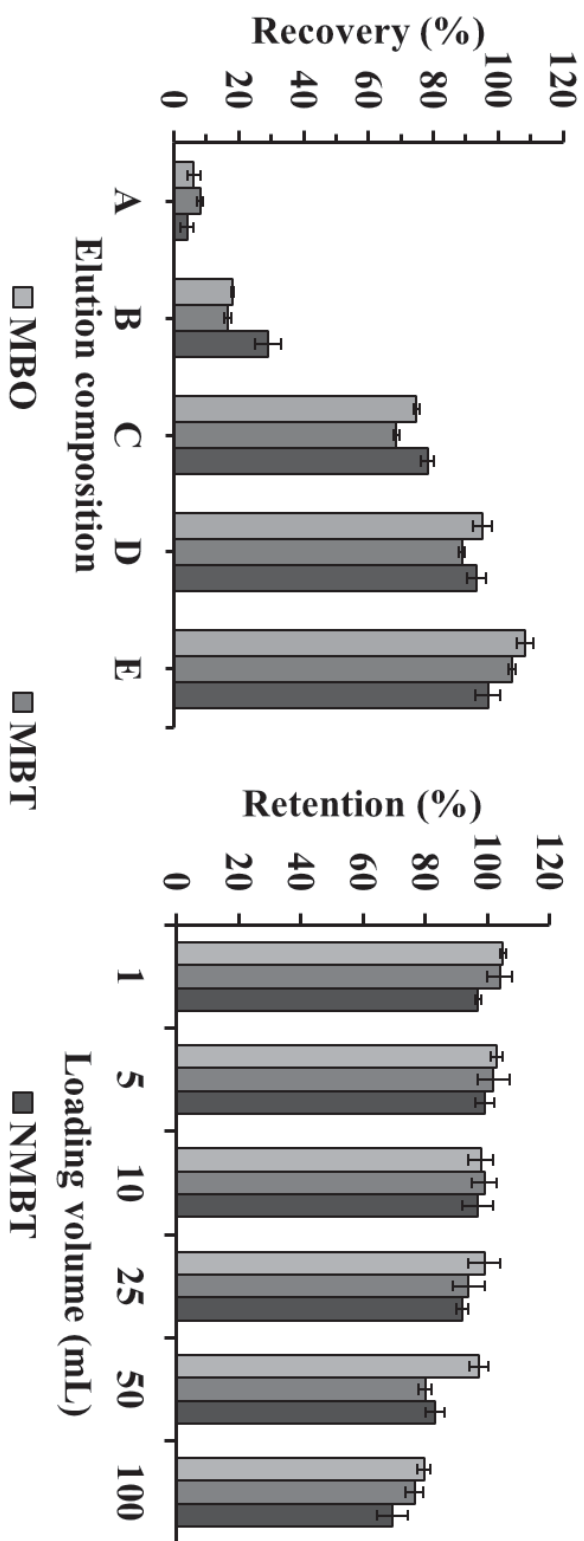
#### 6.3.4. Figures of merit and application to real samples

The developed SPE procedure using NH<sub>2</sub>-ZIF-8-BA 1 as sorbent, combined with HPLC-UV detection, was validated in terms of linearity, sensitivity and precision under the previously optimized experimental conditions. The obtained results are summarized in **Table 6.2**. As can be seen from this table, a good linearity range ( $r > 0.998$ ) was observed in the chromatographic dynamic range of 7-2500  $\mu\text{g L}^{-1}$  for all analytes. The limits of detection (LOD) and quantification (LOQ) (after applying the extraction protocol) were experimentally obtained as the concentration of the analyte that provided a signal-to-noise ratio (S/N) of 3 and 10, respectively. Thus, the LODs for aqueous samples varied from 16 ng L<sup>-1</sup> to 21 ng L<sup>-1</sup>, whereas the LOQs were in the range 52 ng L<sup>-1</sup> and 69 ng L<sup>-1</sup>. In the case of soil samples, the LOD and LOQ values ranged 0.4-0.5  $\mu\text{g kg}^{-1}$  and 1.3-1.7  $\mu\text{g kg}^{-1}$ , respectively.

**Table 6.2.** Figures of merit of the developed material used as SPE sorbent in the extraction and analysis of benzomercaptans.

Analyte	Calibration range ( $\mu\text{g L}^{-1}$ )	Within-device recovery (%) $\pm$ RSD (n=3)	Between-device recovery (%) $\pm$ RSD (n=3)	LOD <sup>a</sup> ( $\mu\text{g L}^{-1}$ )	LOQ <sup>a</sup> ( $\mu\text{g L}^{-1}$ )
MBO	5 – 2500	109 $\pm$ 2	107 $\pm$ 2	1.6	5
MBT	7 – 5000	95 $\pm$ 7	101 $\pm$ 1	2	7
NMBT	7 – 5000	100 $\pm$ 7	95 $\pm$ 1	2	7

<sup>a</sup>Instrumental values (without applying the extraction protocol)



**Figure 6.2.** Effect of elution solvent composition on the recovery values of analytes using  $\text{NH}_2\text{-ZIF-8}$  as SPE sorbent (left part), eluent compositions: A) MeOH, B) 50:50 MeOH:H<sub>2</sub>O (v/v), C) 50:50 MeOH:H<sub>2</sub>O (v/v) with 0.1 M NaOH, D) 50:50 MeOH:H<sub>2</sub>O (v/v) with 0.2 M NaOH and E) 50:50 MeOH:H<sub>2</sub>O (v/v) with 0.5 M NaOH; effect of loading sample volume on the extraction efficiency of benzomercaptans (right part). Error bar = SD (n = 3).

The precision of the method (intra and inter-units), expressed as relative standard deviation (RSD, %) was also determined from standard solutions at a concentration level of 250  $\mu\text{g L}^{-1}$  of each analyte and subjected to the SPE protocol. RSD values comprised between 2.0 and 7.0% were found.

To study the applicability of the developed SPE-HPLC-UV method using  $\text{NH}_2$ -ZIF-8-BA 1 as sorbent, the developed method was applied to monitor the target analytes in environmental complex matrices. The samples were analyzed in order to find any potential presence of the analytes. The results (see **Table 6.3**) showed that none of the target benzomercaptan was detected in the nonspiked real samples. Next, validation samples were prepared using these samples fortified with the three target compounds at concentration level of 5-500  $\mu\text{g L}^{-1}$ .

As shown in **Table 6.3**, the recoveries of analytes were satisfactory, ranging between 74 and 117%. In order to discard matrix effect in sewage water, particularly for that one from Gandía (influent), standard addition calibration curves were done. Several spiked samples at different levels (25-100  $\mu\text{g L}^{-1}$ ) were percolated through cartridges and the slopes obtained in the resulting calibration curves were not statistical different from those found with the external calibration method (confidence level of 95%) As representative examples, **Figure 6.3** (left) shows the chromatograms of a water sample (from influent sewage water) spiked with the analytes without and with SPE pretreatment. On the other hand, the right part of **Figure 6.3** illustrates the eluted fraction corresponding to a blank soil sample and that spiked with the analytes. As observed, an effective enrichment of analytes of interest in both matrices was evidenced, which demonstrated the performance of the synthesized sorbent to be used as preconcentration purposes in complex samples.

**Table 6.3.** Recovery study of benzomercaptans in spiked environmental samples analyzed following the recommended SPE protocol. Recovery (%)  $\pm$  SD (n=3)<sup>a</sup>.

Analyte	Environmental samples											
	Gandia sewage water (influent)	Paterna sewage water (effluent)	Tap water	Soil 1 (Sueca)	Soil 2 (Burjassot)	Soil 3 (Valencia)						
	Spiked level ( $\mu\text{g L}^{-1}$ )				Spiked level ( $\mu\text{g kg}^{-1}$ )							
	5	-	5	-	5	-	500	-	500	-	500	
MBO	< LOD	76 $\pm$ 2	< LOD	94 $\pm$ 2	< LOD	117 $\pm$ 9	< LOD	109 $\pm$ 2	< LOD	100 $\pm$ 7	< LOD	102 $\pm$ 3
MBT	< LOD	76 $\pm$ 5	< LOD	82 $\pm$ 2	< LOD	81 $\pm$ 4	< LOD	103 $\pm$ 1	< LOD	107 $\pm$ 1	< LOD	98 $\pm$ 6
NMBT	< LOD	74 $\pm$ 5	< LOD	75 $\pm$ 6	< LOD	74 $\pm$ 8	< LOD	93 $\pm$ 1	< LOD	84 $\pm$ 10	< LOD	82 $\pm$ 3

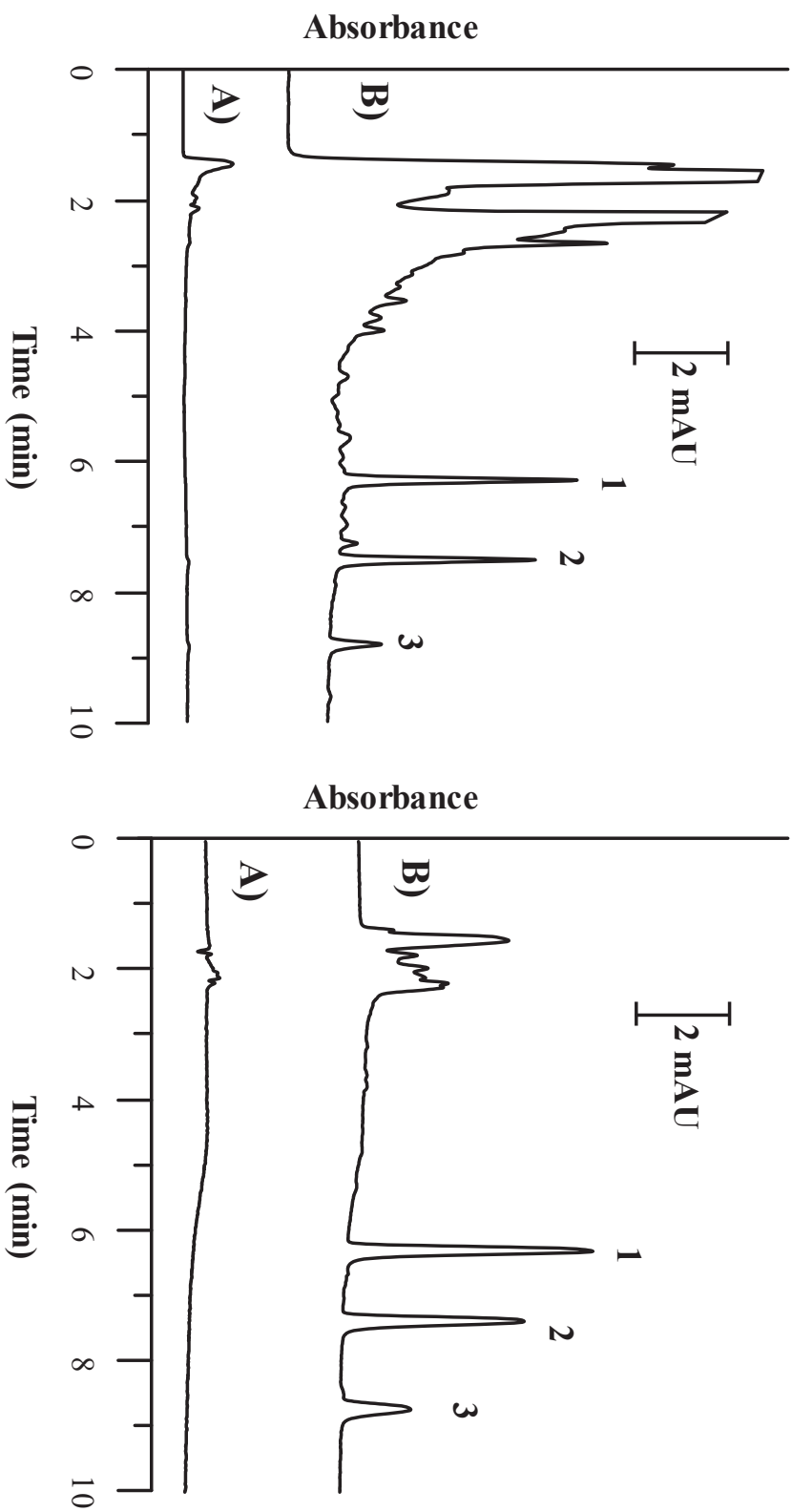
<sup>a</sup>The recovery values were calculated by dividing the concentration found by the concentration added (calibration curves).

### *6.3.5. Comparison with other commercial sorbents and extraction methodologies*

Next, a comparison in terms of extraction performance with one commercial sorbent (silica gel) commonly used for the extraction of benzomercaptans [51, 52] was made. This generic sorbent gave retention values below 50% (see **Figure 6.S8**), which underlines the convenience of using our synthesized sorbent.

Finally, the developed material was compared with other extraction sorbents of target analytes in environmental samples (see **Table 6.4**). Regarding aqueous samples analysis, the recovery values obtained were quite similar to those found in most reported studies; however, in certain works [23, 28] these values were lower than 65%. Regarding the LODs, our values were better than those described by Parham *et al.* [24], and similar to those reported in refs. [28, 30, 31] using a sophisticated and high-cost MS detector. Other advantage found is the less amount (20 mg) of sorbent required compared with single-use commercial SPE sorbents (commonly up to 150-500 mg) [28, 30, 31]. This amount was also similar to a nanomaterial-based method using CuNPs [23, 24] probably due to surface area-to-volume ratio; however, its reusability was quite lower than that found in the present study.

Likewise, in soil monitoring, the present method gave higher recoveries than those described in literature [53, 54]. Concerning LODs, our protocol provided comparable LOD values [53], or higher using MS detection [54]. In any case, this drawback does not reduce the good features of our protocol such as the easy and cheap preparation of the sorbent combined with the accessible equipment required, make this protocol a feasible method to monitor benzomercaptans and their derivatives in environmental samples.



**Figure 6.3.** HPLC-UV chromatograms of sewage water (Gandía's plant) (left part) and extracts of soil samples (right part) spiked with  $5 \mu\text{g L}^{-1}$  of each benzomercaptan, respectively, without applying (A) and applying the proposed SPE protocol (B). The right part shows an extract of soil sample without (A) and with spiking of analytes at  $500 \mu\text{g kg}^{-1}$  (B) subjected to the SPE treatment. Chromatographic conditions are given in Experimental Section and Supplementary Information. Peak identification: 1, MBO; 2, MBT; 3, NMBT.

**Table 6.4.** Comparison with other reported methods for benzomercaptans extraction and analysis.

Analytes	Material (sorbent amount)	Method	Sample matrix	R (%)	LOD (ng L <sup>-1</sup> / ng kg <sup>-1</sup> )	Reusability	EF <sup>a</sup>	Reference
MBT, MBO	Copper oxide nanoparticles (14 mg)	HPLC-DAD	Industrial water samples	56-93	-	3		[23]
MBT, MBO, MBI	Copper oxide nanoparticles (14 mg)		Environmental water sample	96-104	1900-2700	3	200	[24]
MBT	Oasis HLB cartridge (200 mg)	SPE /HPLC-MS	Municipal steewater samples	60-70	16.7	-	7-14	[28]
MBT	Oasis MAX (150 mg)	SPE /HPLC-MS	Environmental water samples	80-118	1-4	-	20-100	[30]
MBT	Oasis HLB (500 mg)	SPE /HPLC-MS	Water samples	70-85	7	-	21-83	[31]
BT, HBT, MTBT, ABT	Strata™-X cartridges (200 mg)	SPE /HPLC-MS/MS	Dewatered sewage sludge	50-116	40 - 13000	-	-	[51]
MBT, HBT, BT, ABT, MTBT	Poly-Sery HLB cartridge (60 mg)	SPE /UPLC-MS/MS	Road dust / Roadside soil	56-105	20-120	-	-	[52]
MBO, MBT, NMBT	NH <sub>2</sub> -ZIF-8-BA 1 (20 mg)	SPE /HPLC-UV	Environmental samples	74-117	16-21 / 400-500	10	4 <sup>b</sup> , 100 <sup>c</sup>	This Work

<sup>a</sup>The EF from the overall SPE protocol was calculated using the ratio between the final (eluent) extract and the maximum sample volume load (for aqueous samples) or the amount of solid weighed (for soil samples); bsoil samples; caqueous samples EF: enrichment factor. MBT: 2-mercaptobenzothiazole, MBO: 2-mercaptobenzoxazole, MBI: 2-mercaptobenzimidazole, NMBT: 2-mercapto-6-nitrobenzothiazole, HBT: 2-hidroxybenzothiazole, MTBT: 2-methyl-thiobenzothiazole, ABT: 2-aminobenzothiazole



## **6.4. Conclusions**

In this research, n-butylamine modulated ZIF-8 nanocrystals were successfully synthesized, characterized and applied as SPE sorbent to the extraction of benzomercaptans in environmental matrices. Prior to the SPE optimization, the addition of BA (at several molar ratios) as modulator to the reaction mixture was done to evaluate its impact on the crystal growth and adsorption capacity of the resulting MOFs. As a result of this study, NH<sub>2</sub>-ZIF-8 containing 10 mmol of BA as modulator was the most appropriate sorbent. Then, several experimental parameters of the SPE protocol (such as sample pH, desorption solvent composition, among others) were investigated in detail using this MOF as SPE phase. The highly selective and efficient retention of benzomercaptans on this MOF take advantages of multiple interactions between these targets and the framework.

Moreover, the fruitful combination of NH<sub>2</sub>-ZIF-8-BA 1 followed by HPLC-UV analysis led to high extraction recovery values, low LODs, excellent enrichment factors and satisfactory reusability. All these figures of merits prove that the present protocol constitutes a simple, cost-effective, and appropriate methodology for extraction and preconcentration of these pollutants in complex environmental samples. As far as we know, this study reports the first study of influence of modulator content on the morphology and extraction performance of organic pollutants and the subsequent application of the best modulated ZIF-8 for the extraction of benzomercaptans and demonstrate that it could be a promising SPE sorbent for further applications.

## 6.5. References

- [1] M. Safaei, M. M. Foroughi, N. Ebrahimpour, S. Jahani, A. Omid, M. Khatami, A review on metal-organic frameworks: synthesis and applications, *Trends Anal. Chem.* 118 (2019) 401–425. doi: 10.1016/j.trac.2019.06.007
- [2] C.C. Hou, Q. Xu, Metal–organic frameworks for energy, *Adv. Energy Mater.* 9 (2019) 1801307. doi: 10.1016/j.chempr.2016.12.002
- [3] L. Joseph, B.M. Jun, M. Jang, C.M. Park, J.C.M. Senmache, A.J.H. Maldonado, A. Heyden, M. Yu, Y. Yoon, Removal of contaminants of emerging concern by metal-organic framework nanoadsorbents: A review, *Chem. Eng. J.* 369 (2019) 928–946. doi: 10.1016/j.cej.2019.03.173
- [4] P. Kumar, E. Vejerano, A. Khan, G. Lisak, J.H. Ahn, K.H. Kim, Metal organic frameworks (MOFs): Current trends and challenges in control and management of air quality, *Korean J. Chem. Eng.* 36 (2019) 1839–1853. doi: 10.1007/s11814-019-0378-8
- [5] A. Shahat, H.M.A. Hassan, H.M.E. Azzazy, Optical metal-organic framework sensor for selective discrimination of some toxic metal ions in water, *Anal. Chim. Acta.* 793 (2013) 90–98. doi: 10.1016/j.aca.2013.07.012
- [6] P.R. Bautista, I.P. Fernández, J. Pasán, V. Pino, Are metal-organic frameworks able to provide a new generation of solid-phase microextraction coatings? - A review, *Anal. Chim. Acta* 939 (2016) 26–41. doi: 10.1016/j.aca.2016.07.047
- [7] X. Gong, Y. Wang, T. Kuang, ZIF-8-based membranes for carbon dioxide capture and separation, *ACS Sustainable Chem. Eng.* 5 (2017) 11204–11214. doi: 10.1021/acssuschemeng.7b03613
- [8] X. L. Xu, H. Wang, J.B. Liu, H. Yan, The applications of zeolitic imidazolate framework-8 in electrical energy storage devices: a review, *J.*

Mater. Sci. Mater Electron 28 (2017) 7532–7543. doi: 10.1007/s10854-017-6485-6

[9] J. Troyano, A.C. Sánchez, C. Avci, I. Imaz, D. Maspoch, Colloidal metal–organic framework particles: the pioneering case of ZIF-8, Chem. Soc. Rev. 48 (2019) 5534–5546. doi: 10.1039/c9cs00472f

[10] H. Zhang, D. Liu, Y. Yao, B. Zhang, Y. Lin, Stability of ZIF-8 membranes and crystalline powders in water at room temperature, J. Membr. Sci. 485 (2015) 103–111. doi: 10.1016/j.memsci.2015.03.023

[11] H. Tanaka, S. Ohsaki, S. Hiraide, D. Yamamoto, S. Watanabe, M. T. Miyahara, Adsorption-induced structural transition of ZIF-8: a combined experimental and simulation study, J. Phys. Chem. C. 118 (2014) 8445–8454. doi: 10.1021/jp500931g

[12] Y. Pan, D. Heryadi, F. Zhou, L. Zhao, G. Lestari, H. Su, Z. Lai, Tuning the crystal morphology and size of zeolitic imidazolate framework-8 in aqueous solution by surfactants, Cryst. Eng. Comm. 13 (2011) 6937–6940. doi: 10.1039/c1ce05780d

[13] H. Lan, T. Rönkkö, J. Parshintsev, K. Hartonen, N. Gan, M. Sakeye, J. Sarfraz, M.L. Riekkola, Modified zeolitic imidazolate framework-8 as solid-phase microextraction. Arrow coating for sampling of amines in wastewater and food samples followed by gas chromatography-mass spectrometry, J. Chromatog. A. 1486 (2017) 76–85. doi: 10.1016/j.chroma.2016.10.081

[14] J. Kong, F. Zhu, W. Huang, H. He, J. Hu, C. Sun, Q. Xian, S. Yang, Sol–gel based metal-organic framework zeolite imidazolate framework-8 fibers for solid-phase microextraction of nitro polycyclic aromatic hydrocarbons and polycyclic aromatic hydrocarbons in water samples, J. Chromatogr. A. 1603 (2019) 92–101. doi: 10.1016/j.chroma.2019.06.063

[15] F. Maya, M. Ghani, Ordered macro/micro-porous metal-organic framework of type ZIF-8 in a steel fiber as a sorbent for solid-phase

microextraction of BTEX, *Microchim. Acta.* 186 (2019) 425. doi: 10.1007/s00604-019-3560-0

[16] J. Pang, Y. Liao, X. Huang, Z. Ye, D. Yuan. Metal-organic framework-monolith composite-based in-tube solid phase microextraction on-line coupled to high-performance liquid chromatography-fluorescence detection for the highly sensitive monitoring of fluoroquinolones in water and food samples, *Talanta.* 199 (2019) 499–506. doi: 10.1016/j.talanta.2019.03.019

[17] M. Rio, C.P. Cabello, V. Gonzalez, F. Maya, J.B. Parra, V. Cerdà, G.T. Palomino, Metal oxide assisted preparation of core–shell beads with dense metal–organic framework coatings for the enhanced extraction of organic pollutants, *Chem. Eur. J.* 22 (2016) 11770–11777. doi: 10.1002/chem.201601329

[18] X. Liu, Z. Sun, G. Chen, W. Zhang, Y. Cai, R. Kong, X. Wang, Y. Suo, J. You, Determination of phthalate esters in environmental water by magnetic zeolitic imidazolate framework-8 solid-phase extraction coupled with high-performance liquid chromatography, *J. Chromatogr. A.* 1409 (2015) 46–52. doi: 10.1016/j.chroma.2015.07.068

[19] D. Ge, H. K. Lee, Zeolite imidazolate frameworks 8 as sorbent and its application to sonication-assisted emulsification microextraction combined with vortex-assisted porous membrane-protected micro-solid-phase extraction for fast analysis of acidic drugs in environmental water samples, *J. Chromatogr. A.* 1257 (2012) 19–24. doi: 10.1016/j.chroma.2012.08.032

[20] D. Ge, H.K. Lee, Sonication-assisted emulsification microextraction combined with vortex-assisted porous membrane-protected micro-solid-phase extraction using mixed zeolitic imidazolate frameworks 8 as sorbent, *J. Chromatogr. A.* 1263 (2012) 1–6. doi: 10.1016/j.chroma.2012.09.016

- [21] Y. Wang, S. Jin, Q. Wang, G. Lu, J. Jiang, D. Zhu, Zeolitic imidazolate framework-8 as sorbent of micro-solid-phase extraction to determine estrogens in environmental water samples, *J. Chromatogr. A.* 1291 (2013) 27–32. doi: 10.1016/j.chroma.2013.03.032
- [22] J. Cravillon, R. Nayuk, S. Springer, A. Feldhoff, K. Huber, M. Wiebcke, Controlling zeolitic imidazolate framework nano- and microcrystal formation: insight into crystal growth by time-resolved in situ static light scattering, *Chem. Mater.* 23 (2011) 2130–2141. doi: 10.1021/cm103571y
- [23] H. Parham, F. Khoshnam, Highly efficient and simultaneous removal of 2-mercaptobenzothiazole and 2-mercaptobenzoxazole from water samples by copper oxide nanoparticles, *J. Chem. Technol. Biotechnol.* 88 (2013) 1736–1743. doi: 10.1002/jctb.4026
- [24] H. Parham, F. Khoshnam, Solid phase extraction–preconcentration and high performance liquid chromatographic determination of 2-mercapto-(benzothiazole, benzoxazole and benzimidazole) using copper oxide nanoparticles, *Talanta.* 114 (2013) 90–94. doi: 10.1016/j.talanta.2013.04.014
- [25] T. Sorahan, Cancer risks in chemical production workers exposed to 2-mercaptobenzothiazole, *Occup. Environ. Med.* 66 (2009) 269–273. doi: 10.1136/oem.2008.041400
- [26] M.H. Whittaker, A.M. Gebhart, T.C. Miller, F. Hammer, Human health risk assessment of 2-mercaptobenzothiazole in drinking water, *Toxicol. Ind. Health.* 20 (2004) 149–163. doi: 10.1191/0748233704th199oa
- [27] NSF International Standard/American National Standard for drinking water additives. Drinking water treatment chemicals – health effect. NSF International, USA. March 9, 2016 (NSI/ANSI 60-2016)
- [28] A. Kloepfer, M. Jekel, T. Reemtsma, Determination of benzothiazoles from complex aqueous samples by liquid

chromatography–mass spectrometry following solid-phase extraction, *J. Chromatogr. A.* 1058 (2004) 81–88. doi: 10.1016/j.chroma.2004.08.081

[29] E. Fries, Determination of benzothiazole in untreated wastewater using polar-phase stir bar sorptive extraction and gas chromatography–mass spectrometry, *Anal. Chim. Acta.* 689 (2011) 65–68. doi: 10.1016/j.aca.2011.01.015

[30] I. Carpinteiro, B. Abuin, M. Ramil, I. Rodríguez, R. Cela, Simultaneous determination of benzotriazole and benzothiazole derivatives in aqueous matrices by mixed-mode solid-phase extraction followed by liquid chromatography–tandem mass spectrometry, *Anal Bioanal Chem.* 402 (2012) 2471–2478. doi: 10.1007/s00216-012-5718-z

[31] C.H. Loi, F. Buseti, K.L. Linge, C.A. Joll, Development of a solid-phase extraction liquid chromatography tandem mass spectrometry method for benzotriazoles and benzothiazoles in wastewater and recycled water, *J. Chromatogr. A.* 1299 (2013) 48–57. doi: 10.1016/j.chroma.2013.04.073

[32] Z. Xiang, C. Fang, S. Leng, D. Cao, An amino group functionalized metal–organic framework as a luminescent probe for highly selective sensing of Fe<sup>3+</sup> ions, *J. Mater. Chem. A.* 2 (2014) 7662–7665. doi: 10.1039/c4ta00313f

[33] C. Gecgel, U. B. Simsek, B. Gozmen, M. Turabik. Comparison of MIL-101(Fe) and amine-functionalized MIL-101(Fe) as photocatalysts for the removal of imidacloprid in aqueous solution. *J. Iran. Chem. Soc.* 16 (2019) 1735–1748. doi: 10.1007/s13738-019-01647-w

[34] C. Li, L. Zhu, W. Yang, X. He, S. Zhao, X. Zhang, W. Tang, J. Wang, T. Yue, Z. Li, Amino-functionalized Al–MOF for fluorescent detection of tetracyclines in milk, *J. Agr. Food Chem.* 67 (2019) 1277–1283. doi: 10.1021/acs.jafc.8b06253

[35] Y. Yuan, X. Zheng, H. Lin, Y. Li, M. Yang, X. Liu, C. Deng, Z. Fan, Development of a hydrophilic magnetic amino-functionalized metal-

organic framework for the highly efficient enrichment of trace bisphenols in river water samples, *Talanta*, 211 (2020) 120713. doi: 10.1016/j.talanta.2020.120713

[36] F. Maya, C.P. Cabello, S. Clavijo, J.M. Estela, V. Cerdà, G.T. Palomino, Zeolitic imidazolate framework dispersions for the fast and highly efficient extraction of organic micropollutants, *RSC Adv.* 5 (2015) 28203–28210. doi: 10.1039/c5ra01079a

[37] J. Cravillon, S. Münzer, S.J. Lohmeier, A. Feldhoff, K. Huber, M. Wiebcke, Rapid room-temperature synthesis and characterization of nanocrystals of a prototypical zeolitic imidazolate framework, *Chem. Mater.* 21 (2009) 1410–1412. doi: 10.1021/cm900166h.j

[38] ISO (2005). Soil Quality–Determination of pH (ISO 10390: 2005). ISO (1994). Soil Quality—Determination of the Specific Electrical Conductivity. ISO (2003) Soil quality -- Determination of soil water content as a volume fraction on the basis of known dry bulk density - Gravimetric method (ISO 16586:2003)

[39] Z. Zhang, N. Ren, Y.F. Li, T. Kunisue, D. Gao, K. Kannan, Determination of benzotriazole and benzophenone UV filters in sediment and sewage sludge, *Environ. Sci. Technol.* 45 (2011) 3909–3916. doi: 10.1021/es2004057

[40] C.Y. Sun, C. Qin, X.L. Wang, G.S. Yang, K.Z. Shao, Y.Q. Lan, Z.M. Su, P. Huang, C.G. Wang, E.B. Wang, Zeolitic imidazolate framework-8 as efficient pH-sensitive drug delivery vehicle, *Dalton Trans.* 23 (2012) 6906–6909. doi: 10.1039/c2dt30357d

[41] F. Yan, Z.Y. Liu, J.L. Chen, X.Y. Sun, X.J. Li, M.X. Su, B. Li, B. Di, Nanoscale zeolitic imidazolate framework-8 as a selective adsorbent for theophylline over caffeine and diprophylline, *RSC Adv.* 4 (2014) 33047–33054. doi: 10.1039/c4ra05293e

[42] J.C. Ma, D.A. Dougherty, The cation- $\pi$  interaction, *Chem. Rev.* 97 (1997) 1303–1324. doi: 10.1021/cr9603744

- [43] I. Ahmed, N.A. Khan, J.W. Yoon, J.S. Chang, S.H. Jung, Protonated MIL-125-NH<sub>2</sub>: remarkable adsorbent for the removal of quinoline and indole from liquid fuel, *ACS Appl. Mater. Interfaces* 9 (2017) 20938–20946. doi: 10.1021/acsami.7b01899
- [44] A. Schaate, P. Roy, A. Godt, J. Lippke, F. Waltz, M. Wiebcke, P. Behrens, Modulated synthesis of Zr-based metal–organic frameworks: from nano to single crystals, *Chem. Eur. J.* 17 (2011) 6643–6651 doi: 10.1002/chem.201003211
- [45] Q. Liu, L.N. Jin, W.Y. Sun, Coordination modulation induced and ultrasonic-assisted synthesis of size-controlled microporous metal–imidazolate framework crystals with enhanced adsorption performance, *Cryst. Eng. Comm.* 15 (2013) 8250–8254. doi: 10.1039/c3ce41133h
- [46] G. Wißmann, A. Schaate, S. Lilienthal, I. Bremer, A. M. Schneider, P. Behrens, Modulated synthesis of Zr-fumarate MOF, *Micropor. Mesopor. Mat.* 152 (2012) 64–70. doi: 10.1016/j.micromeso.2011.12.010
- [47] S. Diring, S. Furukawa, Y. Takashima, T. Tsuruoka, S. Kitagawa, Controlled multiscale synthesis of porous coordination polymer in nano/micro regimes, *Chem. Mater.* 22 (2010) 4531–4538. doi: 10.1021/cm101778g
- [48] Y.N. Wu, M. Zhou, B. Zhang, B. Wu, J. Li, J. Qiao, X. Guan, F. Li, Amino acid assisted templating synthesis of hierarchical zeolitic imidazolate framework-8 for efficient arsenate removal, *Nanoscale* 6 (2014) 1105–1112. doi: 10.1039/c3nr04390h
- [49] J. Li, Y. N. Wu, Z. Li, B. Zhang, M. Zhu, X. Hu, Y. Zhang, F. Li, Zeolitic imidazolate framework-8 with high efficiency in trace arsenate adsorption and removal from water, *J. Phys. Chem. C.* 118 (2014) 27382–27387. doi: 10.1021/jp508381m
- [50] C. S. Wu, Z. H. Xiong, C. Li, J.M. Zhang, Zeolitic imidazolate metal organic framework ZIF-8 with ultra-high adsorption capacity bound



tetracycline in aqueous solution, *RSC Adv.* 5 (2015) 82127–82137. doi: 10.1039/c5ra15497a

[51] Y. Liu, Q. H. Zou, M. X. Xie, J. Han, A novel approach for simultaneous determination of 2-mercaptobenzimidazole and derivatives of 2-thiouracil in animal tissue by gas chromatography/mass spectrometry, *Rapid Commun. Mass Spectrom.* 21 (2007) 1504–1510. doi: 10.1002/rcm.2989

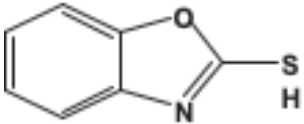
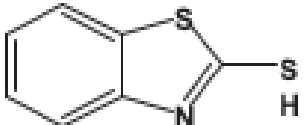
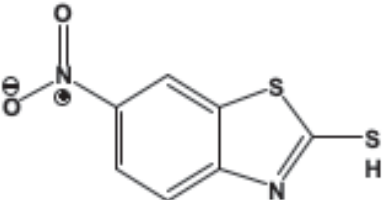
[52] M. Lõhmus, K. Kallaste, B. Le Bizec, Determination of thyreostats in urine and thyroid gland by ultra high performance liquid chromatography tandem mass spectrometry, *J. Chromatogr. A* 1216 (2009) 8080–8089. doi: 10.1016/j.chroma.2009.04.005

[53] A.G. Asimakopoulos, A. Ajibola, K. Kannan, N.S. Thomaidis, Occurrence and removal efficiencies of benzotriazoles and benzothiazoles in a wastewater treatment plant in Greece, *Sci. Total Environ.* 452-453 (2013) 163–171. doi: 10.1016/j.scitotenv.2013.02.041

[54] J. Zhang, X. Zhang, L. Wu, T. Wang, J. Zhao, Y. Zhang, Z. Men, H. Mao, Occurrence of benzothiazole and its derivatives in tire wear, road dust, and roadside soil, *Chemosphere* 201 (2018) 310–317. doi: 10.1016/j.chemosphere.2018.03.007

## 6.6. Supporting Material

Table 6.S1. Structures and properties of the studied benzomercaptans.

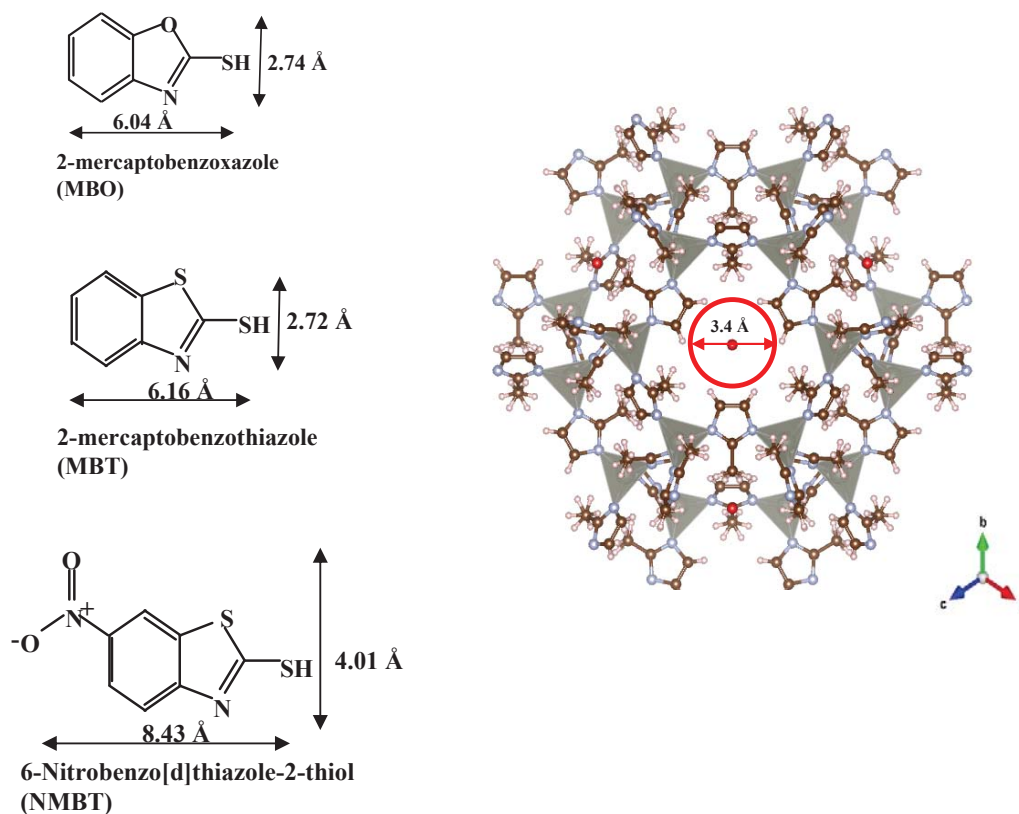
Compound	Structure	Log $P_{O/W}^a$	pK <sub>a</sub>	Ref.
2-mercaptobenzoxazole (MBO)		2.1	6.6	[1]
2-mercaptobenzothiazole (MBT)		2.9	7.0	[2]
6-Nitrobenzo[d]thiazole-2-thiol (NMBT)		3.6	7.8	[3]

**Table 6.S2.** HPLC gradient composition and detection wavelength program for the HPLC-UV analysis.

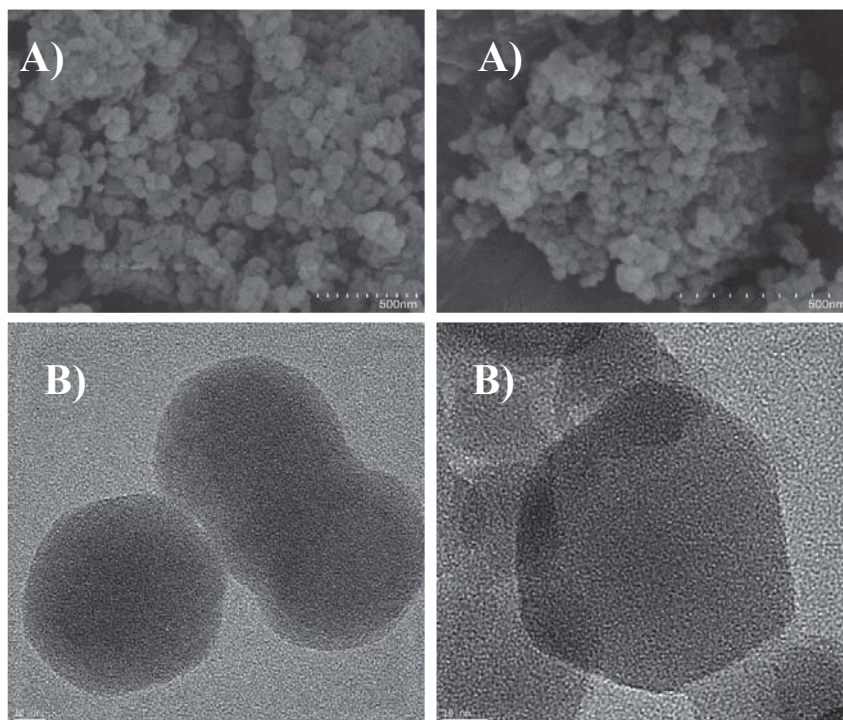
HPLC Gradient		Detection wavelength program	
Time (min)	% B (v/v) mobile phase	Time (min)	Detection wavelength (nm)
0-2	35		
2-5	35-50	0-7	300
5-9	50		
9.0-9.1	50-80	7-8	322
9.1-11.5	80		
11.5-11.6	80-35	8-13	361
11.6-13.0	35		

**Table 6.S3.** Physical–chemical characteristics (or parameters) of the soil samples collected in different sites.

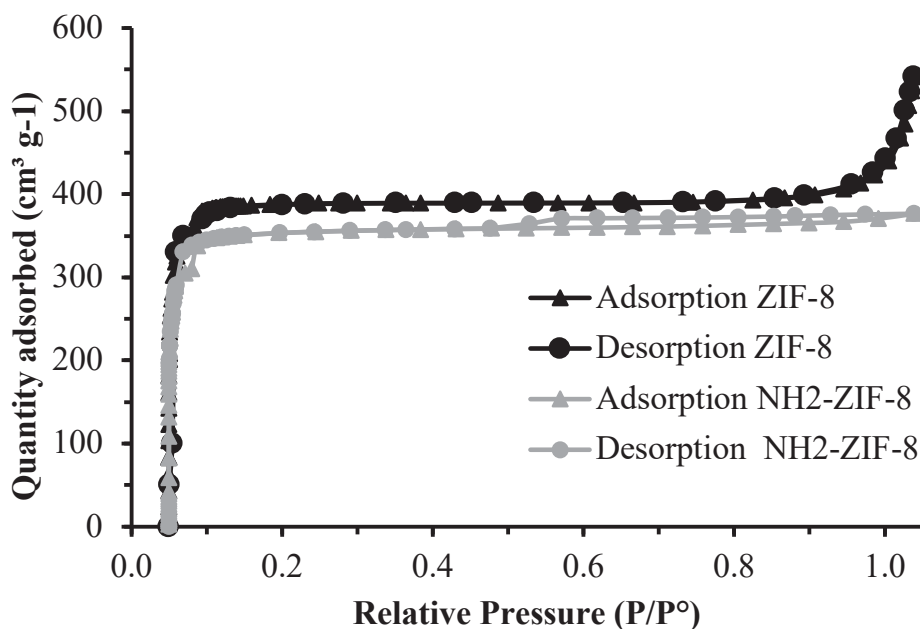
Soil source	Humidity (% wt.)	Conductivity ( $\mu\text{S cm}^{-1}$ )	pH
Sueca	$2.5 \pm 0.1$	$36.4 \pm 0.8$	$9.56 \pm 0.1$
Burjassot	$2.0 \pm 0.2$	$39.3 \pm 0.5$	$9.57 \pm 0.3$
Valencia	$3.3 \pm 0.3$	$35.1 \pm 0.9$	$9.44 \pm 0.2$



**Figure 6.S1.** Molecular sizes of the target benzomercaptans and ZIF-8. Colors' code: N atoms (blue), H atoms (pale pink), C atoms (brown) and Zn atoms (grey inside of tetrahedrals). The structures of analytes were obtained from Chem3D. To obtain the sizes, an energetic minimization was done using MM2 model at 300K. (Minimum RMS Gradient = 0.0100).



**Figure 6.S2.** SEM (A) and TEM (B) images of NH<sub>2</sub>-ZIF-8-BA 2 (left part) and NH<sub>2</sub>-ZIF-8-BA 3 (right part) materials.



**Figure 6.S3.** N<sub>2</sub> adsorption/desorption isotherms at 77 K of the ZIF-8 NH<sub>2</sub>-ZIF-8-BA 1 materials. Circles and triangles indicate the adsorption and desorption isotherms, respectively.

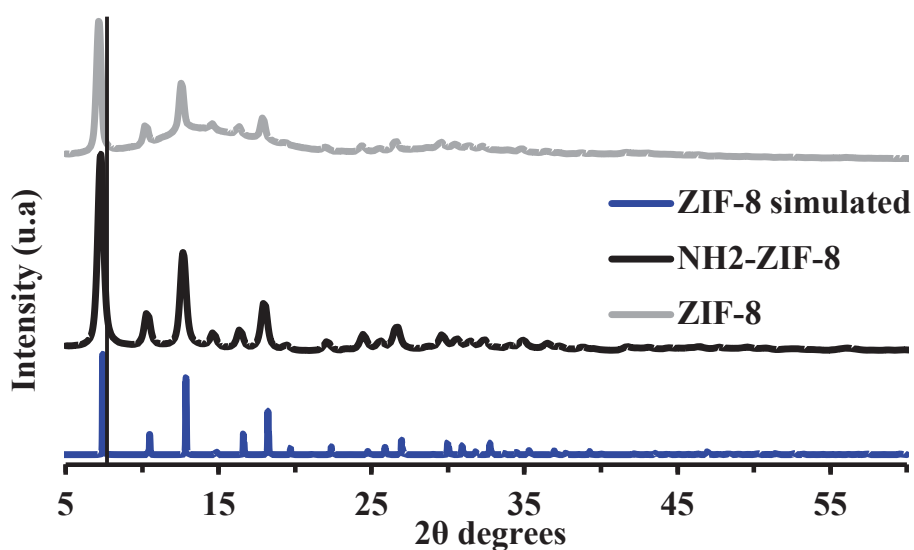


Figure 6.S4. Powder XRD patterns of zeolitic materials (ZIF-8 and NH<sub>2</sub>-ZIF-8-BA 1) and the simulated one obtained from the crystallographic data of Crystallography Open Database (COD, ID: 4128139).

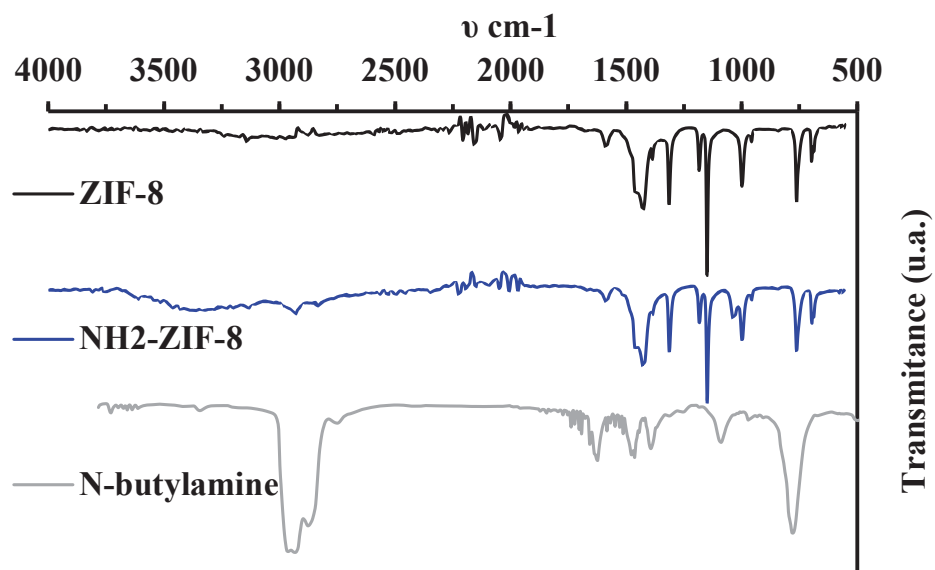
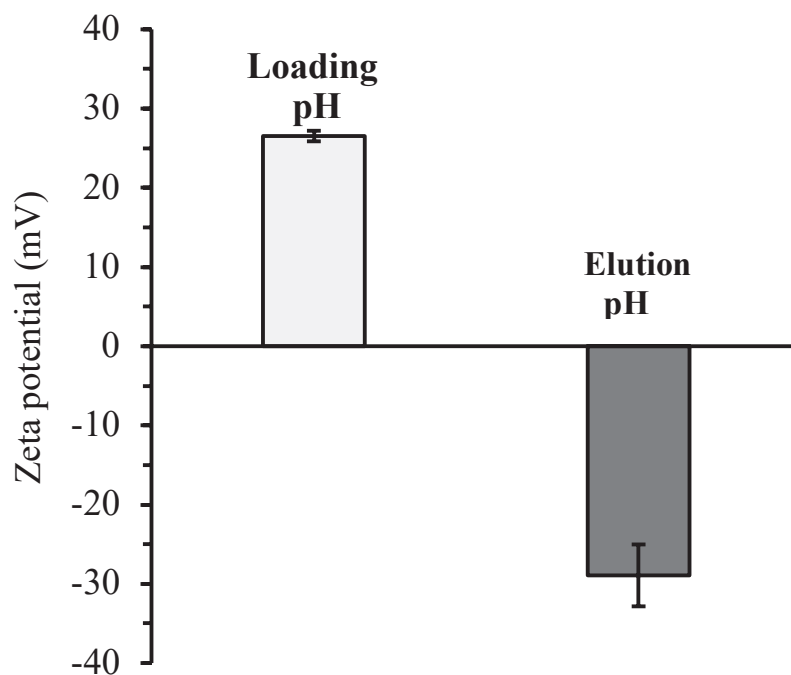
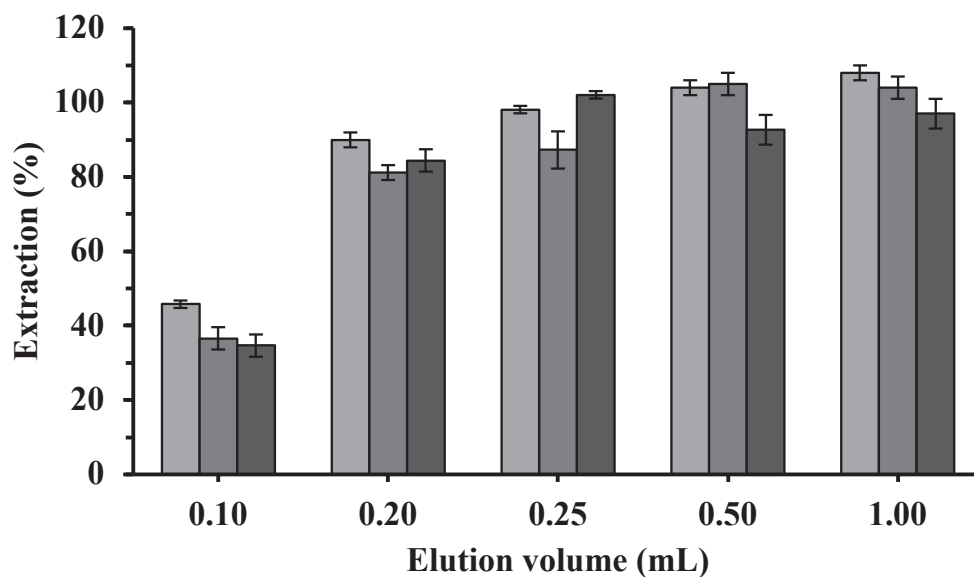


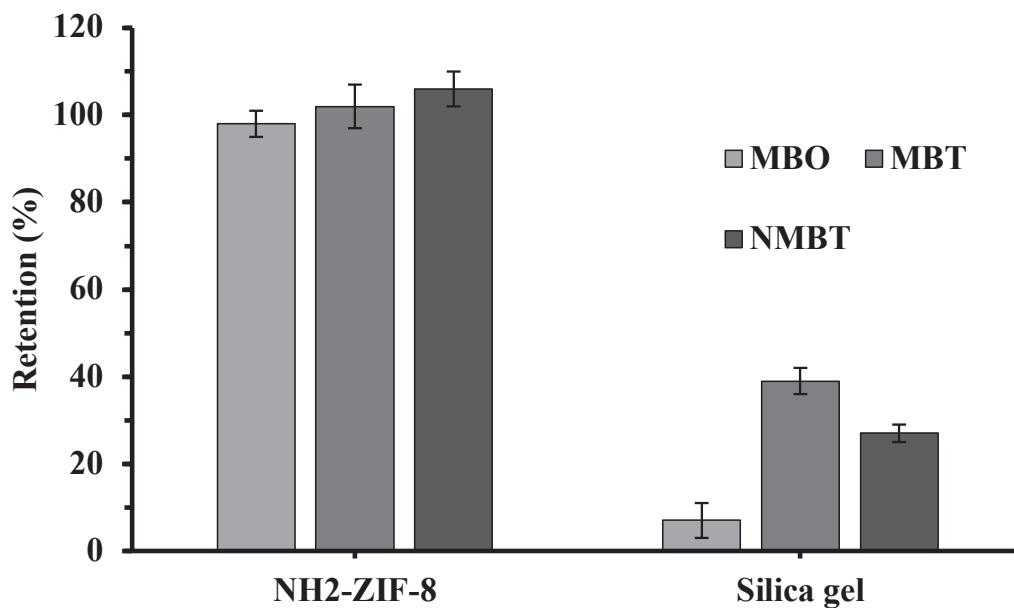
Figure 6.S5. FT-IR spectra of zinc-based MOF (ZIF-8 and NH<sub>2</sub>-ZIF-8-BA 1) and n-butylamine.



**Figure 6.S6.** Zeta potential of NH<sub>2</sub>-ZIF-8-BA 1 at different SPE conditions. Error bar = SD (n = 3).



**Figure 6.S7.** Effect of the elution volume on the extraction efficiency of the benzomercaptans using NH<sub>2</sub>-ZIF-8- BA 1 as sorbent. Error bar = SD (n = 3).



**Figure 6.S8.** Comparison of benzomercaptans extraction efficiency of NH<sub>2</sub>-ZIF-8-BA 1 sorbent and commercial silica-based cartridges. Error bar = SD (n = 3).

## References

- [1] D. R. Lide Jr. CRC Handbook of Chemistry and Physics.
- [2] ECHA database <https://echa.europa.eu/substance-information/-/substanceinfo/100.005.216> (accessed April 2020).
- [3] Calculated using Advanced Chemistry Development (ACD/Labs) Software V11.02 (© 1994-2020 ACD/Labs).



**Bloque III. Aplicación de materiales  
monolíticos en técnicas cromatográficas  
miniaturizadas**



**Capítulo 7. Poly(ethylene glycol) diacrylate based  
monolithic capillary columns for the analysis of polar  
small solutes by capillary electrochromatography**





RESEARCH ARTICLE |  Full Access |

## **Poly(ethylene glycol) diacrylate based monolithic capillary columns for the analysis of polar small solutes by capillary electrochromatography**

María Vergara-Barberán, Óscar Mompó-Roselló, José Manuel Herrero-Martínez, Ernesto Francisco Simó-Alfonso 

Monolithic stationary phases based on poly(ethylene glycol) diacrylates for capillary electrochromatography were developed. Several poly(ethylene glycol) diacrylates ( $M_n$  250, 575, and 700) were used as single monomers and the resulting columns were carefully compared. Methanol and ethyl ether were selected as porogenic solvents, and in all cases UV radiation was selected as initiation method to prepare polymeric monoliths. The influence of the monomer chain length and ratio monomer/porogen on the morphological and electrochromatographic properties of the resulting monoliths was investigated. Several families of compounds with different polarity (alkyl benzenes, organophosphorous pesticides, benzoic acid derivatives and sulfonamides) were selected to evaluate the performance of the fabricated monolithic columns. The best results were obtained for poly(ethylene glycol) diacrylate 700 monoliths affording efficiencies of 144,000 plates  $m^{-1}$  for retained polar aromatic small molecules and excellent reproducibility in column preparation (RSD values below 2.5%).

**Keywords:** Capillary electrochromatography, poly(ethylene glycol) diacrylate, polymeric monolith, polar compounds

## **7.1. Introduction**

Capillary electrochromatography (CEC) is a separation technique defined as a hybrid of capillary electrophoresis (CE) and high-performance liquid chromatography (HPLC) [1], which combines the selectivity of HPLC with the high efficiency of CE [2,3]. This technique has demonstrated its higher efficiency over pressure-driven systems due to the flat flow profile of electroosmotic flow (EOF). Currently, separation columns which are either particle-packed or silica/polymeric monoliths are used in CEC. In the case of polymeric stationary phases, the most extended materials for CEC applications have been based on acrylate and methacrylate monoliths [1,4]. The advantages of these stationary phases are their easy *in situ* preparation, high permeability, chemical stability in a wide pH-range, and an extensive variety of monomers available [4-6]. Indeed, several variables (choice of monomers, cross-linkers, porogenic solvents, polymerization time and temperature, and post-modification treatment, etc) can be modified to tailor the morphological and chromatographic properties of monoliths [7,8]. In fact, all these routes have been extensively used in the literature by different research groups with a widely differing success and recently reviewed [8].

One of these smart strategies is based on the use of single cross-linkers as monomers in the polymerization mixture. In this sense, single monomers based on dimethacrylate [9], diacrylate [9,10], divinylbenzene [11,12], N,N-methylenebis(acrylamide) [13], 1,2-bis(p-vinylphenyl)ethane [14,15], and tetrakis(4-vinylbenzyl)silane [16,17] have been reported. In particular, Lee's group [18] have explored the influence of linking alkyl length in alkylene dimethacrylates on separation performance of monolithic capillary columns reaching column efficiencies of 54,000 plates  $m^{-1}$ . The same group has described the photopolymerization of monoliths based on poly(ethylene glycol) diacrylate (PEGDA) with different length of ethylene glycol chains to efficiently separate proteins by hydrophobic interaction chromatography

[19,20]. Monoliths prepared with average molecular weight of the PEG bridge between 250-258 provided the best results (or high permeability beds with enough hydrophobic interaction sites) to successfully separate even immunoglobulin G subclasses and variants [20]. In another work, Aggarwal *et al.* [21] have also described the fabrication of monoliths based on PEGDA monomers with different ethylene-oxide (EO) chain length to separate small molecules by reversed-phase (RP) capillary liquid chromatography. A careful selection and a very-fine tuning of porogenic solvents is essential to obtain monoliths with flow-through properties. All these works based on the use of a single-monomer system highlighted the easy and simple optimization of polymerization conditions, the large surface area of resulting monolithic columns and its enhanced reproducibility. However, the extension of these highly cross-linked monoliths to strongly polar aromatic molecules (such as sulfonamides) and its use in CEC mode has not been yet applied.

In this study, the preparation and characterization of several PEGDA-based monolithic columns for CEC was done. For this purpose, several parameters such as PEGDA monomer (with different EO chain length), porogenic content and polymerization temperature were optimized. The influence of these variables on monolith morphology and its CEC performance was evaluated by scanning electron microscopy (SEM) and by measuring the retention factor and efficiency of a test mixture of alkylbenzenes, respectively. In order to demonstrate the capability of the optimized PEGDA-based column, several polar aromatic small compounds (organophosphorous pesticides, benzoic acid derivatives and sulfonamides) were separated under CEC.

## 7.2. Materials and methods

### 7.2.1. Reagents

Poly(ethyleneglycol) diacrylate (PEGDA,  $M_n$  250, 575, and 700), [2-(methacryloyloxy)ethyl]trimethyl ammonium chloride (META) and 3-(trimethoxysilyl)propyl methacrylate (TPM) were from Aldrich (Milwaukee, WI, USA). HPLC-grade acetonitrile (ACN), ethyl ether ( $\text{Et}_2\text{O}$ ) and methanol (MeOH) were from Scharlau (Barcelona, Spain). 2,2-dimethoxy-2-phenylacetophenone (99%, DMPA) were from Fluka (Buchs, Switzerland). Hydrochloric acid (37%) was supplied by Panreac (Barcelona, Spain). Uracil as EOF marker, and several alkylbenzenes and organophosphorus (OPPs) (chlorpyrifos, dialifos, fensulfothion, malathion, prophenofos, sulprofos) compounds from Riedel-de Haën (Seelze, Germany), were used. Benzoic acid derivatives [22] (benzoic acid ( $\text{pK}_a = 4.2$ ); phthalic acid ( $\text{pK}_{a1} = 2.94$ ,  $\text{pK}_{a2} = 5.41$ ); iodobenzoic acid ( $\text{pK}_a = 2.86$ ) and salicylic acid ( $\text{pK}_a = 2.97$ )) were from Fluka. Sulfonamides (sulfadiazine ( $\text{pK}_{a1} = 1.64$ ,  $\text{pK}_{a2} = 6.50$ ); sulfathiazole ( $\text{pK}_{a1} = 2.31$ ,  $\text{pK}_{a2} = 7.24$ ); sulfapyridine ( $\text{pK}_{a1} = 2.90$ ,  $\text{pK}_{a2} = 8.54$ ); sulfamethazine ( $\text{pK}_{a1} = 1.95$ ,  $\text{pK}_{a2} = 7.45$ ); sulfisoxazole ( $\text{pK}_{a1} = 1.52$ ,  $\text{pK}_{a2} = 4.83$ ); sulfamonomethoxine ( $\text{pK}_{a1} = 1.42$ ,  $\text{pK}_{a2} = 6.67$ ); sulfaguanidine ( $\text{pK}_{a1} = 2.75$ ,  $\text{pK}_{a2} = 12.10$ ) [23]) were purchased from Sigma-Aldrich (St. Louis, MO, USA). Unless otherwise stated, other chemicals used were of analytical grade. Deionized water was obtained with a B30 water purification system (Adrona, Rīga, Latvia). Standard solutions of uracil (EOF marker), alkylbenzenes, OPPs, benzoic acids and sulfonamides were prepared at  $1 \text{ mg mL}^{-1}$  each in ACN and were kept at  $4 \text{ }^\circ\text{C}$  until use. Test mixtures of these solutions ( $0.1 \text{ mg mL}^{-1}$  uracil and each analyte) were prepared daily by dilution with the mobile phase. Uncoated fused-silica capillaries of 33.5 cm total capillary length (25.0 cm of effective monolithic bed length) and 375  $\mu\text{m}$  O.D.  $\times$  100  $\mu\text{m}$  I.D. with UV-transparent external coating (Polymicro Technologies, Phoenix, AZ, USA) were used.



### *7.2.2. Instrumentation*

To initiate polymerization, the capillaries were placed into an UV crosslinker chamber (Model CL1000, UVP, Upland, CA, USA) equipped with five UV lamps ( $5 \times 8$  W, 254 nm). An HPLC pump (1100 series, Agilent Technologies, Waldbronn, Germany) was used to achieve surface modification of the capillary wall. SEM images of monolithic columns were taken with a scanning electron microscope (S-4100, Hitachi, Ibaraki, Japan) provided with a field emission gun, and an EMIP 3.0 image data acquisition system (Rontec, Normanton, UK). CEC experiments were performed on a HP<sup>3</sup>DCE instrument (Agilent) equipped with a diode array UV detector, and pressurized at both capillary ends with an external nitrogen supply. Data acquisition was performed with the ChemStation Software (Rev.A.10.01, Agilent).

### *7.2.3. Preparation of poly(ethylene glycol) diacrylate-based monoliths*

Prior to the column preparation, and in order to ensure covalent attachment of the monolith to the inner wall of the fused-silica capillaries, surface modification with TPM was performed according to Cifuentes *et al.* [24]. The two ends of the capillary were sealed with rubber septa until further use. Polymerization mixtures were prepared by weighing PEGDA (monomer), META (a positively charged monomer to generate EOF), DMPA (initiator) and porogen solvents (MeOH and/or Et<sub>2</sub>O). **Table 7.1** shows the composition of all the assayed columns. Then, the mixture was quickly vortexed (for 2 min) and the preconditioned capillary was filled with the polymerization mixture up to a length of 25.0 cm. Photo-polymerization was accomplished by irradiation of the capillaries within the UV irradiation chamber at 0.9 J/cm<sup>2</sup> for 10 min. Polymerization was done at room temperature or at ~0°C, which was achieved by placing the capillary on a copper plate freeze-mounted on ice in advance. After UV polymerization, an HPLC pump was used to flush the

columns with MeOH for 30 min to remove the pore-forming solvents and possible unreacted monomers, and finally pumped with the mobile phase.

#### *7.2.4. CEC*

Prior to use, all mobile phases for CEC were degassed by sonication. The monolithic column, placed in the CEC instrument, was equilibrated with the mobile phase by progressively increasing the applied voltage from 0 kV to -30 kV, until a constant current and a stable baseline were observed. Separations were performed at 25 °C (at several voltages). In all cases, the inlet and outlet vials were pressurized at 1 MPa with nitrogen. The test mixtures were injected electrokinetically under -30 kV for 7 s. The mobile phase was composed by 50:50 (v/v) ACN-water containing 5 mM acetic/acetate buffer at pH 3.0. Detection was performed at 214 nm.

**Table 7.1.** Composition of polymerization mixtures, experimental conditions used for polymerization, efficiency and permeability for the PEGDA-based monoliths investigated in this study.

Column	Monomer:Porogen (wt:wt, %)	MeOH:Et <sub>2</sub> O (wt:wt, %)	Polymerization Conditions	H <sub>min</sub> <sup>a</sup> (μm)	Permeability (K <sub>0</sub> ) <sup>b</sup> (10 <sup>-14</sup> m <sup>2</sup> )
<b>PEGDA 250</b>					
C1	32.2:67.8	100:0	10 min, 0°C	-	-
C2	28.5:71.5	100:0	10 min, 0°C	-	-
C3	28.4:71.6	99.1:0.9	10 min, 0°C	165	8.1
C4	21.4:78.6	98.3:1.7	10 min, 0°C	107	11.1
C5	21.4:78.6	95.9:4.1	10 min, 0°C	35.2	13.0
<b>PEGDA 575</b>					
C6	21.4:78.6	17.1:82.9	10 min, 0°C	-	-
C7	21.4:78.6	17.1:82.9	10 min, RT	43.4	4.2
<b>PEGDA 700</b>					
C8	21.4:78.6	0.7:99.3	10 min, RT	13.2	2.8

<sup>a</sup> Values obtained for hexylbenzene

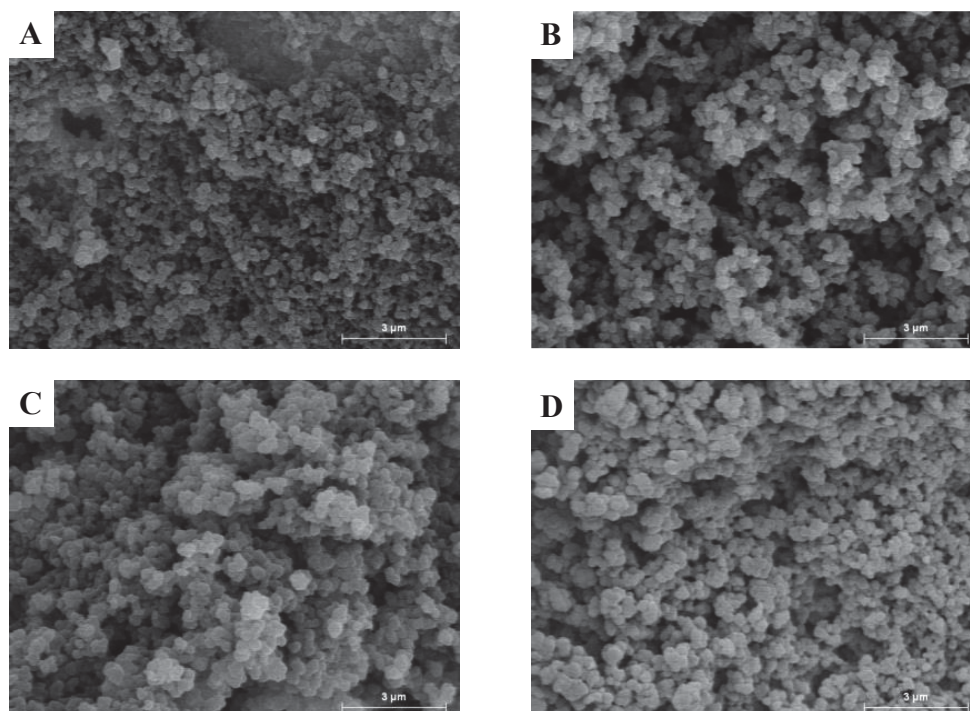
<sup>b</sup> Evaluated as  $K_0 = \frac{L\eta u}{\Delta P}$ , where L is the column length,  $\eta$  is the mobile phase viscosity (50:50, v/v ACN:H<sub>2</sub>O), u the linear flow velocity, and  $\Delta P$  is the pressure drop across the column

### **7.3. Results and discussion**

#### *7.3.1. Preparation and characterization of UV-polymerized poly(ethylene glycol) diacrylate-based monoliths*

To prepare the PEGDA-based monolithic columns, UV-polymerization was selected since presents some advantages over thermal initiation such as fast preparation, higher bed uniformity, and easy selection of polymerization regions by using masks [18, 19, 21, 25]. The conditions to prepare PEGDA-based monoliths were adapted from a previous work [19]. Thus, PEGDA 250 was firstly investigated, and the initial composition of the polymerization mixture was 32.2 wt.% monomers (99.6 wt.% PEGDA 250 and 0.4 wt.% META) and 67.8 wt.% porogens (100 wt.% MeOH and 0 wt.% Et<sub>2</sub>O). A 1 wt.% DMPA with respect to the monomer was also added. The polymerization was carried out at 0°C. However, the resulting column (**Table 7.1**, Column C1) showed a very low permeability, due to the highly dense polymeric bed formed. This is well evidenced in the SEM micrograph of this monolith (**Figure 7.1A**). For this reason, polymerization mixtures containing higher porogen weight fraction were prepared. When the porogenic solvent was increased to 78.5 wt.% (column C2), the bed permeability also remained low. The interpretation of this morphological behaviour could be explained by considering that the formation of monolithic bed is highly depending of solvating conditions for the growing polymers of PEGDA monomer [19, 21]. Indeed, these authors have demonstrated that MeOH is a good solvent for the growing polymer chains during polymerization, giving a polymer with extremely small pores. Consequently, the MeOH content in the porogenic solvent was reduced (**Table 7.1**, columns C3-C5). These monoliths showed better permeability (with values comprised between 8.1 and 13.0·10<sup>-14</sup> m<sup>2</sup>, see **Table 7.1**) than columns prepared with MeOH (columns C1-C2). It was also confirmed in **Figures 7.1B-D**, where slightly larger globules were evidenced, and these columns were chromatographically tested. The column efficiency was evaluated by measuring the minimum plate height ( $H_{\min}$ ) of hexyl

benzene as test solute. As observed in **Table 7.1**, with decreasing methanol content, a decrease in  $H_{\min}$  values in PEGDA 250 monoliths was obtained.

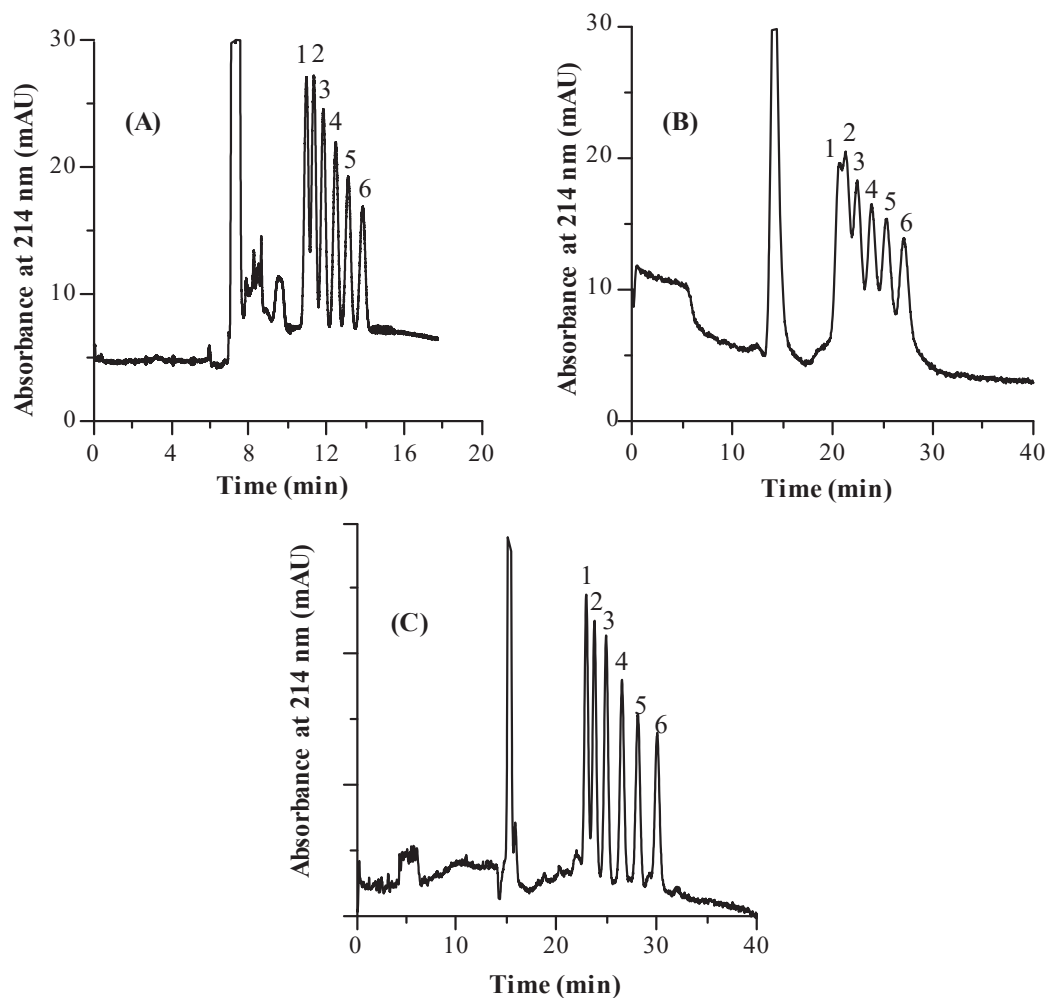


**Figure 7.1.** SEM micrographs of PEGDA 250-based monolithic columns: C1 (A), C3 (B), C4 (C) and C5 (D). Details of the polymerization composition and conditions are given in **Table 7.1**.

However, monoliths prepared at contents 93.5 wt.% of methanol or even lower contents partially polymerized in small segments within the capillary, likely caused by a poor solvation of growing nuclei in the initial stages of polymerization. **Figure 7.2A** shows the electrochromatogram of a test mixture of alkyl benzenes obtained on the column C5 that provided the best  $H_{\min}$ .

Once the PEGDA 250 monolithic column composition was optimized, the influence of other PEGDA monomers (PEGDA 575 and 700) containing different length of ethylene glycol chains or units was also investigated. For this purpose, using the best polymerization conditions found for PEGDA 250 monoliths (column C5), but replacing this monomer by PEGDA 575,

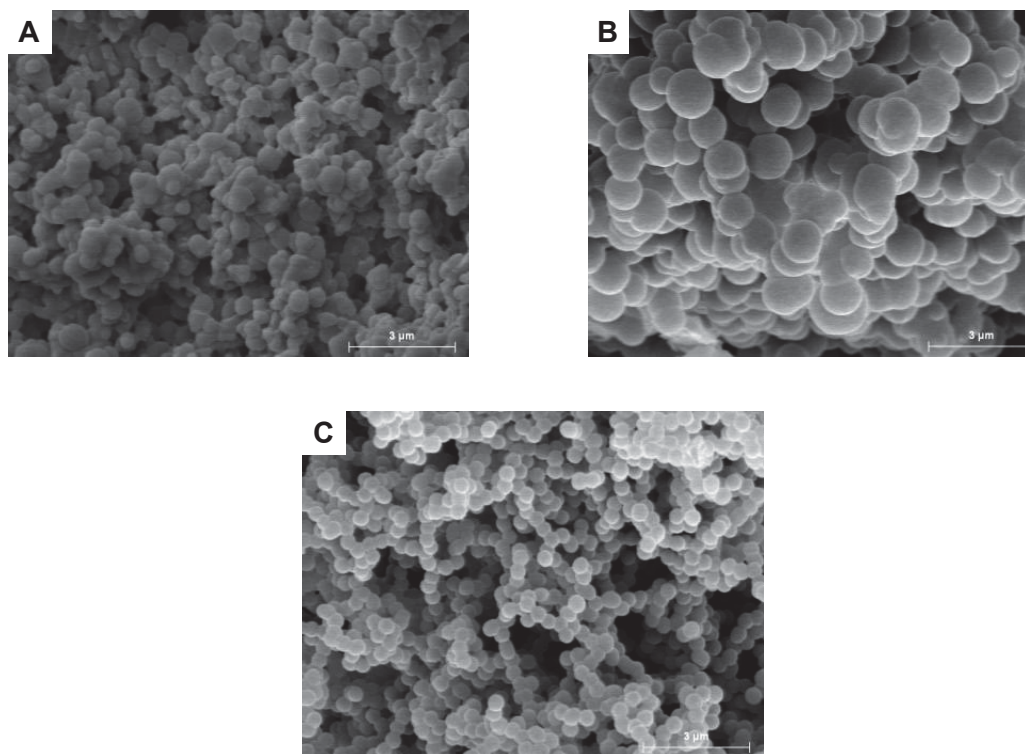
monolithic columns were prepared at *ca.* 0°C. However, a transparent wax was formed with extremely small pores (data not shown).



**Figure 7.2.** CEC separation of alkylbenzenes with different PEGDA-based monoliths: PEGDA 250 (column C5) (A), PEGDA 575 (column C7) (B); PEGDA 700 (column C8) (C). Details of the polymerization composition and conditions are given in **Table 7.1**. Experimental conditions: mobile phase, 50:50 (v/v) ACN-water containing 5 mM acetic/acetate buffer at pH 3.0; electrokinetic injection, 10 kV  $\times$  7 s; separation voltage, -30 kV. Peak identification: 1, uracil; 2, toluene; 3, ethylbenzene; 4, propylbenzene; 5, butylbenzene; 6, pentylbenzene and 7, hexylbenzene.

This behavior can be explained by an increase in ethylene glycol units (from ~ 4-5 to ~ 9-10 from PEGDA 250 to PEGDA 575) making that MeOH be better solvent for the growing polymer chains during polymerization [19,21]. The content of MeOH was also reduced (up to 17.1 wt%, column C6); however, the permeability of the resulting column was really low. In order to improve this feature, polymerization of this monolith was conducted at room temperature. As already reported [19,26-29], temperature affects both the decomposition rate of initiator (nucleation rate) and solvating properties of the solvent of polymer. At room temperature, the formation of nuclei with longer chain lengths should be expected compared to polymerization at lower temperatures, which would translate into large globules and pores. Indeed, SEM pictures taken of columns C6 and C7 (**Figures 7.3A** and **B**, respectively) corroborated this behavior. This last column exhibited a plate height of 43.4  $\mu\text{m}$ . Lower MeOH contents (up to 10.5 wt%) were tried; however, the columns gave efficiency values quite similar to column C7, accompanied by a slight reduction in its permeability ( $< 3.5 \cdot 10^{-14} \text{ m}^2$ ). Taking into account all these above considerations, a similar optimization study of the MeOH content in porogenic solvent was also performed for PEGDA 700. The conditions and composition details that provided the best permeability (**Figure 7.3C**) and efficient monoliths for PEGDA 700 (column C8) are indicated in **Table 7.1**.

Then, mixture of alkylbenzenes was also carried out under the best polymerization conditions achieved for columns synthesized with PEGDA 575 and PEGDA 700 (**Figures 7.2B** and **C**, respectively) under same separation conditions. As can be seen, when PEGDA 250 is used (**Figure 7.2A**), a satisfactory separation of analytes was observed in reasonable short times (less than 15 min). When PEGDA 575 was selected, a loss of resolution in the separation of alkylbenzenes with a concomitant increase in retention time (*ca.* 30 min) was evidenced (**Figure 7.2B**).



**Figure 7.3.** SEM micrographs of several PEGDA-based monolithic columns: PEGDA 575 (column C6) (A), PEGDA 575 (column C7) C3 (B), and PEGDA 700 (column C8) (C). Details of the polymerization composition and conditions are given in **Table 7.1**.

On the other hand, PEGDA 700 columns showed a good separation of test solutes, exhibiting better resolution than that obtained with PEGDA 250 at expense of longer analysis time. As suggested Lee and co-workers [19,21], these changes in retention and efficiency cannot be ascribed to the differences in the ethylene glycol chain length (from PEGDA 250 to PEGDA 700), and other factors such as the polymerization conditions may induce changes in retention but also changes in monolith morphology. Taking into account the higher performance of PEGDA 700 monolith, it was selected for further studies. The CEC column efficiencies (approx. 76,000 plates  $m^{-1}$ ) found for this polymer monolith were favorably compared to those reported by others for highly cross-linked monoliths evaluated using capillary LC [19,21]. For example, our column efficiencies were better than the values of 60,000 plates  $m^{-1}$  obtained by Liu *et al.* [18] for alkylbenzenes using poly(pentaerythritol

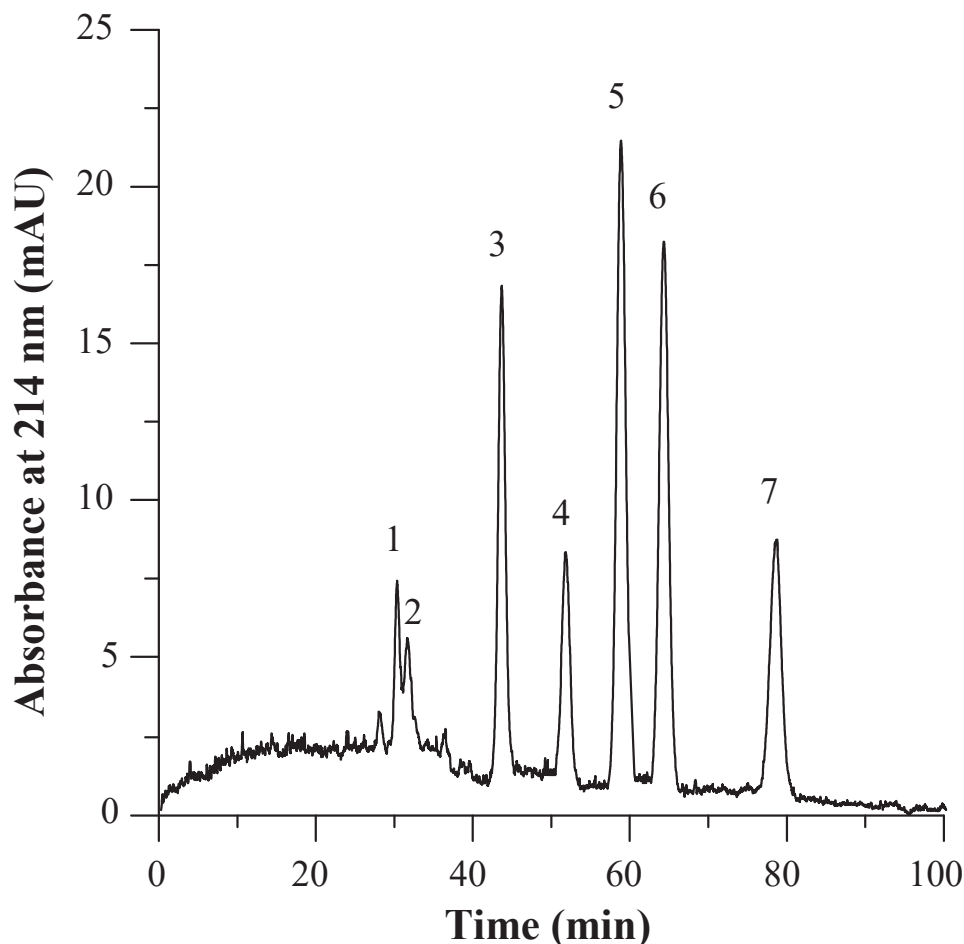


tetraacrylate) monoliths. Also, our plate numbers were slightly lower than those reported (up to 100,000 plates  $m^{-1}$ ) for PEGDA-700 monolith using alkylparabens as test solutes [21].

### *7.3.2. Separation of small polar compounds*

The CEC performance of the PEGDA-700 monolithic columns containing was then evaluated using different mixtures of polar test analytes. **Figure 7.4** shows the separation of a mixture of OPPs under the mobile phase same conditions as in **Figure 7.2**. These compounds were satisfactorily resolved with column efficiencies of up to 64,000 plates  $m^{-1}$ . These analytes also showed a decrease of retention when the ACN content increased (data not shown), thus indicating a predominant RP mechanism. Indeed, the plots of log retention factor *versus* the 1-octanol-water coefficient ( $\log P_{o/w}$ ) of these solutes showed positive correlations ( $r > 0.999$ ), which confirmed these findings.

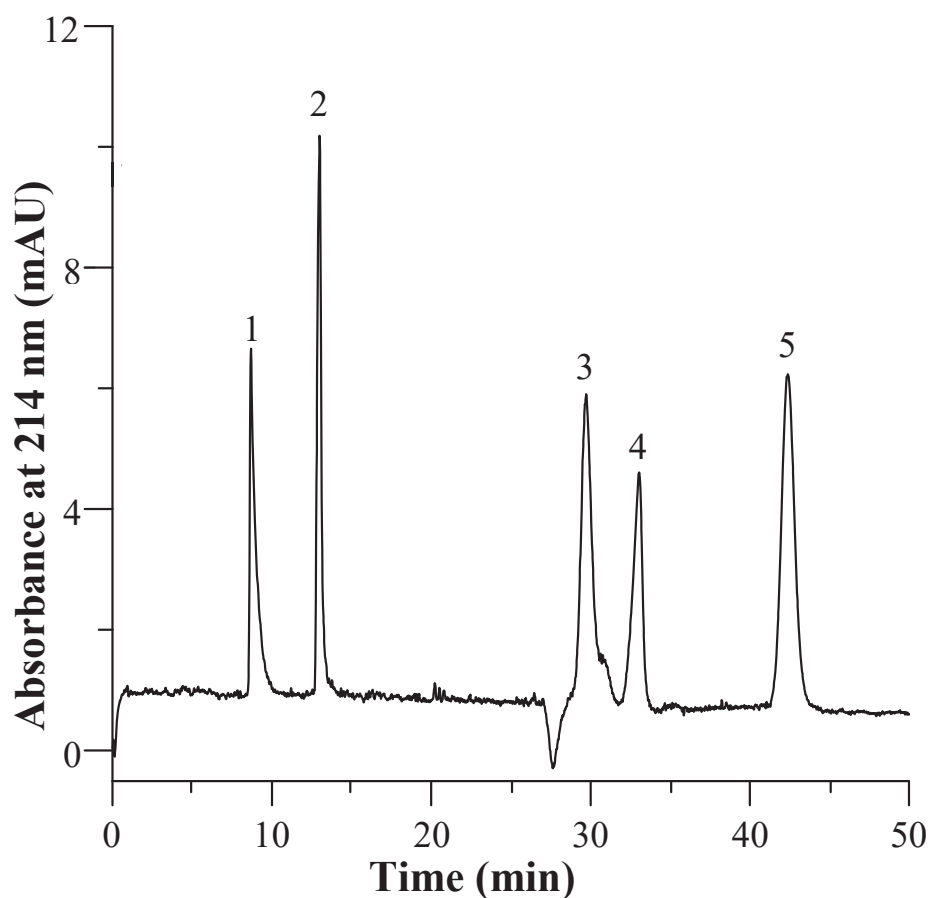
To further demonstrate the excellent performance of PEGDA-700 monolith, mixtures of hydroxyl benzoic acids and sulphonamides were analyzed. Thus, the separation of four benzoic acids (including phthalic, salicylic, 2-iodobenzoic and benzoic acids) was accomplished (see **Figure 7.5**). Under these conditions, the mixture of these acids was baseline resolved with large efficiency values (up to 80,000 plates  $m^{-1}$ ). In this case, the separation mechanism of these compounds on this column was a combination of electrophoretic mobility, electrostatic interactions of these solutes with the ionizable META moieties, and hydrogen bonding or dipole-dipole interactions with polar ethylene chains on the PEGDA monolith surface. In any case, the retention behaviour of this charged sample demonstrates that the main separation mechanism is still RP mechanism.



**Figure 7.4.** CEC separation of OPPs on a PEGDA 700 monolithic column (column C8). CEC conditions as in **Figure 7.1**, but the separation voltage was -20 kV. Peak identification: 1, uracil; 2, fensulfotion; 3, malathion; 4, prophenofos; 5, dialifos; 6, chlorpyrifos; 7, sulprofos.

Sulfonamides, a group of commonly used veterinary drugs, was also used to evaluate the applicability of PEGDA-700 monolith. As can be seen in Fig. 9.6, a satisfactory separation of seven sulfonamide antibiotics was evidenced with efficiency values up to 144,000 plates  $m^{-1}$  with very low tailing. At the mobile phase conditions selected (pH 3.0), the sulfonamides were mainly in their molecular form, and their elution order was strongly correlated with  $\log P_{o/w}$ , which supports again that the hydrophobic interaction with stationary phase played a key role in their separation. The efficient separation obtained here was better than those reported in previous studies [30, 31], where polar

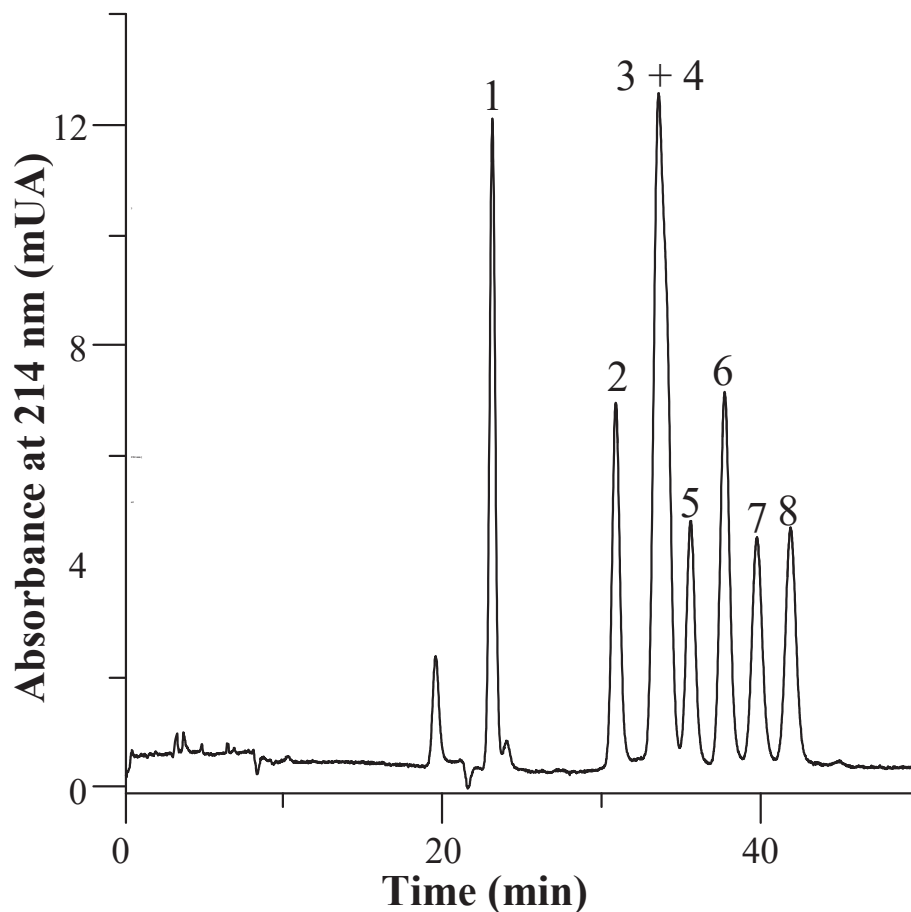
monomers (such as hexanediol ethoxylate diacrylate or methacrylic acid) were incorporated to alkyl methacrylate monolithic columns failed in the capillary LC separation of these polar solutes. Recently, the same authors have described poly(alkyl methacrylate-co-divinylbenzene) monolithic columns under gradient elution mode, showing acceptable efficiencies (given in terms of peak widths below 21 s), which could be favourably compared with our results.



**Figure 7.5.** CEC separation of benzoic acid derivatives on a PEGDA 700 monolithic column (column C8). CEC conditions as in **Figure 7.4**. Peak identification: 1, phthalic acid; 2, salicylic acid; 3, uracil; 4, 2-iodobenzoic acid and 5, benzoic acid.

The repeatability of monolithic columns prepared using PEGDA 700 was also evaluated. For this purpose, several CEC parameters (EOF time, retention factor and  $H_{\min}$  of hexylbenzene) were determined. The run-to-run repeatability was evaluated from series of three injections of the alkylbenzene

test mixture at the conditions given **Figure 7.2C**, while the column-to-column reproducibility was estimated from three columns prepared using the same polymerization mixture. For all tested parameters, the RSD values were below 2.5%, which confirmed the good reproducibility of column fabrication process.



**Figure 7.6.** CEC separation of sulfonamides on a PEGDA 700 monolithic column (column C8). CEC conditions as in **Figure 7.4**. Peak identification: 1, uracil; 2, sulfaguanidine; 3, sulfadiazine; 4, sulfathiazole; 5, sulfapyridine; 6, sulfamethazine; 7, sulfomonomethoxine and 8, sulfoxazole.

## **7.4. Conclusions**

In this work, a series of PEGDA-based monolithic columns for CEC separation of small molecules have been synthesized and characterized. Different monomers of PEGDA with different PEG chain length (PEGDA 250, 575 and 700) were investigated and thoroughly compared to separate efficiently small molecules. The results showed that PEGDA 700 monolithic column was found to provide the best separation performance with respect to efficiency, permeability and reproducibility. The feasibility of this column for separating small polar analytes (OPPs, benzoic acid derivatives and sulfonamides) has also demonstrated. Indeed, large chromatographic efficiencies (up to 144,000 plates  $m^{-1}$ ) were achieved, particularly, for certain “problematic” solutes (*e.g.* sulfonamides), where satisfactory separation performances were found compared to prior results obtained using other alkyl methacrylate-based monolithic columns containing highly hydrophilic monomers. Besides, the fabricated columns exhibited excellent reproducibility with RSD values below 2.5%, which strongly remarks the benefits of using this highly cross-linked single monomer.

## 7.5. References

- [1] Z. Deyl, F. Svec, *Capillary Electrochromatography*, Journal of Chromatography Library, Vol. 62, Elsevier, Amsterdam 2001.
- [2] C. Legido-Quigley, N.D. Marlin, V. Melin, A. Manz, N.W. Smith, *Advances in capillary electrochromatography and micro-high performance liquid chromatography monolithic columns for separation science*, *Electrophoresis* 24 (2003) 917–944. doi: 10.1002/elps.200390136
- [3] S. Eeltink, W.T. Kok, *Recent applications in capillary electrochromatography*, *Electrophoresis* 27 (2006) 84–96. doi: 10.1002/elps.20050055
- [4] Z. Deyl, F. Svec, T.B. Tennikova, *Monolithic materials, preparation properties and applications*, Elsevier, Amsterdam 2003.
- [5] F. Svec, *Porous polymer monoliths: amazingly wide variety of techniques enabling their preparation*, *J. Chromatogr. A* 1217 (2010) 902–924. doi: 10.1016/j.chroma.2009.09.073
- [6] R.D. Arrua, M. Talebi, T.J. Causon, E.F. Hilder, *Review of recent advances in the preparation of organic polymer monoliths for liquid chromatography of large molecules*, *Anal. Chim. Acta.* 738 (2012) 1–12. doi: 10.1016/j.aca.2012.05.052
- [7] F. Svec, *Quest for organic polymer-based monolithic columns affording enhanced efficiency in high performance liquid chromatography separations of small molecules in isocratic mode*, *J. Chromatogr. A* 1228 (2012) 250–262. doi: 10.1016/j.chroma.2011.07.019
- [8] F. Svec, Y. Lu, *Advances and recent trends in the field of monolithic columns for chromatography*, *Anal. Chem.* 2015, 87, 250–273. doi: 10.1021/ac504059c
- [9] T. Kubo, N. Kimura, K. Hosoya, K. Kaya, *Novel polymer monolith prepared from a water-soluble crosslinking agent*, *J. Polym. Sci. Part A-Polym. Chem.* 45 (2007) 3811–3817. doi: 10.1002/pola.22130

- [10] Z. Wu, K.J. Frederic, M. Talarico, D. De-Kee, Porous polymer monolith templated by small polymer molecules, *Can. J. Chem. Eng.* 87 (2009) 579–583. doi: 10.1002/cjce.20190
- [11] K. Kanamori, K. Nakanishi, T. Hanada, Rigid macroporous poly (divinylbenzene) monoliths with a well-defined bicontinuous morphology prepared by living radical polymerization, *Adv. Mater.* 18 (2006) 2407–2411. doi: 10.1002/adma.200601026
- [12] J. Hasegawa, K. Kanamori, K. Nakanishi, T. Hanada, S. Yamago, Pore formation in poly (divinylbenzene) networks derived from organotellurium-mediated living radical polymerization, *Macromolecules* 42 (2009) 1270–1277. doi: 10.1021/ma802343a
- [13] J. Hasegawa, K. Kanamori, K. Nakanishi, T. Hanada, S. Yamago, Rigid crosslinked polyacrylamide monoliths with well-defined macropores synthesized by living polymerization, *Macromol. Rapid Commun.* 30 (2009) 986–990. doi: 10.1002/marc.200900066
- [14] A. Greiderer, S.C. Ligon, C.W. Huck, G.K. Bonn, Monolithic poly (1, 2-bis (p-vinylphenyl) ethane) capillary columns for simultaneous separation of low-and high-molecular-weight compounds, *J. Sep. Sci.* 32 (2009) 2510–2520. doi: 10.1002/jssc.200900211
- [15] A. Greiderer, S.C. Ligon, C.W. Huck, G.K. Bonn, Influence of the polymerisation time on the porous and chromatographic properties of monolithic poly (1, 2-bis (p-vinylphenyl)) ethane capillary columns. *J. Chromatogr. A* 1216 (2009) 7747–7754. doi: 10.1016/j.chroma.2009.08.084
- [16] S.H. Lubbad, M.R. Buchmeiser, Highly cross-linked polymeric capillary monoliths for the separation of low, medium, and high molecular weight analytes, *J. Sep. Sci.* 32 (2009) 2521–2529. doi: 10.1002/jssc.200900188
- [17] S.H. Lubbad, M.R. Buchmeiser, Fast separation of low molecular weight analytes on structurally optimized polymeric capillary monoliths,

J. Chromatogr. A 1217 (2010) 3223–3230. doi: 10.1016/j.chroma.2009.10.090

[18] K. Liu, H.D. Tolley, M.L. Lee, Highly crosslinked polymeric monoliths for reversed-phase capillary liquid chromatography of small molecules, J. Chromatogr. A 1227 (2012) 96–104. doi: 10.1016/j.chroma.2011.12.081

[19] Y. Li, H.D. Tolley, M.L. Lee, Monoliths from poly (ethylene glycol) diacrylate and dimethacrylate for capillary hydrophobic interaction chromatography of proteins, J. Chromatogr. A 1217 (2010) 4934–4945. doi: 10.1016/j.chroma.2010.05.048

[20] C.T. Desire, R.D. Arrua, M. Talebi, N.A. Lacher, E.F. Hilder, Poly (ethylene glycol)-based monolithic capillary columns for hydrophobic interaction chromatography of immunoglobulin G subclasses and variants, J. Sep. Sci. 36 (2013) 2782–2792. doi: 10.1002/jssc.201300558

[21] P. Aggarwal, J.S. Lawson, H.D. Tolley, M.L. Lee, High efficiency polyethylene glycol diacrylate monoliths for reversed-phase capillary liquid chromatography of small molecules, J. Chromatogr. A 1364 (2014) 96–106. doi: 10.1016/j.chroma.2014.08.056

[22] E.P. Serjeant, B. Dempsey, Ionisation constants of organic acids in aqueous solution, International Union of Pure and Applied Chemistry (IUPAC). IUPAC Chemical Data Series No. 23, 1979

[23] M.J. Ruiz-Angel, S. Carda-Broch, M.C. Garcia-Alvarez-Coque, A. Berthod, Effect of ionization and the nature of the mobile phase in quantitative structure-retention relationship studies, J. Chromatogr. A 1063 (2005) 25–34. doi: 10.1016/j.chroma.2004.11.062

[24] A. Cifuentes, P. Canalejas, A. Ortega, J.C. Díez-Masa, Treatments of fused-silica capillaries and their influence on the electrophoretic characteristics of these columns before and after coating, J. Chromatogr. A 823 (1998) 561–571. doi: 10.1016/s0021-9673(98)00295-7



- [25] C. Yu, M. Xu, F. Svec, J.M. Fréchet, Preparation of monolithic polymers with controlled porous properties for microfluidic chip applications using photoinitiated free-radical polymerization, *J. Polym. Sci. Part A-Polym. Chem*, 40 (2002) 755–769. doi: 10.1002/pola.10155
- [26] F. Svec, J.M. Frechet, Temperature, a simple and efficient tool for the control of pore size distribution in macroporous polymers, *Macromolecules* 28 (1995) 7580–7582. doi: 10.1021/ma00126a044
- [27] O. Okay, Macroporous copolymer networks, *Prog. Polym. Sci.* 25 (2000) 711–779. doi: 10.1016/s0079-6700(00)00015-0
- [28] C. Gelfi, A. Orsi, F. Leoncini, P.G. Righetti, Fluidified polyacrylamides as molecular sieves in capillary zone electrophoresis of DNA fragments, *J. Chromatogr. A* 689 (1995) 97–105. doi: 10.1016/0021-9673(94)00861-3
- [29] M. Szumski, B. Buszewski, Effect of temperature during photopolymerization of capillary monolithic columns, *J. Sep. Sci.* 32 (2009) 2574–2581 doi: 10.1002/jssc.200900220
- [30] S.L. Lin, Y.R. Wu, T.Y. Lin, M.R. Fuh, Preparation and evaluation of 1, 6-hexanediol ethoxylate diacrylate-based alkyl methacrylate monolithic capillary column for separating small molecules, *J. Chromatogr. A* 1298 (2013) 35–43. doi: 10.1016/j.chroma.2013.05.003
- [31] S.L. Lin, C.C. Wang, M.R. Fuh, Chromatographic selectivity of poly (alkyl methacrylate-co-divinylbenzene) monolithic columns for polar aromatic compounds by pressure-driven capillary liquid chromatography, *Anal. Chim. Acta* 939 (2016) 117–127. doi: 10.1016/j.aca.2016.08.034



**Bloque IV. Resumen de resultados y  
conclusiones**



## **A. Evaluación del potencial de nuevos materiales porosos en técnicas de (micro)extracción**

### *A.1. In syringe hybrid monoliths modified with gold nanoparticles for selective extraction of glutathione in biological fluids prior to its determination by HPLC*

En este trabajo se diseñaron y sintetizaron monolitos modificados con AuNPs como sorbentes de SPE para el aislamiento de GSH en fluidos biológicos. En primer lugar, se prepararon monolitos genéricos de GMA, los cuales se modificaron posteriormente con varios ligandos (amoníaco, cisteamina y cistamina), y finalmente se funcionalizaron con AuNPs. La caracterización morfológica de los materiales obtenidos se llevó a cabo por técnicas tales como SEM y microanálisis. El material funcionalizado con cistamina dio lugar a un mayor contenido de AuNPs, y por ello se seleccionó como sorbente para los estudios posteriores.

Con respecto al procedimiento SPE, tras la optimización de las etapas de extracción, se lograron valores de recuperación entre 86 y 105% y un LOD muy bajo ( $1,5 \text{ ng mL}^{-1}$ ). La efectividad del sorbente sintetizado quedó demostrada por su satisfactoria aplicación a muestras biológicas, donde jugó un papel fundamental en la limpieza de la matriz de la muestra y preconcentración del GSH. Esto puede explicarse en base a la fuerte afinidad entre el grupo tiol presente en el GSH y las AuNPs localizadas en la superficie de la matriz polimérica durante la etapa de retención.

En comparación con otros métodos actuales basados en nanomateriales usados en la preparación de muestras conteniendo GSH, la metodología desarrollada resultó más simple y rentable, gracias a la buena reutilización mostrada por el material. Por lo tanto, la metodología propuesta representa una alternativa prometedora para la extracción de compuestos relevantes tiolados en muestras biológicas.

*A.2. Boronate affinity sorbents based on thiol-functionalized polysiloxane-polymethacrylate composite materials in syringe format for selective extraction of glycopeptides*

En este estudio se sintetizaron materiales monolíticos con grupos boronato para aislar y preconcentrar glicopéptidos. Para ello, se partió de un monolito genérico (GMA) el cual fue modificado, de forma sucesiva, con PMPMS y VPBA obteniéndose el material GMA-PMPMS-VPBA. Por otro lado, se preparó un monolito funcionalizado con AuNPs, al que posteriormente se le incorporaron PMPMS and VPBA (material GMA-SH@AuNP@PMMPS-VPBA). Ambos materiales se caracterizaron mediante SEM, FTIR y análisis elemental.

En lo referente al protocolo SPE, el material GMA-SH@AuNP@PMMPS-VPBA mostró una mayor eficiencia en la retención de glicopéptidos, lo cual se puede atribuir a la mayor cantidad de grupos boronato presentes en su estructura. Además, dicho material mostró una preconcentración selectiva de glicopéptidos (24 glicopeptidos de un total de 27), una elevada capacidad de adsorción ( $25 \text{ mg g}^{-1}$ ), alta sensibilidad ( $0.5 \text{ fmol}/\mu\text{L}$ ) y selectividad, así como una buena reproducibilidad y reutilización (hasta 10 ciclos sin pérdidas apreciables en los valores de recuperación).

Además, la metodología desarrollada representó una herramienta sencilla y efectiva para la extracción satisfactoria de glicopéptidos en muestras biológicas complejas, como suero humano, sin ningún pretratamiento adicional.

*A.3. Extraction of  $\beta$ -blockers from urine with a polymeric monolith modified with 1-allyl-3-methylimidazolium chloride in spin column format*

En este trabajo se prepararon sorbentes monolíticos funcionalizados con un líquido iónico ([AMIM][Cl]) en columnas de microcentrífuga para su aplicación en la extracción de  $\beta$ -bloqueantes en muestras de orina humana. Tras optimizar la composición del monolito de partida, se abordaron dos rutas

para la incorporación del IL al monolito: i) la generación *in situ* del IL sobre la superficie del monolito base (GMA) y ii) la adición del IL en la mezcla de reactivos seguido de polimerización.

De las dos aproximaciones, la segunda vía proporcionó un material con la suficiente resistencia mecánica, así como permeabilidad y porosidad apropiadas para llevar a cabo el proceso extractivo. A continuación, se optimizó el protocolo SPE para obtener el mayor rendimiento de extracción posible evaluándose aspectos tales como el contenido de [AMIM][Cl] en el sorbente polimérico, el pH de la disolución de carga y la composición del disolvente de elución

Así pues, la presencia de [AMIM][Cl] en el sorbente resultante proporcionó un aumento en la retención de los analitos (en comparación con el polímero base de GMA) debido a interacciones electrostáticas, enlaces por puente de hidrógeno, interacciones  $\pi$ - $\pi$ , y fuerzas hidrofóbicas. Bajo las condiciones óptimas de SPE, el sorbente desarrollado mostró altas recuperaciones (> 90 %), LODs entre 1,4 y 40  $\mu\text{g L}^{-1}$ , una capacidad de carga de 2,5  $\mu\text{g}$  por mg sorbente y una reutilización satisfactoria (hasta 20 ciclos).

El método desarrollado se aplicó a la extracción de propranolol en muestras de orina humana, observándose una limpieza efectiva (*clean up*) de la matriz de la muestra, preservando así la integridad estructural de la columna cromatográfica.

En comparación con otros métodos de tratamiento de muestra de  $\beta$ -bloqueantes publicados, el método propuesto supone una reducción en la cantidad de reactivos, un menor impacto medioambiental y reducido coste. Además, el formato de sorbente monolítico en columna de microcentrífuga permite el procesamiento de un mayor número de muestras debido a la sencilla manipulación del material requerido en el proceso y por tanto podría extenderse a aplicaciones bioanalíticas de rutina.

*A.4. Determination of benzomercaptans in environmental complex samples by combining zeolitic imidazolate framework-8-based solid-phase extraction and high-performance liquid chromatography with UV detection*

En este trabajo se sintetizaron y caracterizaron nanocristales de ZIF-8 modulados con BA para su posterior evaluación como sorbente de SPE de benzomercaptanos en matrices medioambientales.

En primer lugar, se estudió el efecto de la cantidad de BA en la mezcla de síntesis del MOF sobre el crecimiento cristalino y la capacidad de adsorción del MOF resultante. La caracterización morfológica del material sintetizado se llevó a cabo por técnicas tales como SEM, TEM, EDAX incluyéndose también medidas de área superficial. El material que mejores resultados proporcionó fue el ZIF-8 que contenía 10 mmol de BA como modulador.

En segundo lugar, se investigaron varios parámetros experimentales del protocolo SPE (pH de la muestra, composición y volumen del disolvente de elución, y reutilización). La fructífera combinación del ZIF-8 como extractante seguido de la determinación mediante HPLC-UV proporcionó elevados rendimientos de extracción, LODs bajos, excelentes factores de preconcentración y una reutilización satisfactoria.

Los resultados obtenidos demuestran que el protocolo desarrollado constituye una metodología simple, barata y apropiada para la extracción y preconcentración de estos contaminantes en muestras medioambientales complejas.

Este trabajo supone el primer estudio de la influencia del contenido de modulador en la morfología y rendimiento de extracción de MOFs orientados a la evaluación de contaminantes orgánicos, y en concreto, benzomercaptanos. La estrategia propuesta podría extenderse al desarrollo de otros MOFs y su aplicación en el ámbito analítico e industrial.



## **B. Aplicación de materiales monolíticos en técnicas cromatográficas miniaturizadas**

### *B.1. Poly(ethylene glycol) diacrylate based monolithic capillary columns for the analysis of polar small solutes by capillary electrochromatography*

En este trabajo se sintetizaron y caracterizaron una serie de columnas monolíticas basadas en PEGDA para la separación de moléculas pequeñas por CEC.

En primer lugar, se optimizó la composición de las mezclas de polimerización (concentración y longitud de cadena del PEGDA, concentración de porógenos y temperatura de polimerización). Se caracterizó la morfología de las fases monolíticas mediante SEM, y se evaluó la eficacia de separación de las columnas sintetizadas de una mezcla de alquilbencenos obteniendo valores cercanos a 76,000 platos  $m^{-1}$  con una mezcla de PEGDA 700.

Posteriormente, se demostró la viabilidad de esta columna para la separación de analitos de muy diversa polaridad (OPP, derivados del ácido benzoico y sulfonamidas). De hecho, se alcanzaron elevadas eficacias cromatográficas (hasta 144.000 platos  $m^{-1}$  para las sulfonamidas). Además, las columnas sintetizadas exhibieron excelentes reproducibilidades con valores de CVs por debajo del 2.5 %, lo cual confirma los beneficios de usar PEGDA como único monómero en las mezclas de polimerización, y la capacidad de proporcionar estructuras altamente entrelazadas que ofrezcan buenas prestaciones cromatográficas.